目次

1. 主論文

A geochemical study of naturally occurring arsenic-contaminated groundwater in Bangladesh: Factors controlling spatial variation of arsenic concentration in groundwater

(バングラデシュにおける自然発生のヒ素汚染地下水に関する地球化学的研究: 地下水中のヒ素濃度の空間分布を規制する要因について)

Takaaki Itai

2. 公表論文

(1) Itai, T., Kusakabe, M., 2004. Some practical aspects of an on-line chromium reduction method for D/H analysis of natural waters using a conventional IRMS. Geochemical Journal 38, 435-440.

(2) Itai, T., Masuda, H., Takahashi, Y., Mitamura, M., Kusakabe, M., 2006. Determination of As^{III}/As^{V} ratio in alluvial sediments of the Bengal Basin using X-ray absorption near-edge structure. Chemistry Letters 35, 866-867.

(3) Itai, T., Takahashi, Y., Uruga, T., Tanida, H., Iida, A., 2008a. Selective detection of Fe and Mn species at mineral surfaces in weathered granite by conversion electron yield X-ray absorption fine structure. Applied Geochemistry 23, 2667-2675.

(4) Itai, T., Masuda, H., Seddique, A. A., Mitamura, M., Maruoka, T., Li, X., Kusakabe, M., Dipak, B. K., Farooqi, A., Yamanaka, T., Nakaya, S., Matsuda, J., Ahmed, K. M., 2008b. Hydrological and geochemical constraints on the mechanism of formation of arsenic contaminated groundwater in Sonargaon, Bangladesh. Applied Geochemistry 23, 3155-3176.

3. 参考論文

(1) Shimizu, K., Itai, T., Kusakabe, M., 2006. Ion chromatographic determination of fluorine and chlorine in silicate rocks following alkaline fusion. The Journal of Geostandards and Geoanalysis 30, 121-129.

(2) Mitamura, M., Masuda, H., Itai, T., Minowa, T., Maruoka, T., Ahmed, K. M., Seddique, A. A., Biswas, D. K., Nakaya, S., Uesugi, K., Kusakabe, M., 2008. Geological structure of an arsenic-contaminated aquifer at Sonargaon, Bangladesh. Journal of Geology 116, 288-302.

(3) Seddique, A. A., Masuda, H., Mitamura, M., Shinoda, K., Yamanaka, T., Itai, T., Maruoka, T., Uesugi, K., Ahmed, K. M., Biswas, D. K., 2008. Biotite releasing arsenic into Holocene groundwater aquifer in Bangladesh. Applied Geochemistry 23, 2236-2248.

(4) Kashiwabara, T., Mitsunobu, S., Das, A., Itai, T., Tanimizu, M., Takahashi, Y., 2008. Oxidation states of antimony and arsenic in marine ferromanganese oxides related to their fractionation in oxic marine environment. Chemistry Letters 37, 756-757.

(5) Takahashi, Y., Sakuma, K., Itai, T., Zheng, G., Mitsunobu, S., 2008. Speciation of antimony in PET bottles produced in Japan and China by X-ray absorption fine structure spectroscopy. Environmental Science & Technology 42, 9045-9050.

主論文

A geochemical study of naturally occurring arsenic-contaminated groundwater in Bangladesh: Factors controlling spatial variation of arsenic concentration in groundwater

by

Takaaki Itai

Department of Earth and Planetary Systems Science,
Graduate School of Science,
Hiroshima University

Preface

I have investigated geochemical features of As-contaminated groundwater in Bangladesh since my undergraduate year. This study is initiated by the suggestion of Prof. Harue Masuda, Osaka-city University, with a financial support of the grant 15403017 from the Scientific Research Fund of the Japan Society for the Promotion of Science. I accompanied two field surveys in Bangladesh and performed some chemical analyses in Osaka-city University. After completing my BSc, I continued this research in Institute for Study of the Earth's Interior, Okayama University, for two years under supervision by Prof. Minoru Kusakabe. In this period, I accompanied one field survey in Bangladesh, and performed chemical and isotopic analyses. The results of these studies have been reported as my bachelor and master theses. Following these studies, this PhD thesis describes developed parts of my continuous research for last three years in Hiroshima University supervised by Dr. Yoshio Takahashi.

In chapter 1, I firstly reviewed the background studies dealing with mechanism of natural occurrence of As-contaminated groundwater. Because of the great environmental significance, numerous studies have been conducted, not only by field surveys, but also by experimental studies in laboratory. Summarizing of these knowledges is necessary to converge the controversial issues. Because many superior reviews of geochemistry/environmental chemistry on this topic have been published since 2000s, I particularly focused the new important studies to discuss the mechanism of naturally occurrence of As-contaminated groundwater in Bengal Basin.

Chapter 2 entitled "Hydrological and geological background of As-contaminated aquifer in Sonargaon, middle east Bangladesh" describes hydrogeochemical characteristics of As-contaminated groundwater of the study area: Sonargaon, middle-east Bangladesh. Although many data were included in my master's thesis, it took a long time to summarize the findings from these data. In 2007, the result of this study is summalizingly reported at the international conference "*Arsenic in groundwaters in south-east Asia with emphasis of Cambodia and Vietnam*" at Manchester University. This meeting was a greatly meaningful opportunity to join the discussion about the advanced researches for the global As contamination. After the

meeting, the result of my hydrogeochemical study was published in *"Applied Geochemistry"*. One important result of this study is the finding of spatial variability of As concentration in groundwater. This intricate feature gave me another research interest.

Parallel to the study of Chapter 2, another focus of my PhD study was establishment of speciation method of Fe and Mn in solid phases because of the importance of their secondary minerals controlling As behavior as I will emphasize in Chapter 1. Despite their relatively high abundances, speciation of Fe and Mn in secondly mineral using X-ray absorption spectroscopy has intrinsic analytical difficulty, i.e., strong signal interference from unwated primary minerals. In order to overcome this issue, I evaluated the applicability of surface sensitive X-ray method, namely conversion electron yield X-ray absorption fine structure (CEY-XAFS), using some granite having different degree of weathering. I succeeded the selective detection of secondary Fe and Mn phases forming on the mineral surface using this method. Hence, I applied this method to the sediment collected from As-contaminated aquifer in our study area (Chapter 4). Additionally, the availability of this new speciation method was reported in *"Applied Geochemistry"*. The detail of this method is described in Chapter 3 entitled "Development of selective speciation method for secondly Fe and Mn species at mineral surfaces by conversion electron yield X-ray absorption fine structure".

The study described in Chapter 4 entitled "Adsorption properties of As-contaminated sediment: Implication for the factors controlling large variation of As concentration in groundwater" is the most important part of my PhD study. This chapter describes the controlling factor of large variation of As concentration in groundwater. Firstly, I tried speciation of As which has been believed as the key factor controlling mobility of As in subsurface environment. I succeeded to determine the oxidation state of As using X-ray absorption spectroscopy, and this valuable result was immediately reported in the journal *"Chemistry Letters"* in 2006. However, I found that the present spatial distribution of As in groundwater, particularly in vertical direction, can not be explained solely by the change in oxidation state of As. I have seeked another controlling factors of the spatial distribution of As, and focused on the adsorption-desorption reaction of As in contaminated sediment. Combination of X-ray

absorption study and laboratory adsorption experiment gave me a new insight on the partitioning of As between sediment and groundwater.

Summarizing my PhD studies described in Chapters 2 - 4 and common scientific issues regarding to the global groundwater contamination of As mentioned in Chapter 1, I would like to discuss several controversial issues about natural occurrence of As-contamination in Chapter 5.

Aside from my 1 st authored papers, two papers, Mitamura *et al.* (2008) and Seddique *et al.* (2008), give very helpful information to develop my research. Mitamura *et al.* (2008) described geological features of the Sonargaon area based on the survey of 8 drilling cores. Seddique *et al.* (2008) described mineralogical characteristics of As-contaminated aquifer.

Contents

Chapter 4 Adsorption properties of As-contaminated sediment: Implication for the factors controlling large variation of As concentration in groundwater

Chapter 5 Discussion

Abstract

In this thesis, geochemical investigations which aim to clarify the formation process of natural occurrence of As-contaminated groundwater in Sonargaon, middle-east Bangladesh are organized into 6 Chapter. The overview of background studies (Chapter 1), hydrogeochemical approach (Chapter 2), speciation approaches (Chapter 3 and Chapter 4), total discussion (Chapter 5) and conclusion (Chapter 6). The interrelationship of each study is summarized in Fig. A-1.

Background

In Chapter 1, background studies dealing with natural occurrence of As-contaminated groundwater is overviewed. This Chapter is classified into three parts: (i) geochemical perspectives of As-contamination in Bengal Basin, (ii) basic chemical reactions of As in near surface environment, (iii) previous hypotheses for the cause of As-contamination. The objectives and approaches of the PhD studies are summarized in the end of this Chapter.

Hydrogeochemical approach

In Chapter 2, geochemical and hydrological features of As contaminated groundwater in Sonargaon, middle-eastern Bangladesh are described. Samples of groundwater are collected from ca. 230 tube-wells in rainy and dry seasons. Arsenic-contaminated groundwater was found in the Holocene unconfined aquifer (5 ~ 30 m) but not in the Pleistocene aquifer (> 60 m). Concentration of As is varied from <1 to 1200 μg/L in Holocene aquifer. The spatial distribution of As concentration in groundwater is extremely patchy despite the small study area (3 × 3 km^2). The aqueous As concentration was low from surface to 15 m, whereas it becomes high from 15 to 30 m. This vertical distribution corresponds to the typical bell-shaped profile which commonly observed from various parts of Bangladesh. Groundwater in the Holocene aquifer gives Ca-Mg-HCO_3^- type chemistry. Groundwater with a high degree of As contamination is generally characterized by high Fe^{2+} and NH_4^+, whereas NO_3^- and SO_4^{2-} were low, suggesting that As-contaminated groundwater prevails under highly reducing condition. The results of H and O stable isotope ratios and tritium indicated the small scaled circulation of Holocene groundwater with typical residence time being <50 years. This study revealed that reducing environment is clearly favored for the As mobilization. However, the controlling factors of large spatial variation of As concentration is remained as a matter.

Speciation approach

The objective of two studies classified into this approach are to clarify the underlying mechanisms to form (i) bell-shaped depth profile and (ii) patchy spatial distribution of As

concentration in groundwater, based on the speciation of As and relevant solid phases: Fe and Mn oxyhydroxides/oxides.

In Chapter 3, an experimental study to establish the new analytical method using X-ray absorption fine structure (XAFS) is introduced. This study is aimed to establish the selective speciation method of secondly Fe and Mn phases which strongly control the partitioning of As in solid-water system. Generally, XAFS measurement targeting to the speciation of Fe or Mn in bulk sediment is affected interference by strong signal derived from unwanted primary minerals, such as biotite and hornblende. The conversion electron yield XAFS (CEY-XAFS) employed this study reflects information of the species at sub-micrometer scale from particle surface due to limited escape depth of inelastic Auger electron. This feature is potentially advantageous to the selective detection of the signal derived from minor secondly minerals. The surface sensitivity of this method was assessed by the experiments for two samples of granite having different degrees of weathering. The XANES spectra of Fe-K and Mn-K edge gave clearly different information between CEY and fluorescence (FL) modes. These XANES spectra of Fe and Mn show a good fit upon application of the least-squares fitting using ferrihydrite/MnO_2 and biotite as the end members. The XANES spectra collected by CEY mode provided more selective information on the secondary phases which are probably present at mineral surfaces. This study demonstrated that combination of CEY and FL-XAFS will help to identify important minor phases that form at the mineral surfaces.

In Chapter 4, the factors controlling the large spatial variation of As-contaminated groundwater is focused. We hypothesized that the concentration of As in household well waters are controlled by an adsorption–desorption equilibrium between sediment and groundwater. To verify the hypothesis, two factors are focused upon in this study: (i) speciation of As and Fe in the solid phase, and (ii) the adsorption properties of As(III) and As(V) to sediment. The oxidation states of As and Fe in the sediments as determined by FL- and CEY-XANES showed a distinct redox boundary below 5 m from the ground surface, whereas the peak of dissolved As is observed below 15 m. The apparent distribution coefficient ($K_d = C_{solid}/C_{solution}$) of As(V) is always larger than that of As(III) at all the depths. A simulated concentrations of As in the groundwater obtained by multiplying the amount of exchangeable As (extracted by 0.1 M PO_4^{3-} solution) and K_d^{-1} with considering the oxidation state of As is consistent with depth profile of As in groundwater. This suggests that the concentration of dissolved As is strongly controlled by an adsorption–desorption equilibrium between sediment and groundwater. Variation in K_d is controlled by the amount of Fe oxyhydroxides for As(V), whereas surface area is important for As(III). The discrepancy between the depth of the redox boundary and the peak of dissolved As is attributed to the difference in abundance of exchangeable As (mass effect) rather than to a variation of K_d (partition effect). Using these two effects, the mechanism to

form great variation in aqueous As concentration in groundwater can be quantitatively evaluated.

Conclusion

The most important finding throughout the PhD studies are that aqueous As concentration in groundwater is consistent with adsorption-desorption equilibrium. This conclusion indicated that relative contribution of two factors: "mass effect" and "partition effect", must be clarified to discuss the spatial variation of As concentration. Speciation of As and Fe is the key approach to quantify the relative contribution of these effects. Through this study, factors controlling large spatial variation of aqueous As concentration in groundwater are much better understood.

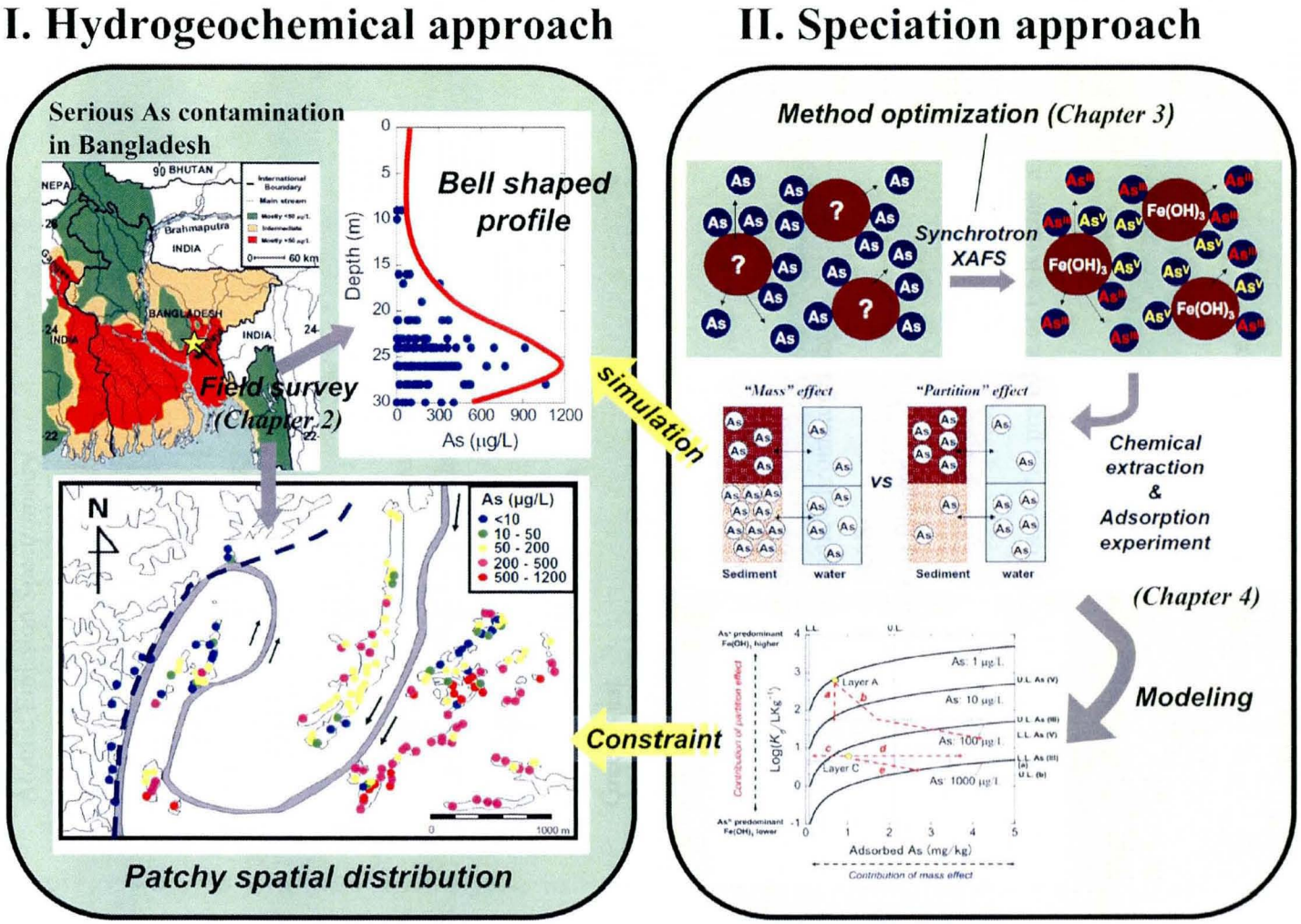

Fig. A-1: A schematic of the relationship of two major approaches conducted by the PhD studies.

List of abbreviations

AAS:	Atomic Absorption Spectrophotometry
AES:	Atomic Emission Spectrometry
ASV:	Anode stripping Voltammetry
AVS:	Acid Volatile Sulfide
BGS:	British Geological Survey
CEY:	Conversion electron Yield
CSV:	Cathode Stripping Voltammetry
CD:	Charge Distribution
DOM:	Dissolved Organic Matter
DOC:	Dissolved Organic Carbon
DPHE:	Department of Public Health and Engeneering
EXAFS:	Extended X-ray Absorption Fine Structure
EY:	Electron Yield
FL:	Fluorescence
GBM:	Ganges-Brahmaputra-Meghna rivers
GR:	Green Rust
HFO:	Hydrous Ferric Oxide
HMO:	Hydrous Manganese Oxide
HAO:	Hydrous Alminum Oxide
HR-ICP-MS:	High Resolution ICP-MS
HPLC:	High Performance Liquid Chromatography
HG-AAS:	Hydride Generation AAS
ICP:	Inductively Coupled on Plasma
MS:	Mass Spectrometry
PF:	Photon Factory
RSC:	Relative Shift of Centroid of the pre-edge of Fe K-edge XANES
TC:	Total Carbon
TN:	Total Nitrogen
TS:	Total Sulfur
XAFS:	X-ray Absorption Fine Structure
XANES:	X-ray Absorption Near the Edge Structure

List of figures

Abstract

Chapter 1

Chapter 2

Chapter 3

Chapter 4

Chapter 5

List of Tables

Chapter 1

Chapter 2

Chapter 3

Chapter 4

Chapter 1
A review of As-contamination in groundwater

1. Chapter introduction

Degradation of groundwater quality has attracted worldwide attention particularly because of increasing dependence on groundwater as a source of water securing for the quality of life. Being different from surface water, remediation of polluted groundwater is quite difficult. In many developing countries, the groundwater problem is particularly serious due to the difficulty to construct the centralized water supply system by economic reasons.

Among various inorganic contaminants, As is recently focused because of its high toxicity and complex geochemical behavior. Arsenic poisoning associating with the consumption of local groundwater and the consequent serious health ailment have been reported from various parts of the world, particularly from Asian countries since late 1980's, e.g. Bangladesh, and West Bengal in India (Garai *et al.*, 1984; Chakraborty and Saha, 1987; Nickson *et al.*, 1998; Chowdhury *et al.*, 1999; Acharyya *et al.*, 2000; Harvey *et al.*, 2002; van Geen *et al.*, 2003), China (Smedley *et al.*, 2003; Gong *et al.*, 2006; Guo et al., 2008), Taiwan (Chen *et al.*, 1994; Lin *et al.*, 2006; Wang *et al.*, 2007; Nath *et al.*, 2008b), Pakistan (Nickson *et al.*, 2005; Farooqi *et al.*, 2007a, 2007b), Nepal (Gurung *et al.*, 2005, 2007), Cambodia (Polya *et al.*, 2005; Rowland *et al.*, 2005, 2007, 2008; Buschmann *et al.*, 2007) and Vietnam (Berg *et al.*, 2001; Agusa *et al.*, 2006; Postma *et al.*, 2007). Despite such a serious situation, the cause of this global pollution is unclear at present due to the lack of any clear sources of As around the polluted region. Although it is generally believed that As in groundwater is geogenic, the mechanism to form As rich groundwater is still extensively debating.

The most serious As-contamination has been reported from Bangladesh and West Bengal since 1980s. In Bangladesh, surface water used to be the main source of drinking water before 1940s. However, surface water sources in Bangladesh have been contaminated with microorganisms, causing a disease and mortality. Infants and children suffered from serious gastrointestinal disease resulting from bacterial

contamination of stagnant pond water (Smith *et al.*, 2000). In the 1970's, international organizations such as UNICEF and nongovernmental organization (NGOs) initially set the example by installing and promoting the use of tube wells in order to avoid microbial pathogens found in surface waters. In 1980s, the vast majority of tube wells in Bangladesh were installed privately by individual households with the recommendation of the government of Bangladesh (van Geen *et al.*, 2002). At present, ca. 97% of people living in Bangladesh rely on the groundwater as the source of drinking water (Yu *et al.*, 2003). This switching strategy of drinking water was initially succeeded, and patients of gastroenteritis drastically decreased. However, extensive use of groundwater brought the other serious problem. In the mid-1980s, the initial discovery of arsenicosis were attributed to the drinking of elevated As groundwater in West Bengal, India (Chakraborty and Saha, 1987). Unfortunately, As was not listed as an items which was routinely analyzed to check the water quality. Hence, extremely serious situation of As-contamination had been overlooked until 1990s. It is now recognized that the affected area in Bangladesh is vast. Approximately 46 % of wells in Bangladesh have As in excess of the drinking standard recommended by WHO (World Health Organization, 2004; As >10 μg/L), and 27% contain more than the national standard of Bangladesh (As >50 μg/L) (BGS & DPHE, 2001).

The observed health effects of exposure to groundwater As are skin abnormalities and lesions: typically pigmentation changes (e.g., hyperpigmentation) on the upper chest, arms and legs, and keratoses of the palms and soles. Long-term exposure can result in skin cancer and in various types of internal cancer, predominantly cancer of the lung, bladder, and liver (Smith *et al.*, 2000; Karim, 2000; Yu *et al.*, 2003). Yu *et al.* (2003) predicted that long-term exposure to present As concentrations will result in approximately 1,200,000 cases of hyperpigmentation, 600,000 cases of keratosis, 125,000 cases of skin cancer, and 3000 fatalities per year from internal cancers based on the statistical analysis using the comprehensive dataset of regional distribution of As-contaminated groundwater (BGS and DPHE, 2001) and dose response functions (Mazumder *et al.*, 1998).

It is generally agreed that the As is geogenic, originated from the sediments from the upland Himalayan catchments (e.g., McArthur *et al.*, 2001; Nickson *et al.*, 2000;

Harvey *et al.*, 2002). These studies also indicated that the aquifers in Bangladesh do not contain high levels of solid As, and the prevailing of certain chemical condition, which is favorable to mobilize As, is rather important to lead to anomalously high As in groundwater. However, the specific geologic, hydrologic, and geochemical conditions to form As-contaminated groundwater are still unclear.

In order to clarify the mechanism of natural occurrence of As-contaminated groundwater, background for the geochemical behavior of As in near surface environment is needed. The aim of this review chapter is to strengthen the existing knowledge about the geochemical characteristics of As-contaminated groundwater, basic chemistry of As, and various hypothesis about formation process of As-contaminated groundwater. This chapter is divided into 3 parts. In the first part (section 2 to 6), a distribution and circulation of As in Bengal Basin is briefly reviewed, then the common geochemical features of As-contaminated groundwater are described. In the second part (section 7 to 10), laboratory studies and theoretical modeling which focus basic reaction of As in water-rock system are reviewed. Because numerous laboratory and modeling studies have conducted since 1990s, I highlighted a variety of new report since 2000. In the third part (section 11 to 13), some hypotheses of the mechanism of natural occurrence of As in groundwater are introduced to clarify the controversial point of this global problem. I did not mention the studies focusing on the mitigation strategy, and human health effect, although these studies have also been emphasized as well as mechanism of the contamination. Finally, I would like to pick up some commonly discussed issues, and introduce the approaches of my PhD studies.

Part I: Geochemical perspective of As-contamination in Bengal Basin

2. *Distribution of As-contaminated groundwater in Bengal Basin*

After 1990s, many hydrogeochemical surveys have been performed to investigate the distribution of As-contaminated groundwater. The biggest survey was initiated by British Geological Survey and Department of Public Health and Engeneering for entire part of Bangladesh. In this survey, groundwaters had been collected from ca. 3500 house hold tube-wells from 1998 to 1999 (BGS and DPHE, 2001). This survey gives

clear regional distribution of As-contaminated groundwater (Fig.1−1). The highest concentration is observed in the south and south-east and the lowest concentrations in the north and north-west. Comparison of regional variation of As-contaminated groundwater and geology of Bengal Basin (Fig. 1−2), low-As groundwater is clearly linked to the relatively oxic, uplifted Pleistocene aquifers, whereas high groundwater As concentrations is in reducing Holocene aquifers. The BGS study has shown that water from shallow aquifers with recent alluvial sediments carries distinctly higher As than the groundwater from deeper aquifers with pre-Holocene sediments: only 1% of wells in the depth range of 150−200 m have aqueous As above 50 μg/L (0.7 mM; BGS and DPHE, 2001). The BGS study reveals relationships between the occurrence of aqueous As, the geology, geomorphology and hydrogeology of the area, as well as land and water use. These observations demonstrate that As concentrations in groundwater are controlled by a complex processes.

Although the extent is smaller than Bangladesh, serious contamination is also reported from West Bengal, India. The extent of As-contaminated region has been updated, not only in the West Bengal, but also other provinces, e.g., Bihar (Chakraborty *et al.*, 2003), Uttar Pladesh (Ahamed *et al.*, 2006). Many surveys have performed by the group of Jadavpur University, India, headed by Dr. Chakraborti who has been greatly contributed to inform the serious As-contamination in West Bengal and Bangladesh to the world since 1980s. The map of the distribution of As-contaminated groundwater can be found from following web site (http://www.soesju.org/).

3. *Geological and hydrological settings of Bengal Basin*

Tectonic processes have played a major role in the development of the Ganges-Brahmaputra-Meghna (GBM) delta system. The Bengal Basin, at the junction of the Tibetan, Indian and Burmese continental plate, formed after the separation of the Indian plate from the southern continent of Gondwana (Curray and Moore, 1974). Initially, marine sediments were deposited within the basin during Cretaceous times. During the Eocene, the Indian Plate collided with the Burmese Plate, and sediments eroded from the uplifted Burmese Hills were deposited within the basin. The Indian Plate further collided with the Tibetan and Burmese Plates during Miocene times,

causing a large influx of sediment into the basin south of the Himalayas and west of the Burmese Hills.

Quarternary sediments of the GBM system were deposited in two geomorphologically distinct environments to the north and to the south of the Ganges and lower Meghna rivers. To the north, continental fluviatile sediments were deposited within mountain front fan deltas and flood plains of the major rivers (Fig. 1–2). To the south, thinly bedded alluvial sediments were deposited within an estuarine delta environment.

During the Quarternary, patterns of river incision and sediment deposition in the GBM system were mainly controlled by climatic change and sea-level oscillations related to periods of glaciation (Umitsu, 1993). Sediments derived from erosion of the Himalayas and the Indo-Burman Hills were deposited in this area by major river systems. Changes in the courses of the Brahmaputra, Tista, Ganges and other rivers of the GBM system have been caused by tectonic activity. The main geomorphorogy and near surface geology of the Bengal Basin can be classified as following (see Fig. 1–2).

(i) Mountain front fan deltas of the Tista and Brahmaputra.

(ii) Fluvial floodplains of the Ganges, Brahmaputra, Tista and Meghna rivers.

(iii) The delta plain of the lower GBM system south of the Ganges-Meghna valleys, including the moribund Ganges delta and the Chadina Plain.

(iv) Pleistocene terraces of the Barind and Madhupur Tracts and associated fault systems.

(v) Subsiding basins within the eastern Ganges tidal delta and Sylhet basin adjacent to the Dauki Fault.

The large amounts of detrital are annually transported from Himalaya to Ganges-Brahmaputra rivers (GBR). The drainage area of the GBR is ~2×10^6 km^2 (Holeman, 1968; Coleman, 1969), and its floodplain in Bangladesh and India is estimated to be 2.5×10^5 km2 (modified from Morgan and McIntire, 1959). The discharge of the GBR to the Bay of Bengal varies considerably over the year; Subramanian (1979) reported a total yearly discharge of $1.0 \pm 0.1 \times 10^{12}$ m^3.

The Ganges River flows through highly weathered sediments, resulting in a heavy

clay load, whereas the Brahmaputra River drains very young and unweathered sedimentary rocks, producing a silty and sandy bedload (Coleman, 1969). Galy and France-Lanord (2001) reported that the GBR sediment load is composed of quartz, clays, primary micas, and carbonates. Within the GBR floodplain, the Bengal Basin consists of mostly quaternary deltaic sediments of the GBR and the alluvial deposits from the weathering of the Himalayas.

The hydrology of the Bengal Basin is complex because of the complicated interfingerings of coarse and fine-grained sediments from the numerous regressions and transgressions. Silts and sands dominate the upper valley deposits, whereas in the lower delta, there are silts, clays, and peats (Coleman,1969). Figure 3 indicates the geological sections derived from the boreholes data by the study of BGS & DPHE (2001). At the northern end of the section, subsidence occurs along the Himalayan Main Boundary Fault, accommodating a wedge of coarse sediments deposited as course grained sand. This layer becomes thinner to the south of the Rangpur Saddle uplift zone. Within this zone, there has been incision of the main Brahmaputra valley along which basal fan-delta sediments were deposited between uplifted Pleistocene Tracts. These coarse-grained sediments become thinner and pinch out south of the Hinge Zone and pass laterally into sandy deltaic deposits within the subsiding Faridpur Trough. Several fining-upward sequences have been deposited on the Faridpur Trough during a glacial/interglacial cycle. In the coastal zone, this sandstones and silts contains saline water above fresh water in a series of discrete aquifers. Away from the coastal zone of saline intrusion, these aquifers tend to form a single body of fresh water (Fig. 1–3).

4. *Source of As*

There are several hypothesis about the primary source and origin of As. Generally, As-contaminated groundwater occurs in the Holocene basins developed along the large river, such as Ganges, Brahmaputra, Megkong, and Indus rivers (Berg *et al.*, 2001; Polya *et al.*, 2005; Nickson *et al.*, 2005). Because most of these rivers originated from Himalaya, many researchers believe that the source material of As is derived from certain rocks in Himalaya.

Although various minerals have been proposed as a source, one important solid is

sulfides, because (i) some sulfide potentially can contain high concentration of As, and (ii) sulfide is easily weathered under oxic environment. Acharyya *et al.* (1999) suggested some possible origin of As in GBM delta as following by summarizing previous researches: (i) the Gondwana coal seams in Rajmahal basin contain up to 200 mg/kg of As (the overlying basaltic volcanics are not enriched in As), (ii) the As mineral lollingite and pyrite, which occur sporadically in association with pegmatites in the mica-belt of Bihar, have an As content in mineralized rocks that ranges from 0.12 to 0.018%, (iii) pyrite-bearing shale from the Proterozoic Vindhyan range, with its Amjhore mine, contains 0.26% As, (iv) the gold belt of the Son Valley has an As content in the bedrock that locally reaches 2.8% to 1000 mg/kg, (v) isolated outcrops of sulfides contain up to 0.8% As in the Darjeeling Himalayas, and (vi) in outcrops in the upper reaches of the Ganges River system.

Possible sources other than sulfide have also been proposed. Guillot and Charlet (2007) proposed that the Indus-Tsangpo suture zone dominated by arc-related rocks and more particularly by large volume of serpentinites enriched in arsenic could be one of the primary source of arsenic. Seddique *et al.* (2008) found that biotite buried in Holocene aquifer contains relatively high concentration of As (up to up to 49 mg/kg). They suggested that primary source of As is biotite, and weathering of this mineral can be the principal cause of As-contamination.

Although it is no wonder that to specify the source mineral of As around the Himalaya is important to prove that As is ultimately derived from Himalayan rocks, estimation of the flux of As from Himalaya to Bengal delta through the large river flow should firstly be evaluated. Concentrations of As as dissolved and particulate forms in river have been poorly reported despite great importance of this estimation. Stummeyer *et al.* (2002) reported the concentration of various trace elements in particulate matters collected from off-shore of the Bay of Bengal, and assessed their chemical forms using selective chemical extraction. The average concentration of As in particulate matter was 15 ± 1.5 mg/kg, and >90% of As was the constituent of chemically recalcitrant phases, such as crystalline Fe oxides and silicates. This As concentration is higher than the average value in world rivers (ca. 5 mg/kg, Martin and Meybeck, 1979). Because Stummeyer *et al.* (2002) was conducted during dry season, similar study in rainy season

is needed to estimate the annual flux of As from Himalaya to GBM delta. Sampling of particulate matters should also be conducted from inland regions because greatly different water composition between river and estuary waters must differentiate the speciation of As. A research group of Hiroshima University including me recently conducted a comprehensive sampling of particulate matter along the Ganges river during rainy season. Speciation of As in these samples will be important to discuss the flux of As from Himalaya to GBM delta.

Although the ultimate source of As is almost universally believed to be Himalayan source, seawater was also proposed as the ultimate source because of the precipitation of the iron oxides and organic matter due to transgression/regression cycle during the Terminal Pleistocene-Holocene (Chatterjee *et al.*, 2005). This hypothesis is consistent with the increase of As-contamination toward the coastal region. Additionally, they pointed out that the lower As content of bed load sediment samples from Ganga (1.2 to 2.6 mg/kg), Brahmaputra (1.4 to 5.9 mg/kg) and Meghna (1.3 to 5.6 mg/kg) than from BDP bore hole samples (~8 to 18 mg/kg, Datta and Subramanian 1998) is inconsistent with inland source hypothesis. Although geochemical data supporting marine origin hypothesis is still poor, it is valuable hypothesis to be tested.

5. *Spatial and temporal variations of As in groundwater*

5.1. Spatial variation

Recent intensive studies at various areas in Bangladesh and West Bengal have revealed that spatial distribution of As-contaminated groundwater is far more complex in localized scale relative to the global trend of As distribution in national scale. Van Geen *et al.* (2003) measured As concentration in groundwater pumped from 6000 wells within a 25 km^2 area of Araihazar upazilla, Narayanganj district, middle east Bangladesh. The range of concentration was <5 to 900 μg/L in the study area. The proportion of wells that exceed the Bangladesh standard for drinking water of 50 μg/L As increases with depth from 25% between 8 and 10 m to 75% between 15 and 30 m, then declines gradually to less than 10% at 90 m. Some villages within the study area do not have a single well that meets the standard, while others have wells that are nearly all acceptable. This contrastive distribution is, at least in part, related to the age of the

sediments. Holocene (<10 ka) alluvial and deltaic deposits generally contain groundwater elevated in As; while concentrations are rarely elevated in older Pleistocene sediments (<40 ka). They suggested that this is indicated by the very high fraction (99%) of wells deeper than 150 m containing >50 μg/L As (Department of Public Health Engineering (DPHE), Mott MacDonald Ltd (MMD), and British Geological Survey (BGS) (DPHE/MMD/BGS), 1999). Even shallow tube wells that reach these older deposits in uplifted terraces (e.g. Barind and Madhupur tracts) yield groundwater that is systematically low in As.

Similar feature was also reported from other researchers. Mitamura *et al.* (2008) reported the complex spatial variation of groundwater from ca. 230 wells within a 10 km^2 area of Sonargaon upazilla, Narayanganj district. The range of dissolved As concentrations are varied from <1 to 1200 μg/L in Holocene aquifer, whereas that are <4.3 μg/L in Pleistocene aquifer. To clarify the factor controlling this contrast is of primarily importance to seek the most effective mitigation strategy. This result is also reported in detail in Chapter 2 of this thesis.

Vertical distribution of As concentration is also investigated at various regions. One of the most important features of As concentrations is distinct change between shallow and deep wells. BGS and DPHE (2001) reported that wells deeper than 150–200 m show a sharp reduction in average As concentration, whereas contamination is significant in shallow wells with maximum concentration being found in the 15–30 m. This "bell-shape" profile is most clearly visualized by the report of BGS and DPHE (2001), and is commonly observed among intensive study areas, e.g., Araihazar (van Geen *et al.*, 2003), Sonargaon (Mitamura *et al.*, 2008), and Munshiganji (Harvey *et al.*, 2002). To clarify the formation process of this distinct profile is important to reveal the mechanism of natural occurrence of As-contaminated groundwater. I would like to further discuss about the formation process of the "bell-shape" profile in Chapter 4.

5.2. Temporal variation

Temporal variation of As concentration is very important information to predict the change in scale of global contamination with time. However, there is a paucity of systematic information about the variation of As concentration with time. Recent

discussion among Cheng *et al.* (2005, 2006), Ravenscroft *et al.* (2006), and Sengupta *et al.* (2006) on the journal of Environmental Science & Technology focused on the degree of temporal variation of As in groundwater. Cheng *et al.* (2005) reported a limited temporal variation within 15% at Araihazar, based on the continuous monitoring of As in ten shallow wells above 20 m over three years, although two of the shallowest wells about 8 m deep showed a significant seasonal variation of 21–63%. They concluded that groundwater As concentrations typically do not vary over time. However, Ravenscroft *et al.* (2006) and Sengupta *et al.* (2006) cast some doubt for this conclusion, particularly for the generalization of limited temporal variation for entire part of Bangladesh. They proposed several cases showing the change in As concentration with time, and argued that limited temporal variation of As concentration can not be generalized. Cheng *et al.* (2006) summarized the available monitoring data as much as possible in the response to comments (Table 1 – 1). Although As level changes with time in some places and not in other places, one important point is to compare the credible data only.

There are several reports of significant changes in As concentrations in groundwater over time. A striking example was the case of a highly-contaminated private well of unreported depth at Ramnagar in West Bengal, India, that was monitored biweekly between July 1992 and June 1993 and showed occasional variations of ~30% around an average of ~2700 μg/L (Chatterjee *et al.*, 1995). The same group observed a long term rise in groundwater As concentration in a number of private wells in 23 villages out of 100 villages of West Bengal where initially water with low As (<50 μg/L) exceeded 50 μg/L over time, although the data were not reported (Chakraborti *et al.*, 2002). There is more convincing evidence that As concentration declined between September to December, 1999, and during May 2000 in many of the 68 wells sampled twice in four districts of the Red River delta, Vietnam (Berg *et al.*, 2001).

6. *Chemical features of As-contaminated aquifer*

The typical chemical features of the high-As groundwaters of the Bengal Basin are high Fe, Mn, HCO_3^-, NH_4^+, and often PO_4^{3-}, and low Cl^-, SO_4^{2-}, NO_3^- and F^-, with a typical range of pH from 6.5 to 8.0. Such reducing features are consistent with the commonly low redox potential (Eh <100 mV; BGS and DPHE, 2001). Typical range of

Fe, Mn, HCO_3^-, NH_4^+ and PO_4^{3-} are >0.2 mg/L, >0.5 mg/L, >500 mg/L, 1 mg/L and >0.5 mg/L, respectively. However, the correlations between As and redox sensitive elements are usually not good. One commonly observed relationship is a negative correlation between As and SO_4^{2-} concentrations (e.g., BGS and DPHE, 2001; Ahmed *et al.*, 2004; McArthur *et al.*, 2004; Itai *et al.*, 2008b). This anticorrelation suggests that As mobilization occurs under the most strongly reducing conditions, coincident with SO_4^{2-} reduction. Some of the groundwaters of Bangladesh are sufficiently reducing to generate CH_4 (Harvey *et al.*, 2002). In contrast to the As-rich aquifer, As free deeper aquifers generally show Na-HCO_3 type chemistry, with relatively little dissolved NH_4^+, Fe, and Mn (Zheng *et al.*, 2005; Itai *et al.*, 2008b; Chapter 2 of this thesis) suggesting the oxic nature of this aquifer.

Saturation states of several secondary minerals are calculated by various research groups. Generally, As-contaminated groundwater is often equilibrated with calcite and dolomite. Because of reducing nature, some groundwater saturated with siderite ($FeCO_3$) and vivianite ($Fe_3(PO_4)_2 \cdot 8H_2O$) (Ahmed *et al.*, 2004; McArthur *et al.*, 2004; Itai *et al.*, 2008b; Chapter 3 of this thesis).

The sediments collected from As-contaminated aquifers in the Bengal Basin typically have total As concentrations in the range from <2 to 20 mg/kg. Permeable layers consisting of sandy sediments generally have As <10 mg/kg. This is not exceptional by reported world-average values: 1.5 ~ 5.7 mg/kg (Taylor and McLennan, 1995; Gao *et al.*, 1998; Rudnick and Gao, 2003; Hu *et al.*, 2008). These sediments are derived from the drainage systems of 3 major rivers (Ganges, Brahmaputra, and Meghna) which are originated from a wide area of the Himalaya. Therefore, it is commonly believed that the majority of As in the Bengal Basin sediments is derived from specific mineralized areas in the source region in the Himalaya.

The mineralogy of Holocene sediments is Generally dominated by quartz, feldspar, mica, chlorite and amphibole (BGS and DPHE, 2001; Akai *et al.*, 2004). The clays are dominated by a smectite-illite-chlorite clay mineral assemblage with minor amounts of kaolinite and contain variable amounts of fine grained calcite. The sediments contain variable amounts of organic matter, often less than 0.5%, although concentrations are sometimes much greater due to presence of peat horizon (BGS & DPHE, 2001).

7. *Speciation of As in contaminated aquifer*

Speciation of As is a basic information to understand the chemical behavior of As in natural environment. Arsenic can take various species in near surface environment, and show different chemical behavior depending on the speciation. Some results of the speciation analysis are briefly introduced here with analytical method and cautions for interpretation.

Speciation of certain element in solution can be estimated by the thermodynamic calculation if the solution composition is known. In the case of As, concentrations of both As(III) and As(V) must be individually determined. Species specific analytical method has been extensively developed. The most commonly used speciation techniques are combination of chromatographic separation with spectrometric detection. Among them, HPLC combined with ICP-AES/MS is the most widely used speciation method for organic and inorganic As species (Gong *et al.*, 2002). Hydride generation (HG) technique is another useful choice. HG coupled with atomic absorption (AAS), atomic emission, atomic fluorescence, and mass spectrometry (MS) have applied for the determination and speciation of trace levels of As. Because these methods are quite well established, the point of geochemically meaningful speciation analysis for natural sample is preservation method of As speciation after sampling rather than the choice of the analytical methods. On site separation using anion exchange column is the best way to avoid alteration after sampling. Alternatively, anodic or cathodic voltammetries (ASV and CSV) are a potential on site analytical method (Hung *et al.*, 2004 and reference therein). Even if these methods are difficult to be applied, suitable preservation procedures of aqueous As species are proposed form various researchers (Table 1–2). However, it seems that there is no universally agreed way. Optimum filtration immediately after the sampling followed by the addition of some acids with some complexing agent is a general procedure. A method proposed by Gault *et al.* (2005b) assuming the nearest composition of As-contaminated groundwater in Bengal Basin, recommended that simple acidification by hydrochloric acid is the best way to preserve oxidation state of As for Fe rich reducing groundwater.

Here, most reliable speciation results obtained by on-site separation using anion

exchange kit or on-site voltammetric analysis are highlighted. Bhattacharya *et al.* (2002) reported base on ground water chemistry from 9 districts {Rajshahi, Ishwardi, Meherpur, Faridpur, Munshiganj, Magura, Brahman Baria Sadar, Satkhira, and Laksmipur (Fig. 1–4)}, that As(III) is the dominant species representing about 67 to 99% of total As. Zheng *et al.* (2004) collected the water sample from 6 sampling sites (Sripur, Dhaka, Araihazar, Sonargaon, Ramganj, and Senbag) and reported that fraction of As (III) was mostly 50 to 90 %. Swartz *et al.* (2004) collected water samples from various depths at their field site in Munshiganji district, and reported that 80 to 97% is As(III) where aqueous As concentration is more than 100 μg/L (18 to 61 m), whereas fractions of As(III) were 35 to 90% where aqueous As is less than 100 μg/L (<18 m and >61 m). van Geen *et al.* (2006b) employed CSV to determine the As(III)/As(V), and reported that total dissolved As concentrations measured by high resolution (HR) ICP-MS was very good agreed with dissolved As(III) concentrations measured by CSV over the entire range of concentrations (up to ~600 μg/L). All reports indicated that As(III) is the dominant species in As contaminated groundwater.

Speciation of As in sediment is generally more difficult than that of solution due to the variability of host phase of As in sediment. Additionally, the As concentrations in sediments are generally too low to apply the spectroscopic techniques such as XAFS. Hence, selective chemical extraction techniques have been most widely used.

Despite the well-known defects of selective chemical extractions, e.g., re-adsorption, poor reproducibility, and lack of selectivity, many workers have developed both single and sequential extraction chemical procedures for As in soils and sediments (e.g., van Herreweghe *et al.*, 2003; Hudson-Edward *et al.*, 2004; Jung *et al.*, 2006). There is no universally agreed standard method for single or sequential extractions of As in sediments, and various methods have been applied to the sediment from Bengal Basin (Table 1–3).

The results of these extraction studies show large variation. Some researchers reported that amorphous Fe-oxyhydroxide fraction is the major host phase of As (e.g, BGS & DPHE, 2001; Akai *et al.*, 2004; Nath *et al.*, 2008a), whereas some reported that contribution of As in residual phase is high (e.g., Anawar *et al.*, 2003; Swartz *et al.*, 2004; Seddique *et al.*, 2008). When discuss the water-rock interaction in relatively short

time scale (day to week order), only concentrations of As in labile phases (e.g., exchangeable, amorphous Fe oxyhydroxide) are important. However, in a long time scale (>10 years), As in residual phase (e.g., crystalline oxides, sulfides and silicates) can release and move to laible phases. To identify the host of As in the residual phase is an important issue for the speciation of As in solid phase. This issue is further discussed in Chapter 5.

XAFS is the superior speciation method in terms of its non-destructivity. Generally low concentration of As in sediment disables us to directly determine the host phase by EXAFS, whereas some studies applied XANES to determine the oxidation state of As (Takahashi *et al.*, 2003; Smith *et al.*, 2005). Itai *et al.* (2006, and Chapter 4 in this thesis) determined depth profile of oxidation state of As in cored sediment using XAFS, and revealed that As in sediment is mostly arsenate and arsenite. Arsenate is dominant near the surface, while arsenite is dominant in the depth where high As groundwater is prevailing. Redox boundary between arsenate and arsenite exists around the depth of water table. Polizzotto *et al.* (2005, 2006) reported similar results based on the μ-XANES technique for the soil. They also found the presence of micro-meter ordered As-bearing sulfide from Holocene aquifer. Lowers *et al.* (2007) also proposed that authigenic framboidal and massive pyrite (median values 1500 and 3200 mg/kg As, respectively), is the principal host phase of As in sediments collected from Rajoir and Srirampur districts.

Part II: Basic reactions of As in near surface environment
: Laboratory experiment and modeling studies

In this part, basic chemical reactions controlling mobility of As in natural aquifer are introduced based on the recently published laboratory based studies. Despite the wealth of recent studies, there remain considerable gaps between fundamental aspects of As chemistry and behavior of As in natural system. I classified numerous studies into three groups. First group investigates the molecular structure of As in solution, solid phase, and solid-solution interface. These studies mainly apply the spectroscopic methods, particularly infrared, X-ray absorption, and X-ray photoelectron spectroscopy to investigate the molecular structure. Another main approach is quantum calculation.

Although this type of study is very important to determine the chemical reaction occurring in nature, I do not focus this approach in this thesis, and some fundamental structural information is included in the next section. Second group investigates the solid-water interactions, such as precipitation-dissolution, adsorption-desorption, and coprecipitation in simple system. Simple batch experiments are most common approach. Development of surface complexation modeling is also classified into this group. Adsorption experiments and possible effect on ionic competition are particularly focused. Although there are other important reactions, i.e., surface precipitation and coprecipitation, I do not mention in this thesis. The third group is conducted under most complex system. The studies using contaminated sediment are classified into this group, e.g., incubation experiment and adsorption experiment. Before highlight the new experimental result, basic chemistry of As in low temperature environment is introduced in next section.

8. Fundamental aspects of geochemical behavior of As in near surface environment

8.1 Aqueous chemistry

Speciation of dissolved As is important to determine the extent of reaction with the solid phase, and hence the mobility of As in groundwater. Because of the high ionic potential of As(III) and As(V), these are dissolved as various oxyanions. Under oxidizing conditions, H_2AsO_4 is dominant at low pH (less than about pH 6.9), whereas at higher pH, $HAsO_4^{2-}$ becomes dominant. Under reducing conditions at pH less than about pH 9.2, the uncharged arsenite species $H_3AsO_3^0$ will predominate (Fig. 1–5). Although inorganic As is likely dominant in most groundwater, some organic As, such as dimethylarsenic acid (DMAA; $(CH_3)_2AsO(OH)$) and monometylarsonic acid (MMAA; $CH_3AsO(OH)_2$) can form after catalyzed by microbial activities (Smedley and Kinniburgh, 2002; O'Day et al., 2006).

The molecular structure of aqueous As has been investigated by vibration spectroscopy (e.g., Myneni *et al.*, 1998) and quantum calculation (e.g., Tossel, 1997). The tetrahedral structure of arsenate is similar to the phosphate. The first coordination

sphere is composed of 4 oxygen atoms forming a pyramid, and the symmetry of the molecule is affected by the protonation, hydration, and metal complexation (Fig. 1–6). Structure of aquo-complex of arsenite is rather asymmetric. The first coordination sphere of arsenite is composed of 3 oxygen atoms forming a pyramid (Fig. 1–6).

Complexation of arsenate and arsenite with various metals are generally limited in surface and groundwater. Only some water having high salinity, however, metal-arsenate (or arsenite) complex can be important. Marini and Accornero (2007) re-investigated standard thermodynamic properties of arsenate and arsenite using revised Helgeson-Kirkham-Flowers (HKF) equations, and evaluated stability constants with various metals. Using the data, they calculated speciation of As in seawater. Main species of dissolved arsenate is the $NaAsO_4^{2-}$ (55% of total dissolved arsenate) aqueous complex followed by $HAsO_4^{2-}$ (14%), $MgAsO_4^-$ (14%), $MgHAsO_4^0$ (9%), with minor contributions of $NaHAsO_4^-$, $CaAsO_4^-$, $CaHAsO_4^0$, and $KAsO_4^{2-}$.

Thioarsenic species are recently well investigated to clarify the behavior of As under sulfate reducing condition. There has been some debate about the identity of the aqueous As species in sulfidic solution. Previously, it has been believed that thioanions produced at saturation with As_2S_3 were best represented as trimers: $H_xAs^{III}{}_3S_6^{x-3}$ (x = 1–3), and monometric thioanions ($H_xAs^{III}S_3^{n-3}$, $H_xAs^{III}S_2^{n-3}$) would be more likely for solutions undersaturated with As_2S_3 (Heltz *et al.*, 1995). However, Heltz and Tossell (2008) recently argued that the chemistry of As in sulfidic waters is much more complex than those previously believed, and suggested that all earlier thermodynamic data on stabilities of As thioanions require revision. Following this situation, molecular structure is intensively studied by molecular quantum calculation (Tossell and Zimmermann, 2008) and XAFS (Beak *et al.* 2008).

Formation of As(III)-carbonate complex has been proposed by Kim *et al.* (2000) and Lee and Nriagu (2003). Kim *et al.* (2000) suggested that $(AsCO_3)^+$, $As(CO_3)_2^-$, and $As(OH)_2CO_3^-$ might be the most stable inorganic As species in the aquatic environment. They suggested the several facts as the evidence of As(III)-carbonate complex: (a) high concentrations of HCO_3^- (0.02 to 0.6 M) promote leaching of As from aquifer materials (this is also mentioned by Anawar *et al.*, 2004, using sediment collected from Bangladesh), (b) ion exchange chromatograms of solutions containing CO_2 saturated

arsenite show anomalous features compared to solutions containing only arsenite, (c) extrapolation of stability constants for lanthanide carbonate complexes vs. ionic radius suggests that carbonate complexes of As^{3+} would have large stability constants and (d) formation of extremely stable As(III)-carbonate complexes can explain As(III) leaching from sulfide minerals in anaerobic aquifers. Neuberger *et al.* (2005) evaluated the importance of this complexation reaction by measuring the solubility of As_2O_3 in concentrated (up to 0.72 M) bicarbonate solutions at near-neutral pH under 25 °C. They observed a small, but statistically significant solubility enhancement in $NaHCO_3$ containing solutions compared to NaCl solutions of essentially the same ionic strength. They concluded that As(III)-carbonate complexes can form under extremely carbonate rich condition, but is likely negligible at carbonate concentrations found in most natural waters.

There are some reports dealing with complexation of As with dissolved organic matter. Buschmann *et al.* (2006) reported distribution coefficient for As(III) and As(V) binding onto Suwannee River humic acid and Aldrich humic acid using dialysis analysis. They found that As(V) was more strongly bound than As(III) from pH 4.6 to 8.4. Maximum binding was observed around pH 7. As a result, they estimated that about 10% of total As(V) may be bound to dissolved organic matter (DOM) under environmentally relevant conditions, whereas >10% of As(III) is bound to DOM at only very low As/DOM ratios. Lin et al. (2004) examined the complexation of As(V) with humic substance by dialysis and ion exchange techniques. From 30% to 51% of added As(V) reacted with organic substance in water extract of compost to form an As-metal-organic complex. This was verified as a hydrophobic organic fraction after separation of As-metal-organic complex fraction from the hydrophilic fraction by XAD-8 resin. The separated material was also identified as humic substances by the method of proton binding formation function determination. They suggested that cations, such as Ca and Mg, and especially Fe, Al, and Mn act in cation bridging in the complexation of As(V) with humic substance. Formation of aquatic arsenate-Fe(III)-DOM is also confirmed by Ritter et al. (2006) using dialysis experiment for natural organic matters. They also pointed out that arsenate-Fe(III)-DOM associations are at least partially colloidal in nature.

8.2 Arsenic in minerals

There are more than 200 kinds of As mineral, including native As, sulfides, oxides, arsenates and arsenites. Most are ore minerals or their alteration products. Except for some sulfides, solubility product of these As minerals are generally very high. Tables 1–4 and 1–5 show the formation free energies and solubility product of major arsenate and arsenite minerals. This feature indicates that concentration of As in groundwater is not controlled by the solubility of As mineral.

Arsenic can be incorporated into various rock forming minerals as a minor component (Fig. 1–6). Because of chemical similarity of S to As, sulfides can incorporate As up to percent order. Concentrations in pyrite, chalcopyrite, galena and marcasite can be very variable, even within a given grain, but in some cases exceed 10 wt% (Smedley and Kinniburgh, 2002). Arsenic is present in the crystal structure of many sulfide minerals as a substitute for S (Foster, 2003). High As concentrations are also found in many oxide minerals and hydrous metal oxides, either as part of the mineral structure or as sorbed species. These type of As is most important in sedimentary environment like As-contaminated groundwater, and is described more detail in next section.

8.3 Solid-water interface

Arsenic concentrations observed in most groundwaters are orders of magnitude less than the solubilities of most As-bearing minerals. Hence, adsorption reactions between As and mineral surfaces are generally the most important factor controlling the dissolved As concentration. Adsorption of As is a complex function of the relationship between the properties of the solid surface, pH, As concentration, competing ions, and As speciation. Many studies that investigated the effects of different geochemical parameters on adsorption of As species used laboratory experiments to evaluate adsorption of As by pure mineral phases, e.g., Fe, Al, and Mn (hydr)oxides, and clay minerals. The distribution coefficient (K_d) of As and these solid phases at circum-neutral pH are listed in an excellent review paper by Smedley and Kinniburgh (2002). This indicates that amorphous Fe hydroxides (often named hydrous ferric oxide: HFO) have

the highest K_d for both arsenate and arsenite. Manganese oxides, Al oxides, and clay minerals can also adsorb significant amount of As, but the role of these phases are not primarily important (Smedley and Kinniburgh, 2002; Table 1–6). Manganese oxides are important as not only adsorbent, but also as the strong oxidant of arsenite. Rapid oxidation of arsenite on the surface of manganese oxides has been reported (Chiu *et al.*, 2000; Manning *et al.*, 2002; Tournassat *et al.*, 2002; Mitsunobu *et al.*, 2006).

Structures of surface complex of arsenate and arsenite have been investigated using various spectroscopic techniques. For HFO and several Fe oxyhydroxides, both arsenate and arsenite form inner sphere complex, probably dominantly bidentate, binuclear surface complex (Farquhar et al., 2002; Foster, 2003; Sherman and Randall, 2003; Ona-Nguema *et al.*, 2005; Zhang *et al.*, 2005). The ratios of outer sphere/inner sphere complexes depend on the solution composition. Generally, contribution of outer sphere complex is significant for arsenite, particularly at low concentration of As (Sverjensky and Fukushi, 2006). Arsenate tends to form inner sphere complex for HFO. Similar to HFO, both XAFS and surface complexation modeling proved that arsenite can form outer sphere and inner sphere complex on the surface of hydrous aluminum oxides (AlO) depending on the solution composition, whereas arsenate forms inner sphere complex (Arai *et al.*, 2001; Fukushi and Sverjensky, 2007).

Because of highest affinity of HFO for both arsenite and arsenate, adsorption behavior of these species was intensively studied under various conditions (Piers and Moore, 1982; Wilkie and Hering, 1996; Raven *et al.*, 1998; Jain *et al.*, 1999; Dixit and Hering, 2003). The relative affinity of arsenate and arsenite to Fe oxyhydroxides is dependent on the pH, crystalliny, and total As in system. Generally, As(V) sorption is more favorable than As(III) at lower pH values, but the opposite is true at higher pH values (Dixit and Hering, 2003). Despite higher mobility of arsenite in natural environment, this is not always supported by the adsorption experiment (Manning *et al.*, 1998; Dixit and Hering, 2003; Harbel *et al.*, 2006). Higher mobility of arsenite than arsenate in natural environment is often explained as the result of difference of adsorption structure: arsenite forms a larger fraction of outer-sphere complex including hydrogen bonding, which is weaker adsorption mode than inner-sphere complexation (Sun and Doner, 1996; Sverjensky and Fukushi, 2006).

9. *Experimental studies on adsorption and competition*

9.1 Adsorption experiment

Various laboratory experiments conducted before 2000s have evidenced that Fe oxyhydroxide is the most important solid controlling adsorption behavior of As in soil and aquifer systems. This general understanding has not changed despite various laboratory studies being conducted after 2000 (Table 1−6). One important recent trend is to investigate the adsorption behavior of As to secondly minerals which are only stable under reducing condition, because HFO is not stable under reducing condition. According to the Eh-pH diagram of Fe, various secondly minerals can form depending on the Eh (Fig. 1−7). As noted, siderite is often supersaturated in the As-contaminated groundwater in Bengal Basin (Chapter 1 section 5). Some researchers pointed out the importance of authigenic magnetite in contaminated aquifer (Horneman *et al.*, 2004; Seddique *et al.*, 2008). Green rusts (GR) are a group of Fe(II, III) hydroxyl compounds characterized by a layered structure, and highly reactive mineral phase found in moderately reducing condition. Jöhnson and Sherman (2008) investigated the adsorption mechanism of arsenate and arsenite to carbonate GR (fougerite), magnetite, and siderite by batch adsorption experiment coupled with XAFS. They found that arsenate sorbs to fougerite, magnetite, and siderite by forming inner-sphere surface complexes resulting from corner sharing between AsO_4 groups and FeO_6 octahedra without reduction of arsenate. Arsenite also forms inner-sphere surface complexes on magnetite and fougerite but only a (presumably) weak outer-sphere complex on siderite. Arsenate desorbs from magnetite, fougerite and siderite at pH>8, however, arsenite sorption to all three phases is enhanced with increasing pH. They argued that reduction of iron oxides followed by precipitation of fougerite, magnetite or siderite will released dissolved arsenate at pH>8. However, if arsenate is also reduced to arsenite, sorption of As will be enhanced.

Whereas adsorption onto HFO and various secondly Fe minerals are the most important reactions under oxic condition, adsorption onto sulfide becomes important under strongly reducing condition. Adsorption of arsenite onto sphalerite, galena, troilite,

and pyrite were investigated by batch adsorption experiments coupled with X-ray absorption fine structure (Bostick *et al.*, 2003; Bostick and Fendorf, 2003). For all sulfides, amount of adsorbed As tends to increase with increasing pH. This is opposite trend to the typical adsorption envelope of As to Fe oxyhydroxides. They concluded that adsorption of arsenite is controlled by formation of polymerized complex, e.g., $As_3S_3(SH)_3$, and surface precipitate rather than ligand exchange with OH^- or SH^- based on the XAFS results. According to this report, adsorption of arsenite onto sulfide is not a reversible reaction, and cannot be controlled by adsorption-desorption equilibrium.

Calcite is ubiquitous mineral in aquifer system. Many As-contaminated groundwaters in Bengal Basin are equilibrated or oversaturated with calcite (Ahmed *et al.*, 2004; McArthur *et al.*, 2004; Itai *et al.*, 2008b). Some previous studies suggest that calcite could be important in controlling the aqueous concentrations of As, especially at higher pH (Stollenwerk *et al.*, 2003 and reference therein). The reaction between arsenite and calcite is particularly important because calcite can be stable under reducing condition where Fe oxyhydroxides are unstable. There are two completely different idea about this reaction. Cheng *et al.* (1999) allowed a solution of As(III) to react with calcite. Using data from X-ray standing wave diffraction, they concluded that As(III) was removed from solution and occupied the carbonate sites on the calcite surface. Róman-Ross *et al.* (2006) examined the arsenite sorption on calcite by conventional batch experiment. They also confirmed that arsenite can adsorb on or co-precipitate with calcite. Contrastingly, Sø *et al.* (2008) found that arsenate can adsorb on the surface of calcite, whereas adsorption of arsenite is almost negligible from pH7.5 to 8.1. This argument is consistent with Yokoyama *et al.* (in prep) who performed coprecipitation experiment of arsenate and arsenite to calcite coupled with XAFS.

9.2 Ionic competition

Many inorganic and organic aqueous species have influences on As adsorption. The following researches deal with those elements that are commonly found in groundwater. Solutes can directly compete with As for available surface binding sites and can indirectly influence adsorption by alteration of the electrostatic charge at the solid surface. Both processes are influenced by pH, solute concentration, and the

intrinsic binding affinity of the solid. Effect of competition is generally evaluated by batch experiment under dual or multiple ion system. Additionally, various surface complexation models are also important to describe the mechanism of competition.

Because of the chemical similarity, phosphate is the most important competitor for adsorption of arsenate and arsenite to various solid phases in solid-water system. Jain and Loeppert (2000) show the influence of phosphate on adsorption of arsenate and arsenite to ferrihydrite as a function of pH. The P/As ratios (1:1 and 10:1) used in these experiments are within the range reported for many groundwaters. Adsorption of both arsenate and arsenite decreased with increasing phosphate concentration. For arsenate, the decrease was significant over the entire pH range, and the greatest effect on arsenite adsorption observed at lower pH values. For arsenite, adsorption of arsenite decreased by only a few percent at pH 9, even at the highest phosphate concentration, suggesting that the neutral $H_3AsO_3^0$ was better to compete for surface complexation sites with HPO_4^{2-} at higher pH.

Silicic acid ($H_4SiO_4^0$) has also been shown to effectively compete with As for adsorption sites. Meng *et al.* (2000) evaluated the effect of Si for arsenite and arsenate adsorption to ferrihydrite. Adsorption of arsenite (300 μg/L) and arsenate (500 μg/L) at pH 6.8 start to decrease in the presence of 1 mg/L of Si, and adsorption decreased by 70% for As(V) and 80% for As(III) at 10 mg/L of Si. Swedlund and Webster (1999) suggested that the decrease in As adsorption at high Si concentration is attributed to the combination of competition for surface sites and polymerization of Si resulting in an increase in negative surface charge.

Competition by carbonate recently collected attention because some reports suggested the possible enhancement of mobility of As under the carbonate rich solution (e.g., Appelo *et al.*, 2002; Anawar *et al.*, 2003). Radu *et al.* (2005) evaluated the competition of carbonate for arsenate and arsenite adsorption to ferrihydrite using by column experiment. They found that increasing carbonate concentrations had relatively little effect on arsenate adsorption to the iron oxide coated sand surface at pH 7. The adsorption of arsenate decreased only marginally when the $CO_2(g)$ partial pressure increased from $10^{-3.5}$ to $10^{-1.8}$ atm, despite a 50-fold increase in total dissolved carbonate (0.072 to 3.58 mM). Increasing the $CO_2(g)$ partial pressure to $10^{-1.0}$ atm resulted in only

a slight decrease in arsenate adsorption, despite a >300-fold increase in total dissolved carbonate (to 22.7 mM). Minor competition effect by carbonate is also found for the arsenite to ferrihydrite. They concluded that when compared to phosphate, carbonate mobilized adsorbed arsenate to a lesser degree than phosphate, even when present in much higher concentrations than phosphate.

Competition with dissolved organic matter has also been investigated. Simeoni *et al.*(2003) conducted adsorption experiment of arsenate to ferrihydrite and gibbsite in the presence of fulvic acid at pH 4, 6 and 8. Arsenate adsorption on both gibbsite and ferrihydrite decreases with increasing concentrations of fulvic acid. The effect was highest at pH 4, and decreased at pH 6 and 8. Bauer *et al.* (2006) evaluated effect and mechanism of competition by DOM for adsorption of As to goethite, natural soils, and sediments using batch experiment. In goethite suspensions with pre-sorbed As, dissolved concentrations increased up to 6 times in the presence of 25 mg/L DOM compared to samples without DOM. They suggested that the primary mechanism for the As release from solid phases is competition between As and organic anions for sorption sites, whereas redox reaction promoting by the presence of DOM were probably of minor importance.

Finally, a modeling study conducted by Stachowicz *et al.* (2008) is introduced. They employed charge distribution (CD) model for the adsorption of arsenite and arsenate in the presence of Ca^{2+}, Mg^{2+}, PO_4^{3-}, and CO_3^{2-}. Although this study does not consider the silicic acid, the following summary is almost consistent with the laboratory experiments shown above.

(i) Both Ca^{2+} and Mg^{2+} ions promote the adsorption of PO_4^{3-}. This promotion is of an electrostatic nature. Since AsO_4^{3-} is chemically comparable with PO_4^{3-} and has a very similar interfacial charge distribution, the same type of electrostatic effect is expected for the interaction of Ca^{2+} and Mg^{2+} with AsO_4^{3-}. In natural systems, such interactions should be taken into account.

(ii) The presence of Ca^{2+} ions has a minor effect on the As(III) adsorption in Ca-As(III) systems, only occurring at very high pH. In the pH range, relevant for natural groundwater (pH 6 to 9), no significant effect is observed. For Mg^{2+} ions, no significant effect on the arsenite binding is found over a very large pH

range.

(iii) Adsorbed phosphate ions have a strong ability of competition with both $As(OH)_3^0$ and AsO_4^{3-} and therefore PO_4^{3-} is of critical importance in groundwater systems. Interaction between PO_4^{3-} and AsO_4^{3-} is stronger than the interaction of PO_4^{3-} and $As(OH)_3$. The difference is related to the amount of charge that is introduced by the adsorbed As(III) and As(V) ions in the electrostatic 1-plane. The sensitivity of As(III) oxyanion for changes in the phosphate concentrations is smaller than the sensitivity of As(V) oxyanion for phosphate at pH 7. Therefore, the release of As from a sediment due to biogeochemical reduction of As(V) to As(III) will depend on the phosphate level.

(iv) In 3-component experiments with $As(OH)_3$, PO_4^{3-}, and divalent cations, the arsenite concentration is dominantly regulated by phosphate. The phosphate concentration is regulated by arsenite with influences of Ca^{2+} and Mg^{2+}. The Ca^{2+} and Mg^{2+} concentrations are mainly regulated by the adsorption of the PO_4^{3-} ions.

(v) Bicarbonate is a very weak competitor in a 3-component goethite system with AsO_4^{3-}-PO_4^{3-}-HCO_3^-. Therefore, the presence of carbonate ions is not relevant for the competitive release of As from iron oxides under natural groundwater conditions.

10 Laboratory studies in complex reaction systems

10.1. Incubation experiment using contaminated sediment

Because the important roles of microbial activity for redox reaction of As have been demonstrated (e.g., Jones *et al.*, 2000; Zobrist *et al.*, 2000; Stolz and Oremland, 1999; Oremland and Stolz, 2003, 2005), incubation experiment, which aims to clarify the role of biotic reaction for As mobilization, have been conducted by various groups (Table 1–7). Islam *et al.* (2004) used sandy sediment collected from As-affected region in West Bengal. They prepared four types of batches: (a) aerobically; (b) anaerobically; (c), anaerobically with 4 g/L sodium acetate as a proxy for organic matter, (d) 'abiotic' control sediments autoclaved before incubation with added acetate. They reported that

high level of As dissolution occurred only batches (b) and (c). Particularly, maximum aqueous As concentration (ca. 110 μg/L) was observed in the batch (c). This report confirmed that microbial mediation can enhance the mobility of As under anaerobic condition. Interestingly, they also reported that As does not mobilize at the same time of mobilization of Fe^{2+}, and which starts to mobilize several days after the Fe^{2+} release.

Van Geen *et al.* (2004) conducted incubation experiment for several sediment having different features in terms of lithology, color (as redox indicator), and collected depth. They reported that 30 ~ 80% of hot HCl extractable As was mobilized under the acetate added batch, whereas release of As was not significant or almost negligible under the antibiotic batch containing Guillard reagent, suggesting the impact of microbial mediation in As desorption. Radloff *et al.* (2007) used sediment collected from same site to the van Geen's study. They employed needle sampler and carefully preserved sample to maintain the anaerobic condition followed by the 11 month incubation. This study also supports the importance of microbial mediation to form reducing condition.

Akai *et al.* (2004) used glucose, polypepton, and N rich urea and fertilizer to test the availability of various nutrients for bacterium. Arsenic was released with decreasing Eh as well as other incubation studies, and only glucose and polypepton were effective to decrease Eh and mobilization of As.

Polizzotto *et al.* (2006) proposed different conclusion from the researches shown above. They used a sandy sediment collected from the depth where maximum dissolved As was observed. They reported that more than 10% of As in sediment is leached from both sterilized and non-sterilized samples. They found that Fe oxyhydroxides are not contained in the sediment based on the XAFS results. They consequently concluded that aqueous As concentration in aquifer is not controlled by the amount of Fe oxyhydroxides.

10.2. Adsorption experiment using contaminated sediment

Adsorption-desorption reaction may be the most important reaction to control large variation of aqueous As in contaminated aquifer due to rapid kinetics relative to

precipitation-dissolution and oxidation-reduction reactions. Some researchers focused on the apparent partitioning ratio of As between sediment and water. There are roughly two approaches: (i) batch adsorption experiment to determine the apparent distribution coefficient, and (ii) comparison of labile As in both sediment and water phases based on the analysis of natural samples. Although both approaches are important, laboratory experiments are highlighted in this section.

Itai *et al.* (in revision, Chapter 4 in this thesis) determined the apparent distribution coefficient of arsenate and arsenite at pH 7.3 using sediments collected from various depths in aquifer hosted by Holocene sediments. The range of K_d were 7 to 84 L/kg for arsenite and 15 to 560 L/kg for arsenate. They also suggested that the controlling factor of apparent K_d is amount of Fe oxyhydroxide and surface area based on the correlation between K_d and redox state of Fe in sediment. The profile of simulated concentration of aqueous As in aquifer was consistent with the actual profile with the assumption of adsorption equilibrium. They proposed that aqueous As concentration is controlled by adsorption-desorption equilibrium.

Stollenwerk *et al.* (2007) conducted adsorption experiment to the oxic sediment collected from Pleistrocene aquifer. They intended to assess the ability of attenuation of aqueous As level when contaminated groundwater flow into the Pleistocene aquifer. According to the adsorption isotherm, the apparent K_d at concentration of aqueous arsenite being 600 μg/L was ca. 10 L/kg. This value is not higher than the apparent K_d value for Holocene aquifer determined by Itai *et al.* (in revision). Hence, capacity of adsorption of arsenite to Pleistocene sediment is not necessary high. The apparent K_d of arsenate was, contrastively, ca. 100 L/kg when aqueous arsenate is 600 μg/L. This result indicates that the reason of low As concentration in Pleistocene aquifer is not attributed to the high adsorption capacity of oxic sediment. Oxidation state of As can be a more important factor.

10.3. Relative importance of Fe and As reduction

The field observation and laboratory studies shown above indicated that one important question to answer the factor controlling mobility of As is relative importance of Fe and As reduction for As mobilization. The research group of Stanford University

have performed a series of column experiment to emphasize the relative importance of these reductive reactions and role of specific bacteria.

Harbel *et al.* (2006) compared relative mobility of arsenite and arsenate through the column filled by synthetic ferrihydrite coated sand. They used active cultures of the Fe(III) and As(V) respiring bacterium *Sulfospirillium barnesii* (an Fe and As respiring organism), As(V) respiring *Bacillus benzoevorans* (an organism capable of As(V) but incapable of dissimilatory Fe(III) reduction) to compare the relative importance of As and Fe reduction. They found that although reductive dissolution of ferrihydrite induces the mobilization of As due to reduction of available surface area, biotically generated Fe(II) appears to induce As sequestration within the ferrihydrite coated sand matrix. They also pointed out that arsenite is more easily mobilized than arsenate under dynamic flow condition despite greater amount of arsenite was adsorbed than arsenate at pH 7.4 in batch experiment. They concluded that the greatest threats to environmental quality within Fe-rich environments appears from either (1) having arsenite retained on Fe hydroxides under advective flow or (2) prevailing the moderately reducing conditions. Continued production of high Fe(II) levels within ferrihydrite dominated systems actually results in a suppression of As release to the aqueous phase. Kocar *et al.* (2006) combined the similar column experiment with XAFS to characterize the transformation of Fe in column. They also concluded that reduction of arsenate most importantly contributes to the mobilization of As. The mechanism of arsenite sequestration under high Fe(II) condition is still debating. Presently, Stanford group proposed that although reductive dissolution of Fe(III) phases such as goethite and hematite can lead to secondary precipitation of ferrous phases such as siderite or green rust, formation of these phases does not appear to retain appreciable quantities of As. Arsenic retention is rather dependent on recrystallization of ferrihydrite to goethite and, particularly, magnetite (Tufano and Fendorf, 2008; Tufano *et al.* 2008).

Pedersen *et al.* (2006) investigated the behavior of trace amounts of arsenate coprecipitated with ferrihydrite, lepidocrocite and goethite during reductive dissolution and phase transformation of the iron oxides using [^{55}Fe]- and [^{73}As]-labelled iron oxides. For ferrihydrite and lepidocrocite, all the arsenate remained associated with the surface, whereas for goethite only 30% of the arsenate was desorbable. During reductive

dissolution of the iron oxides, arsenate was released incongruently with Fe^{2+} for all the iron oxides. For ferrihydrite and goethite, the arsenate remained adsorbed to the surface and was not released until the surface area became too small to adsorb all the arsenate. In contrast, arsenate preferentially desorbs from the surface of lepidocrocite. Their findings suggested that during Fe^{2+} catalyzed transformation of ferrihydrite and lepidocrocite, arsenate became bound more strongly to the product phases.

Burnol *et al.* (2007) conducted the incubation experiments using synthesized 2-line ferrihydrite, with which arsenate was preliminarily coprecipitated, in the presence of phosphate-rich growth medium and a community of Fe(III)-reducing bacteria under strict anoxic conditions for two months. Their conclusions are (1) As(V) is not reduced during the first incubation month with high Eh values, but rather re-adsorbed onto the ferrihydrite surface, and this state remains until arsenic reduction is energetically more favorable than iron reduction, and (2) the release of As during the second month is due to its reduction to the more weakly adsorbed As(III) which cannot compete against carbonate ions for sorption onto ferrihydrite.

To assess the relative importance of Fe and As reduction is important to understand the scattered relationship of aqueous Fe and As in As-contaminated groundwater (Chapter 2 of this thesis).

Part III : Previous hypotheses about the cause of As-contamination

11. Biogeochemical trigger for As mobilization

Two major hypotheses have been proposed as the biogeochemical trigger of global As-contamination: pyrite oxidation hypothesis and Fe oxyhydroxides reduction hypothesis. Although latter hypothesis is broadly agreed as the main mechanism of As mobilization, other hypotheses are also reviewed to discuss the mechanism from various points of views.

11.1. Pyrite oxidation hypothesis

The pyrite oxidation was a firstly proposed hypothesis as the mechanism of

As-contamination by West Bengal scientists (Chatterjee *et al.*, 1995; Das *et al.*, 1996; Mallick and Rajagopal, 1996; Mandal *et al.*, 1996; Chowdhury *et al.*, 1999). They proposed that arsenopyrite, or As-rich pyrite, was initially present in the sediments and has been at least partially oxidized as a result of the recent seasonal lowering of the water table. This lowering has been attributed to the use of groundwater for irrigation. This hypothesis therefore supports the notion that the release of As to the groundwater is a recent phenomenon induced by human activities. Because of the vulnerability of sulfides, which are certainly present in at least some part of contaminated aquifer under oxic condition, the pyrite oxidation is possible in principle. However, the following evidences are strongly against such a hypothesis.

(i) Although presence of pyrite is confirmed at least some of the sediments, the amounts are usually small and difficult to be observed.

(ii) Oxidation of pyrite releases large amounts of sulfate. However, sulfate concentration reported from various contaminated regions are consistently low, often <1 mg/L.

(iii) Sulfide oxidation involves release of proton and induces the decrease of pH. However, highly contaminated groundwater generally shows circum neutral or slightly alkaline pH.

(iv) The pyrite oxidation hypothesis would predict that As concentrations would be greatest in the shallowest groundwaters close to the water table since this is where the influence of oxidation would be greatest. However, as noted in Chapter 4, high-As groundwater is generally observed significantly lower depth from surface.

Pyrite oxidation hypothesis is consequently not believed as the major mechanism of As contamination. However, chemistry of sulfide in aquifer is being addressed due to the possibility of As fixation coupled with sulfide formation under reducing condition (O'Day e*t al.*, 2004b; Polizzotto *et al.*, 2005; Lowers *et al.*, 2007).

11.2. Iron oxyhydroxide reduction hypothesis

The Fe oxyhydroxide reduction hypothesis, As released with the microbial

reductive dissolution of Fe oxyhydroxides, is now widely accepted as the principal mechanism of As mobilization in the groundwaters of the alluvial aquifers of the GBM Delta. (Bhattacharya et al., 1997; Nickson et al., 1998, 2000; Ravenscroft et al., 2001; McArthur et al., 2001; Dowling et al., 2002; Harvey et al., 2002, and Anawar et al., 2003). This hypothesis is supported by an observed elevated concentration of Fe in As-contaminated groundwater, and enrichment of As in Fe oxyhydroxide fractions in sediments (Nickson et al., 2000; BGS and DPHE 2001; Swartz et al., 2004).

Despite a common title, the hypothesis has many variations and various researchers have interpreted it in significantly different ways. One important and controversial point is the timing of As release during various reductive reactions. Generally, dissolved As and Fe are poorly correlated. If As is released coupled with the reductive dissolution of Fe, positive correlation is expected. Because of this complex situation, relative importance of reductive "desorption" of As and reductive "dissolution" of Fe oxyhydroxides are under debating. Although reducing condition is favorable for As mobilization, sulfate reduction can induce the sequestration of As with sulfide precipitates. Role of secondly formed Fe(II) minerals is also under debating.

Another controversial point is the source of redox driver. The Fe oxyhydroxides reduction hypothesis is based on the assumption that the contaminated aquifer was initially under an oxidizing condition and this was followed by a change to a reducing state. The source of the reducing agent necessary for changing the redox condition remains a matter of debate. To the best of my knowledge, there are four kinds of hypotheses about the source of organic matter: (i) surface origin hypothesis (Harvey et al., 2002), (ii) co-deposition hypothesis (Smedley and Kinniburgh, 2002; Meharg et al., 2006), (iii) peat origin hypothesis (McArthur et al., 2001, 2004; Ravenscroft et al., 2001), and (iv) petroleum origin hypothesis (Rowland et al., 2006; van Dongen et al., 2008). Discussion about the source of organic matter is further considered in Chapter 5.

11.3. Anion exchange hypothesis

Aside from the two major hypotheses, there are some other potential processes to induce As mobilization. Anion exchange is an important process affecting the adsorption-desorption equilibrium of As. Acharrya *et al.*, (1999) pointed out that

leaching of phosphate fertilizers as the primary source of high P groundwaters and indirectly to As-rich groundwaters through the competitive desorption of As from the sediments. This mechanism does not seem to be the primary cause of the global contamination, because there are As-rich groundwaters that are not P-rich (and *vice versa*). However, the effect of phosphate for mobility of As in aquifer should be considered.

Effect of carbonate species are also examined from various perspectives. Appelo *et al.* (2002) hypothesized that displacement of As by dissolved carbonate is an alternative mechanism for the natural occurrence of high As groundwater. They re-evaluated the surface complexation constant of CO_3^{2-} and Fe^{2+} on ferrihydrite in Dzombak and Morel's database. Using the updated constant, they concluded that sorption of carbonate at groundwater level significantly reduces the sorption capacity of As on ferrihydrite. Kim *et al.* (2000) have shown that HCO_3^- is effective in increasing the As concentration in dissolution experiments with pyrite containing rock, under both aerobic and anaerobic conditions. They suggested that formation of aqueous As-HCO_3 complexes solubilize As. Because carbonate species are ubiquitous in aquifer, the mobility of As is valuable to be tested.

12. Cause of patchy distribution of As-contaminated groundwater

The patchy spatial distribution of As-contaminated groundwater is a crucial feature of naturally occurring As-contamination. Many researchers have carefully considered the process of formation of this distribution. Both biogeochemical reaction and transport of As in aquifer need to be considered in order to understand the process of formation of patchy spatial variation. The hypotheses shown in the previous section are basically focused on the biogeochemical reactions under subsurface system, and the relation to local hydrology has been poorly understood. There are some interesting reports about the relationship between As distribution and local hydrology.

In earlier studies, age of groundwater has been estimated by measuring ^3H (Aggawal *et al.*, 2000; Zheng *et al.*, 2004). However, precise dating by ^3H analyses is recently difficult due to lowering of background concentration of ^3H. The first study applied $^3H/^3He$ dating to the As-contaminated groundwater is Klump *et al.* (2006) at

Munshiganji district. They reported that the age of groundwater increased from <5 to 70 years with the increase in the depth. Such dating is very important to constrain the timing of As release from aquifer materials. Stute *et al.* (2007) found that groundwater having longer residence time (determined by $^{3}H/^{3}He$) shows higher As concentration. They proposed two kinds of interpretations: variation of As concentration in groundwater is controlled by (i) the kinetics of As mobilization or (ii) the removal of As by groundwater flushing. If As has been released from certain solid in aquifer, amount of As in aquifer must decrease with time. van Geen *et al.* (2008) estimated the rate of decrease of As concentration in groundwater according to the analytical solution of the advection-dispersion transport model and suggested that local patterns of dissolved As in shallow groundwater could primarily reflect the different flushing histories of sand formations deposited in the region over the past several thousand years.

Some researchers focused on the relationship between As-rich water and physical property of subsurface sediment or soil (van Geen *et al.*, 2006b; Hoque *et al.*, 2008; Aziz *et al.*, 2008; Mitamura *et al.*, 2008; Nath *et al.*, 2008c; Pal *et al.*, 2009). Hoque *et al.* (2008) applied electromagnetic method to shallow subsurface sediment from a small area in the southeastern Bangladesh. They suggested that the variations in As concentration within the very shallow Holocene aquifers are constrained by the heterogeneity in near surface sediments that seems to control recharge and rate of aquifer flushing at shallow depths. They observed that low-As aquifers are located underneath the areas with relatively thinner top-silt layer or sandy surface materials with higher permeability and hydraulic conductivity at slightly elevated topography. Possibly, finer materials on the surface act as potential barriers to downward percolation and infiltration of oxygenated water from precipitation and runoff into the shallow aquifers and thus control groundwater As mobilization in the very shallow aquifers.

In order to clarify the controlling factor of patchy As distribution, both biogeochemical and hydrological factors should be considered in the same study area. I will mention about the factors controlling variation of As concentration in Chapter 4.

13. From the other Asian regions

Natural occurrence of As-contaminated groundwater is not limited in the Bengal

Basin, but also in other parts of Asian countries (Fig. 1–8). Vulnerable areas for arsenic contamination are typically young Quaternary deltaic and alluvial sediments comprising highly reducing aquifers (Charlet and Polya, 2006). The EAWAG (Swiss Federal Institute of Aquatic Science and Technology) research group has studied As-contamination in Red river delta and Mekong delta in Vietnam since 2001 (Berg *et al.*, 2001, 2006, and 2008), and Manchester group has conducted various field surveys in Cambodia since 2005 (Polya *et al.*, 2005; Rowland *et al.*, 2005, 2007, 2008). Berg *et al.* (2006) overviewed As pollution in the Mekong delta: As concentrations ranged from 1–1610 μg/L in Cambodia (average 217 μg/L) and 1–845 μg/L in southern Vietnam (average 39 μg/L), respectively. They also evaluated the situation in Red River delta: As concentrations in groundwater vary from 1–3050 μg/L (average 159 μg/L). The sediments of 12–40 m deep cores from the Red River delta contain arsenic levels of 2–33 mg/kg (average 7 mg/kg) and show a remarkable correlation with the concentration of Fe bound to sediments. The situations of Mekong and Red River delta are similar to the case in Bengal Basin in terms of geology and chemistry of As-affected aquifer. One difference is the short history of groundwater use, i.e., tube-well water is only used over the past 11 to 14 years in Mekong delta (Hug *et al.*, 2008).

Because of the less developed groundwater use, Mekong delta is the suitable site to discuss the mechanism of natural occurrence of As contaminated groundwater without considering the anthropogenic perturbation. A research group of Stanford University conducted hydrogeological study in Cambodia, and proposed that As is released from near-surface, river-derived sediments, and transported through the underlying aquifer (Polizzotto *et al.*, 2008). They also proposed that the As-contaminated groundwater is finally back to the river in a hundreds years timescale. Their finding can give great implication for the future prospect of As contamination. If the flux of As from river to surface wet land is identical to that from aquifer to river as they proposed, the As level in contaminated groundwater will not decrease for long time, at least for the next several tens years.

Serious As contamination is also reported from some inland regions. Arsenic problems have been recognized in groundwater used for potable supplies in a number of areas of mainland China over the last few decades. The first As problems were

identified during the 1980s in groundwater from deep boreholes in a rural area of Xinjiang Province in north-western China (Wang, 1984 cited by Smedley *et al.*, 2003). Smedley *et al.* (2003) conducted a geochemical study at Huhhot Basin, Inner Mongolia. The As-contaminated aquifer in Huhhot Basin show many similarities to other As affected aquifer in Asia. High As concentrations occur in anaerobic groundwaters from low-lying area and are associated with moderately high dissolved Fe as well as high Mn, NH_4^+, DOC, HCO_3^- and P concentrations. The observed range of total As concentrations in sediments is 3 – 29 mg/kg (n=12) and the concentrations correlate positively with total Fe. Up to 30% of the As is oxalate-extractable and taken to be associated largely with Fe oxides.

Inland type contamination is also reported from Nepal, although amount of published data is still poor. In lowland Nepal, known as Terai, where almost half (12 million) of the Nepalese population resides, the people have been using groundwater for all domestic purposes including drinking since 1990s (Shrestha *et al.*, 2003). It was reported that 29% of more than 20,000 tube wells had As concentrations exceeding the WHO standard. Approximately 0.5 million people in Terai were at risk of consuming water with the As concentration >50 μg/L.

Systematic prediction of As-affected regions is also attempted. Winkel *et al.* (2008) produced maps pinpointing areas at risk of groundwater arsenic concentrations exceeding 10 μg/L by combining geological and surface soil parameters in a logistic regression model, calibrated with 1756 aggregated and geo-referenced groundwater data points from the Bengal, Red River and Mekong deltas. They showed that Holocene deltaic and organic-rich surface sediments are key indicators for arsenic risk areas. Their predictions are in good agreement with the known spatial distribution of arsenic contamination, and further indicate elevated risks in Sumatra and Myanmar, where no groundwater studies exist.

14. The approaches of this study

In this Chapter, I have overviewed the geochemical characteristics of

As-contaminated groundwater in Bengal Basin coupled with the basic chemistry of As in subsurface environment. Based on the numerous studies, there are several common controversial issues. Following questions are the key to make clear the mechanism.

- What is the primary source of As? (Section 4)
- What factors are controlling the spatial distribution of As? (Section 5)
- Why is the bell-shaped depth profile common in Bangladesh? (Section 5)
- What is the reason of different trend of temporal variation of As in well water? (Section 5)
- Why are Pleistocene aquifers generally not contaminated by As? (Section 5, 6)
- What is the speciation of As in aquifer? Particularly for solid phase. (Section 7)
- Why is arsenite more mobile than arsenate in the aquifer? (Section 8)
- What amount of Fe oxyhydroxides is available in contaminated aquifer? (Section 12)
- What is the origin of organic matter? (Section 12)
- Why is natural occurrence of As contamination remarkable in Asia? (Section 13)

Although the problems shown above are associated each other, to focus the all issue is difficult. I decided to focus the speciation of As and Fe in aquifer in my PhD study, because this information is obviously lacking, and it should be important to interpret the factors controlling complex spatial variation of As rich groundwater. Continuous approach of my PhD study is summarized as follows.

This study started from the hydrogeochemical survey in the Sonargaon area, middle east Bangladesh to clarify the geochemical features of As-contaminated groundwater, and its relevance with aquifer structure. According to the geology of Bangladesh, we expected that both contaminated and uncontaminated aquifers exist in relatively shallow depth (~ 100 m). Hence, this site is suitable to discuss the specific geochemical condition where As tends to mobilize. I have conducted chemical and isotopic analyses for more than ca. 230 groundwaters. We collected groundwaters in both rainy and dry seasons to evaluate the seasonal change in water and isotopic compositions. Residence time of groundwater is roughly estimated by ^{3}H analyses.

Aquifer structure is clarified by geological survey summarized by Mitamura *et al.* (2008). Combining the aquifer structure and water chemistry, the geochemical and hydrological characteristics of the study area is revealed.

Parallel to the above approaches, I have tried to establish the speciation method of As and Fe in solid phase. As mentioned in this Chapter, speciation of As and Fe is critically important to discuss the water-rock interaction in aquifer. I attempted various XAFS method for the speciation. One succeeded approach, conversion electron yield XAFS (CEY-XAFS), is applied to the sediment form contaminated aquifer. The surface sensitivity of this method brought us a new insight about the speciation of Fe in aquifer. Detail methodology and applicability of this method is described in Chapter 3.

Following the hydrogeochemical characteristics of As-polluted region, I initiated the speciation study of As and Fe using the cored sediment collected from Sonargaon area. XAFS techniques were employed to determine the redox state of As and Fe with depth. Additionally, formation process of "bell-shape" vertical profile is discussed based on the XAFS results. Adsorption experiment and chemical extraction were also conducted to discuss the adsorption properties of As coupled with the characterization of redox states of Fe and As in sediment. This approach, which might be an orthodox way in chemical point of view but nobody has attempted, brought us important constraints to discuss the controlling factor of spatial distribution of As.

The datasets of this study coupled with the geological and mineralogical studies (Mitamura *et al.*, 2008; Seddique *et al.*, 2008) are sufficient to constrain the answer of questions shown above. In Chapter 5, I would like to discuss the controversial issues listed above including some implications for mitigation and future prospects for the problem of As-contaminated groundwater.

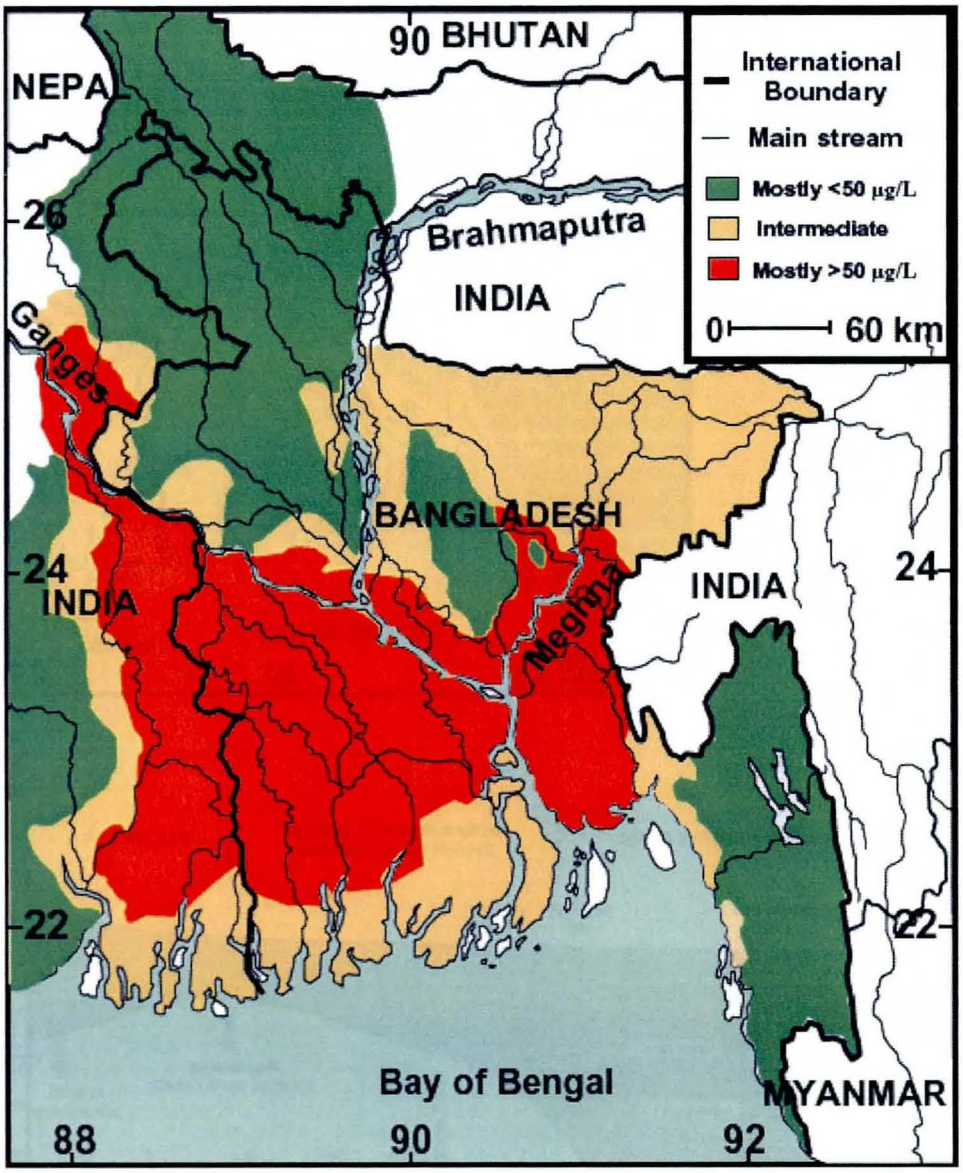

Fig. 1-1. Regional distribution of As contaminated groundwater in Bangladesh and West Bengal.

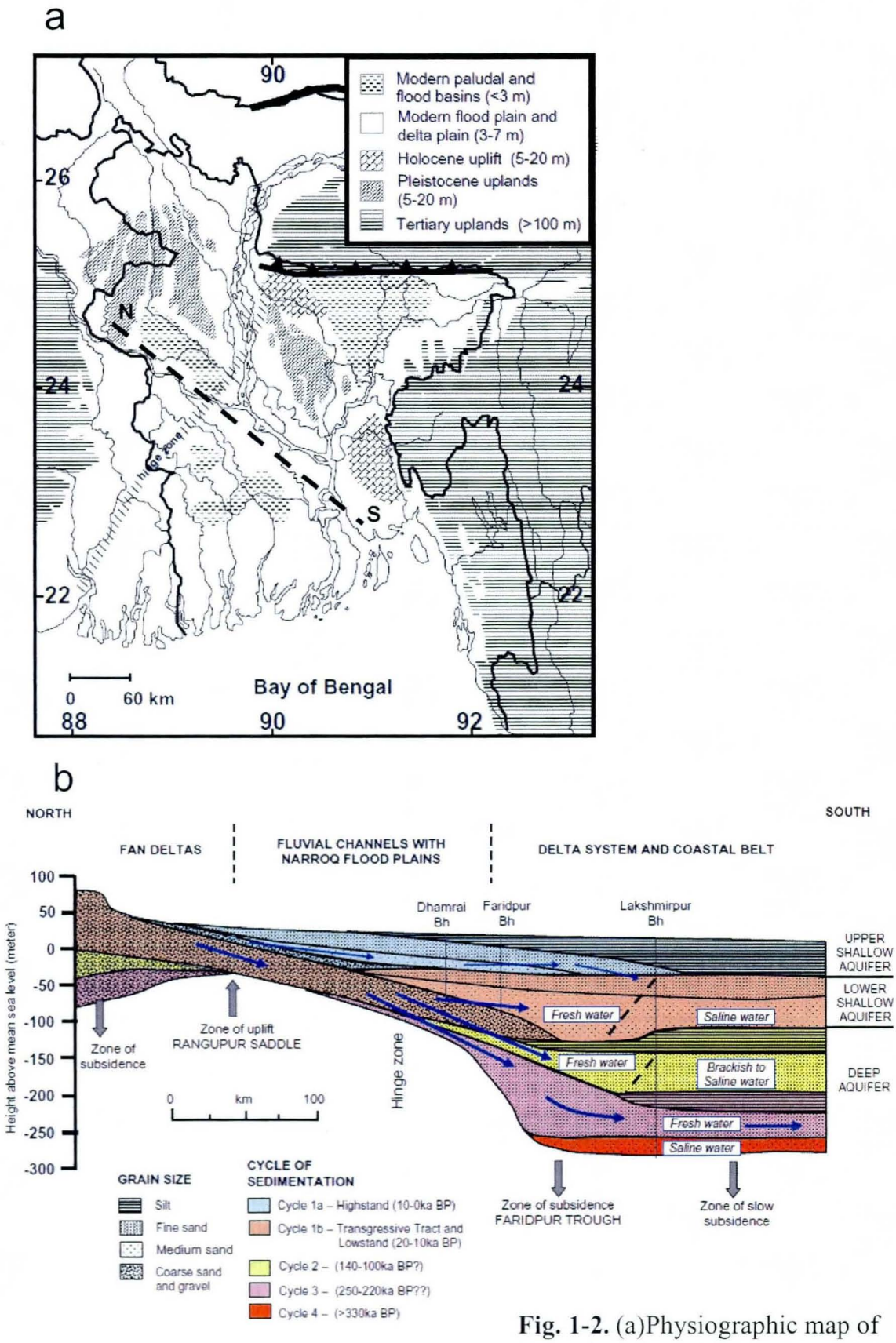

Fig. 1-2. (a)Physiographic map of Bengal Basin and (b) hydrogeological cross-section from north to south across Bangladesh.

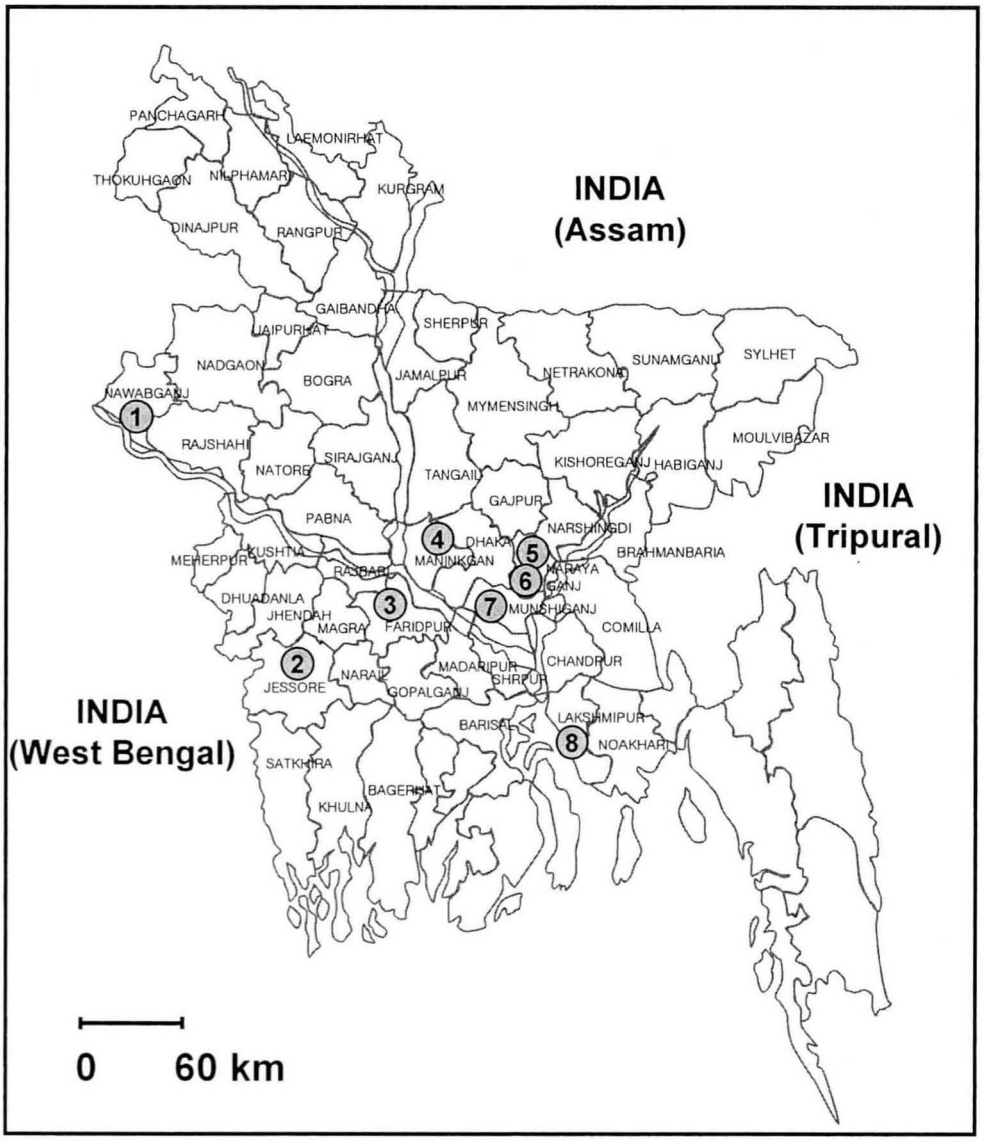

Fig. 1-3. District map of Bangladesh. Numbers indicated intensive study areas by this and previous surveys: 1. Nawabganj (BGS and DPHE 2001), 2. Samta, Jessore (AAN, 2001), 3. Faridpur, (BGS and DPHE, 2001), 4.Maninkganj (Stollenwerk, 2007) 5. Araihazar, Narayaganj (e.g., van Geen *et al.,* 2003) 6. Sonargaon, Narayaganj, (this study), 7. Munshiganj (e.g., Harvey *et al.,* 2002), 8. Laksmipur (BGS and DPHE, 2002)

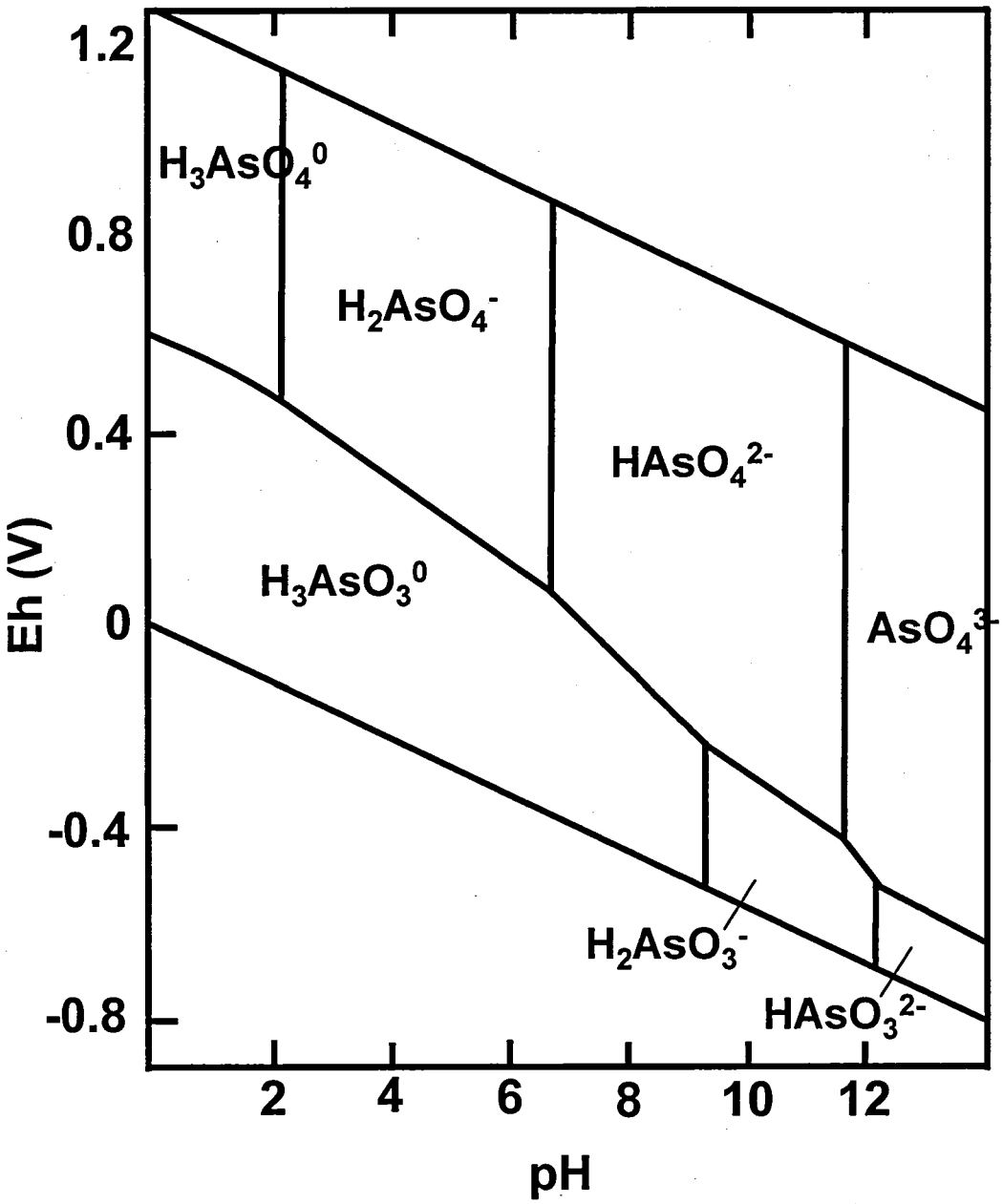

Fig. 1-4. The Eh-pH diagram of As under As-O_2-H_2O system, 25 degree, 1 atm. Activity of total As is 10^{-9} M.

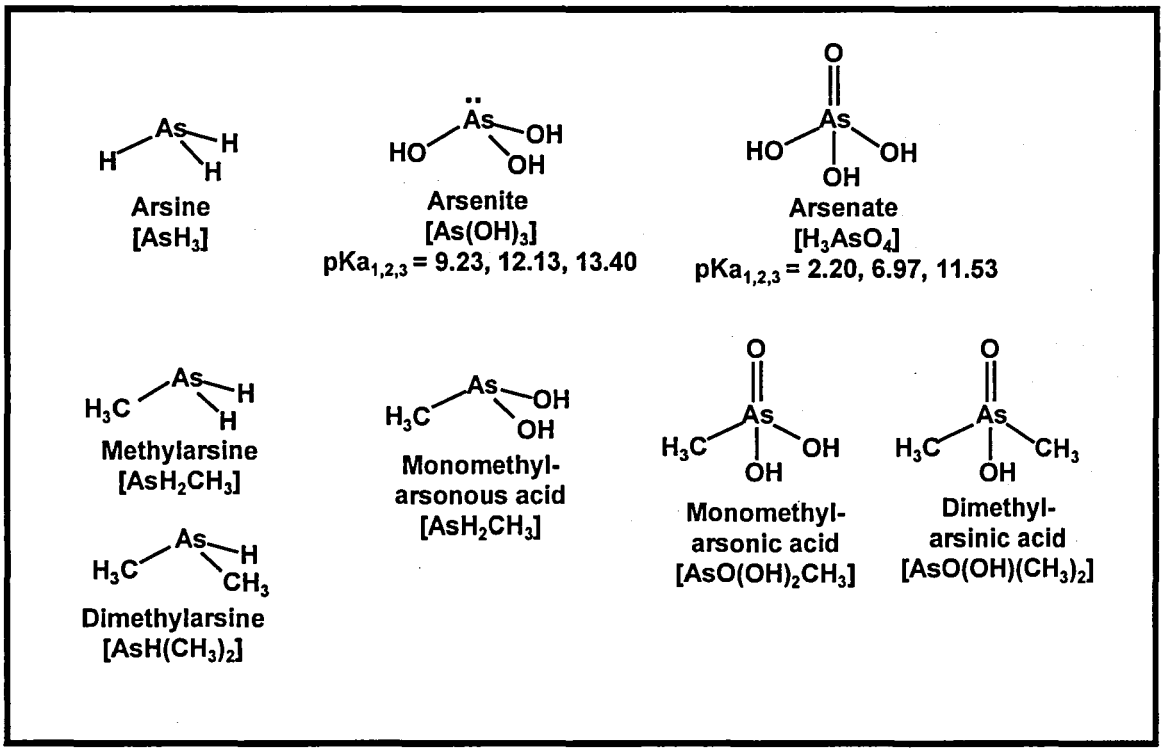

Fig. 1-5. Summary of important inorganic, organic arsenic in the environment. For inorganic aqueous species, stepwise acid dissociation constants are given.

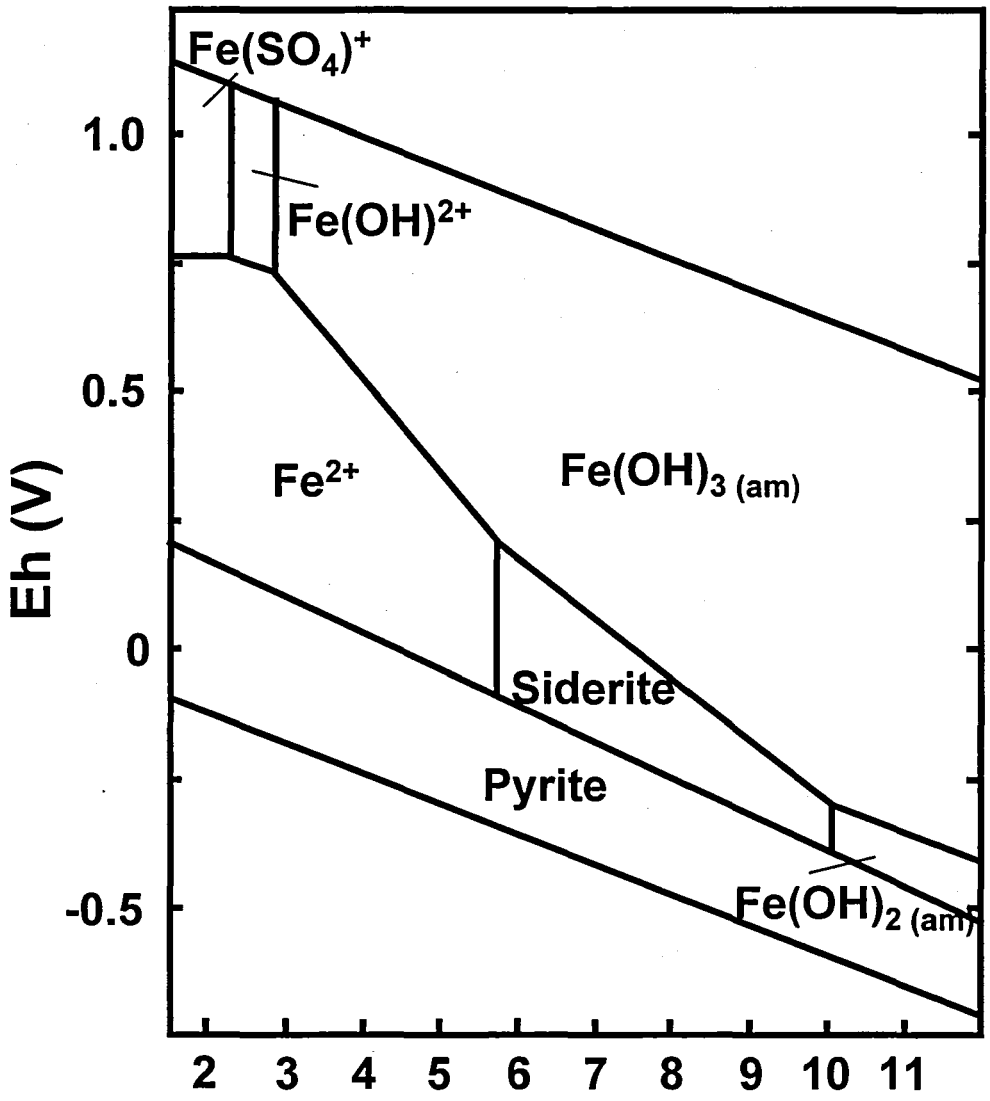

Fig. 1-6. The Eh-pH diagram of Fe under Fe-CO_2-S-O_2-H_2O system, 25 degree and 1 atm. Activity of total Fe, CO_2, and S are 10^{-6}, 10^{-3}, 10^{-4} M, respectively.

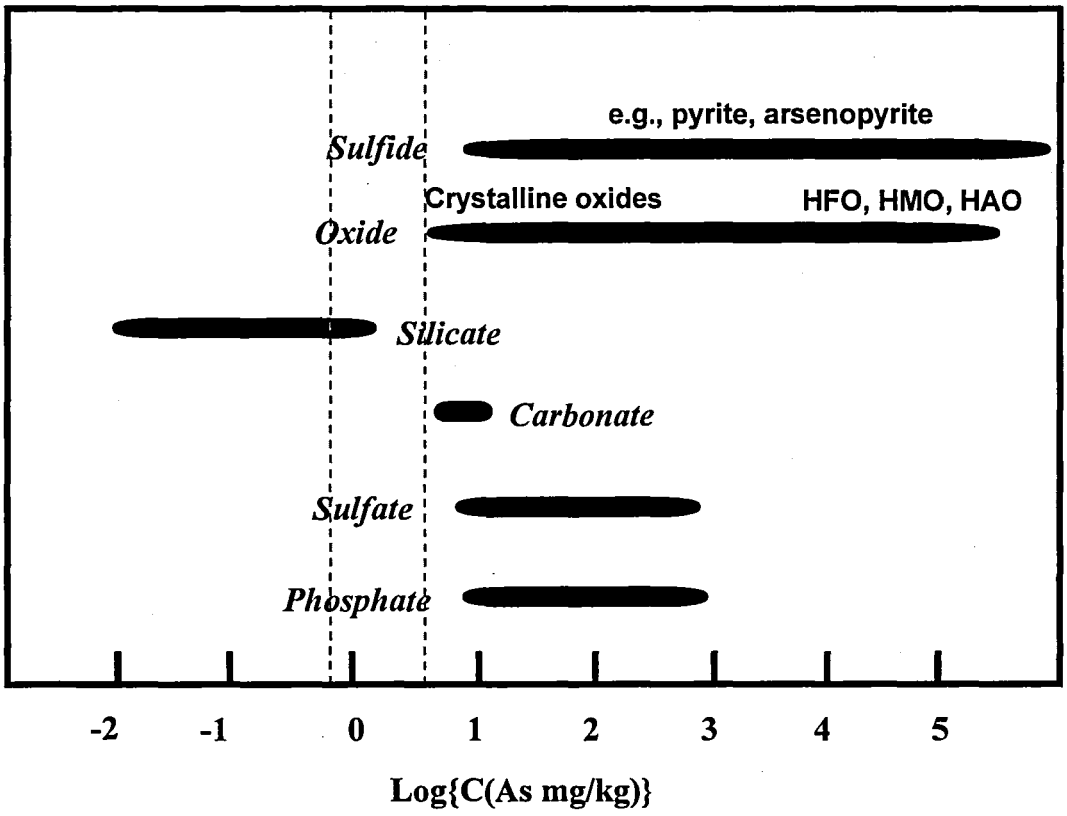

Fig. 1-7. The range of As concentration for various minerals according to the data given in Smedley and Kinniburgh (2002) Table 3. Dotted region is the range of background concentration of As in upper continental crust.

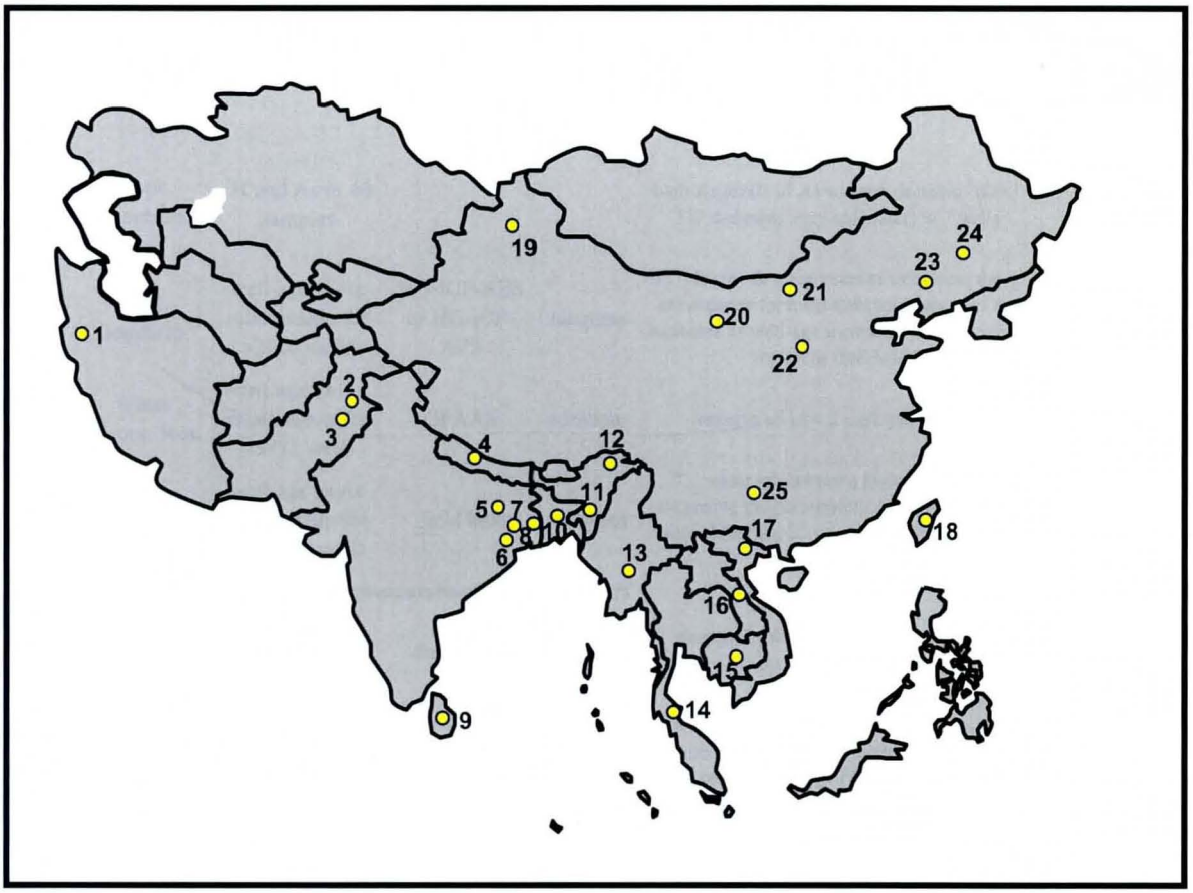

1 Kurdistan, IRAN
2 Jhelum, PAKISTAN
3 Fujrat, PAKISTAN
4 Terai, NEPAL
5 Uttar Pradesh, INDIA
6 Jharkhand, INDIA
7 Bihar, INDIA
8 West Bengal, INDIA
9 SRILANKA
10 BANGLADESH
11 Assam, INDIA
12 Assam, INDIA
13 MYANMAR
14 Ronphibun, THAILAND
15 CAMBODIA
16 LAO, PDR
17 Hanoi, VIETNAM
18 TAIWAN
19 Xinjiang, CHINA
20 Ningxia, CHINA
21 Inner Mongolia, CHINA
22 Shanxi, CHINA
23 Liaoning, CHINA
24 Jillin, CHINA
25 Gulzhou, CHINA

Fig. 1-8. The map of the distribution of As-contaminated groundwater in Asia.

Table 1-1. Summary of reported As monitoring data for Bangladesh, Inda, and Vietnam

reference	form of publication	type of data	analytical method	data quility	main conclusion	data shown?
indirect evidence over decades						
Aggawal et al. (2000)	report	^{3}H and As in 11 samples			Eight samples with significantly elevated As levels do not contain any detectable ^{3}H.	yes
BGS-DPHE (2001)	report	^{3}H and As in 31 samples			"The finding of very low tritium concentrations (<1 TU) at depth... while at the same time finding high concentrations of As (in 8 wells)... is a strong indication that the As release rodates the 1960s."	yes
Zheng et al. (2004) and Stute et al.(2007)	Appl. Geochem.	^{3}H and As in 40 samples			high As levels of As without dectable ^{3}H (<1 TU; indicates very old water) in 7 wells	yes
McArthurr et al. (2004)	Appl. Geochem.	well age vs As relationship for >2000 wells	HG-ICP-AES or HG-ICP-AFS	adequate	"..for the first ten years of existence, the exceedance for most threshold values of As increases as well-age increases, irrespective of region or threshold."	yes
van Geen et al. (2003)	Water Resour. Res.	well age vs As relationship for >5971 wells	GFAAS	adeauate	increase of 16 ± 2 µg/L per decade.	yes
Rosenboom (2004)	report	well age vs As relationship for ~300000 wells	field kits	adequate	"... older wells have a higher chnace of exceeding the permissible As level (75% for wells older than 25 years, against 65% for all wells)."	yes
Direct measurements over > 2years						
SOES-DCH cited by BGS-DPHE (2000)	report	unspecified	unspecified	unknown	"...deep wells that were once As-free are now As-contamianted."	no
Chakraborti et al. (2001)	conference volume	31 wells sampled in 1995 and 2000	FI-HG-AAS	high	"Out of 31 tube wells in 18 we found increased As concentration. Rest 13 either remained close to previous value (± 15%) or decreased."	yes
Sengupta et al. (2004)	conference abstract	unspecified number of wells from 9 arsenic-affected districts of West Bengal sampled in 1997 and 2003	FI-HG-AAS	high	"...some villages in the 9 As-affected districts of West Bengal where safe or very less contaminated, got contamination with time..."	yes
Cheng et al. (2006)	Environ. Sci. Technol.	20 wells for 3 years.	HR-ICP-MS	high	"Significant change in As concentration was only observed from very shallow depth "	yes
van Geen et al. (2008)	J. Environ. Sci. Health A	51 deep wells for 5 years.	HR-ICP-MS	high	"Although majority of deep well did not show significant increase, 4 out of 51 wells provides a clear warning: concentrations of As will inevitably rise in a (hopefully small) fraction of deeper wells. "	yes
Dhar et al. (2008)	J. Contam. Hydrol.	37 wells for 2-3 years with 2-4 weeks interval.	HR-ICP-MS		" As and P concentrations generally varied by <30%, whereas concentrations of the major ions (Na, K, Mg, Ca and Cl) and the redox-sensitive elements (Fe, Mn, and S) varied over time by up to ±90%. "	yes
Direct measurements over <2 years						

Table 1-1. Summary of reported As monitoring data for Bangladesh, Inda, and Vietnam (Continued)

reference	form of publication	type of data	analytical method	data quility	main conclusion	data shown?
Burren, cited by Ravenscroft et al.	thesis	unspecified	unspecified	unknown	"...data strongly suggest a trend of increasing As concentration over time"	no
CGWB cited by BGS-DPHE	book	unspecified	unspecified	unknown	"Monitoring in West Bengal has indicated that As concentrations in tube wells are lowest during the months August - September."	no
Asia Arsenic Network	report	5 observation wells at different depths	AAS or fiels kit	unknown	"...the concentration is generally higher in the rainy season than in the dry season..."	yes
DPHE, cited by PHED pumping test	report	unspecified	unspecified	unknown	"...very slight increase in As toward the end of eight hour pumping tests, though the significance of these very slight increases is unclear. However, the general short-term trend indicates little change."	yes
DPHE, cited data from 18 district Towns project	report	6 randomly selected wells	unspecified	unknown	"Of the six wells rancomly selected... only one or two appear to show a consistent increase with time, and they are still well below the Bangladesh standard. The other wells appear to show no overall trend to increase or reduce."	yes
Berg et al.	Environ. Sci. Technol.	68 wells sampled three times in 1999-2000	HG-AAS	adequate	"The highest As concentrations occurred at the rainy season to dry season and the lowest at the end of the dry season."	yes
BGS-DPHE	report	32 wells sampled biweekly over 1 year	HG-ICP-AES or HG-ICP-AFS	adequate	"Arsenic cncentrations show little notable temporal variation in most of the monitored wells"	yes
van Geen et al.	Bull. W.H.O.	6 wells sampled monthly for 1 year	HR-ICP-MS	high	"The six currently safe wells that were sampled more frequently over a year showd no indication of signifiant seasonal fluctuations in As concentrations..."	yes
Savarimuthu et al. (2006)	J. Health Popul. Nutr.	74 selected tubewells ranging in depth from 40 to 500 feet for 1 yeaar.	FI-HG-AAS	high	"...As concentration in water show the minimum average concentration in the summer season (694 µg/L) and the maximum in the monsoon season (906 µg/L)..."	yes
van Geen et al.	Bull. W.H.O.	7 deep wells sampled biweekely for 1 year	HR-ICP-MS	high	"...There were no noticeable seasonal variations in As concentrations."	yes
van Geen et al.	Environ. Sci. Technol.	344 wells sampled in 2001 and 2003	HR-ICP-MS	high	"No systematic temporal trend can be inferred from the data."	yes

Table 1-2. Recommended preservation method of inorganic As.

references	recommendation
Daus et al. (2002)	Arsenite was stable with in 9 days with 0.01 M phosphoric acid under 6 °C after filtration. Freezing should be avoided. HCl, NTA, HAc were not suitable.
McCleskey (2004)	Addition of hydrochloric or sulfuric acid with EDTA to prevent the oxidation by Fe3+. Preserve in the dark is recommended.
Gault et al. (2005)	Immediate filtration and acidification with HCl followed by refrigerated storage was found to be the most effective strategy for minimizing the oxidation of inorganic As(III) during storage. To use EDTA is not simply better choise and even problematic for Ca nad Mg rich groundwater.
Samanta (2005)	EDTA-HAc could preserve the inorganic As(III/V) species efficiently for more than 30 days. This method is better than the use of H_2SO_4 or H_3PO_4.

Table 1-3. Summary of chemical extraction using the sediment from Bangladesh or West Bengal

references	sample	leaching steps	results	references of extraction methods.
Nickson et al. (2000)	Nadia district, West Bengal, India	*diagenetically available As* : 12 N boiled HCl for 1 min.	More than 75% of total As is diagenetically available As.	Raiswell et al. (1994)
BGS and DPHE (2001)	Chapai Nawabganj, Faridpur, Laksmipur districts, Bangladesh	*coprecipitated with oxides and clays* : ammonium oxalate extraction (although detail procedure is not given, this method is well established and is widely used.)	Mean values of oxalate extractable As are 1.79, 0.84, and 2.13 mg/kg in Chapai Nawabganj, Faridpur, and Lakshmipur, respectively.	Tessier et al. (1978)
Anawar et al. (2003)	Faridpur district, Bangladesh	(1) *carbonate phase* : 0.1 M acetic acid at pH 5.0 for 5 hours. (2) *Fe and Mn oxyhydroxide phases* : 0.2 M NH_2OH•HCl at 96 °C for 12 hours. (3) *organic matter phase* : 0.1 M sodium pyrophosphate at pH 10 for 12 hours. (4) *sulfide and silicate phases* : mixture of concentrated HCl and pottasium chlorate.	oxide phase: 30 to 60% organic phase: 7 to 35% residual phase: 25 to 50% Oxide phase increased below 25 m, whereas residual phase decreased in this depth.	Thomas et al. (1994) modified
Swartz et al. (2004)	Munshiganji district, Bangladesh	(1) *weakely adsorbed* : 1 M $MgCl_2$ at pH8 for 2 hours. (2) *strongly adsorbed* : 1 M Na_2HPO_4 at pH 4-5 for 24 hours. (3) *coprecipitated with carbonate, AVS, amourphous metal oxide, and magnetite* : 1 M HCl 1 hour followed by 0.2 M oxalic acid at pH 3 for 2 hours. (4) *coprecipitated with crystalline Fe oxides and amorphous sulfides* : 0.5 M titanium(III) chloride-sodium citrate-tetrasodium EDTA-bicarbonate at pH.7 for 2 hours. (5) *coprecipitated with silicate* : 10 M HF for 24 hours. (6) *coprecipitated with pyritic phase* : concentrated nitric acid for 2 hours. (7) *crystalline sulfides and other recalcitant phase* : hot concentrated nitric acid and 30% hydrogen peroxide .	For all samples, 41 to 75% was extracted at HF step. Arsenic extracted from step 3 and step 4 are generally higher in shallow part than deep part.	Keon et al. (2001)
Akai et al. (2004)	Samta village, Jessore district, Bangladesh	(1) *carbonate phase* : 0.1 M acetic acid at pH 5.0 for 5 hours. (2) *Fe and Mn oxyhydroxide phases* : 0.2 M NH_2OH•HCl at 96 °C for 12 hours. (3) *organic matter phase* : 0.1 M sodium pyrophosphate at pH 10 for 12 hours. (4) *sulfide and silicate phases* : mixture of concentrated HCl and pottasium chlorate.	Dominant As forms in the most samples are Fe- and/or Mn-oxides, organic matter and sulfides, although relative abundances differ among the samples. Little As is adsorbed to minerals and fixed in carbonates.	Thomas et al. (1994) modified
Zheng et al. (2005)	Araihazar, Narayangonji district, Bangladesh	(1) *P-extractable As:* 1 M NaH_2PO_4 at pH5 for 16 hours.	Average of P-extracted As is 1.7 ± 1.2 and 1.4 ± 2.0 mg/kg in Holocene sediment, while 0.2 ± 0.3 and 0.1 ± 0.1 mg/kg in Pleistocen aquifer.	Keon et al. (2001)

Table 1-3. Summary of chemical extraction using the sediment from Bangladesh or West Bengal (Continued)

references	sample	leaching steps	results	references of extraction methods.
Nath et al. (2007)	Nadia district, West Bengal, India	(1) *weakely adsorbed*: 1 M $MgCl_2$ at pH8 for 2 hours. (2) *strongly adsorbed*: 1 M Na_2HPO_4 at pH 4-5 for 24 hours. (3) *coprecipitated with carbonate, AVS, Mn oxides, and very amourphous Fe oxide* : 1 M HCl 1 hour. (4) *coprecipitated with amorphous Fe oxyhydroxides: 0.1 M ascorbic acid, 0.2 M trisodium citrate, 0.6 M sodium hydrogen carbonate at pH8 for 24 hours.* *(5) coprecipitated with crystalline Fe oxyhydrooxides:* 0.3 M sodium dithionite, 0.35 M sodium acetate, 0.2 M sodium citrate at pH4.4 under 60 °C for 5 hours. (6) orpiment and recalcitrant As minerals: 35% hydrogenperoxide at pH2 under 85 °C for e hours.	The total extracted As concentration was 7.0 and 8.9 mg/kg for the silt fraction and 2.7 and 3.2 mg/kg for the sand fraction. Of the different extractant pools, the amorphous Fe-oxyhydroxide (34 ± 10% of total extracted As; step 4) is a major sink for As.	Keon et al. (2001) Kotska and Luther (1994) Tessier (1979)
Seddique et al. (2008)	Sonargaon, Narayangonji district, Bangladesh	(1) *carbonate phase* : 0.1 M acetic acid at pH 5.0 for 5 hours. (2) *Fe and Mn oxyhydroxide phases* : 0.2 M $NH_2OH{\cdot}HCl$ at 96 °C for 12 hours. (3) *organic matter phase* : 0.1 M sodium pyrophosphate at pH 10 for 12 hours. (4) *sulfide and silicate phases* : mixture of concentrated HCl and pottasium chlorate.	More than 80% of total As is extracted after step 3. In Holocene aquifer, 40 to 56% of As are in insoluble phase, and 35 to 50% are in organic phase. Majority of insoluble As is attributed to the As in biotite.	Thomas et al. (1994) modified

Table 1-4. Solid-solution distribution coefficients (K_d) calculated from experimental data at or near pH 7.

material	As/mineral ratio (μmol/g)	K_d (L/kg)	LogK_d (L/kg)	ionic strength	pH	comments	reference	remarks
arsenite								
HFO	3300	27000	4.4	0.01 M $NaClO_4$	7	Fig. 2	Dixit and Hering (2003)	
HFO	1700	57000	4.8	0.01 M $NaClO_4$	7	Fig. 2	Dixit and Hering (2003)	
HFO	830	86000	4.9	0.01 M $NaClO_4$	7	Fig. 2	Dixit and Hering (2003)	
HFO	330	300000	5.5	0.01 M $NaClO_4$	7	Fig. 2	Dixit and Hering (2003)	
Fe hydroxide (am)	40	78000	4.9	0.01 M NaCl	7	Fig. 2	Goldberg (2002)	
goethite	200	3300	3.5	0.01 M $NaClO_4$	7	Fig. 2	Dixit and Hering (2003)	
goethite	100	8000	3.9	0.01 M $NaClO_4$	7	Fig. 2	Dixit and Hering (2003)	
goethite	50	18000	4.3	0.01 M $NaClO_4$	7	Fig. 2	Dixit and Hering (2003)	
goethite	20	38000	4.6	0.01 M $NaClO_4$	7	Fig. 2	Dixit and Hering (2003)	
siderite	190	830	2.9	0.01 M $FeClO_4$	7	Fig. 10	Jönsson and Sherman (2008)	Sideite was partially dissoluted below pH7.
siderite	19	250	2.4	0.01 M $FeClO_4$	7	Fig. 10	Jönsson and Sherman (2008)	Sideite was partially dissoluted below pH7.
green rust	1300	11000	4.0	0.01 M $FeClO_4$	7	Fig. 2 fougerite	Jönsson and Sherman (2008)	GR was partially dissoluted below pH8. Amount of sorbed As(III) is renormalized to the amount of remaining fougerite.
magnetite	300	1800	3.2	0.01 M $NaClO_4$	7	Fig. 2	Dixit and Hering (2003)	
magnetite	200	2700	3.4	0.01 M $NaClO_4$	7	Fig. 2	Dixit and Hering (2003)	
magnetite	100	6000	3.8	0.01 M $NaClO_4$	7	Fig. 2	Dixit and Hering (2003)	
magnetite	1700	6000	3.8	0.01 M $FeClO_4$	7	Fig. 8	Jönsson and Sherman (2008)	Magnetite was partially dissoluted below pH8.
calcite				0.073 M KCl or LiCl	7.53	rarely adsorbed	Sø et al. (2008)	
galena	50	13000	4.1			Fig. 4	Bostic et al. (2003)	
sphalerite	50	4000	3.6			Fig. 4	Bostic et al. (2003)	
pyrite	55	2100	3.3	0.001 M NaCl	7	Fig. 6	Bostick and Fendorf (2003)	

Table 1-4. Solid-solution distribution coefficients (K_d) calculated from experimental data at or near pH 7. (Continued)

material	As/mineral ratio (μmol/g)	K_d (L/kg)	LogK_d (L/kg)	ionic strength	pH	comments	reference	remarks
troilite	55	1600	3.2	0.001 M NaCl	7	Fig. 6	Bostick and Fendorf (2003)	
biotite	3.2	550	2.7	0.001 M $NaNO_3$	7	Fig. 4	Chakraborti et al. (2007)	Maximum adsorption observed around pH 5.
muscovite	3.2	220	2.3	0.001 M $NaNO_3$	7	Fig. 2	Chakraborti et al. (2008)	Maximum adsorption observed around pH 5.
kaolinite	0.50	11	1.0	0.01 M NaCl	7	Fig. 3	Goldberg (1999)	
kaolinite	0.016	22	1.3	0.05 M NaCl	7	Fig. 1	Manning and Goldberg, (1997)	
montmorillonite	0.50	7.9	0.9	0.01 M NaCl	7	Fig. 5	Goldberg (2002)	
montmorillonite	0.016	68	1.8	0.005 M NaCl	7	Fig. 1	Manning and Goldberg, (1997)	
illite	0.50	17	1.2	0.01 M NaCl	7	Fig. 4	Goldberg (2002)	
illite	0.016	27	1.4	0.015 M NaCl	7	Fig. 1	Manning and Goldberg, (1997)	
Al hydroxide (am)	20.0	2300	3.4	0.01 M NaCl	7	Fig. 1	Goldberg (2002)	
Al hydroxide (am)	0.16	1800	3.3	0.02 M NaCl	7	Fig. 1	Manning and Goldberg, (1997)	
arsenate								
HFO	3300	16000	4.2	0.01 M $NaClO_4$	7	Fig. 1	Dixit and Hering (2003)	
HFO	1700	39000	4.6	0.01 M $NaClO_4$	7	Fig. 1	Dixit and Hering (2003)	
HFO	1200	73000	4.9	0.01 M $NaClO_4$	7	Fig. 1	Dixit and Hering (2003)	
HFO	330	3300000	6.5	0.01 M $NaClO_4$	7	Fig. 1	Dixit and Hering (2003)	
Fe hydroxide (am)	40	78000	4.9	0.01 M NaCl	7	Fig. 2	Goldberg (2002)	
goethite	200	2000	3.3	0.01 M $NaClO_4$	7	Fig. 1	Dixit and Hering (2003)	
goethite	100	11000	4.1	0.01 M $NaClO_4$	7	Fig. 1	Dixit and Hering (2003)	
goethite	50	N/A	N/A	0.01 M $NaClO_4$	7	Fig. 1	Dixit and Hering (2003)	almost all adsorbed
goethite	20	N/A	N/A	0.01 M $NaClO_4$	7	Fig. 1	Dixit and Hering (2003)	almost all adsorbed

Table 1-4. Solid-solution distribution coefficients (K_d) calculated from experimental data at or near pH 7. (Continued)

material	As/mineral ratio (μmol/g)	K_d (L/kg)	LogK_d (L/kg)	ionic strength	pH	comments	reference	remarks
siderite	190	11000	4.1	0.01 M $FeClO_4$	7	Fig. 10	Jönsson and Sherman (2008)	GR was partially dissoluted below pH7.
siderite	19	2200	3.3	0.01 M $FeClO_4$	7	Fig. 10	Jönsson and Sherman (2008)	GR was partially dissoluted below pH7.
green rust	1400	2800000	6.4	0.01 M $FeClO_4$	7	Fig. 2 fougerite	Jönsson and Sherman (2008)	As(V) is completely sorbed below pH8.
green rust	700	1400000	6.1	0.01 M $FeClO_4$	7	Fig. 2 fougerite	Jönsson and Sherman (2008)	As(V) is completely sorbed below pH8.
green rust	140	280000	5.4	0.01 M $FeClO_4$	7	Fig. 2 fougerite	Jönsson and Sherman (2008)	As(V) is completely sorbed below pH8.
magnetite	1700	3400000	6.5	0.01 M $FeClO_4$	7	Fig. 8	Jönsson and Sherman (2008)	Magnetite was partially dissoluted below pH8.
biotite	3.2	1800	3.3	0.001 M $NaNO_3$	7	Fig. 3	Chakraborti et al. (2008)	Maximum adsorption observed around pH 5.
muscovite	3.2	220	2.3	0.001 M $NaNO_3$	7	Fig. 2	Chakraborti et al. (2008)	Maximum adsorption observed around pH 5.
kaolinite	0.50	N/A	N/A	0.01 M NaCl	7	Fig. 3	Goldberg (2002)	almost all adsorbed
montmorillonite	0.50	17	1.2	0.01 M NaCl	7	Fig. 5	Goldberg (2002)	
illite	0.50	180	2.3	0.01 M NaCl	7	Fig. 4	Goldberg (2002)	
Al hydroxide (am)	20.0	N/A	N/A	0.01 M NaCl	7	Fig. 1	Goldberg (2002)	almost all adsorbed

Table 1-5. Reported ΔG_f^0 value at standard states for the minerals.

Arsenic minerals	ΔG_f^0 (kcal/mol)	References
$FeAsO_4 \cdot 2H_2O$	-305.96	Robins, 1990
$FeAsO_4$	-184.66	Sadiq and Lindsay, 1981
$AlAsO_4 \cdot 2H_2O$	-408.4	Naumov et al., 1974
$AlAsO_4$	-306.13	Sadiq and Lindsay, 1981
$Mn_3(AsO_4)_2$	-518.03	Sadiq and Lindsay, 1981
$Mn_3(AsO_4)_2 \cdot 8H_2O$	-969.2	Naumov et al., 1974
$Mg_3(AsO_4)_2$	-663.3	Itagaki and Nishimura, 1986
$Mg_3(AsO_4)_2 \cdot 10H_2O$	-1230.2	Nishimura et al., 1981
$MgHAsO_4$	-283.8	Itagaki and Nishimura, 1986
$MgHAsO_4 \cdot 7H_2O$	-680.6	Nishimura et al., 1981
$Ca_3(AsO_4)_2$	-731.5	Nishimura et al., 1981
$Ca(H_2AsO_4)_2$	-490.9	Nishimura et al., 1981
$Ca_5H_2(AsO_4)_4$	-1347.2	Nishimura et al., 1981
Ca_2AsO_4OH	-475.1	Nishimura et al., 1981
As_2S_2	-36.22	Naumov et al., 1974; Wagman et al., 1968
As_2S_3	-23.06	Webster, 1990

All data are cited from Ryu et al. (2002) Geochim. Cosmochim. Acta

Table 1-6. Reported Log*K* values of some dissolution reactions of As minerals.

Arsenic minerals	Log *K*	References
$FeAsO_4 \cdot 2H_2O + H^+ = Fe^{3+} + HAsO_4^{2-} + 2H_2O$	-13.02	Ryu et al., 2002
$FeAsO4 \cdot 2H2O + H^+ = Fe^{3+} + HAsO_4^{2-}$	-8.59	Sadiq et al., 1983
$AlAsO_4 \cdot 2H_2O + H^+ = Al^{3+} + HAsO_4^{2-}$	-13.47	Ryu et al., 2002
$AlAsO_4 + H^+ = Al^{3+} + HAsO_4^{2-}$	-4.7	Sadiq et al., 1983
$Mn_3(AsO_4)_2 + 2H^+ = 3Mn^{2+} + 2HAsO_4^{2-}$	8.51	Sadiq et al., 1983
$Mn_3(AsO_4)_2 \cdot 8H_2O + 2H^+ = 3Mn^{2+} + 2HAsO_4^{2-} + 8H_2O$	-7.66	Ryu et al., 2002
$Mg_3(AsO_4)_2 + 2H^+ = 3Mg^{2+} + 2HAsO_4^{2-}$	3.26	Ryu et al., 2002
$Mg_3(AsO_4)_2 \cdot 10H_2O + 2H^+ = 3Mg^{2+} + 2HAsO_4^{2-} + 10H_2O$	3	Nishimura et al., 1981
$MgHAsO_4 + H^+ = Mg^{2+} + H_2AsO_4$	3.62	Ryu et al., 2002
$MgHAsO_4 \cdot 7H_2O + H^+ = Mg^{2+} + HAsO_4^- + 7H_2O$	3.6	Nishimura et al., 1981
$Ca_3(AsO_4)_2 + 2H^+ = 3Ca^{2+} + 2HAsO_4^{2-}$	5.2	Nishimura et al., 1981
$Ca(H_2AsO_4)_2 = Ca^{2+} + 2H_2AsO_4^{2-}$	1.1	Nishimura et al., 1981
$Ca_5H_2(AsO_4)_4 + 2H^+ = 5Ca^{2+} + 4HAsO_4^{2-}$	-1.8	Nishimura et al., 1981
$Ca_2AsO_4OH + H^+ = 2Ca^{2+} + AsO_4^{3-} + H_2O$	0.88	Nishimura et al., 1981
$As_2S_2 + 16H_2O = 2HAsO_4^{2-} + 2SO_4^{2-} + 11e^- + 15H^+$	-180.42	Sadiq et al., 1983
$0.5As_2S_3 + 3H_2O = H_3AsO_3^0 + 1.5HS^-$	-23.11	Webster, 1990

This table is cited from Ryu et al. (2002) Geochim. Cosmochim. Acta

Table 1-7. Summary of incubation experiment conducted various parts of Bengladesh and West bengal.

References	Sampling point	Sample	Duration of incubation	Nutrient	Comment	Result
Islam et al. (2004)	Nadia district, West Bengal, India	Sand from Holocene aquifer	40 days	4 g/L acetate	Four types of batches were used: aerobically; anaerobically; anaerobically with acetate; anaerobically with acetate using autoclaved sediment.	Large amount of As (>100 nM) is released from only anaerobically with acetate batch. Fe(II) released to water after 8 days, whereas As(III) released after 24 days.
Akai et al. (2004)	Samta village, Jessore district, Bangladesh	Mad from Holocne aquifer	14 days	0.5 g/L glucose 20 g/L polypepton urea fertilizer	Scanning electron microscopic observation was also conducted.	Polypepton and glucose were effective to mobile As.
van Geen et al. (2004)	Araihazar, Narayanaganji district, Bangladesh	One orange sands and two gray sands from Holocene aquifer, whereas one orange sand from Pleistocene aquifer.	70 days	1 g/L acetate	Guillard reagent was used to make antibiotic condition.	Release of As was marked from acetate amended biotic batch. As was not released from orange sand without addition of acetate.
Polizzotto et al. (2006)	Munshigunji district, Bangladesh	Holocene sand from 30 m depth where maximum dissolved As observed.	30 days	1.5 mM lactate	Compare the sterilized and non-sterilized sediment using gamma irradiation.	Approximately 15% or the total arsenic is released from sediment from both sterilized and non-sterilized sediment.
Gault et al. (2005)	Nadia district, West Bengal, India	Holocene clays and sands from 8, 18, 24, 26, 30, and 45 m.	1 month	20 mM acetate	Combined the analysis of microbial community.	Significant arsenic release was noted in sediment collected from 24 m and 45 m depth, with some Fe(III) reduction also observed in the 24 m sample.
Radloff et al. (2007)	Araihazar, Narayanaganji district, Bangladesh	Holocene sand from 5, 12, and 38 m.	11 months	1.5 μM acetate	Groundwater and sediment were collected simultaneously using a device coined the needle sampler, and placed immediately under anaerobic conditions in the field.	Small periodic additions of oxygen suppressed the release of As from sediments at all three depths.

Chapter 2
Hydrological and geological background of As-contaminated aquifer in Sonargaon, middle east Bangladesh

1. Chapter introduction

There have been many hydrogeochemical studies carried out in Bangladesh and West Bengal. Early research on the occurrences of local scale As contaminated groundwater had been carried out in mid to late 1990's (summarized in Smedley and Kinniburgh, 2002; Chapter 1 of this thesis). A nation-wide field survey was first carried out by BGS & DPHE (2001) to document the spatial distribution of As contaminated groundwater; i.e., 3534 wells were collected with a sampling density of approximately one per 37 km^2 or an average about 6 km distance among each wells for the entire landmass of the country. As results, the As contaminated groundwater exists in the aquifers within the Holocene delta and the flood plains of Ganges, Brahmaputra, and Meghna (GBM) rivers. Aquifers in the Pleistocene terrace deposits were not contaminated (Chapter 1, Fig. 1−1). The level of As contamination varies in the local scale; e.g., van Geen *et al.* (2003) analyzed about 6000 tube wells within a 25 km^2 area, and found the contaminated and uncontaminated groundwaters in adjacent wells 10 m apart in the Holocene aquifers. Many authors noticed the similar occurrences of As contaminated groundwaters in the different areas of that country (Harvey *et al.*, 2002; McArthur *et al.*, 2004; Zheng *et al.*, 2005).

Reductive dissolution of Fe oxyhydroxide is almost the consensus to explain the mechanism of mobilization of As into the groundwater in the GBM delta (Nickson *et al.* 1998; Harvey *et al.* 2002; McArthur *et al.* 2004). According to this hypothesis, As is released via reduction and decomposition of Fe oxyhydroxides associated with biodegradation of organic matter in the aquifer. However, this process has not been fully supported in terms of several controversial points; e.g., source of organic matter (Harvey *et al.* 2002, McArthur *et al.* 2004; Rowland *et al.* 2006), chemical form of reduced Fe oxyhydroxides/oxides (Horneman *et al.* 2004; van Geen *et al.* 2004), and transportation process of As (Harvey *et al.* 2005; Polizzotto *et al.* 2005).

In order to document the formation mechanism of the As contaminated groundwater in the Holocene aquifer, I and co-investigators drilled into the Holocene and underlying Pleistocene aquifers in Sonargaon, located at the edge of Pleistocene terrace in central Bangladesh. Lithology and mineralogy in the study area are reported in Mitamura *et al.* (2008) and Seddique *et al.* (2008). Prior to the drilling, well waters were geochemically studied to document the spatial distribution of As groundwater. In this report, first, chemical and stable isotopic characteristics of the groundwaters are described in detail. Then, I interpret the process of releasing As into the aquifer in relation to the hydrogeology and mineralogy of the studied area, and explain the principal mechanism of formation of As contaminated groundwater in the GBM delta.

2. *Geological settings*

The Bengal Basin, located downstream of the GBM river system, is one of the most active deltaic plains (GBM delta) in the world. A large volume of detritus eroded from the Himalayas has been transported to form the GBM delta. Goodbred and Kuehl (1999) estimated that a long-term total annual sediment load of 10^{12} kg/year, of which approximately one third has been deposited in the subaerial delta and flood plain. Erosion of the ultramafic rocks of the northern parts of the Himalayas and granitic and high grade metamorphic rocks of the central and southern parts, have produced these sediments and provided the dominant mineral assemblage of quartz, biotite, and feldspar (BGS and DPHE, 2001). More detail geological background of GBM delta is described in Chapter 1 (section 3).

Fig. 2–1 shows the surface geology of Bangladesh (Goodbred *et al.*, 2003). The country is geologically divided into four parts, i.e., modern delta plain in the south, alluvial flood plain in the central, Pleistocene terraces in the north-west (Barind Tract) and central (Madhupur Tract), and a subsided basin (Sylhet Basin) in the upstream Meghna river.

Our study area, located at the southeastern edge of the Pleistocene terrace deposit, Madhupur Tract, is approximately 3 × 3 km^2 in the Sonargaon thana (sub-district). A geographic map of the study area is presented in Fig. 2–2a, in which the meandering Old Brahmaputra River is running. This river was the main channel of the Brahmaputra

river presently flowing several hundred km westward as Meghna River (Goodbred and Kuehl., 2000). Dissected terraces, where reddish brown oxidized mud and sand layers are exposed, occur in the western part of the study area separated by the Line A from the alluvial floodplain in the eastern part. Natural banks, where settlements commonly exist, are located along the present and abandoned channels. Except for such banks, the flood plain is mostly covered with water during the rainy season (June to September). In the dry season, the channel of the Old Brahmaputra river is almost dry, and the land is used for cultivation.

Observation of the drill core revealed the underlying geology and aquifer structure in this area (Mitamura *et al.*, 2008). Simplified geological cross section is shown in Fig. 2–2b. The results can be summarized as given below.

(i) Quaternary strata in the study area above the depth of 100 m is divided into three formations; lower sand, middle mud, and upper sand layers.

(ii) The age of middle mud formation was determined to be >54 Ka by ^{14}C dating. The sedimentation ages of the three formations are estimated to be Plio-Pleistocene (the lower sand layer), Middle-Upper Pleistocene (the middle mud layer), and Holocene (the upper sand layer).

(iii) At the western terrace, which was uplifted due to fault movement, the lower sand layer is exposed on the ground surface.

(iv) The middle mud layer works as the aquitard dividing the upper and lower aquifers. Surface of this layer is mostly flat in E-W direction, while undulating irregularly in N-S direction with various depressions of sizes.

(v) Two aquifers can be identified in the study area; an unconfined aquifer shallower than ca. 30 m deep hosted by upper Holocene sand layer, and a confined aquifer beyond the depth of 40 m hosted by lower Pleistocene sand layer. In the northeastern part of the study area, in which Pleistocene sediment is directly exposed, groundwater in Pleistocene aquifer exists in even shallower (<30 m) depth.

(vi) Lower half of the upper Holocene sand layer generally consists of middle to coarse grained sand, suggesting high permeability. Majority of the tube wells draw groundwater from this layer.

3. *Methods*

3.1. Sampling and in situ analyses

Tube wells installed in shallow aquifers of ~30 m depth locally called "hand tube well", are densely distributed in the settlements to satisfy the daily use of water. Groundwaters from 232 tube wells were collected at the end of rainy season in September 2003 along with waters from 228 wells previously sampled at the end of dry season in February 2004. Because hand tube well is generally not fully screened, and only 3-6 m length screen is attached on the end of the installed pipe, length of well pipes can be regarded as depth of taking groundwater. Location of the sampling wells was positioned using a portable GPS receiver (eTrex Vista, GARMIN) with an error limit of <10 m.

Oxidation reduction potential (ORP), pH, and electrical conductivity (EC) were measured *in situ* using portable instruments (D-55, Horiba Techno Service, Ltd. and SC82, Yokogawa electric co.). The pH was measured by glass electrode. ORP was measured as the potential difference between platinum electrode and Ag/AgCl reference electrode, and the measured ORP values were converted to Eh (vs. standard hydrogen electrode) using the following equation recommended by Horiba Techno Service, Ltd.

$$Eh\ (V) = ORP\ (V) + 0.206 - 0.007 \times (T - 25)$$

where T is the water temperature in °C. Groundwater was sampled during continuous pumping after the readings of pH, ORP, EC, and water temperature became stable. Alkalinity was analyzed in situ by titration with 0.1 N (or 0.16 N) HCl using the mixture of bromcresol green and methyl red (BCG-MR) as the indicator at pH 4.8.

Each groundwater sample was split and stored in four bottles and treated in the field as follows. (i) Acidified with HCl to 0.06 N HCl solution for determination of total As including particulate and dissolved As; (ii) filtered with 0.45 μm membrane-filter for analysis of major anions, dissolved organic acids (formate, acetate and oxalate ions), δD, and $\delta^{18}O$; (iii) filtered with 0.45 μm membrane-filter and acidified to 0.06 N HCl solution for analysis of major cations and NH_4^+, dissolved As and Fe, and $\delta^{34}S_{SO4}$ and

dissolved organic carbon (DOC); and (iv) filtered with 0.45 μm membrane-filter and acidified to 0.09 N H_2SO_4 solution for analysis of As^{III} and $\delta^{15}N_{NH4}$. McCleskey *et al.* (2004) suggest that acidification by H_2SO_4 is a suitable way to avoid As^{III} oxidation during preservation. Samples (i), (ii), and (iii) were preserved in polyethylene bottles, and samples (iv) were kept in air-tight glass vials. In addition to those samples, one liter of groundwater was also collected from each of the 7 wells, i.e., [*LDD3* (60 m; Ledemi), *BKB6* (75 m; Bara Khater Bhulua), *NKD5* (90 m; Darikandi), *GLG3* (26 m; Gulnagar), *DRK35* (18 m Darikandi), and *MCC22* (23 m; Mucharchar), *DLD6* (21 m; Daulaudi) in December 2004 for tritium analysis. The samples were selected based on the following concepts; (i) to collect from both Holocene and Pleistocene aquifer, and (ii) the samples having typical water chemistry and $\delta^{18}O$ within the regions based on the analytical data of groundwaters in the rainy season. Riverwater and rainwater were collected monthly from March to December 2004. The sampling location of riverwater is shown in Fig. 2−2a. Rainwater was taken after the first shower at Dhaka-Mirpur or sampling site. The sampling procedure of them was same as sampling of groundwater. Chemical fertilizers, i.e., urea, Thiobit, ZnS, $(NH_4)_2SO_4$, and $MgSO_4$ were purchased in Darikandi village to analyze N and S isotopes.

3.2. Analytical methods

Major anions and dissolved organic acids were determined by ion chromatography (DX-120, Dionex for the anion analyses). Ca and Mg were determined with EDTA titration, and Na and K were quantified with atomic absorption spectrophotometer (SAS7000, Seiko Instruments). Detection limits of these compounds were ~0.1 mg/L. Dissolved organic carbon (DOC) was measured by TOC analyzer (TOC-5000, SHIMADZU). Since the sample water is evaporated during the pretreatment, the above dissolved organic acids are excluded from the concentration of DOC. Saturation index of secondary minerals, e.g., calcite, dolomite, siderite, ferrihydrite, etc., were calculated using MINTEQA2 ver. 2.30 (Allison *et al.* 1991) for the groundwaters collected in February 2004, 14 samples from the Pleistocene aquifer and 143 samples from the Holocene aquifer.

Total dissolved arsenic was determined by a hydride generation atomic absorption

spectrophotometer (SAS7000, Seiko Instruments). As^{III} was determined with the cathode stripping voltammetry (Holak, 1980) after filtration in the laboratory with a solid-phase extraction disk (Milli-pore) to remove the dissolved organic matters which interfere with the accurate determination of As^{III} using a potentiostat/galvanostat (AUTOLAB model PG-STAT 10, Eco chemie) interfaced with the multi-mode electrode (VA 663, Metrohm). The As^{III} analysis was completed within 3 months of sampling. NH_4^+ concentration was determined with colorimetric Indo-phenol method within 3 weeks after sampling. Dissolved Fe concentration was determined by colorimetric o-phenanthroline method.

Hydrogen and oxygen isotope ratios of water were determined from hydrogen gas produced by the on-line Cr reduction method (Itai and Kusakabe, 2004) and a conventional H_2O-CO_2 isotopic equilibration method (Epstein and Mayeda, 1953), respectively, using a mass spectrometers (SIRA10, VG-Micromass, and PRISM, Fison). The hydrogen and oxygen isotopic compositions are expressed in terms of δD and $\delta^{18}O$ (‰) relative to the VSMOW (Vienna Standard Mean Ocean Water). Precision of the analytical data was within ± 0.5 ‰ (δD) and ± 0.1 ‰ ($\delta^{18}O$) respectively (1σ). For tritium analysis, one liter of sampled groundwater was distilled to remove dissolved matters, and then condensed electrically to 50 mL using Solid Polymer Electrolysis for tritium enrichment (TriPure, Permelec Electrode ltd.), before measuring of the tritium content using a liquid scintillation analyzer (Aloka model LB3).

3.3. Water table monitoring

Three observation wells (W1, W2 and W3) were drilled at southern end of Darikandi village (specified as "M" in Fig. 2–2a) within 10 m in diameters to monitor the seasonal variation of groundwater table during January to December in 2005. The depths of screens are 6–12 m for W1, 18–27 m for W2, and 45–54 m for W3.

4. Results

In order to constrain the relationship between geology and the occurrence of As

contamination, the investigated groundwaters are classified into two groups based on the locality and the depth of the wells installed. One group comprises most of the groundwaters drawn from the wells shallower than 36 m located in the alluvial plain, where the Holocene sediments host the unconfined aquifer. The other group comprises groundwater drawn from depths greater than 50 m from the wells installed in the Pleistocene sediments beneath the alluvial plain and all groundwaters collected from the western Pleistocene terrace (Gulnagar village), which is a recharge zone of the studied groundwater in the Pleistocene aquifer. According to this classification, number of groundwaters in the Holocene and Pleistocene aquifers were 178 and 23 samples, respectively. The groundwaters drawn from the wells of 36 ~ 50 m depth are excluded from these two categories, since the aquifer cannot be specified without information of subsurface geology. Thus, these groundwaters are tentatively classified into the third groups named "unspecified". Because groundwaters drawn from the wells >100 m depth is too deep to know hydrological relationship to those in the shallower aquifers, those are used only as reference data.

4.1. Major chemical composition of groundwater

All the 178 groundwaters collected from the Holocene aquifer have pH within the range 6.5 to 7.4. The studied groundwaters are dominantly Ca-Mg-HCO_3 type (Fig.2–3), similar to those previously reported for other areas in Bangladesh (e.g., Zheng *et al.*, 2004, Ahmed *et al.*, 2004). The key diagram of cations shows more than 90% of the groundwaters plotted in the region where Ca, Mg, and Na+K fractions are >0.4, 0.2 ~ 0.4 and <0.3, respectively. With increasing Ca concentration, Ca : Mg ratio approaches 7 : 2 ~ 7 : 3. Less than 10% of groundwater from the Holocene aquifer, mostly found in Daulaudi and Temdi, have Ca fraction <0.4, and Na+K increases with decreasing Ca fraction. Most dominant anion is HCO_3^-, where equivalent fraction among total anion is up to 0.99 with mean value of 0.82. Some waters, mostly collected from Mammudi and Daulaudi, contain HCO_3^- fraction of <0.60 and concentration of Cl^- (up to 5.1 meq/L), plausibly derived from anthropogenic sources, increases instead of HCO_3^-. Fraction of sulfate in a total anion is generally <0.1. Among the 17 samples collected from Mammudi village, however, 7 samples in rainy season and 6 samples in dry season

show a exceptionally high sulfate fraction of >0.1 with a maximum value of 0.14. SO_4^{2-}/Cl^- ratio ranged from 0.0 to 580 μM/mM. In Bangladesh, surface waters show SO_4^{2-}/Cl^- ratios ranging from hundreds to 3000 μM/mM (Galy and France-Lanord, 1999). Based on the $\delta^{34}S_{SO4}$ analysis, Zheng *et al.* (2004) suggested that very low SO_4^{2-}/Cl^- ratio (<10 μM/mM) in some regions of Bangladesh is primarily a result of sulfate reduction and not due to recharge of low sulfate water. Thirty-three samples of our studied groundwaters give SO_4^{2-}/Cl^- ratio <10 μM/mM, and most of them are distributed in the southern part of Harihardi, Darikandi, and Bara Khater Bhulua.

Groundwaters of the Pleistocene aquifer comprises 10 samples from the shallow wells in the western terrace, and 13 from the wells of >50 m depth beneath the alluvial plain. The former groundwaters have pH ranging 6.9 to 7.1, and the latter have a range of 6.8 to 7.0. Despite the two different depths of the installed wells, the major chemical composition of these groundwaters is similar and distinct from most of the groundwaters from the Holocene aquifer. Equivalent fraction of HCO_3^- in total anion of the shallow well waters from the terrace is up to 0.93 with a mean value of 0.75, and that of Ca^{2+} in total cation was <0.46 with a mean value of 0.40. Those fractions are similar to those of HCO_3^- and Ca^{2+} of the deep groundwaters beneath the alluvial plain, which are 0.71 and 0.43 respectively. Na+K fraction increases with decreasing Ca fraction. SO_4^{2-}/Cl^- ratio of the groundwater in Pleistocene aquifer ranged from 10 to 453 μM/mM. No sample show lower SO_4^{2-}/Cl^- ratio than 10 μM/mM, indicating limited occurrence of sulfate reduction.

Groundwater from the Holocene aquifer show NH_4^+ concentrations >0.1 mg/L in 139 samples of rainy season and 136 samples of dry seasons with the maximum values being 7.3 and 8.6 mg/L, respectively. NH_4^+ rich groundwaters mostly occur in the southern part of Harihardi, Darikandi and Bara Khater Bhulua. Most of the groundwaters do not contain detectable NO_3^- (<0.1 mg/L), while the groundwaters collected in the rainy season occasionally contain high amounts of NO_3^- >2 mg/L and the maximum concentration is about 16 mg/L. This observation suggests that oxic water contaminated with nitrate infiltrates the aquifer in the rainy season, while that such an infiltration rarely occurs in the dry season. More than 0.1 mg/L of PO_4^{3-} was detected in 61 groundwaters in the rainy season and 52 in the dry season with the maximum value

of 12 and 4 mg/L, respectively.

Analysis of dissolved Organic Carbon (DOC) was conducted on 40 samples collected in the dry season. Three samples collected from Pleistocene aquifer ranged in values from 1.2 to 2.2 mg/L, while 37 samples from Holocene aquifer showed a range 1.1 to 7.9 mg/L. Among Holocene aquifer, high DOC (>4 mg/L) tend to be observed in the southern parts (e.g., Darikandi and Bara Khater Bhulua), while low DOC (<2 mg/L) were in the northern part of study area (e.g., Harihardi and Mammudi). Acetate ion is ubiquitous in both Holocene and Pleistocene aquifers. In the Holocene aquifer, concentration of acetate varied between 1.4 to 11.4 and 1.4 to 14.4 mg/L in rainy and dry seasons, respectively. Low-acetate groundwater (<4 mg/L) was often observed in northern part of Harihardi, Temdi, and Mammudi, while the acetate was generally high (>8 mg/L) in Darikandi and Bara Khater Bhulua.

4.2. Relationships of major chemistry and As and redox components

Concentrations of total As, including particulate and dissolved forms, was almost the same as that of dissolved As within analytical precision for more than 80% of samples, and hereafter the concentration of dissolved As is used as total As for discussion. Horizontally spatial distribution of As concentration of the groundwaters from the wells shallower than 36 m is shown in Fig. 2–4a. Concentration of As of all groundwaters from western terrace (Gulnagar village) is within the limit of WHO standard 0.01 mg/L. Arsenic concentration varies widely in groundwaters from the Holocene aquifer. Highly As contaminated groundwater occasionally occurs as an island which is a few tens meters of wide and a few hundred meters long (sometimes called As hotspot). Kumarchar, middle to southern part of Harihardi, and Darikandi are such areas. On the other hand, groundwaters free from or low in As occur in three areas, i. e., Daulaudi, south-eastern part of Mucharchar, and northern part of Harihardi. In these areas, As free groundwater is occasionally found from the wells which are within a few tens of meters away from the highly contaminated well.

In order to trace the process of evolution of As contaminated groundwater chemistry, Ca, Mg and redox components (total Fe, NH_4^+, and As) of groundwaters from the Holocene aquifer are plotted against alkalinity (given as HCO_3^-) in Fig. 2–5.

The groundwaters are grouped according to each villages in this figure to observe the local scale variation of the chemistry. Relationships between HCO_3^- and Ca^{2+} and Mg^{2+} show good linear correlation, indicating that those components are mostly dissolved along the chemical weathering process of silicates, which is a hydration reaction promoted by mainly H^+ produced from the dissociation of dissolved soil CO_2 due to the respiration of soil organisms.

Alkalinity also increases in the groundwater in association with the biodegradation of organic matters. Fe (>5 mg/L) and NH_4^+ (>2 mg/L) rich groundwaters mostly occur in the southern part of Harihardi, Darikandi, and Bara Khater Bhulua villages, and tend to contain high HCO_3^- (>3 mM). However, HCO_3^- (>3 mM) rich groundwater does not always contain high Fe and NH_4^+. Arsenic (>400 μg/L) rich groundwaters mainly occur in northern and southern part of Harihardi, Darikandi, and Kumarchar villages. Slightly different distribution of As and Fe and/or NH_4^+ implies different mobilization process of these components via decomposition of organic matter in aquifer.

Major chemical compositions do not change very much in the groundwater collected from the same well in different seasons, although seasonal changes in Eh are significant. The Eh of the groundwater collected in the rainy season is with a narrow range of 0.165 to 0.226 V, while that in the dry season is highly variable (0.037 to 0.383 V). As shown in Fig. 2–4b, most of the groundwaters show negative ΔEh [Eh(dry season) – Eh(rainy season)]; (i. e., the Eh is higher in the rainy season than the dry season), especially for the groundwaters collected from southern part of the study area, such as Darikandi, Bari Khater Bhulua, and Kumarchar villages. However, some of the studied groundwaters, especially in the northern area, i.e., northern part of Harihardi, Mammudi, and Daulaudi, becomes noticeably more oxic in the dry season than in the rainy season.

Fig. 2–6 shows the relationships between redox components and Eh. The Eh does not vary significantly in the rainy season, and the relationships between Eh and concentrations of As, Fe and NH_4^+ are not clear. On the other hand, in dry season, concentration of As, Fe, and NH_4^+ generally increase with decreasing Eh. However, NH_4^+ and As concentrations occasionally high in the groundwaters giving high Eh

values of 0.25 ~ 0.35 V. Comparably high amount of As and NH_4^+ containing groundwater with high Eh among the sample would indicate that those components are dissolved via different process from the reduction. Change in As [$\Delta As\ (\%) = (As_{dry}-As_{rainy})/As_{mean}\times 100$] content of the groundwaters collected from the same well in different seasons are mostly < 20% (Fig. 2–6), while changes in the concentration of NH_4^+ and Fe were significant. Increase of Fe concentration in the dry season was obvious in southern part of Harihardi. Variable Fe concentration in relation to the Eh implies dissolution and precipitation of secondary Fe minerals such as Fe oxyhydroxide, siderite and vivianite. Precipitation of Fe sulfide such as mackinawite is also possible as a fixing mechanism of Fe in reducing condition. Concentration of NH_4^+ also increases in the dry season in the southern part of Harihardi, but the extent of change is smaller than that of Fe. Small seasonal changes in As and NH_4^+ concentrations might be attributed to their slower redox reaction rates than that of Fe.

Fig. 2–7 shows the relationships of redox components of the groundwaters sampled in the dry season. Arsenic concentration increases with increasing NH_4^+ and decreasing SO_4^{2-}, implying that dissolution of As and NH_4^+ increases with the intensification of the reducing environment as reported previously in other regions of Bangladesh (Anawar *et al.*, 2003; McArthur *et al.*, 2001; Zheng *et al.*, 2004; Ahmed *et al.*, 2004). Arsenic is believed to be released from Fe oxyhydroxide undergoing decomposition in reducing condition (e.g., De Vitre *et al.* 1991). However, it is known that As does not always behave in tandem with Fe (BGS and DPHE., 2001; McArthur *et al.*, 2001; 2004; Ahmed *et al.*, 2004), i.e., As rich groundwater is not always rich in Fe. This erratic behavior is noticeable in our studied groundwaters. For example, Fe concentration is low when the As concentration is high in the groundwater from in the northern part of Harihardi.

Groundwaters in Holocene aquifer were often saturated with calcite ($-1.33 < SI_{cal} < 0.64$) and dolomite ($-2.66 < SI_{cal} < 1.04$) as suggested by previous researches (e.g., Ahmed *et al.* 2004; McArthur *et al.* 2004), indicating that elevated concentration of HCO_3^- in Holocene groundwater was not attributed to dissolution of carbonate minerals. More than half of the groundwaters (55 %) including all samples containing > 0.1 meq/L of Fe are saturated or oversaturated with siderite (Fig. 2–8). Saturation index of

siderite was up to 1.3. These oversaturation implies that siderite is precipitated in the aquifer when groundwater alkalinity and Fe concentration increase. Stable Fe mineral in studied groundwater condition was estimated by Eh-pH diagram (Fig. 2–8). If ignore the precipitation of siderite, Fe oxyhydroxides are stable in measured Eh and pH region. Considering precipitation of siderite, stability field of both Fe oxyhydroxides becomes decrease. Although goethite is still stable under this condition, ferrihydrite ($Fe(OH)_3$) becomes unstable toward lower Eh and pH. Groundwaters collected from Darikandi which were generally reducing and slightly alkaline were plotted close to the boundary of $Fe(OH)_3/FeCO_3$, while $Fe(OH)_3$ was stable in groundwaters from the other regions; i.e., northern part of Harihardi (oxic and slightly alkaline) and Daulaudi (oxic and slightly acidic).

4.3. H and O isotopic character of waters

Fig. 2–9 shows the relationship between δD and $\delta^{18}O$ of the groundwaters. All groundwaters are plotted around the global meteoric water line (MWL: $\delta D = 8\delta^{18}O + 10$, Craig, 1961), indicating that all groundwaters originate from meteoric water. Variation of isotopes ranged from -46.3 to -5.7‰ in δD and -7.2 to -2.0‰ in $\delta^{18}O$. This range of $\delta^{18}O$ is similar to, and δD slightly higher, than those of groundwaters in Bangladesh reported by Aggarwal *et al.* (2000) (δD = -50 to -12‰, $\delta^{18}O$ = -7.2 to -2.4‰).

Isotopic composition of riverwater reflects most recent rainfall (overland-flow) and discharge of unconfined groundwater (base-flow) (Criss, 1999). Fig. 2–10a shows the monthly record of $\delta^{18}O$ of Old Brahmaputra riverwater during the period April to December 2004, when the values varied from -7.6 to -1.1‰(Fig. 2–10b). $\delta^{18}O$ value gradually increases during dry season due to discharging of unconfined groundwater to stream (Harvey *et al.*, 2005) and evaporation. The $\delta^{18}O$ of rain were -9.1, -3.7, -10.6, and -3.5‰, in middle of June, July, August and September, respectively. $\delta^{18}O$ of the rainwater largely vary, and no systematic variation with the sampling months. It is known that the stable isotope ratios of rain changes with the variation of volume and duration of precipitation and sampling timing during raining. Thus, those values do not reflect the average of rain at each month.

The isotope ratios of the groundwaters of the Pleistocene aquifers show a large

variation, i.e., $\delta^{18}O$ between -7.1 ~ -4.2 ‰ and δD between -47 and -25 ‰, respectively. The oxygen isotope ratios are consistent with those of riverwater during June to September. Thus, the groundwater in this aquifer must be recharged during the peak of rainy season without much contamination of surface water. The isotope ratios of groundwaters from the Holocene aquifer range between -6.2 to -2.0 ‰ for $\delta^{18}O$ and -40 and -8 ‰ for δD, much higher than those of the Pleistocene aquifer, implying that the surface water remained in the flood plain (mostly in ponds and channel) is contaminated into the aquifer after finishing the rainy season.

Table 2−1 shows the seasonal variation of $\delta^{18}O$ value of groundwaters collected in September-2003, end of rainy season; February-2004, end of dry season; and December-2004, middle of dry season. The $\delta^{18}O$ value of groundwaters in Pleistocene aquifers collected at different times do not show any change except for 3 groundwaters, where$\delta^{18}O$ varies by >0.5‰, and those collected from the shallow depths at the western terrace. This result indicates that residence time of these groundwaters is long enough to homogenize $\delta^{18}O$. The $\delta^{18}O$ of groundwaters from Holocene aquifers have similar values for samples collected in September-2003 and February-2004, except for only four groundwaters that show a change in $\delta^{18}O$ by >0.2‰. However, 52% of groundwaters from Holocene aquifers (13 out of 25) show in $\delta^{18}O$ value >0.2‰ difference between the samples collected in February and December, 2004. The $\delta^{18}O$ of the groundwaters taken in the February is higher than those in the December (10 out of 13), indicating the contamination of ^{18}O enriched water into the aquifer in the February.

Change in water table level clearly responded to the amount of precipitation (Fig. 2−10b). Since the groundwater table of Holocene aquifer is consistent with the level of surface water, the lowest water table in May is attributed to the drying up the surface water and also may be due to excessive drawing of groundwater during dry season. Sharp rising water table from May to July reflects recharge of rainwater. Change in water table becomes small from July to September due to saturation of aquifer.

A rough estimation of the residence time of the groundwaters can be made based on the ^{3}H data. Tritium was not detected (<0.5 TU) in the four groundwaters collected from the Pleistocene aquifer [60 m depth at Harihardi (*LDD 3*), 75 m Bara Khater Bhulua (*BKB 6*), 90 m Darikandi (*NKD5*), and 26 m Gulnagar (*GLG3*)] and one sample

from the Holocene aquifer [21 m at Daulaudi (*DLD6*)]. On the other hand, measurable ^{3}H was detected in the two groundwaters collected from the Holocene aquifer; one from a 18 m deep well in Darikandi (*DRK35*, 1.49 ± 0.38 TU) and the other from a 23 m deep well in the south of Mucharchar (*MCC22*, 2.84 ± 0.37 TU). Thus, the groundwaters collected from the Pleistocene aquifer have a longer residence time of more than at least 50 years, while the Holocene aquifer hosts groundwater recharged after 1953. Those results are consistent with the fact that large contribution of freshly recharged surface water in Holocene aquifer and less contribution in Pleistocene aquifer. Moreover, my results are roughly consistent with the estimation of residence time of unconfined groundwaters in the Munshiganji district by Klump *et al.* (2006), who suggested that residence time of groundwater in Holocene aquifer is gradually increased with depth, and varied from ca. 35 ~ 80 years from 10 to 40 m based on the $^{3}H/^{3}He$ measurements.

5. *Discussions*

5.1. Redox reaction in Holocene groundwater

The groundwaters in the sturdy area have the same geochemical characteristics with the previously reported As contaminated groundwaters; i.e., they contains low SO_4^{2-} and high NH_4^{+}, implying that As rich groundwater is formed under reducing condition. However, the concentrations of As are occasionally high in the groundwaters that have less or are even free from dissolved Fe, which is sensitive to ambient redox condition. Similar relationship between As and Fe has been observed by previous researchers who have studied several areas of Bangladesh; e.g., BGS&DPHE (2001), McArthur *et al.*, (2001) and Ahmed *et al.* (2004). Harvey *et al.* (2005) argued in detail about the relationship between Fe oxyhydroxide and As, and they noticed that the As rich groundwaters were mostly found in reducing grey Holocene sediments from not only their own study (Harvey *et al.*, 2002) but also in other studies (e.g., BGS and DPHE, 2001; van Geen *et al.*, 2003; McArthur *et al.*, 2004). However, since only a small amount of Fe oxyhydroxide is needed to explain the As concentration in the groundwater (Swartz *et al.*, 2004), Harvey *et al.* (2005) concluded that the aquifer sediments must be poised in a geochemical state where the inventory of Fe

oxyhydroxides was nearly (or recently) exhausted, yet As had not been flushed away by the flowing groundwater. Thus, the controversial observation has been neglected for hypothesizing the mechanism.

Concentration of NO_3^-, one of the strongest oxidants among major anions in the natural waters, of the groundwaters widely varies in the rainy season with the high values reaching 16 mg/L, while it is mostly <2 mg/L in the dry season even when the Eh is high. Reported values of NO_3^- in several regions of Bangladesh are generally lower than the values observed in this study, e.g., <0.22 mg/L (Bhattacharya *et al.* 2002), <1.32 mg/L (McArthur *et al.* 2004). NO_3^- produced from nitrification of soil organic matters does not commonly increase by >2 mg/L in the groundwater that is in close association with the natural biological process in common soil and sediments (Mueller and Helsel, 1996). Hence, seasonal variation of NO_3^- likely reflects impact of anthropogenic pollutants from surface during rainy season. Reduction of the groundwater occurs in the aquifer when the recharge stops after the rainy season. However, in some areas such as Daulaudi, Mammudi and northern Harihardi, where the Eh of groundwater increases in dry season, contribution of oxic water becomes more prominent. Lithology of the sediment column in Daulaudi and Mammudi demonstrate the absence of a silt/fine sand layer in the aquifer sediments, indicating higher permeability of the aquifer of those villages in comparison to the other villages in the studied area (Mitamura *et al.*, 2008). Thus, the vertical infiltration affects the permeable part of the aquifer more than the other parts. Such spatial variation of permeability related on the lithology of subsurface is reported from other studied sites (e.g., Métral *et al.* 2008). However, even if permeability is high, observed seasonal variation is very astonishing. Infiltrating water is very unlikely to reach greater depths in a couple of weeks or months in the environment formed by completely natural process. I suppose that presence of permeable flow path along well pipe or abandoned well causes this phenomenon.

Based on the hydraulic head data during pumping test and the $\delta^{18}O$ values of groundwaters at Munshiganji, 30 km south of Dhaka, Harvey *et al.* (2005) mentioned that there was convergent vertical flow that mixes water at a depth of about 30 m, and the circulation cell of groundwater flow scales within 10's and 100's of meters. They

also indicated that the aquifer was recharged in June when monsoon flooding began. Geochemical features of studied groundwaters are concordant with their results. $\delta^{18}O$ values of different seasons show only minor changes but chemical components, especially those derived from anthropogenic pollution such as Cl^-, show large variation, which indicate that the convergent flow is affected by the local source of chemicals. Reduction of the groundwater occurs in the aquifer when the recharge stops after the rainy season. However, in some areas such as Daulaudi, Mammudi and northern Harihardi, where the Eh of groundwater increases in dry season, contribution of oxic water becomes more prominent. Lithology of the sediment column in Daulaudi and Mammudi demonstrate the absence of a silt/fine sand layer in the aquifer sediments, indicating higher permeability of the aquifer of those villages in comparison to the other villages in the studied area (Mitamura *et al.*, 2008). Thus, the vertical infiltration affects the permeable part of the aquifer more than the other parts.

Dissolved Fe concentration is likely to be controlled by the solubility of Fe containing mineral(s) at a given redox condition. Ferrihydrite and goethite are stable in Holocene groundwater as shown in Fig. 2−8. Actually, brown patches believed to be Fe oxyhydroxides were occasionally found in the grey aquifer sediment (Mitamura *et al.*, 2008), and goethite was identified as an alteration product of magnetite in the Holocene aquifer sediment by XRD analysis (Seddique *et al.*, 2008). If Fe oxyhydroxide is stable in Holocene aquifer, it is wonder that where dissolved Fe coming from? According to the thermodynamic prediction, Fe can be dissolved in reducing groundwater in study area; e.g., groundwaters from Darikandi village (Fig. 2−8). Both Fe and HCO_3^- rich groundwaters, appeared in southern part of Harihardi, Darikandi, Bara Khater Bhulua villages, were supersaturated with siderite. If precipitation of siderite occurred in groundwaters giving high alkalinity, decomposition of Fe hydroxide is promoted by following reactions.

$$Fe^{2+} + CO_3^{2-} = FeCO_3(c)$$

$$Fe(OH)_3 + 3H^+ = Fe^{2+} + 3H_2O$$

Progressing this reaction, Fe^{2+} released from Fe hydroxide is finally fixed as siderite.

Because rate of inorganic precipitation of siderite is 8 orders lower than calcite in same saturation state (Concepcíon and Christopher, 2004), high saturation state needs to precipitate siderite. In Fig. 2–8, increase in Fe^{2+} plateaus when SI_{sid} becomes 1, implying that precipitation of siderite occurred $SI_{sid} > 1$. Once formed siderite can decompose again via intrusion of oxygenic water. Hence, relatively large change in Fe over the season likely reflects various redox transformation processes in response to water circulation. In addition to the redox transformation process, release of Fe via chemical weathering of biotite should be considered as noted in latter section (5.3).

Unlike dissolved Fe, As concentration does not change much in the groundwaters (mostly <20%) collected in different seasons. Groundwaters showing considerable change in the concentration of As, e.g., *DLD19*, *DRK36*, *GLK3*, and *TMD8* (Table 2–1) also show relatively large change in $\delta^{18}O$, i.e., -2.7 to -4.1, -3.9 to -3.3, -3.5 to -3.6, and -4.3 to -7.2‰ during rainy and dry seasons, respectively. The observed large variation of $\delta^{18}O$ indicates a large variation of influx of surface water into the aquifer. Arsenic concentration is obviously higher in rainy season in *DLD19*, *DRK36*, and *TMD8*, when the Eh is higher. The Fe concentration drastically increased (<0.1 mg/L to 8.6 mg/L) in *DRK36* in the dry season despite a considerable decline in As concentration (314 to 40 μg/L). Those are notable examples of different change in As and Fe corresponding to different redox condition.

Ionic valence controls mobility of As in groundwater. Dissolved As in groundwater are mostly inorganic oxyanions, such as trivalent arsenite and pentavalent arsenate (Smedley and Kinniburgh, 2002). Because mobility of arsenite is higher than arsenate, reduction of arsenate can be a trigger for As mobilization (e.g., Zobrist *et al.* 2000; Takahashi *et al.* 2004; Islam *et al.* 2004). As^{III}/total As ratio was determined only for the groundwaters collected in the dry season. The As^{III}/total As ratio does not correspond well to the Eh, i.e., it tends to be higher in the lower Eh groundwater, while being occasionally comparable in value to the higher Eh ones. Many researchers have reported that As^{III} is dominant in the As rich groundwaters of GMB delta, e.g., Bhattacharya *et al.*, (2002) suggested that 67 ~ 99% of As was As^{III} in nine As affected districts in Bangladesh. Long storage time until the analysis (~ 3 months at the maximum) is not the only reason for this discrepancy. As^{III} is high in the groundwaters

from the northern part of Harihardi and Mammudi, where As/Fe ratio and Eh is higher in the dry season than the rainy season. Some researchers have suggested that reduction of arsenate to arsenite is a dominant factor to mobilize As rather than the reduction of Fe oxyhydroxide based on field observation (Mitsunobu *et al.* 2006) and laboratory studies (Harbel and Fendorf, 2006; Kocar *et al.* 2006). In the study area, highest concentration of As is observed under moderately reducing condition (northern part of Harihardi) rather than more reducing condition (e.g., Darikandi and Bara Khater Bhulua). Low concentration of dissolved Fe in northern part of Harihardi indicates that Fe oxyhydroxides likely precipitate in the region. Our result suggests that As can mobilize regardless of stability of Fe oxyhydroxides.

5.2. Chemical weathering as controlling factor of groundwater chemistry

Groundwater chemistry in the study area indicates degree of chemical weathering. Ca^{2+}-HCO_3^- type major compositions of groundwaters from the Holocene aquifer indicate that Ca^{2+} is dissolved via chemical weathering of plagioclase, which is one of the primary controlling factors of the major chemical compositions of natural waters (Drever, 2002). Mg^{2+} has a weak positive relationship with HCO_3^- indicating that concentrations of Mg^{2+} is also attributed to the chemical weathering of basic minerals such as biotite and hornblende. Because concentrations of these cation in groundwater is obviously higher than riverwater, chemical weathering of minerals after recharging must be a primary factor to control chemical composition of groundwater. Additionally, Seddique *et al.* (2008) pointed out that plagioclase and biotite have higher concentrations in the Holocene aquifer than the Pleistocene sediments that host the confined aquifer and the overlying aquitard mud layer based on the mineralogical and chemical composition of the sediments of the aquifer drilled at Darikandi,.

If biotite is weathered in the aquifer sediment, the following reaction would occur;

$$2KMgFe_2AlSi_3O_{10}(OH)_2 + 14CO_2 + 15H_2O =$$

$$Al_2Si_2O_5(OH)_4 + 4Fe^{2+} + 2K^+ + 2Mg^{2+} + 14HCO_3^- + 4H_4SiO_4$$

When this reaction occurs in anoxic condition, Fe^{2+} can continue to exist in the

groundwater. High Fe and HCO_3^- groundwaters occur in the southern part of Harihardi, Darikandi, and Bara Khater Bhulua, that constitute an area which becomes reducing during the dry season. If the reaction occurs in oxic condition, then iron oxyhydroxide is precipitated by the following reaction;

$$2Fe^{2+} + O_2 + 2H_2O = 2FeOOH + 2H^+$$

When slightly oxic environment, where NO_3^-, SO_4^{2-} are available, Fe oxyhydroxide can be formed by consuming dissolved Fe present in the groundwater. Such an environment appears in the Holocene aquifer in the rainy season. Low Fe but high HCO_3^- occurs in the areas (Daulaudi, Mammudi, northern part of Harihardi) where the groundwater is more oxic and slightly acidic.

Detrital minerals are the likely primary source of As in GBM delta plain, although specific source mineral(s) and transport process of As from the river upstream has been rather neglected compared with explaining the As release from the secondary Fe oxyhydroxides. Sulfide minerals derived from granitic and metamorphic regions of the Himalaya is suggested as a source of As (Polizzotto *et al.* 2006). Some researchers suggested that As is highly concentrated in the silicate and/or sulfide phases of the sediments in GBM delta based on the selective chemical extraction (e.g., Anawar *et al.* 2003; Swartz *et al.* 2004). In the study area, however, As fixed in sulfide should be minor according to the low abundance of sulfide mineral (Seddique *et al.* 2008) and As K-edge XANES (Itai *et al.* 2006; Chapter 4 in this thesis). Most likely candidate of As fixing phase is biotite. Sengupta *et al.* (2004) measured As concentration in biotite, which is up to 9 mg/kg. In the studied area, the biotite from lower part of the Holocene aquifer contains more than 50 mg/kg of As at the maximum (Seddique *et al.* 2008). Because weathering rate of biotite is relatively fast among detrital silicate minerals, release of As from biotite via chemical weathering should be tested.

Combining the groundwater chemistry and the mineralogical evidence of the aquifer sediments, it is possible that the As is released from detrital biotite and/or other basic minerals via chemical weathering. Since the rate of weathering of detrital minerals is controlled by the solubility of SiO_2, the rate of weathering must increase with the increasing the flow rate the groundwater. Harvey *et al.* (2005) mentioned that As was

mobilized by the infiltration of modern water into the aquifer. Our studied groundwater chemistry also support accelerated groundwater flow in the Holocene aquifer.

6. Conclusion

In this chapter, I overviewed geochemical features on the As-contaminated groundwater in Sonargaon, in the mid-eastern Bangladesh. The range of dissolved As concentrations are varied from <1 to 1200 μg/L in Holocene aquifer, whereas that are <4.3 μg/L in Pleistocene aquifer. Groundwater in the Holocene aquifer gives Ca-Mg-HCO_3^- type chemistry to be formed via chemical weathering of detrital minerals such as plagioclase and biotite. General reducing features of As-contaminated groundwater is consistent with other part of Bangladesh. However, redox behavior between As and Fe is not straightforward. Concentration of dissolved Fe which likely originated from detrital biotite is controlled by precipitation/dissolution of Fe oxyhydroxide and siderite at a given redox condition. Reduction of arsenate to arsenite is also contributed to mobilize As.

Patchy distribution of high-As groundwater in Holocene aquifer is marked in our study area as well as some previous studies. Large variation of $\delta^{18}O$ indicates that shallow groundwater is circulated in spatially small scale. Accelerated vertical infiltration of surface water, which can be induced by lowering of water table due to excessive drawing of groundwater, plausibly promotes the water-sediment interaction in the Holocene aquifer, where relatively unaltered detrital minerals still exist. I believe the observed facts are applicable for other As-contaminated modern aquifers.

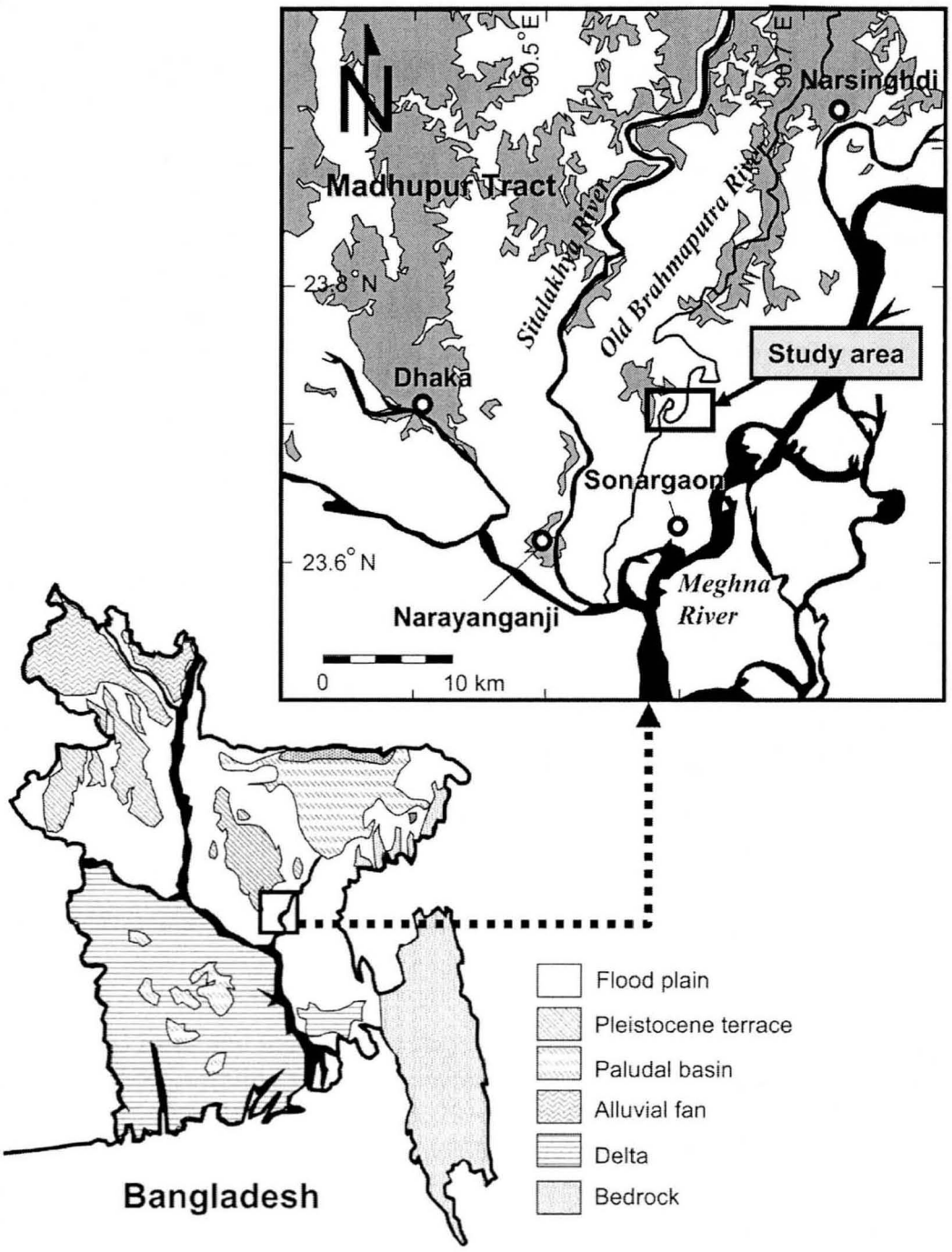

Fig. 2-1. (a) Physiographic map of Bangladesh. (b) Location map of the study area.

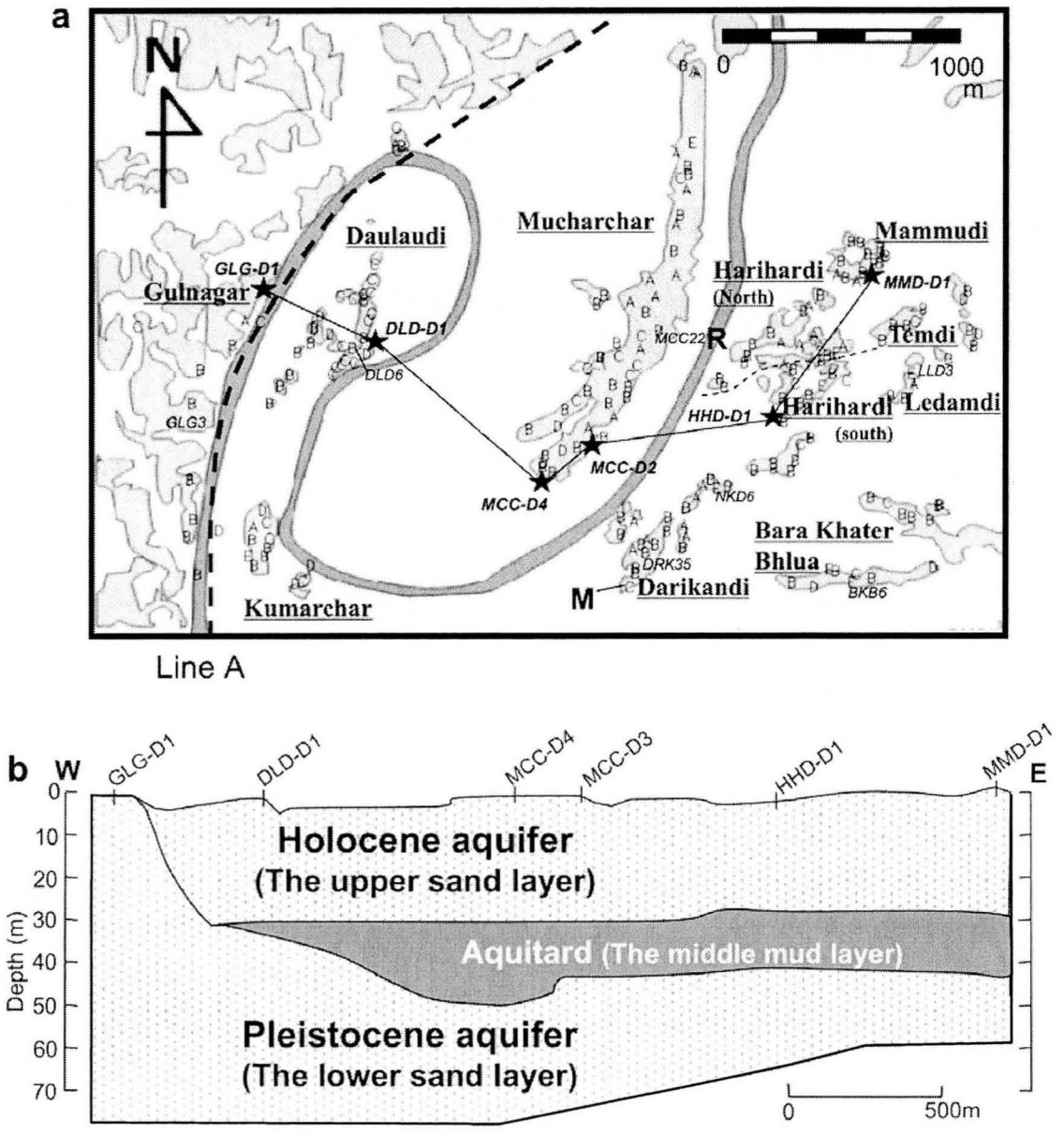

Fig. 2-2. (a) Enlarged topographic map of the study area. Plotted symbols corresponds to the location of sampling wells. The symbols of A, B, C, D, and E represent samples collected from 8 ~ 20 m, 20 ~ 28 m, 28 ~ 36 m (Holocene aquifer), 36 ~ 60 m (unspecified groundwater), and below 60 m (confined groundwater), respectively. The location of drill sites are represented by star symbol. Italicised names are the specific names of the wells where ^{3}H was analyzed. Line A is the approximate boundary that separates Madhupur Tract (west) from the alluvial plain (east). "R" represents the sampling place of river water. "M" represents the location of monitoring wells. (b) Schematic geological cross section of study area.

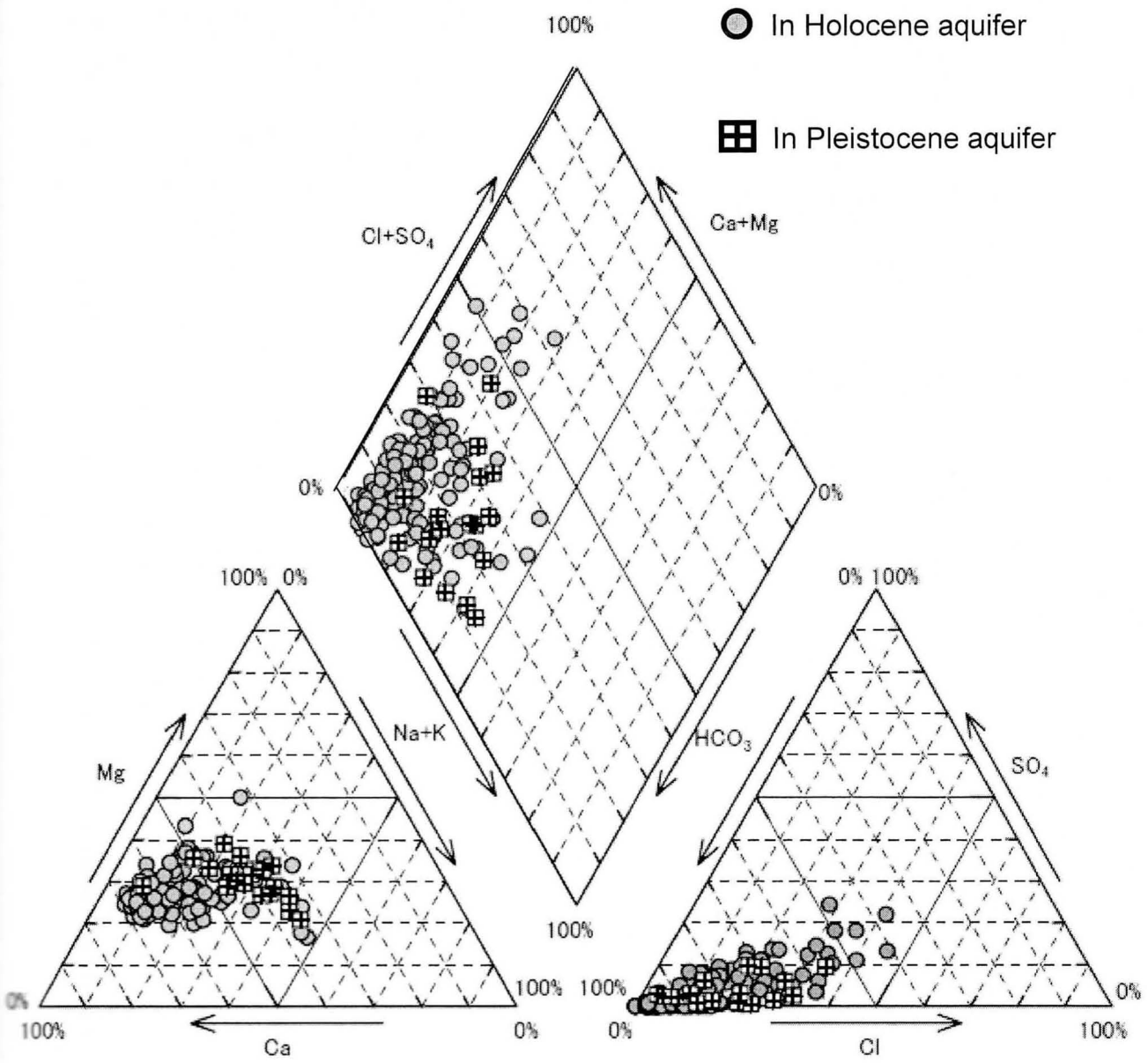

Fig. 2-3. Piper diagram plotted on the aqueous components of well waters. Shaded circle represents groundwater from Holocene aquifer. Square with cross represents groundwater from Pleistocene aquifer.

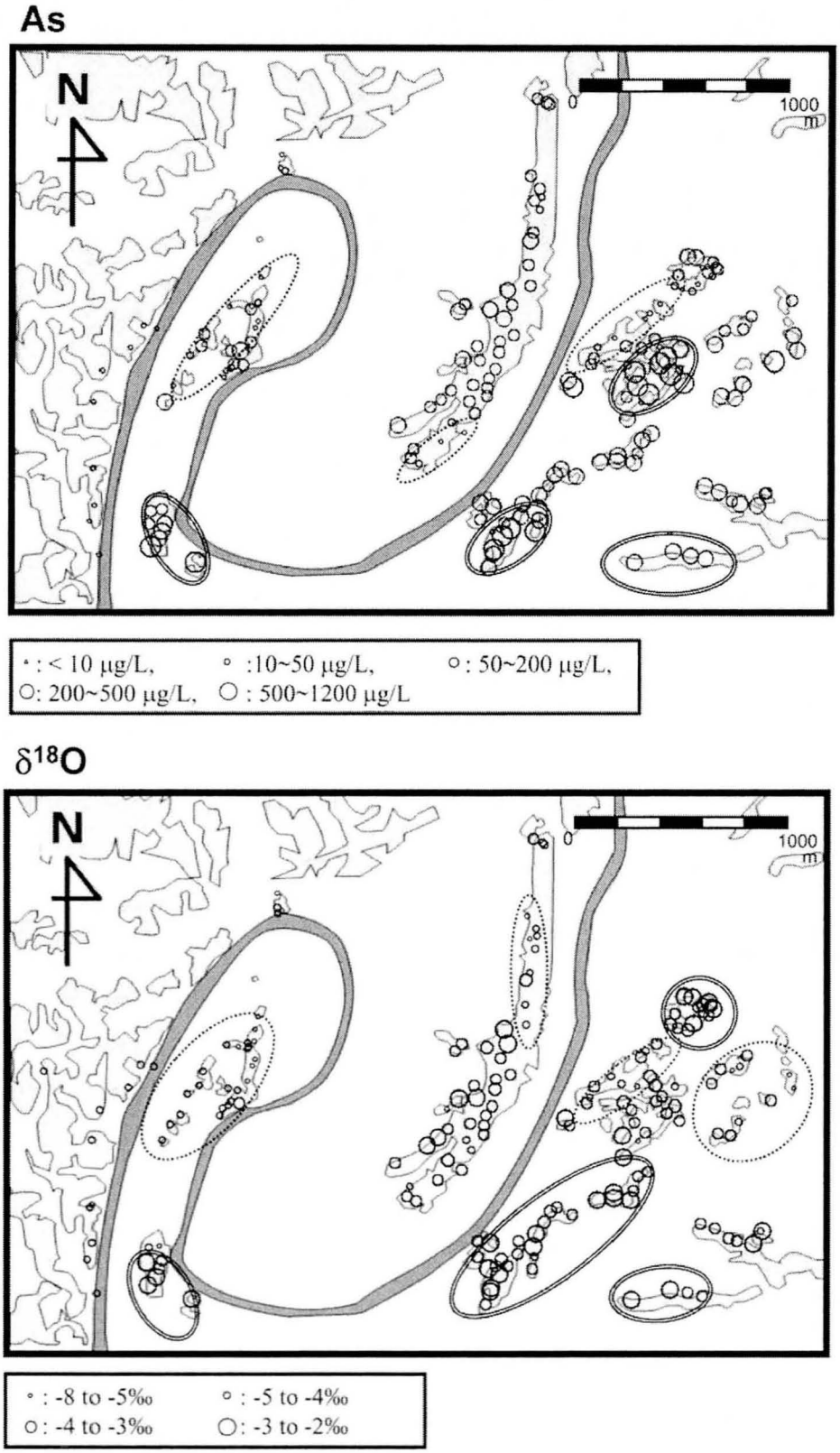

Fig. 2-4. Map of the distribution of (a) As and (b) $\delta^{18}O$ in dry season. Data of shallow groundwater (<36 m) only are plotted. Regions of high As (or $\delta^{18}O$) are encircled by double lines, while regions of low values (or $\delta^{18}O$) are encircled by dotted lines.

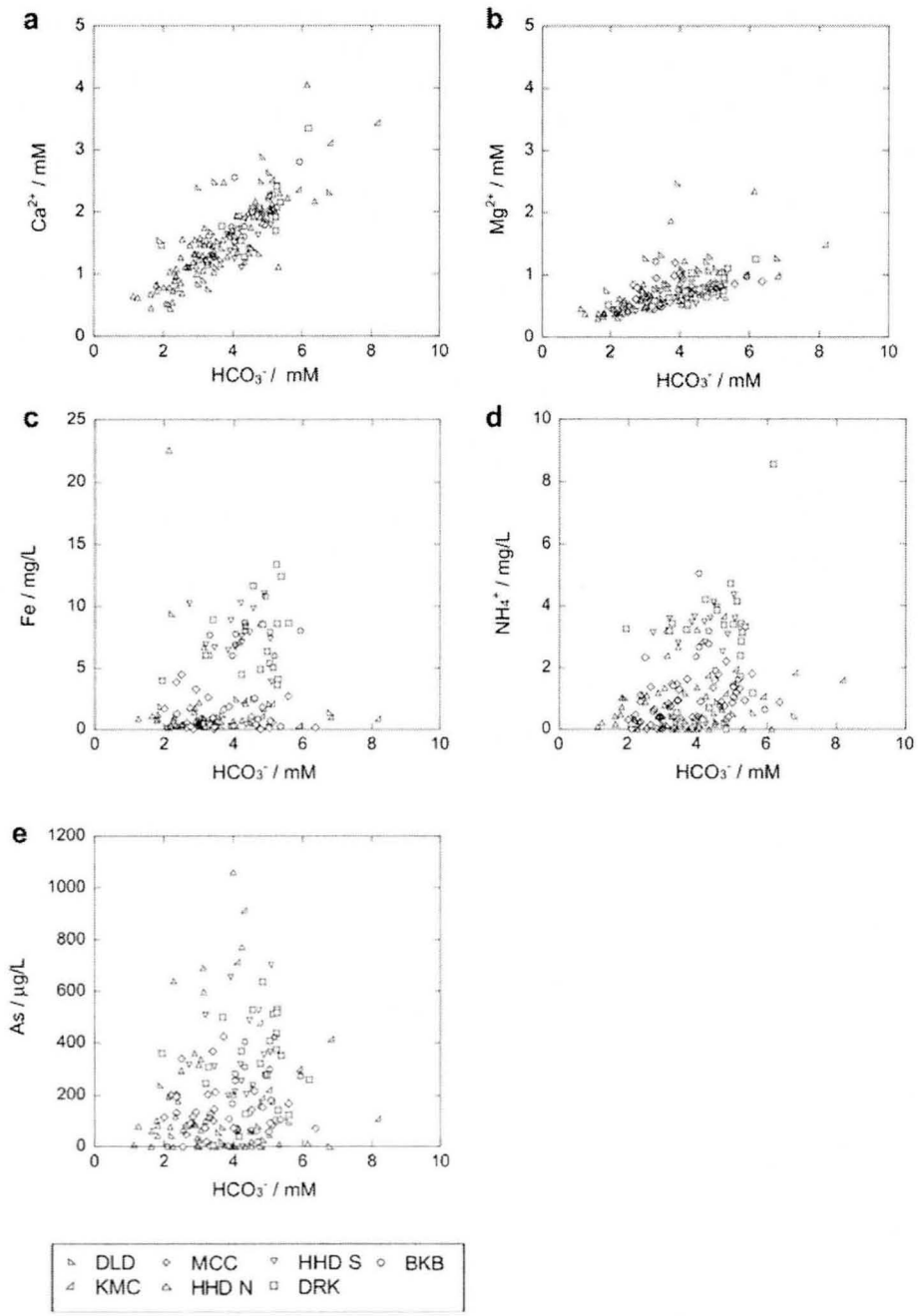

Fig. 2-5. Relationships between HCO_3^- and some dissolved components. The results for dry season are shown. Each symbol represents an area where well water was collected. DLD: Daulaudi, KMC: Kumarchur, MCC: Mucharchar, HHD N: north Harihardi, Mammudi, and Temdi, HHD S: south Harihardi, DRK: Darikandi, and BKB: Bara Khater Bhulua.

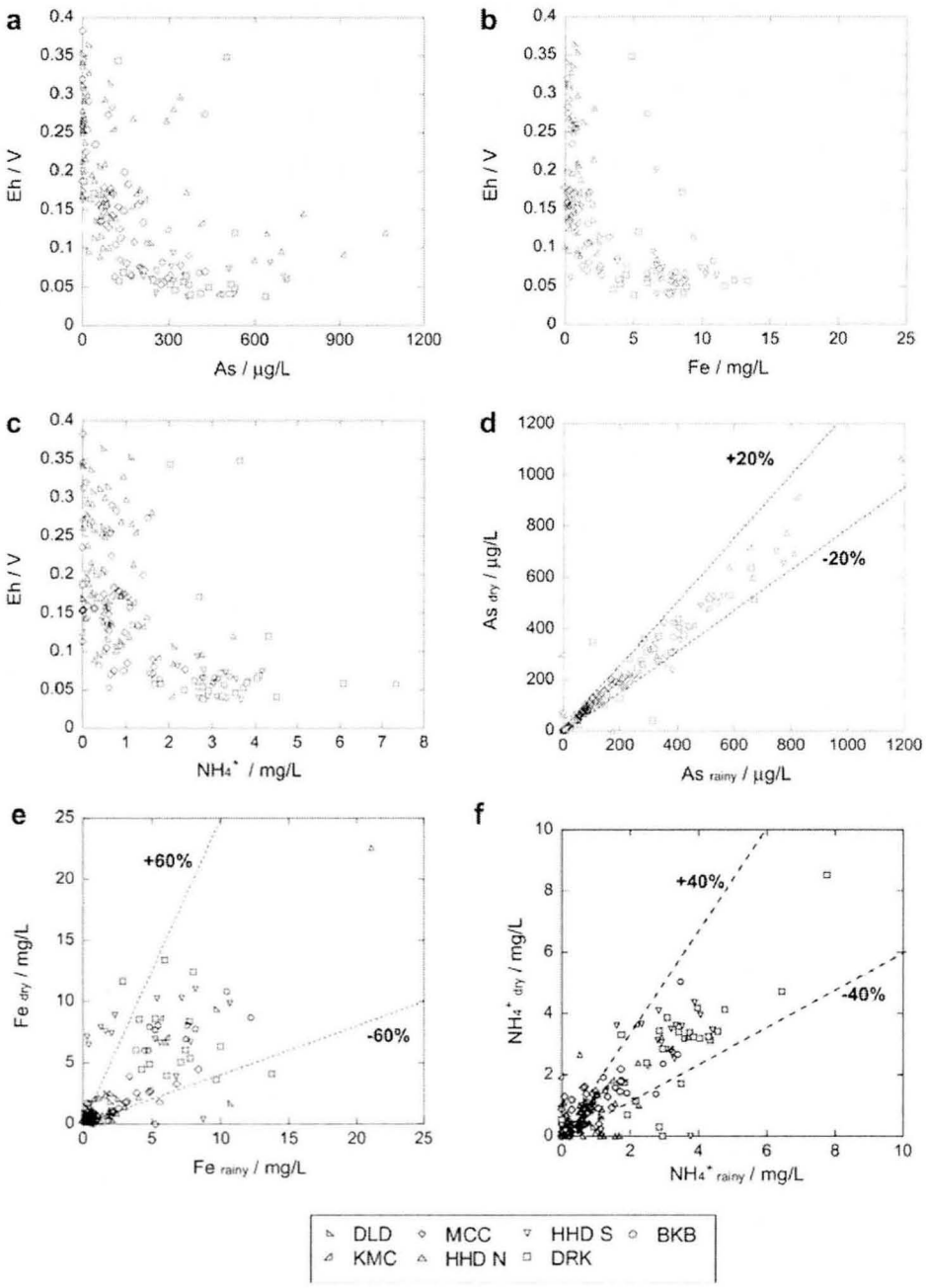

Fig. 2-6. (a)~(c): Relationships between Eh and other dissolved components. Abbreviated village name are as described in Fig. 2-5. Solid symbols represent samples of the rainy season, while open symbols represent samples of the dry season. (d)~(f): variation in concentration of As, Fe, and NH4+ between rainy and dry season.

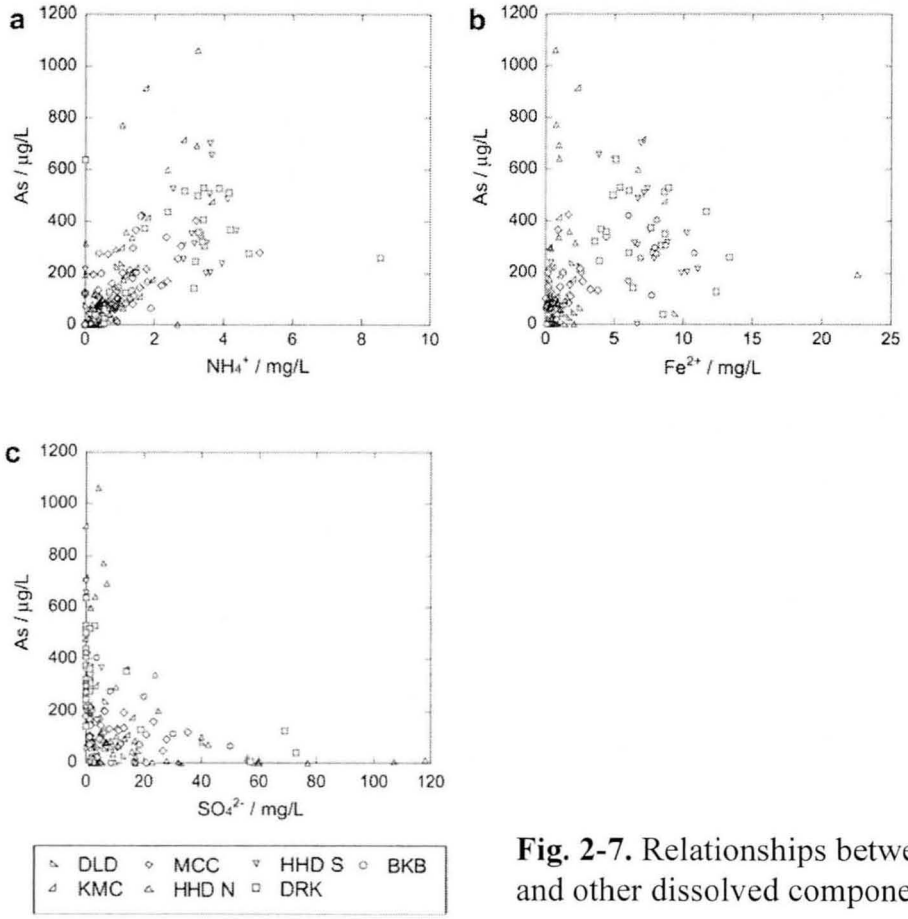

Fig. 2-7. Relationships between As and other dissolved components.

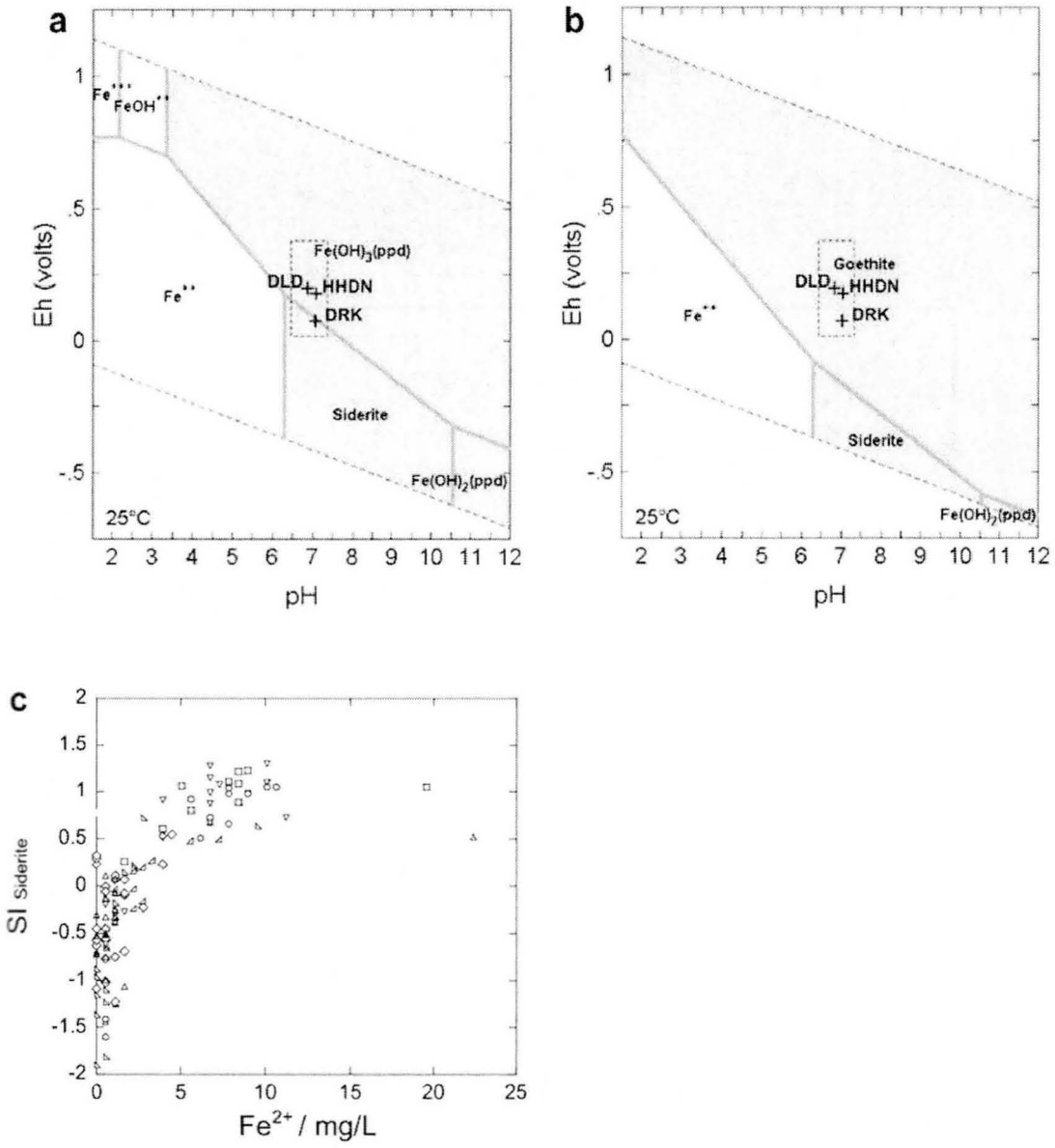

Fig. 2-8. (a)-(c) Eh-pH diagram for the system Fe-O_2-CO_2-H_2O, assuming total dissolved carbonate equals $10^{-2.2}$ mol/kg, and total dissolved Fe is 10^{-3} mol/kg. The diagram is drawn using the Geochemist's Workbench version 6.0 (Bethke, 2006) with following constraints. (a) Precipitation of hematite, goethite, magnetite, FeO(c) and siderite are suppressed, (b) siderite is allowed to precipitate, and (c) siderite and goethite are allowed to precipitate. The regions framed by dotted line indicate range in Eh-pH in Holocene groundwater. Three symbols plotted in (b) represents average of groundwater collected from each village. (d) Relationship between saturation index of siderite and concentration of Fe^{2+}. Symbols are as described in Fig. 2-5.

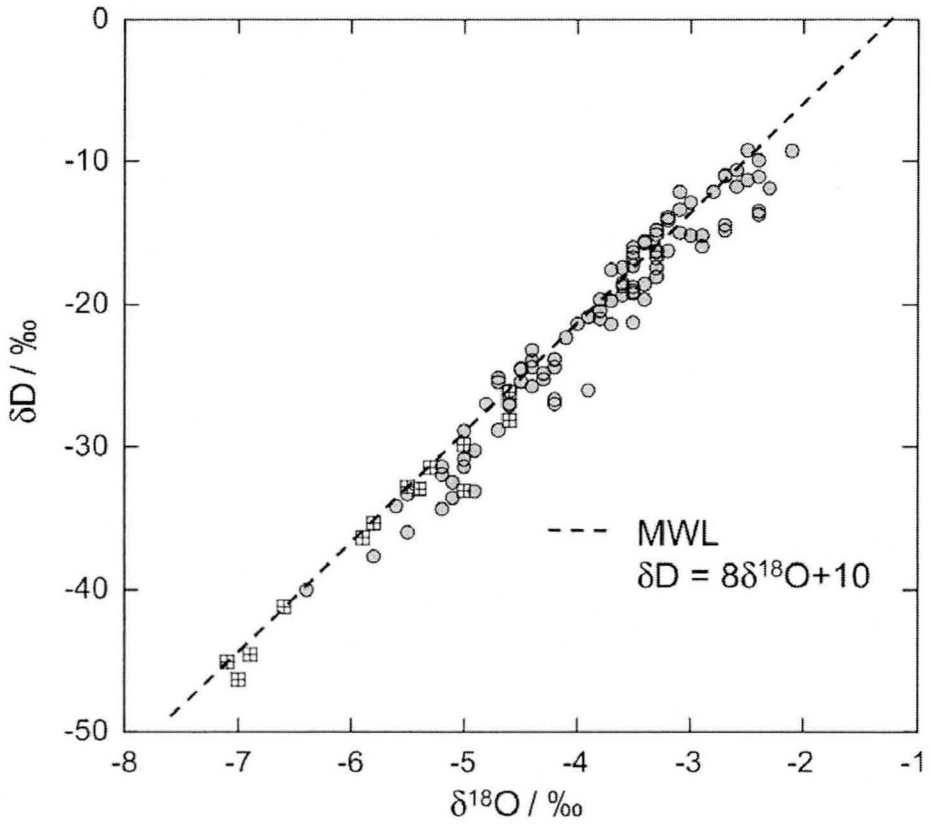

Fig. 2-9. Relationships between δ D and δ ^{18}O of groundwater. The results for dry season are shown. Symbols are as described in Fig. 2-3.

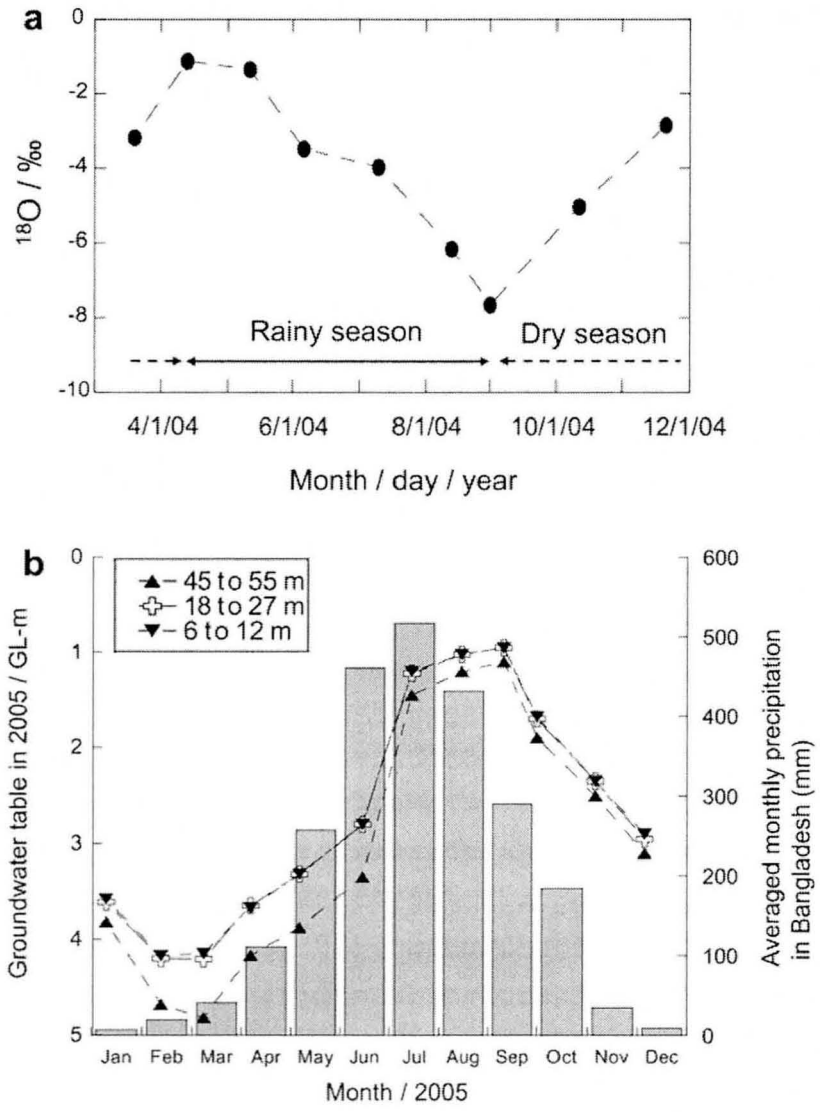

Fig. 2-10. (a) Seasonal variation in $\delta^{18}O$ value of the Old Brahmaputra river during the period April to December 2004. (b) Seasonal variation in groundwater table and monthly averaged rainfall in Bangladesh during 2005. Water table was monitored from the monitoring well (specified in Fig. 2-2). Each symbol specifies the depth of the screen. The averaged rainfall is inferred from the data cited on the web site of Bangladesh Meteorological Department (http://www.bangladeshonline.com/bmd/).

Table 1. Chemical composition of groundwaters collected from Holocene aquifer (unit: mg/L, except for Eh, As, and $\delta^{18}O$)

Sample	Village	Depth (m)	pH Sep	pH Feb	Eh (V) Feb	As (μg/L) Sep	As (μg/L) Feb	% As^{III} Feb	Na^+ Feb	K^+ Feb	Ca^{2+} Feb	Mg^{2+} Feb	NH_4^+ Sep	NH_4^+ Feb	Cl^- Sep	Cl^- Feb	NO_3^- Sep	NO_3^- Feb	SO_4^{2-} Sep	SO_4^{2-} Feb	PO_4^{3-} Sep	PO_4^{3-} Feb	Fe Sep	Fe Feb	DOC Feb	Acetate Sep	Acetate Feb	$\delta^{18}O$ (‰) Sep	$\delta^{18}O$ (‰) Feb	$\delta^{18}O$ (‰) Dec
Holocene aquifer																														
DLD1	Daulaudi	31	6.9	6.9	0.207	3.2	1.8	U.D.	7.6	0.9	67	19	0.3	0.2	42	32	U.D.	U.D.	8.1	5.5	U.D.	0.6	0.1	0.9	N/A	7.0	8.1	-4.5	-4.7	N/A
DLD2	Daulaudi	29	7.0	7.1	0.319	U.D.	2.4	U.D.	15	U.D.	100	26	0.4	0.2	59	70	U.D.	0.8	8.6	5.1	0.2	U.D.	0.1	0.2	N/A	8.3	9.6	-4.4	-4.4	N/A
DLD3	Daulaudi	29	7.0	7.0	0.171	25	26	U.D.	18	0.9	116	31	0.5	0.3	72	101	U.D.	1.2	12	13	U.D.	U.D.	11	1.7	N/A	8.5	9.8	-4.4	-4.4	N/A
DLD4	Daulaudi	34	7.1	6.9	0.143	56	47	U.D.	22	1.1	105	27	0.7	0.5	72	83	U.D.	1.1	19	18	U.D.	U.D.	2.5	2.1	N/A	8.7	9.9	-4.1	-4.2	N/A
DLD5	Daulaudi	31	7.2	7.1	0.165	75	76	U.D.	7.7	U.D.	56	14	0.6	U.D.	2.5	3.5	0.1	U.D.	0.7	1.7	U.D.	U.D.	0.7	1.2	N/A	6.9	8.1	-3.7	-3.7	N/A
DLD6	Daulaudi	21	7.1	7.1	0.114	196	238	46	20	1.0	61	18	2.1	1.0	26	25	0.1	0.6	5.8	6.6	0.1	0.3	1.9	1.9	N/A	7.5	8.6	-4.8	-4.8	-5.3
DLD8	Daulaudi	27	7.2	7.4	0.123	61	65	66	23	3.2	58	18	0.6	0.3	27	17	0.1	0.6	U.D.	3.9	12	U.D.	1.6	2.5	N/A	7.3	8.2	-5.0	-5.2	N/A
DLD10	Daulaudi	32	7.2	7.1	0.173	8.8	U.D.	U.D.	48	U.D.	100	32	0.6	0.4	14	16	U.D.	0.5	1.4	3.1	0.1	U.D.	2.1	0.4	N/A	N/A	7.6	-5.2	-5.2	N/A
DLD11	Daulaudi	34	7.1	7.1	0.261	U.D.	U.D.	U.D.	27	2.5	44	15	0.5	0.2	13	12	U.D.	0.5	0.9	1.8	U.D.	U.D.	0.1	0.4	N/A	6.5	7.6	-5.1	-5.2	N/A
DLD13	Daulaudi	27	7.0	6.9	0.316	U.D.	U.D.	U.D.	32	1.3	64	26	0.2	0.1	51	48	0.1	0.7	17	17	0.1	U.D.	0.3	0.3	N/A	6.2	10	-4.7	-4.7	N/A
DLD14	Daulaudi	32	7.1	7.2	0.372	16	20	U.D.	21	2.7	49	13	0.5	0.4	13	13	U.D.	0.6	0.7	1.9	0.3	0.4	0.1	0.7	N/A	6.3	9.2	-5.1	-5.1	N/A
DLD15	Daulaudi	32	7.1	6.9	0.361	U.D.	U.D.	U.D.	26	U.D.	37	17	1.1	0.1	13	13	0.1	0.6	0.7	1.7	0.2	U.D.	0.1	0.9	N/A	N/A	7.3	-5.2	-5.2	N/A
DLD16	Daulaudi	29	7.0	6.6	0.344	U.D.	U.D.	U.D.	30	U.D.	31	19	0.2	U.D.	13	13	U.D.	0.5	0.7	1.7	0.1	U.D.	0.2	0.6	N/A	6.1	7.4	-5.1	-5.1	N/A
DLD17	Daulaudi	24	7.0	6.9	0.114	231	225	N/A	12	1.3	57	16	0.8	0.8	8.5	8.5	0.1	U.D.	0.8	1.6	U.D.	U.D.	2.0	2.5	N/A	7.7	9.1	-4.3	-4.2	N/A
DLD18	Daulaudi	21	7.2	6.7	0.184	U.D.	U.D.	U.D.	17	U.D.	57	26	0.3	0.2	21	18	U.D.	0.6	24	21	U.D.	U.D.	0.1	0.5	N/A	7.7	9.2	-5.0	-4.9	N/A
DLD19	Daulaudi	21	7.1	6.8	0.267	138	U.D.	U.D.	13	U.D.	50	21	0.7	1.1	24	14	U.D.	0.5	12	5.1	U.D.	U.D.	1.8	0.6	N/A	5.3	7.9	-2.7	-4.1	N/A
DLD20	Daulaudi	21	7.0	6.9	0.103	24	21	U.D.	13	U.D.	46	19	0.4	0.3	15	13	U.D.	0.5	0.9	2.1	0.2	U.D.	0.1	0.2	N/A	N/A	7.5	-4.4	-4.4	N/A
DLD21	Daulaudi	23	7.0	7.1	0.177	57	55	4	16	U.D.	61	21	U.D.	0.4	32	33	U.D.	0.6	3.5	6.3	0.1	U.D.	0.8	1.0	N/A	6.8	7.9	-4.5	-4.5	-5.0
DLD25	Daulaudi	21	6.9	7.1	0.320	U.D.	U.D.	U.D.	38	3.7	64	60	U.D.	0.2	101	154	0.1	1.2	65	60	0.1	U.D.	0.3	0.3	N/A	9.1	10	-4.3	-4.3	N/A
DLD27	Daulaudi	34	6.9	7.1	0.349	U.D.	U.D.	U.D.	12	U.D.	53	29	U.D.	0.2	26	27	U.D.	0.5	0.8	1.8	0.1	U.D.	0.1	0.1	N/A	6.6	8.6	-4.8	-4.6	N/A
DLD28	Daulaudi	31	6.9	6.5	0.270	U.D.	U.D.	U.D.	19	2.2	93	31	0.5	0.4	51	77	U.D.	0.8	1.2	2.6	U.D.	U.D.	0.1	1.4	N/A	N/A	9.7	-5.3	-5.1	N/A
DLD30	Daulaudi	34	6.8	6.9	0.266	U.D.	U.D.	U.D.	33	0.2	54	25	0.3	0.5	48	52	0.2	0.7	9.9	11	0.1	U.D.	0.2	0.6	N/A	7.3	9.1	-4.6	-4.4	N/A
DLD31	Daulaudi	35	6.6	6.9	0.176	U.D.	U.D.	U.D.	35	1.7	96	31	0.3	0.4	64	88	0.1	1.8	32	33	U.D.	U.D.	0.2	0.3	N/A	8.1	7.3	-4.6	-4.4	N/A
DLD33	Daulaudi	26	6.6	7.0	0.121	46	42	77	24	U.D.	18	7.8	0.9	0.3	8.0	8.1	U.D.	0.9	2.9	3.6	U.D.	U.D.	9.7	9.4	N/A	4.9	5.4	-5.2	-5.2	N/A
DLD34	Daulaudi	18	6.6	7.0	0.273	2.9	2.6	U.D.	28	U.D.	34	17	0.2	0.1	12	12	U.D.	0.8	1.2	2.0	0.5	0.5	0.2	0.8	N/A	6.5	7.2	-4.9	-4.9	-5.0
KMC2	Kumarchar	34	6.9	6.7	0.068	656	716	67	7.8	4.0	70	16	3.0	2.7	21	17	0.3	U.D.	U.D.	U.D.	U.D.	U.D.	6.2	7.1	N/A	7.2	7.1	-2.5	-2.6	N/A
KMC7	Kumarchar	31	6.9	6.6	0.262	104	110	38	37	4.2	138	36	1.3	1.5	43	53	1.5	0.2	18	15	U.D.	U.D.	0.5	0.9	N/A	11	8.5	-5.4	-5.5	N/A
KMC8	Kumarchar	20	6.8	6.6	0.179	194	190	45	15	8.7	73	21	0.9	1.1	14	14	0.1	U.D.	1.3	1.6	0.4	0.3	2.1	1.1	N/A	8.3	13	-4.4	-4.3	N/A
KMC9	Kumarchar	21	6.8	6.7	0.162	205	176	41	22	3.6	101	25	U.D.	1.9	U.D.	59	0.1	U.D.	14	16	U.D.	0.8	0.8	2.1	N/A	8.7	8.7	-3.1	-2.7	N/A
KMC10	Kumarchar	31	7.2	6.7	0.171	267	222	70	15	3.7	91	18	1.2	1.4	6.0	6.6	1.5	U.D.	0.7	1.3	U.D.	0.2	0.5	0.6	2.7	8.2	8.2	-3.7	-3.8	N/A
KMC12	Kumarchar	24	7.1	6.8	0.049	511	478	42	18	11	77	17	2.1	3.5	19	19	0.1	U.D.	U.D.	U.D.	U.D.	U.D.	5.7	8.7	N/A	7.5	7.2	-2.8	-2.7	N/A
KMC13	Kumarchar	23	7.2	6.9	0.140	460	416	52	16	5.6	125	24	1.4	1.7	22	24	0.1	0.1	U.D.	U.D.	0.2	U.D.	0.5	1.0	N/A	9.4	9.0	-3.7	-3.5	-3.7
KMC14	Kumarchar	21	7.3	6.5	0.099	826	914	48	12	3.2	77	15	1.8	1.7	13	23	0.4	U.D.	0.6	U.D.	U.D.	U.D.	1.6	2.4	N/A	4.9	7.3	-2.8	-2.4	N/A
MCC1	Mucharchar	24	7.0	6.9	0.092	155	131	57	5.9	U.D.	39	11	1.0	0.9	5.9	7.0	1.1	U.D.	17	11	U.D.	0.3	3.4	3.9	N/A	4.5	4.8	-3.5	-3.3	N/A
MCC3	Mucharchar	24	7.0	7.0	0.298	18	20	U.D.	6.6	U.D.	50	13	0.7	0.7	12	5.1	0.7	0.1	11	3.8	0.3	U.D.	0.3	U.D.	N/A	5.0	5.8	-3.6	-3.4	N/A
MCC5	Mucharchar	15	6.7	6.8	0.242	50	45	30	15	U.D.	45	20	U.D.	0.1	27	32	0.4	U.D.	21	27	U.D.	U.D.	0.8	0.5	N/A	5.5	5.6	-3.8	-3.7	-3.9
MCC11	Mucharchar	20	7.1	7.1	0.179	90	82	39	8.0	1.3	44	11	0.7	1.3	4.1	6.0	U.D.	0.1	0.8	1.7	U.D.	0.2	0.7	0.2	N/A	N/A	3.6	-3.0	-2.8	N/A
MCC12	Mucharchar	21	6.9	6.9	0.112	118	116	63	7.6	1.8	32	11	0.6	0.3	11	9.5	U.D.	0.1	8.1	6.0	U.D.	U.D.	3.1	1.7	1.5	4.3	4.6	-4.1	-4.2	-4.4
MCC14	Mucharchar	23	7.0	7.0	0.352	1.2	2.6	U.D.	16	49	51	24	U.D.	U.D.	43	24	U.D.	0.2	35	17	U.D.	U.D.	0.3	U.D.	2.9	5.6	5.8	-4.1	-3.9	-4.5
MCC15	Mucharchar	21	7.0	7.2	0.390	U.D.	U.D.	U.D.	13	3.0	52	23	U.D.	0.4	25	44	U.D.	U.D.	11	21	U.D.	U.D.	0.3	U.D.	2.0	5.2	5.1	-4.0	-3.8	N/A
MCC16	Mucharchar	18	7.0	6.9	0.138	89	84	43	9.4	1.7	44	15	0.6	0.6	42	15	0.1	U.D.	32	6.0	U.D.	U.D.	3.1	1.7	N/A	N/A	4.1	-5.0	-4.9	N/A
MCC17	Mucharchar	23	6.9	7.0	0.281	95	90	27	16	U.D.	59	19	0.1	0.6	40	50	U.D.	U.D.	23	28	U.D.	U.D.	0.7	0.2	N/A	6.5	4.5	-3.9	-3.7	N/A
MCC18	Mucharchar	31	7.1	7.1	0.206	65	71	25	11	4.2	78	23	0.6	0.8	27	35	U.D.	U.D.	13	19	0.1	U.D.	0.3	U.D.	4.4	6.6	8.0	-3.5	-3.5	N/A
MCC19	Mucharchar	32	7.1	7.2	0.181	89	74	76	12	3.9	65	25	0.5	0.4	5.7	25	U.D.	U.D.	4.0	12	U.D.	U.D.	1.8	0.3	N/A	7.4	5.4	-3.5	-3.3	N/A
MCC20	Mucharchar	18	7.0	7.1	0.156	134	144	60	8.2	1.8	70	18	0.6	1.5	4.2	8.0	U.D.	U.D.	0.9	5.0	U.D.	U.D.	2.1	1.1	N/A	N/A	6.2	-3.8	-3.7	N/A
MCC21	Mucharchar	35	7.0	7.1	0.162	78	84	34	15	2.1	86	18	0.3	1.1	42	4.5	U.D.	U.D.	22	1.5	U.D.	U.D.	1.1	0.6	N/A	N/A	7.3	-3.6	-3.6	N/A
MCC22	Mucharchar	23	6.9	6.9	0.178	124	108	51	21	3.9	65	29	1.1	0.4	7.3	39	2.5	U.D.	1.3	21	0.2	U.D.	3.2	1.8	N/A	N/A	6.1	-3.8	-3.9	-4.4
MCC23	Mucharchar	25	7.1	7.1	0.141	216	213	99	6.2	1.3	51	12	1.3	1.2	4.2	8.5	U.D.	U.D.	0.9	1.7	U.D.	0.6	1.0	0.3	N/A	N/A	4.4	-3.3	-3.5	N/A
MCC24	Mucharchar	20	7.0	7.1	0.082	209	203	N/A	7.2	U.D.	47	11	0.9	1.4	6.0	4.8	3.0	U.D.	5.7	1.8	U.D.	U.D.	4.8	2.6	N/A	N/A	4.3	-3.0	-3.1	N/A
MCC25	Mucharchar	20	7.0	7.3	0.082	173	202	36	6.6	1.7	39	9	0.7	1.0	21	6.4	0.8	U.D.	11	6.4	0.1	1.1	2.6	1.3	N/A	N/A	3.1	-2.9	-2.8	N/A
MCC26	Mucharchar	20	7.0	7.0	0.161	104	125	N/A	12	0.2	59	14	U.D.	U.D.	40	24	U.D.	U.D.	3.2	12	U.D.	0.3	0.7	0.4	N/A	5.2	4.5	-3.6	-4.1	-4.3
MCC31	Mucharchar	18	7.0	7.1	0.134	81	93	45	10	2.2	81	19	0.6	1.0	49	31	U.D.	U.D.	8.0	4.7	U.D.	U.D.	1.0	0.7	N/A	8.1	6.3	-4.3	-4.2	N/A
MCC32	Mucharchar	18	6.9	6.9	0.132	105	131	35	10	1.6	79	18	1.0	1.3	15	45	U.D.	U.D.	0.3	8.0	U.D.	U.D.	1.4	U.D.	N/A	6.9	5.7	-4.7	-4.8	N/A
MCC33	Mucharchar	21	7.1	7.2	0.115	175	181	31	8.5	U.D.	82	17	0.9	1.3	11	15	U.D.	U.D.	0.8	U.D.	0.4	U.D.	2.4	U.D.	4.5	7.2	6.2	-3.2	-3.3	N/A
MCC34	Mucharchar	23	7.1	7.2	0.087	144	153	43	18	2.7	82	19	1.6	2.1	48	11	U.D.	U.D.	0.8	1.4	8.9	U.D.	5.6	1.8	2.7	8.3	6.7	-4.6	-4.5	-4.6
MCC37	Mucharchar	23	6.6	7.1	0.150	95	104	54	10	U.D.	81	19	0.1	1.2	3.0	3.2	0.8	U.D.	1.0	1.5	0.3	0.4	0.4	U.D.	N/A	N/A	6.8	-5.7	-4.1	N/A
MCC38	Mucharchar	24	7.0	6.9	0.261	35	18	U.D.	8.5	3.6	82	17	0.6	0.8	16	4.1	U.D.	U.D.	0.9	2.0	0.3	U.D.	0.8	0.8	N/A	8.2	6.1	-4.1	-4.1	N/A
MCC39	Mucharchar	32	6.9	6.8	0.290	81	105	47	27	1.4	92	26	0.8	0.9	4.8	15	U.D.	U.D.	1.8	1.4	0.2	0.3	0.2	0.2	N/A	9.4	7.2	-5.2	-5.3	N/A
MCC40	Mucharchar	14	7.1	7.2	0.232	17	12	U.D.	12	2.0	75	19	0.7	0.9	2.4	5.2	U.D.	U.D.	0.3	2.4	U.D.	0.3	0.2	U.D.	N/A	7.9	7.4	-4.9	-4.9	-4.8
MCC41	Mucharchar	21	7.0	7.2	0.072	162	169	51	8.8	2.7	89	21	1.7	1.7	3.4	3.0	U.D.	U.D.	0.9	1.1	U.D.	U.D.	5.0	2.7	1.5	8.5	7.8	-4.6	-4.6	N/A

Table 1. Chemical composition of groundwaters collected from Holocene aquifer (unit: mg/L, except for Eh, As, and $\delta^{18}O$)

Sample	Village	Depth	pH		Eh (V)	As (μg/L)		% As^{III}	Na^+	K^+	Ca^{2+}	Mg^{2+}	NH_4^+		Cl^-		NO_3^-		SO_4^{2-}		PO_4^{3-}		Fe		DOC	Acetate		$\delta^{18}O$ (‰)		
		(m)	Sep	Feb	Feb	Sep	Feb	Feb	Feb	Feb	Feb	Feb	Sep	Feb	Sep	Feb	Sep	Feb	Sep	Feb	Sep	Feb	Sep	Feb	Feb	Sep	Feb	Sep	Feb	Dec
MCC42	Mucharchar	20	7.1	7.2	0.078	241	216	58	8.6	1.8	77	18	1.6	1.7	3.2	3.7	U.D.	U.D.	1.0	1.3	0.2	U.D.	3.9	2.5	N/A	8.1	6.9	-3.9	-3.9	N/A
MCC43	Mucharchar	27	7.0	7.0	0.164	59	60	N/A	12	2.5	89	21	0.3	0.8	4.8	3.4	U.D.	U.D.	U.D.	1.5	U.D.	U.D.	0.5	0.1	1.9	9.0	8.1	-4.1	-4.0	N/A
MCC50	Mucharchar	23	6.7	6.9	0.084	275	340	70	5.7	1.0	34	10	2.4	2.2	37	5.2	U.D.	U.D.	5.7	1.3	U.D.	U.D.	8.4	4.5	N/A	4.1	3.9	-3.8	-3.9	N/A
MCC53	Mucharchar	23	7.1	7.3	0.185	130	99	56	8.0	1.9	58	12	0.8	0.9	8.7	5.3	U.D.	U.D.	0.1	1.4	0.1	0.3	0.8	U.D.	N/A	6.1	5.5	-3.0	-3.0	-3.1
MCC54	Mucharchar	29	7.1	7.1	0.186	73	74	37	7.4	2.7	59	13	0.9	0.8	15	8.2	0.6	0.1	8.5	2.0	0.1	0.2	0.3	U.D.	N/A	6.3	5.5	-2.5	-2.4	N/A
MCC55	Mucharchar	23	6.8	7.0	0.166	168	200	31	6.3	U.D.	42	11	0.1	0.4	24	12	3.0	U.D.	18	6.5	0.2	0.5	0.5	0.2	N/A	5.0	4.3	-3.9	-3.5	N/A
MCC56	Mucharchar	21	6.9	7.0	0.164	185	193	61	7.2	U.D.	43	13	1.1	0.2	37	18	U.D.	U.D.	19	13	U.D.	0.8	0.7	U.D.	N/A	4.8	4.7	-3.4	-3.4	N/A
MCC57	Mucharchar	21	6.9	6.7	0.120	124	135	51	11	4.3	53	17	U.D.	0.4	30	30	U.D.	U.D.	13	13	U.D.	U.D.	6.8	3.3	N/A	4.9	5.1	-3.8	-3.7	N/A
MCC58	Mucharchar	32	7.1	7.0	0.142	59	61	25	16	2.3	87	19	0.6	0.7	4.7	26	1.8	U.D.	1.6	11	U.D.	U.D.	1.0	0.4	N/A	7.4	7.2	-3.0	-2.9	N/A
MCC59	Mucharchar	24	7.1	7.1	0.206	119	146	N/A	6.4	U.D.	55	13	1.4	0.9	4.6	4.6	2.2	0.2	U.D.	1.7	U.D.	1.1	0.6	0.2	N/A	5.8	6.2	-3.4	-3.4	-3.5
MCC60	Mucharchar	23	7.2	7.1	0.097	387	369	43	10	3.4	53	13	1.6	1.4	5.2	5.0	U.D.	0.2	U.D.	1.3	U.D.	1.2	2.2	0.9	N/A	4.6	5.7	-3.8	-3.8	N/A
MCC62	Mucharchar	31	7.1	7.0	0.194	U.D.	U.D.	U.D.	42	U.D.	28	12	U.D.	U.D.	7.4	28	U.D.	0.1	0.8	2.6	0.4	U.D.	0.2	U.D.	2.1	1.4	4.9	-5.5	-5.6	N/A
MCC63	Mucharchar	23	7.2	7.1	0.077	353	426	86	7.6	1.6	62	13	0.7	1.5	10	7.3	U.D.	0.2	U.D.	0.4	U.D.	U.D.	0.3	1.7	1.7	N/A	6.6	-2.8	-2.8	-2.8
MMD12	Mammudi	26	7.2	7.1	0.288	384	317	88	12	U.D.	52	12	1.6	U.D.	22	U.D.	1.0	U.D.	7.1	U.D.	U.D.	U.D.	4.1	2.2	N/A	6.7	7.1	-2.2	-2.1	N/A
MMD13	Mammudi	23	7.3	7.3	0.305	315	339	61	12	U.D.	63	14	1.0	1.3	26	33	1.4	0.2	20	24	0.3	U.D.	2.0	1.0	N/A	4.0	4.7	-2.3	-2.3	N/A
MMD14	Mammudi	21	7.0	7.0	0.299	6.7	6.3	U.D.	67	17	99	45	0.2	U.D.	115	148	10	U.D.	115	107	0.1	U.D.	U.D.	U.D.	N/A	4.9	4.6	-3.1	-3.0	N/A
MMD16	Mammudi	23	7.0	7.0	0.162	60	64	56	12	0.4	59	16	0.5	0.7	23	29	U.D.	U.D.	12	11	0.1	0.6	0.4	0.3	N/A	3.9	4.1	-2.4	-2.1	-2.3
MMD17	Mammudi	14	6.9	6.9	0.108	82	92	41	12	2.7	48	15	0.8	0.4	23	21	0.4	0.1	15	13	U.D.	U.D.	3.1	1.4	N/A	4.5	4.5	-3.1	-3.3	N/A
MMD18	Mammudi	21	6.9	7.0	0.146	97	118	64	4.1	U.D.	36	12	0.5	0.2	11	12	0.3	U.D.	5.9	5.1	0.2	0.3	0.9	0.4	N/A	3.2	5.8	-4.0	-3.0	N/A
MMD19	Mammudi	21	7.2	7.3	0.223	13	11	U.D.	65	6.3	163	57	0.2	U.D.	147	178	6.2	6.4	12	118	U.D.	U.D.	U.D.	U.D.	N/A	5.0	N/A	-3.8	-3.9	N/A
MMD20	Mammudi	26	7.3	7.3	0.146	151	101	99	35	U.D.	70	16	0.7	0.7	49	62	0.8	0.1	27	40	0.4	0.6	1.3	0.2	N/A	4.1	N/A	-3.6	-3.8	N/A
MMD21	Mammudi	18	6.8	6.9	0.245	11	10	U.D.	27	U.D.	44	15	0.1	U.D.	95	118	1.3	0.3	88	60	U.D.	0.5	U.D.	U.D.	N/A	5.3	6.6	-3.3	-3.1	N/A
MMD25	Mammudi	24	7.1	7.2	0.154	67	85	41	50	69	62	18	0.4	0.4	44	52	0.4	0.1	20	17	U.D.	U.D.	2.0	0.7	N/A	8.0	5.5	-4.1	-4.0	N/A
MMD27	Mammudi	23	7.1	6.6	0.286	U.D.	1.1	U.D.	20	11	45	21	0.1	U.D.	37	31	0.9	0.3	25	23	U.D.	U.D.	0.3	U.D.	1.6	6.8	7.4	-3.7	-3.8	N/A
MMD28	Mammudi	20	7.2	7.3	0.261	U.D.	U.D.	U.D.	8.0	1.8	27	7.3	0.4	0.4	8.9	8.0	0.5	0.1	10	4.2	U.D.	U.D.	0.4	U.D.	3.2	6.6	6.4	-4.0	-4.2	N/A
MMD29	Mammudi	23	7.0	7.1	0.276	8.7	8.1	U.D.	7.0	16	26	11	0.2	0.1	24	24	1.1	U.D.	31	28	U.D.	0.5	0.3	U.D.	N/A	5.2	5.5	-3.9	-3.9	N/A
LDD1	Ledamdi	24	6.7	7.4	0.046	482	488	57	13	2.7	56	13	2.7	3.9	3.0	3.8	U.D.	U.D.	0.9	U.D.	U.D.	U.D.	1.3	6.7	N/A	N/A	5.2	-3.8	-3.5	N/A
LDD3	Ledamdi	18	6.8	7.2	0.044	335	366	63	24	9.0	90	20	3.7	4.1	41	33	U.D.	U.D.	1.3	5.4	U.D.	U.D.	2.1	7.6	N/A	4.1	4.0	-4.2	-4.2	-4.3
LDD5	Ledamdi	24	7.2	7.1	0.048	562	527	74	17	15	65	17	3.1	2.4	13	4.3	4.8	U.D.	6.1	U.D.	0.2	U.D.	2.2	7.4	N/A	4.1	3.6	-4.0	-3.8	N/A
TMD6	Temdi	21	7.1	7.0	0.217	86	79	42	5.3	4.2	25	9.2	0.2	0.2	31	7.6	U.D.	0.1	21	7.0	0.2	U.D.	2.4	0.9	N/A	4.5	N/A	-3.7	-4.0	N/A
TMD7	Temdi	31	7.1	6.9	0.108	71	71	30	20	52	54	30	0.5	0.4	27	53	7.0	0.1	12	42	U.D.	0.4	U.D.	U.D.	N/A	4.9	4.5	-4.1	-4.0	N/A
TMD8	Temdi	23	7.2	6.7	0.221	176	U.D.	U.D.	53	U.D.	48	23	1.2	U.D.	8.1	39	16	U.D.	7.6	1.8	U.D.	U.D.	1.1	2.1	N/A	5.3	5.1	-4.3	-7.2	N/A
TMD9	Temdi	21	7.2	7.1	0.096	56	61	51	5.8	27	18	9.1	0.3	0.2	27	10	5.3	U.D.	17	8.5	0.3	4.0	1.9	1.1	N/A	5.4	5.5	-4.1	-3.5	N/A
TMD10	Temdi	26	7.1	7.0	0.183	238	201	51	20	4.9	68	21	1.0	1.3	3.7	33	U.D.	0.2	U.D.	25	U.D.	1.7	1.2	U.D.	N/A	5.6	4.8	-2.8	-3.2	N/A
HHD1	North Harihardi	24	7.4	7.3	0.127	1189	1063	71	21	17	67	14	3.5	3.1	21	18	U.D.	U.D.	3.7	4.2	0.8	0.6	1.4	0.7	1.7	5.2	6.6	-3.3	-3.3	-3.7
HHD2	North Harihardi	17	7.3	7.3	0.276	223	176	N/A	6.4	12	31	14	0.9	1.1	11	8.3	0.6	U.D.	8.5	5.0	1.0	1.1	0.5	0.3	N/A	4.8	5.4	-3.6	-3.7	N/A
HHD3	North Harihardi	18	7.0	7.0	0.301	75	78	90	13	11	32	10	0.1	0.3	13	8.0	U.D.	U.D.	10	6.7	0.7	0.8	0.3	0.3	N/A	3.7	4.6	-4.2	-5.0	N/A
HHD5	North Harihardi	20	6.6	7.2	0.166	107	84	60	2.8	2.5	33	9.0	0.5	1.0	8.4	8.0	U.D.	U.D.	9.3	8.5	0.4	0.6	0.7	0.9	1.1	8.8	6.7	-4.1	-4.2	N/A
HHD7	North Harihardi	23	7.0	7.1	0.268	U.D.	U.D.	U.D.	14	27	22	15	U.D.	0.1	32	19	U.D.	U.D.	26	17	U.D.	U.D.	0.4	0.8	N/A	5.5	5.8	-4.4	-4.4	N/A
HHD8	North Harihardi	23	7.3	7.2	0.335	59	24	U.D.	8.2	8.7	49	15	0.9	0.1	42	27.1	0.6	0.6	7.0	17	0.3	0.4	0.3	0.4	N/A	8.5	7.6	-4.3	-3.8	N/A
HHD9	North Harihardi	23	7.2	7.0	0.150	38	65	N/A	6.4	4.0	62	13	0.1	1.0	40	U.D.	0.6	U.D.	28	U.D.	0.4	U.D.	0.3	0.4	N/A	5.5	5.9	-3.7	-4.3	N/A
HHD10	North Harihardi	23	7.0	7.0	0.181	82	102	40	5.9	7.4	33	8.0	0.2	0.5	13	10	0.1	U.D.	11	11	0.3	0.5	0.6	0.7	N/A	N/A	2.7	-3.7	-3.9	N/A
HHD51	North Harihardi	20	7.0	6.9	0.180	324	361	55	21	4.6	53	14	0.9	1.1	70	25	4.1	U.D.	23	14	0.4	1.0	0.4	1.7	N/A	3.2	1.4	-4.4	-4.3	N/A
HHD52	North Harihardi	8	6.9	6.9	0.203	27	33	N/A	28	59	41	12	0.1	0.4	18	42	5.0	0.6	19	9.3	0.4	1.0	0.1	0.5	N/A	3.5	3.1	-3.7	-3.4	N/A
HHD53	North Harihardi	23	7.4	7.3	0.152	785	773	54	19	3.3	65	12	1.5	1.0	30	16	5.3	U.D.	30	6.0	0.5	1.2	0.1	0.8	N/A	3.5	3.5	-3.8	-3.5	N/A
HHD54	North Harihardi	9	7.3	7.3	0.257	3.2	2.1	U.D.	6.3	50	41	13	0.5	2.5	U.D.	19	U.D.	0.6	U.D.	10	U.D.	0.6	0.1	0.6	N/A	5.1	6.1	-3.9	-4.0	N/A
HHD101	North Harihardi	31	6.9	7.0	0.091	665	598	97	6.6	6.0	42	12	2.1	2.3	27	23	U.D.	0.1	1.3	1.7	U.D.	U.D.	6.0	6.7	N/A	4.5	7.5	-3.2	-3.3	-2.8
HHD102	North Harihardi	21	7.3	7.2	0.103	814	693	50	6.6	2.5	52	11	2.8	3.0	16	15	0.1	0.1	5.2	7.3	0.5	0.5	0.6	0.9	N/A	2.9	3.1	-3.4	-3.5	N/A
HHD103	North Harihardi	20	6.9	6.9	0.195	55	42	U.D.	7.0	8.2	29	10	0.2	0.7	15	15	U.D.	0.1	15	16	U.D.	U.D.	0.4	1.2	N/A	6.3	6.3	-3.9	-3.9	N/A
HHD104	North Harihardi	21	6.6	6.8	0.321	197	193	95	9.1	7.1	21	9	1.5	U.D.	21	20	0.1	0.1	0.7	1.4	U.D.	U.D.	21	23	N/A	6.3	6.2	-2.5	-2.4	N/A
HHD105	North Harihardi	23	7.3	7.4	0.126	583	642	72	7.0	8.2	29	10	1.1	U.D.	15	11	0.1	0.1	7.6	3.2	0.8	0.6	0.6	1.0	N/A	8.4	8.0	-3.0	-3.3	N/A
HHD106	North Harihardi	23	7.2	7.3	0.273	327	293	46	7.2	6.7	51	10	1.1	0.8	17	16	1.2	U.D.	12	10	1.7	U.D.	0.5	0.4	N/A	5.9	5.8	-2.8	-2.4	N/A
HHD201	South Harihardi	27	7.1	7.3	0.083	394	309	N/A	9.12	6.4	50	17.9	2.8	2.7	25	26	U.D.	U.D.	0.7	1.2	U.D.	U.D.	5.6	6.7	N/A	N/A	8.3	-3.1	-3.0	N/A
HHD202	South Harihardi	21	6.8	6.9	0.208	2.0	U.D.	N/A	45	0.0	44	18	0.1	0.2	21	21	U.D.	U.D.	0.8	1.5	U.D.	U.D.	0.3	6.7	N/A	N/A	7.0	-6.4	-6.4	-6.8
HHD203	South Harihardi	27	7.2	7.4	0.080	539	509	49	6.2	3.7	47	11	3.3	3.4	6.1	5.2	U.D.	U.D.	0.6	U.D.	U.D.	U.D.	5.3	7.1	N/A	7.0	7.6	-3.4	-3.4	N/A
HHD205	South Harihardi	32	7.2	7.4	0.070	748	702	61	16	3.8	72	16	3.2	3.4	N.A.	4.7	0.1	U.D.	0.9	U.D.	1.5	U.D.	6.8	6.9	1.2	7.4	7.6	-4.0	-3.6	N/A
HHD206	South Harihardi	27	7.3	7.4	0.088	772	656	64	9.1	9.1	55	15	2.2	3.4	5.3	6.7	1.3	U.D.	0.1	U.D.	U.D.	U.D.	2.3	3.9	N/A	N/A	8.3	-3.4	-4.0	N/A
KDK1	South Harihardi	23	7.1	7.1	0.065	303	317	90	7.0	3.9	69	15	3.0	3.3	11	12	0.1	U.D.	U.D.	U.D.	U.D.	U.D.	7.2	8.9	N/A	8.3	7.2	-2.7	-2.7	N/A
KDK2	South Harihardi	21	7.1	7.2	0.078	246	204	49	7.9	4.1	76	17	1.5	3.4	U.D.	20	0.1	U.D.	0.8	U.D.	2.6	U.D.	8.7	10	1.9	7.7	5.4	-2.6	-2.6	N/A
KDK3	South Harihardi	23	7.1	7.3	0.068	382	239	47	7.3	4.3	82	19	3.8	3.7	34	25	U.D.	U.D.	U.D.	U.D.	U.D.	U.D.	11	0.4	1.6	6.3	8.0	-2.6	-2.6	-2.9
KDK4	South Harihardi	23	7.1	7.2	0.081	211	199	86	6.0	3.9	65	15	4.2	3.3	3.6	6.4	U.D.	U.D.	U.D.	U.D.	U.D.	U.D.	0.4	9.9	N/A	8.1	6.9	-3.5	-3.5	N/A

Table 1. Chemical composition of groundwaters collected from Holocene aquifer (unit: mg/L, except for Eh, As, and $\delta^{18}O$)

Sample	Village	Depth	pH		Eh (V)	As (μg/L)		% As^{III}	Na^+		K^+		Ca^{2+}		Mg^{2+}		NH_4^+		Cl^-		NO_3^-		SO_4^{2-}		PO_4^{3-}		Fe		DOC	Acetate		$\delta^{18}O$ (‰)		
		(m)	Sep	Feb	Feb	Sep	Feb	Feb	Feb		Feb		Feb		Feb		Sep	Feb	Sep	Feb	Sep	Feb	Sep	Feb	Sep	Feb	Sep	Feb	Feb	Sep	Feb	Sep	Feb	Dec
KDK5	South Harihardi	21	7.2	7.3	0.101	315	315	57	4.9		2.4		43		10		2.7	3.0	6.2	6.7	U.D.	U.D.	U.D.	1.5	U.D.	0.2	5.4	6.5	N/A	6.6	7.0	-2.9	-2.7	N/A
KDK6	South Harihardi	32	7.1	7.3	0.072	411	356	61	13		3.9		74		19		2.8	2.9	9.7	10	U.D.	U.D.	U.D.	U.D.	U.D.	U.D.	8.2	10	1.6	7.9	7.7	-4.0	-3.9	N/A
KDK7	South Harihardi	23	7.1	6.8	0.071	251	214	58	6.0		2.5		50		14		3.6	U.D.	2.9	3.6	0.1	U.D.	U.D.	U.D.	U.D.	U.D.	7.8	11	N/A	7.5	7.4	-3.2	-3.1	N/A
DRK31	Darikandi	29	7.0	7.2	0.047	423	376	56	11		3.4		77		17		3.3	1.6	3.2	4.0	0.1	U.D.	U.D.	U.D.	0.1	U.D.	7.5	7.7	5.6	8.1	9.2	-3.1	-3.2	N/A
DRK33	Darikandi	27	7.1	7.1	0.127	583	530	21	16		4.5		83		18		4.3	3.2	19	9.4	0.6	U.D.	0.6	U.D.	0.1	U.D.	5.2	5.4	N/A	8.8	9.6	-3.0	-2.9	N/A
DRK34	Darikandi	24	7.1	7.2	0.048	670	513	48	13		3.8		91		20		4.5	3.9	47	34	U.D.	U.D.	U.D.	U.D.	U.D.	U.D.	7.1	8.7	3.4	8.6	9.6	-3.3	-3.1	N/A
DRK35	Darikandi	23	7.3	7.4	0.045	660	638	35	12		2.5		77		17		2.8	U.D.	3.9	4.2	U.D.	U.D.	U.D.	U.D.	0.1	U.D.	4.1	5.1	1.8	8.3	8.9	-3.0	-2.9	-3.8
DRK36	Darikandi	27	7.1	6.8	0.178	314	40	U.D.	10		0.0		78		18		2.7	0.3	75	97	0.2	0.3	86	73	U.D.	U.D.	U.D.	8.6	7.9	9.4	8.7	-3.9	-3.3	N/A
DRK38	Darikandi	21	7.1	7.3	0.056	521	529	54	11		2.5		80		19		2.9	3.7	27	30	0.1	U.D.	0.8	3.0	0.1	U.D.	2.9	8.9	4.8	7.7	5.9	-3.3	-3.5	N/A
DRK40	Darikandi	23	7.0	7.0	0.057	404	438	28	31		3.0		68		18		2.4	2.3	5.8	8.5	0.1	U.D.	U.D.	U.D.	U.D.	U.D.	5.9	12	N/A	8.5	9.6	-3.5	-3.6	N/A
DRK41	Darikandi	23	7.0	6.9	0.064	278	260	85	21		4.9		134		30		7.3	8.1	85	U.D.	0.1	U.D.	0.6	U.D.	U.D.	U.D.	5.1	13	2.5	10	9.9	-3.2	-3.3	N/A
GLK3	Darikandi	23	6.9	7.3	0.064	104	351	37	27		33		86		27		1.7	3.1	50	67	U.D.	U.D.	0.7	14	U.D.	U.D.	8.0	8.7	4.5	7.0	9.6	-3.5	-3.6	N/A
GLK4	Darikandi	23	7.0	7.0	0.065	201	127	30	U.D.		61		51		25		1.8	0.7	40	40	U.D.	U.D.	U.D.	19	U.D.	U.D.	7.8	12	2.3	6.9	7.9	-2.8	-3.6	N/A
GLK5	Darikandi	15	7.1	7.1	0.061	379	306	27	8.9		3.8		46		14		2.7	3.3	58	21	0.2	U.D.	23	1.5	U.D.	U.D.	3.9	8.4	4.0	8.6	5.7	-3.6	-2.4	N/A
NKD1	Darikandi	23	7.0	7.0	0.065	335	277	44	8.9		5.0		76		17		6.1	4.5	44	10	U.D.	0.1	0.8	1.4	U.D.	U.D.	10	6.1	3.0	4.5	7.9	-3.8	-2.8	N/A
NKD2	Darikandi	20	6.9	7.0	0.076	157	142	63	13		5.4		97		22		4.1	3.0	4.1	32	U.D.	U.D.	U.D.	U.D.	1.1	U.D.	14	6.4	1.7	9.1	7.9	-3.0	-3.2	N/A
NKD3	Darikandi	18	7.1	7.2	0.060	336	370	37	10		3.2		61		13		3.7	4.0	6.5	4.0	U.D.	U.D.	U.D.	1.5	U.D.	U.D.	4.3	4.1	N/A	6.1	6.5	-3.1	-3.2	N/A
NKD4	Darikandi	21	7.0	7.4	0.072	284	361	50	10		3.6		58		12		4.1	3.1	22	3.1	U.D.	U.D.	1.2	1.4	U.D.	U.D.	6.1	4.5	N/A	6.5	6.2	-3.1	-3.2	N/A
NKD6	Darikandi	21	7.0	7.2	0.066	261	246	90	9.3		3.4		61		12		3.8	3.0	38	4.0	U.D.	U.D.	1.0	U.D.	U.D.	U.D.	7.5	4.0	N/A	6.2	6.4	-3.1	-3.2	N/A
NMP1	Darikandi	27	7.1	7.2	0.061	512	517	64	38		3.4		96		23		2.8	2.7	12	53	U.D.	U.D.	U.D.	1.4	U.D.	U.D.	9.7	6.1	2.5	7.4	7.6	-3.5	-3.5	N/A
NMP2	Darikandi	18	7.2	7.2	0.053	319	322	44	13		7.2		82		16		3.5	3.2	5.4	11	U.D.	0.1	U.D.	U.D.	U.D.	0.3	4.8	3.6	N/A	7.8	7.2	-4.1	-4.1	N/A
NMP3	Darikandi	20	7.2	7.0	0.355	537	501	51	11		4.6		71		15		3.6	3.1	39	6.0	45	U.D.	U.D.	U.D.	U.D.	U.D.	7.7	4.9	N/A	6.9	7.2	-2.5	-2.7	N/A
ABA1	Bara Khater Bhula	26	7.1	7.2	0.075	405	406	16	8.6		1.0		64		20		3.4	3.0	11	5.0	U.D.	U.D.	0.7	3.7	U.D.	0.2	7.6	8.1	N/A	7.7	N/A	-3.5	-3.5	N/A
ABA2	Bara Khater Bhula	29	7.0	7.0	0.079	353	257	26	11		0.1		102		24		3.2	2.5	78	85	0.1	U.D.	U.D.	20	U.D.	U.D.	7.5	6.9	2.7	7.7	8.2	-3.4	-3.4	N/A
ABA3	Bara Khater Bhula	24	7.0	7.2	0.073	216	169	59	17		2.8		70		18		2.8	2.2	36	27	U.D.	1.1	1.6	3.9	4.2	U.D.	4.8	6.0	3.6	N/A	8.4	-3.4	-3.6	N/A
ABA4	Bara Khater Bhula	23	6.8	7.1	0.073	292	307	38	8.0		1.7		71		17		3.1	2.6	109	20	U.D.	U.D.	7.0	U.D.	3.2	U.D.	12	8.7	6.3	N/A	8.6	-3.5	-3.3	N/A
ABA5	Bara Khater Bhula	27	6.9	7.2	0.063	233	281	69	12		U.D.		61		13		3.3	4.8	57	11	U.D.	U.D.	0.8	U.D.	4.8	U.D.	8.2	7.8	6.0	N/A	8.7	-3.0	-2.5	-3.6
ABA6	Bara Khater Bhula	23	6.9	7.0	0.071	132	113	77	13		23		65		29		1.8	1.3	28	78	0.1	U.D.	6.1	30	0.2	0.2	5.3	7.7	N/A	6.4	7.3	-3.8	-4.3	N/A
BKB1	Bara Khater Bhula	21	7.0	7.4	0.281	389	424	26	5.7		2.5		81		20		1.5	1.5	5.7	6.4	0.1	U.D.	U.D.	U.D.	2.6	1.6	4.5	6.0	N/A	8.8	N/A	-2.1	-2.1	N/A
BKB5	Bara Khater Bhula	21	7.0	7.1	0.089	274	278	27	10		2.9		72		18		0.4	0.4	5.6	6.2	U.D.	U.D.	U.D.	8.3	U.D.	1.2	10	11	2.8	8.8	14	-2.6	-2.5	-2.2
BKB7	Bara Khater Bhula	29	7.1	7.2	0.060	330	274	39	13		14		113		24		0.6	0.6	20	6.9	0.4	U.D.	12	U.D.	U.D.	U.D.	5.5	8.1	N/A	9.9	10	-3.1	-3.2	N/A
CKB1	Bara Khater Bhula	23	7.1	7.2	0.069	359	298	32	9.3		3.5		81		19		2.6	1.3	5.4	4.9	U.D.	U.D.	U.D.	U.D.	U.D.	U.D.	4.8	8.0	1.6	9.3	9.5	-3.4	-3.5	-3
Pleistocene aquifer																																		
GLG1	Gulnagar	21	7.0	6.9	0.209	0.1	U.D.	U.D.	47		U.D.		42		20		0.3	U.D.	11	36	U.D.	U.D.	4.2	6.2	0.5	0.3	0.8	0.8	N/A	7.0	6.0	-4.5	-4.5	N/A
GLG2	Gulnagar	20	7.0	6.8	0.208	0.6	U.D.	U.D.	N/A		N/A		N/A		N/A		0.2	U.D.	36	U.D.	3.9	U.D.	7.0	25	U.D.	0.4	0.5	1.1	N/A	5.6	5.1	-5.0	-4.9	N/A
GLG3	Gulnagar	26	7.1	6.8	0.205	0.9	U.D.	U.D.	26		U.D.		48		27		0.1	0.1	63	220	U.D.	U.D.	23	13	U.D.	0.3	0.5	0.4	N/A	N/A	4.2	-5.0	-4.5	-4.6
GLG4	Gulnagar	21	6.9	6.7	0.213	0.3	U.D.	U.D.	23		U.D.		37		16		0.1	U.D.	12	355	U.D.	U.D.	9.2	5.6	U.D.	0.3	0.3	0.5	N/A	N/A	2.0	-4.6	-4.7	N/A
GLG5	Gulnagar	20	6.8	6.5	0.222	0.9	0.2	U.D.	23		U.D.		28		14		0.2	U.D.	4	15	U.D.	0.38	2.7	5.0	U.D.	0.2	1.3	1.0	1.2	5.9	5.2	-4.6	-4.8	N/A
GLG6	Gulnagar	32	7.0	6.7	0.208	0.4	U.D.	U.D.	20		U.D.		31		12		0.2	U.D.	13	17	U.D.	U.D.	5.3	1.1	U.D.	0.5	0.4	0.3	N/A	6.4	5.8	-4.7	-4.6	N/A
NNK1	Gulnagar	67	7.0	N/A	0.206	0.7	U.D.	U.D.	49.5		U.D.		46.3		20.1		U.D.	U.D.	34	42	U.D.	64	24	U.D.	U.D.	U.D.	U.D.	0.3	N/A	5.8	4.9	-4.2	-4.3	-4.3
NNK3	Gulnagar	26	7.0	6.6	0.216	1.3	1.4	U.D.	25.9		1.9		34.9		14.8		U.D.	U.D.	25	39	U.D.	U.D.	15	14	0.6	U.D.	U.D.	0.2	1.5	4.7	3.9	-5.0	-4.9	N/A
PNG3	Gulnagar	23	6.7	6.3	0.233	2.7	1.2	U.D.	29.0		2.0		42.6		23.7		U.D.	0.2	47	33	U.D.	U.D.	14	4.0	U.D.	U.D.	2.1	4.4	N/A	6.1	4.9	-4.7	-4.8	N/A
PNG4	Gulnagar	23	6.8	6.5	0.224	4.3	4.6	U.D.	37.6		1.5		35.8		21.4		0.4	0.5	32	55	U.D.	U.D.	6.7	6.5	U.D.	U.D.	4.7	9.1	N/A	6.2	4.8	-4.7	-4.7	N/A
PNG5	Gulnagar	26	7.1	6.7	0.209	0.3	U.D.	U.D.	51.7		U.D.		53.3		28.9		0.1	U.D.	70	8.7	U.D.	19	7.6	9.8	0.3	0.1	U.D.	0.2	2.2	7.0	5.5	-4.7	-4.8	N/A
DLD29	Daulaudi	55	6.7	7.0	0.195	U.D.	U.D.	U.D.	N/A		N/A		N/A		N/A		0.2	0.3	114	109	5.6	U.D.	40	57	U.D.	U.D.	U.D.	0.6	N/A	8.9	8.9	-4.7	-4.8	N/A
KMC11	Kumarchar	61	6.7	6.8	0.213	1.9	1.5	U.D.	31.6		U.D.		24.1		11.3		0.1	0.1	22	22	U.D.	U.D.	1.3	0.7	U.D.	U.D.	2.8	2.2	N/A	8.1	4.5	-5.0	-5.1	N/A
MCC36	Mucharchar	67	6.7	7.0	0.221	U.D.	U.D.	U.D.	10.4		1.7		81.6		22.6		0.1	1.2	37	37	U.D.	U.D.	2.6	2.1	U.D.	U.D.	1.0	0.2	N/A	4.1	3.4	-5.7	-5.2	-5.7
HHD6	Harihardi	58	6.7	6.7	0.213	1.1	0.4	U.D.	53.4		U.D.		43.7		18.9		0.2	U.D.	36	37	7.9	U.D.	2.3	1.4	U.D.	U.D.	0.5	0.3	N/A	7.2	8.1	-6.6	-6.6	-6.6
HHD204	Harihardi	61	6.9	6.7	0.220	2.7	0.2	U.D.	51.9		2.3		40.7		15.7		2.3	0.3	20	21	0.44	U.D.	1.5	1.0	1.4	0.1	0.6	0.4	N/A	N/A	7.4	-5.8	-5.8	-5.8
LDD4	Ledamdi	61	6.6	6.5	0.227	1.8	0.3	U.D.	54.5		U.D.		56.9		23.1		U.D.	0.3	51	4.4	U.D.	U.D.	1.4	U.D.	U.D.	U.D.	0.6	0.1	N/A	7.2	8.1	-6.9	-7.1	-7.0
NKD5	Darikandi	92	6.9	6.7	0.219	0.7	0.1	U.D.	63.1		U.D.		43.2		15.6		U.D.	0.6	22	3.4	U.D.	U.D.	1.8	0.0	U.D.	U.D.	U.D.	0.2	N/A	7.2	7.5	-6.4	-6.4	N/A
BKB2	Bara Khater Bhula	58	6.8	6.8	0.204	U.D.	0.5	U.D.	37.7		U.D.		51.3		21.3		U.D.	U.D.	8.6	8.0	3.2	U.D.	8.1	0.7	U.D.	U.D.	0.5	0.1	N/A	8.2	8.9	-5.0	-5.0	N/A
BKB4	Bara Khater Bhula	75	6.9	6.9	0.200	0.3	U.D.	U.D.	29.6		U.D.		63.3		26.9		U.D.	U.D.	6.6	6.1	3.1	U.D.	8.1	0.7	U.D.	U.D.	0.3	0.1	N/A	9.1	10	-4.6	-4.6	N/A
BKB6	Bara Khater Bhula	76	7.0	7.1	0.192	0.3	0.0	U.D.	25.7		U.D.		73.6		32.0		U.D.	U.D.	25	5.9	3.1	U.D.	8.1	0.0	U.D.	U.D.	3.9	0.2	N/A	9.1	11	-4.6	-4.5	-4.9

Note: U.D. means under detection limit.

N/A is not available data.

Chapter 3
Development of selective speciation method for secondly Fe and Mn species at mineral surfaces by conversion electron yield X-ray absorption fine structure

1. Chapter introduction

As mentioned in Chapter 1, mobility of As in sedimentary aquifer is mainly controlled by adsorption-desorption reaction to several secondary minerals. Iron and Mn hydroxides/oxides are particularly important compounds controlling geochemical behavior of As in surface environment. Secondary minerals of Fe(III) and Mn(IV) are readily produced due to their low solubilities (Stumm and Morgan, 1996, see Chapter 1, section 8.3). Chemical forms of these secondary minerals drastically change depending on the surrounding physico-chemical conditions, and reactivity of arsenite and arsenate to these secondary minerals can also be changed. Therefore, development of a speciation method for Fe and Mn in environmental samples is particularly important for my study.

Among the two elements, Fe is initially present as a constituent of minerals in igneous rocks such as biotite, pyroxene, hornblende, olivine, ilmenite, magnetite, and pyrite. Iron in these minerals alters its chemical form into oxides and hydroxides via weathering processes (Wilson, 2004). Although Mn is less abundant in crust relative to Fe, formation processes of secondary Mn oxides via weathering are similar to Fe (Post, 1999). As a result, detrital phases containing Fe or Mn generally coexist with their secondary phases in soil and sediments. Hence, the investigations of speciation of Fe and Mn in solid materials can be difficult, particularly if selective detection of the minor phases in the samples is desired. However, it is considered that the behaviors of As can be controlled by the reactions with the secondary Fe and Mn (hydr)oxides formed at surfaces of primary minerals, even if their ratios to the total Fe and Mn abundances are small. Actually, we observed large abundance of Fe rich primary mineral, such as biotite and chlorite, in sediment collected from our study area (Seddique et al. 2008). Thus, surface sensitive method could play an important role to achieve the speciation of

Fe and Mn for the sediment collected from As-contaminated aquifer.

X-ray absorption fine structure (XAFS) has been used for the speciation of various elements in solid materials (Brown and Sturchio, 2002). Among various techniques in XAFS, electron yield XAFS (EY-XAFS) can prove to be a useful surface sensitive method due to the shallow escape depth of Auger electrons from an atom irradiated by X-ray within a sample (Schroeder, 1996). This technique has been widely used for soft X-ray analysis, because probability for Auger electron emission is inversely proportional to the atomic number (Mcguire, 1970; Kostroun, 1971). For geochemical or environmental samples, EY-XAFS has been applied to speciation of light element in aerosol, e.g., Si (Tohno et al., 1998), P (Tohno et al., 2001), and S (Kawai et al., 1999; Takahashi et al., 2006). Iron and Mn are also possible candidates for investigation by EY-XAFS because (i) their concentrations are generally high (0.01 ~ 1wt.%) in soil and sediment and (ii) they have relatively small atomic number with fairly high probability of Auger electron emission. I hypothesized that conversion electron yield XAFS (CEY-XAFS) is applicable to speciation of Fe and Mn species at mineral surfaces. However, to the best of my knowledge, CEY-XAFS has not been applied for the speciation of Fe and Mn in natural geochemical samples. If the applicability of CEY-XANES for Fe and Mn speciation is confirmed, the technique can apply to the speciation of Fe or Mn secondary minerals, which are probably at low abundance, in the sediment from contaminated aquifer.

In this study, I measured Fe and Mn K-edge XANES spectra of weathered and unweathered granite by both fluorescence (FL) and CEY modes. Major minerals containing Fe and Mn in granite are biotite and hornblende, while secondary minerals, e.g., Fe hydroxide and Mn oxide, are also common in this rock. Abundances of secondary minerals generally increase with the increase in the degree of weathering. Thus, it is expected that the difference of weathered and unweathered granite can be assessed by the combination of FL- and CEY-XAFS by the determination of the chemical forms of Fe and Mn in bulk and at mineral surfaces, respectively. In order to validate the results, I also employed microscopic X-ray fluorescence (XRF) with XAFS analyses and also selective chemical-extraction experiments to determine the amount of secondary minerals.

2. *Methods*

2.1. Sample collection and preparation

The granite samples used in this study were collected from surface outcrop of Tono area, central Japan. Sampling procedure is described in detail in Takahashi *et al.* (2002). I chose two granite samples, ML01 and ML03W, for the experiments in this study, because they were weathered to different degrees. According to the scheme of classification of the degree of weathering proposed by Toyoda *et al.* (1999), ML01 and ML03W are classified to class B (slightly weathered) and class E (disaggregated), respectively. The former is classified as a hard rock indicated by metallic sound when the sample is hit by hammer, while the latter as totally crumbled clay. In terms of chemical index of alteration (CIA) proposed by Nesbitt and Young (1982), CIA_{ML01} and CIA_{ML03W} are 61.3 and 53.6, respectively (calculated by the data shown in Table 2–1). The results also showed that ML03W is weathered to a greater extent than ML01, since a larger CIA value shows that the sample is more intensively weathered. For the XAFS analyses, both samples were pulverized into powder. Major element composition was measured by conventional X-ray fluorescence spectrometry (Philips PW1404) as reported in Takahashi *et al.* (2002).

2.2. XANES data collection

The measurement of macroscopic XAFS spectra of Fe-K edge and Mn-K edge was conducted at BL01B1, SPring-8 (Hyogo, Japan) for Fe analyses and at BL12C, Photon Factory (Tsukuba, Japan) for Mn analyses. For Fe, XANES spectra of ferrihydrite, goethite, hematite, magnetite, pyrite, fayalite, and biotite were measured as the reference materials. For Mn, δ-MnO_2, Mn_2O_3, $MnSO_4$, and biotite were used. Ferrihydrite and goethite were synthesized following the method by Schwertmann and Cornell (2000). The δ-MnO_2 was synthesized following the method by Murray (1974). Hematite and $MnSO_4$ were purchased from Wako Pure Chemical Industry, Ltd (Japan). Magnetite, biotite, fayalite, and pyrite were purchased from Nichika Corp. (Japan). Mn_2O_3 was purchased from Sigma-Aldrich Corp. (USA). During FL-XAFS measurement, references and powdered granite were sealed in oxygen impermeable films. The XANES spectra of reference materials were measured by transmission mode,

while granite samples were measured by fluorescence mode. Among the reference materials, only Mn-K edge spectrum of biotite was measured by fluorescence mode. Samples were positioned at 45° to the incident beam in fluorescence mode. Incident X-ray was tuned by Si(111) monochromater. Energy calibration was performed by assigning a pre-edge position of hematite as 7.110 keV and that of δ-MnO_2 as 6.539 keV for Fe and Mn, respectively. Incident and transmitted intensities were measured by ionization chambers in transmission mode, while fluorescent X-rays by a Lytle detector equipped with Soller slits and Mn or Cr filters for Fe or Mn analyses, respectively. Energy scans for XANES analysis were collected from 7.060 to 7.250 keV for Fe and from 6.438 to 6.740 keV for Mn. All measurements were carried out at room temperature under ambient air conditions.

Measurement of CEY-XAFS was conducted using a CEY detector unit (Teikoku Electric., Japan). Configuration of the detector is illustrated in Fig. 3−1. The powdered sample was placed on electrically conductive carbon tape (DTM9101, JEOL, Japan) at the center of circular-shaped graphite carbon electrode connected to an amplifier. The detector was placed on an alignment stage (θ-2θ type) and covered with a metal box to maintain He atmosphere. Purified He gas was allowed to flow through the cell at 300 mL/min. The detector unit was canted 4° against the incident X-ray. Vertical position of the detector unit against the incident X-ray beam was optimized by scanning the position vertically with the detection of the electron yield. The high voltage power was fixed at 400 V during all measurements.

Contribution of various Fe or Mn species to each sample was estimated by simulating the spectra of the samples by those of reference materials using the least squares fitting. Fitting was conducted in the energy ranges of 7.110 to 7.140 keV and 6.540 to 6.570 keV for Fe and Mn, respectively. The quality of the fit was given by the goodness-of-fit parameter R, defined by

$$R=\frac{\sum\{\chi_{obs}(E)-\chi_{cal}(E)\}^2}{\sum\{\chi_{obs}(E)\}^2} \qquad (1)$$

where $\chi_{obs}(E)$ and $\chi_{cal}(E)$ are experimental and calculated absorption coefficients at a

given energy (E), respectively.

2.3. *Micro XRF and XANES*

Micro XRF elemental mapping was performed at the BL4A, Photon Factory. The samples used for the micro-beam analysis were prepared as a thin section with thickness of ca. 30 μm. Prior to the analyses, distributions of minerals within the thin section were examined by optical microscopy. For the micro X-ray analyses, the thin section was positioned at an angle of 45° against the incident beam, and fluorescence X-ray was recorded by a Si semiconductor. The size of incident X-ray beam was fixed at 5×5 μm^2, which becomes 7 (horizontal) × 5 (vertical) μm^2 on the sample due to the angle of the sample to the incident X-ray beam. The step of the scanning was fixed at 7 and 5 μm for horizontal and vertical scans, respectively. Intensity of incident X-ray was fixed at 8.0 keV. During the scanning, the intensities of fluorescence X-rays of Fe-$K\alpha$, Fe-$K\beta$, Mn-$K\alpha$, K-$K\alpha$, Si-$K\alpha$, Ca-$K\alpha$, and Ti-$K\alpha$ were monitored simultaneously using single channel analyzers tuned for the energy of each fluorescence X-ray.

The XANES spectra were collected for selected points of interest (POI) based on the results of XRF elemental mapping. The micro-XANES spectrum collected for each POI was measured by fluorescence mode. Energy calibration was performed by the same procedure described in the previous section. Energy scans for XANES analysis were collected from 7.059 to 7.197 keV and 6.500 to 6.680 keV for Fe and Mn, respectively. The energy step was typically 0.33 for Fe and 0.50 for Mn in the XANES region. The XANES spectra of powdered reference materials were collected by transmission mode. Reference materials used in the micro-XANES analyses are the same as described in the previous section.

2.4. *Selective chemical-extraction of Fe and Mn species*

Secondary phases of Fe and Mn in the two samples of granites were extracted by wet chemical-extraction following the method proposed by Chao and Zhou (1983) and Koschinsky *et al.* (1995). For Fe, 0.2 g of each sample was reacted with 20 mL of 0.2 M

oxalate/ammonium oxalate (pH 3.0) at 25°C for 4 hours with continuous shaking. This method targets amorphous Fe hydroxide. For Mn, 0.2 g of each sample was reacted with 20 mL of 0.1 M hydroxylamine hydrochloride (pH 2.0) at 25°C for 24 hours with continuous shaking. This method targets Mn oxide. Concentrations of Fe and Mn extracted into the solution were determined by graphite-furnace atomic absorption spectrophotometer (AA-6650, SHIMADZU).

3. *Results*

3.1. Comparison of XANES spectra obtained by FL and CEY modes

Minerals in the two granite samples (unweathered and weathered) were quartz, plagioclase, feldspar, biotite, and lesser abundance of hornblende and chlorite according to the observation by optical microscope. Yellowish secondary Fe mineral is frequently observed in grain boundaries and cracks of quartz, particularly in ML01. Normalized Fe-K edge XANES spectra of ML01 and ML03W in FL and CEY modes show a good fit when subjected to least-squares fitting using the spectra of ferrihydrite and biotite as end members with goodness-of-fit parameter R^2 <0.04 (Fig. 3–2a, Table 3–2). In fluorescence mode, different features were clearly observed between ML01 and ML03W. The XANES spectrum of ML01 in FL mode (ML01-FL) shows similar structure with that of ferrihydrite, and calculated contributions of ferrihydrite and biotite were 0.66 and 0.34, respectively. Dominance of ferrihydrite is consistent with the fact that ML01 was intensively weathered. The XANES spectrum of ML03W-FL exhibits a shoulder around 7.122 keV, whose characteristics are similar to those of biotite. Calculated contributions of ferrihydrite and biotite were 0.31 and 0.69, respectively. Although the XANES spectrum of ML03-FL showed a good fit between ferrihydrite and biotite, height of the peak was slightly lower than that of the calculated spectrum. Because ML03W is a unweathered granite, other silicate minerals containing Fe such as hornblende and chlorite might have contributed to the spectrum. By comparing XANES features between FL and CEY modes for each sample, attenuation of the shoulder around 7.122 keV was notable in CEY mode, i.e., contribution of ferrihydrite increased in the CEY mode. The simulation of the spectra showed that the contribution of

ferrihydrite increased from 0.66 in FL mode to 0.75 in CEY mode for ML01 and 0.31 to 0.47 for ML03W. The larger contribution of ferrihydrite in the spectrum in CEY mode indicates the occurrence of ferrihydrite at mineral surfaces via weathering.

Normalized Mn-K edge XANES spectra are shown in Fig. 3–2b. Because concentration of Mn is lower than that of Fe by a factor of 20 to 30, intensities of signals were weak, particularly in CEY mode. However, all spectra can show a good fit between δ-MnO_2 and biotite with R <0.08. Compared with Fe, more remarkable differences were observed for Mn-K edge XANES between ML01 and ML03W and also between the FL and CEY modes. The XANES spectrum of ML03W-FL is characterized by two distinct peaks at 6.550 and 6.554 keV, which completely overlaps the biotite spectrum, suggesting that the primary Mn bearing mineral in the unweathered granite is biotite. On the other hand, these two peaks were not clear in the ML01-FL spectrum and slightly shifted to higher energy. Calculated contributions of δ-MnO_2 and biotite are 0.58 and 0.42, respectively, for the ML01-FL spectrum. The XANES spectrum of ML01-CEY was clearly different from that of ML01-FL. Contribution of δ-MnO_2 in the CEY mode (= 0.86) obviously increased relative to that for ML01-FL. Difference of the XANES spectra between ML03-FL and CEY was also distinctive. The two peaks (6.549 and 6.554 keV) observed in the biotite spectrum completely disappeared in the CEY mode, suggesting that the contribution of δ-MnO_2 (= 0.91) precipitated in the sample is significant as Mn species at the mineral surfaces, even in the unweathered granite.

3.2. Micro-XRF and XANES

Micro-XRF elemental mapping were performed for several parts in ML03W to determine the spatial distribution of Fe and Mn, some of which were shown in Fig. 3–3. According to the map A, Fe concentration was obviously high in biotite except for its cleavage (specified as spot 3) and margin of the grain (spot 4). Relatively high concentration of Fe was also observed at surface or in crack of the quartz (spot 5). Micro-XANES spectra of Fe K-edge from the points of interest (POI) are illustrated in Fig. 3–3. The XANES spectra of biotite in reference sample and in ML03W (spots 1 and 2) are similar but not identical. The reason for this discrepancy is not clear at

present. It is possible that the difference is partly due to the self-absorption effect, since the spectra of biotite in ML03W was obtained in FL mode irrespective of their high Fe concentrations, while that for the reference material was measured in transmission mode. The XANES spectra from spots 3 and 4 are similar to that of ferrihydrite rather than biotite suggesting that weathering of biotite, and subsequent precipitation of Fe hydroxide within the cleavage and at grain boundaries. The XANES spectrum for the spot 5 was also similar to that of ferrihydrite. Consequently, the micro-beam analysis showed that ferrihydrite is the main secondary phase of Fe formed during weathering.

As was like Fe, Mn also accumulated in the biotite (Map B), but its content is less in the cleavage and at the margin of the grain. The micro-XANES spectra of Mn from biotite regions (spots 6 ~ 8) are characterized by two peaks at 6.547 and 6.553 keV. The positions of these peaks were identical to those found in the XANES spectrum of biotite (reference sample), though the shape of the spectra was slightly different. XANES spectra similar to those of biotite were observed even from the cleavage and margin of the grain (spots 7 and 8). Unlike Fe, secondary phase of Mn was not observed even in the cleavage and margin of minerals. Although various points were analyzed in the thin section of ML03W, presence of Mn oxide was not confirmed by micro-XANES. Consequently, despite biotite is the main Fe and Mn bearing phase in ML03W, spatial distribution of the secondary phase was different between Fe and Mn.

3.3. Comparison of macroscopic and microscopic XANES analyses

As mentioned above, FL- and CEY-XANES gave different information. In the case of Fe, FL-XANES spectra indicate that ferrihydrite and biotite are the dominant Fe phase in ML01 and ML03W, respectively. On the other hand, contribution of ferrihydrite detected by CEY-XANES increased for both ML01 and ML03W. These results are consistent with the microscopic X-ray analyses, where Fe was mainly present in biotite and ferrihydrite in ML03W. Ferrihydrite was found within the cleavage of biotite and at grain boundaries, suggesting that the detection by CEY mode gives selective information for the secondary phase formed at the mineral surfaces. Difference of FL and CEY-XANES was more distinctive in the case of Mn. The FL- and CEY-XANES of Mn in ML03W showed contrasting results, where Mn oxide was not

found in the micro-XANES analyses but dominant in the spectra measured by CEY mode. As shown in the next section, signal detected by CEY-XANES was mainly from Fe and Mn species formed at solid surfaces confined to a depth of 100 nm. This depth is much smaller in magnitude than the beam size of micro-XANES (5×5 μm^2) employed in this study. Possibly, Mn oxide was thinly coated on mineral surfaces in sub micro-meter scale, which cannot be identified by micro XANES. These results showed that Mn oxide was selectively measured in the CEY mode. The present study clearly demonstrates the high potential of CEY-XANES as a selective detection method of thin coating of secondary minerals in sub micro-meter scale.

The relative content of each Fe and Mn phase was also determined by selective chemical-extraction (Table 3–3). For Fe, extracted fractions were smaller than that of ferrihydrite determined by FL-XANES. Particularly, the extracted fraction was less than half of ferrihydrite fraction in ML01. Fe oxide/hydroxide in ML01 might have a more crystalline phase than that in ML03W, which can be resistant to the chemical-extraction. Similar results were reported in La Force and Fendorf (2000) showing that extraction by 0.2 M ammonium oxalate may not remove all the Fe hydroxides from solid phase by comparison of selective chemical-extraction and Fe-K edge XANES. For Mn, extracted fractions were similar to or slightly smaller than that of Mn oxide determined by FL-XANES. The results of CEY-XANES have higher values for the fractions of secondary phases for Fe and Mn than those determined by selective chemical-extraction. Although extracted Mn in ML03W was much smaller than unextracted Mn, the CEY-XANES spectrum for the sample indicates the presence of Mn oxide. Thus, the fraction of the secondary phases determined by CEY-XANES is much larger than those estimated by FL-XANES and selective chemical-extraction. This result also supports the possibility of selective detection of secondary phases by CEY-XANES.

Coating of Mn oxides on mineral surfaces is common in surface environment (Post, 1999). Because such coating is generally fine-grained and poorly crystalline, characterization of Mn oxide is sometimes challenging. Micro- or submicro- scaled spectroscopic methods have been applied to characterization of Mn oxide, e.g., X-ray micro fluorescence, micro X-ray diffraction, and micro EXAFS by Manceau *et al.* (2003), transmission electron microscopy (TEM) by Hochella *et al.* (2005), and electron

energy loss spectroscopy in scanning transmission electron microscopy (STEM-EELS) by Loomer *et al.* (2007). These methods are normally applied to the samples which exhibit Mn-rich area within the samples. Compared with these methods, CEY-XAFS can also be employed to rock samples at early stage of weathering, since this method can give the information of averaged Mn species on surface of minerals in the bulk rock sample, which cannot be characterized by other methods. Besides, sample preparation and analytical procedure of other micro- or submicro- scopic methods are complex and time-consuming relative to CEY-XAFS. Thus, CEY-XAFS has many advantages for speciation of secondary mineral in natural samples.

Although the cause of different spatial distribution of Fe and Mn is unclear, the difference possibly reflects their different redox behavior in nature. Precipitation-dissolution of Mn oxide may be cycled actively in surface environment. Manganese can be soluble due to the concomitant reduction of Mn(IV) with oxidation of metals on the surface of Mn oxide, while dissolved Mn^{2+} is re-precipitated via both biotic and abiotic oxidation (Tebo *et al.* 2005). It is estimated that Mn can recycle 100~300 times during organic matter decomposition in coastal sediments before it is ultimately buried (Canfield *et al.* 1993). On the other hand, since the ability of oxidation by Fe oxide/hydroxide is not intensive, precipitation-dissolution of Fe oxide/hydroxide is expected to be slower than Mn oxide. Thus, ubiquitous thin-coating of Mn oxide possibly reflects its higher mobility coupled with its readily reducible nature of Mn compared to Fe. Separate spatial distributions of Fe hydroxide and Mn oxide is actually observed in natural sample by TEM (Hochella *et al.* 2005), which is consistent with the present results.

3.4. Calculation of probing depth for various compounds

Probing depths of KLL Auger electron of Fe and Mn from selected minerals were estimated using the 'universal curve' proposed by Schroeder (1996). Escape probability P(x) is assessed by *Bethe range* (R_B) which is the average total path length of Auger electron before losing its initial kinetic energy by following equation.

$$P(x) = 0.76 \cdot (1 - \frac{2 \cdot x}{R_B}) \cdot \exp(\frac{-2.7 \cdot x}{R_B}) \quad (5)$$

where x is the origination depth from surface. The R_B is derived from modified Bethe law (Joy and Luo, 1989),

$$R_B = \frac{M}{785 \cdot \rho \cdot Z} \cdot \int_{E_A}^{40eV} \frac{E}{\ln(J/[1.166 \cdot (E + t \cdot J)])} dE \quad (6)$$

where Z is atomic number, ρ the mass density, M the molar mass, t an element-specific dimensionless constant (generally ca. 0.85), and E_A is the KLL electron energy. J is the mean ionization potential estimated using following equation.

$$J = 9.76 \cdot Z + 58.5 \cdot Z^{-0.19} \quad (7)$$

By using the equations above, *Bethe range* of various Fe and Mn compounds (i.e. metallic Fe, ferrihydrite, fayalite, pyrite, and biotite for Fe; metallic Mn, Mn oxide, and biotite for Mn) were calculated.

Bethe range of Fe KLL Auger electron varied from 200 to 550 nm depending on the density of the compounds. Some studies using electron trajectory simulation demonstrated that half length of *Bethe range* (penetration depth; R_P) almost corresponds to the maximum probing depth of Auger electron (Erbil, 1988; Schroeder, 1996). Penetration depth of Fe KLL Auger electron was the lowest for metallic Fe (~ 100 nm), and the highest for the biotite (~ 250 nm). Penetration depth of silicates was longer than oxides (~200 nm) due to lower density of silicates. Because escape probability of Auger electron becomes higher toward mineral surface, more than 90% of the signal comes from the depth less than 100 nm for metallic Fe and pyrite and <160 nm for oxides and silicates. The depth of penetration of Mn KLL Auger electron is almost similar to that of Fe. Calculated penetration depths of Mn for Mn oxide and biotite were ca. 100 and 240 nm, respectively.

Penetration depth of fluorescence X-ray for Fe and Mn in various minerals was roughly estimated based on the absorption coefficients of these elements, and composition and density of minerals. As a result, the penetration depth is mineral dependent, and more than 90% of the signal comes from mineral surface (10–80 μm). This estimation is similar to the result by Dyar *et al.* (2002). Penetration depths of Fe-K edge fluorescence from biotite and ferrihydrite were ca. 50 ~ 70 μm, suggesting that

signal obtained by FL-XAFS was derived from the depth range which can reflect bulk information for minerals. Penetration depths of Mn-K edge fluorescence were in a similar range to that of Fe. The results of calculation for Fe and Mn indicated that probing depth of CEY-XAFS is smaller than FL-XAFS by 2 to 3 orders of magnitude, demonstrating that the combination of both methods can enable us to compare the Fe and Mn species at the surface and in the body of the minerals.

3.5. Possible application of CEY-XAFS for terrestrial samples

I confirmed that CEY-XAFS is applicable for the speciation of Fe and Mn at mineral surfaces in geological materials. Because Fe is the fourth most abundant element in earth's crust, relatively high-quality CEY-XANES spectra can be obtained for Fe. On the other hand, spectra of CEY-XANES for Mn in this study were not of high quality due to the low concentration of Mn in granitic rocks. I confirmed that this technique is likely applicable to the sediment sample collected from As-contaminated aquifer, at least for speciation of secondary Fe species on the mineral surface.

Because Auger electron yield decreases with the increase in atomic number, it is difficult to apply this method to elements heavier than Fe, because their crustal abundance is generally less than 100 mg/kg, or lower than one tenth of Mn. Although Sr is a relatively abundant element, Auger electron yield of Sr is less than half of that of Mn when calculated by fluorescence yield data of various elements proposed by Kostroun (1971). Thus, application of CEY-XAFS for elements heavier than Fe is probably limited to terrestrial samples except for ore minerals. On the other hand, CEY-XAFS is applicable to some elements lighter than Mn such as K, Ca, and Ti, since their crustal abundances and Auger electron yields are sufficiently high.

Combination of FL- and CEY-XAFS is useful to investigate their chemical behavior in various environmental settings. For example, it is important to assess the change in the chemical forms of these elements by weathering to explain the chemical processes. As I noted above, CEY-XAFS is a strong tool to investigate the formation process of secondary minerals in sub-micrometer scale at mineral surfaces. Hence, this method is applicable to evaluate the extent of weathering in the very early stage of the processes.

The selective detection of Fe and Mn oxides are particularly important in terms of the migration of trace (and toxic) elements during water-rock interactions, since Fe and Mn oxides can be important host phases to various ions. CEY-XAFS can detect Fe and Mn oxides at low abundances which can be overlooked by other methods, such as Mn oxide in ML03W sample. However, it is possible that such a minor Mn oxide can act as a host to trace elements in weathered granites. Hence, CEY-XAFS may play an important role to understand the migration of toxic metals and metalloids in surface environment.

When we use CEY-XAFS, preparation of the sample must be carefully conducted, since the method cannot be applied to wet samples due to absorption of emitted electrons by water. Thus, when CEY-XAFS is applied to wet sediments or soils, careful drying processes (e.g. freeze-drying or air-drying under anaerobic condition) are necessary. Evaluation of change in the chemical state during drying processes is an important issue to develop this method for characterization of natural samples.

4. Conclusions

Applicability of CEY-XANES as a speciation method of Fe and Mn in granite has been discussed based on the comparison of FL and CEY-XANES, micro-scale elemental distribution, micro-XANES, and selective chemical-extraction. These results indicate that CEY-XANES can provide the selective information of Fe and Mn in secondary phases which can form on the surface of minerals or as small particles. This method would give valuable information about the speciation of secondary Fe mineral in the As-contaminated aquifer.

I found that CEY-XANES detected extremely small amount of Mn oxide formed at the surface, and it appears to be a powerful tool particularly for investigation of Mn. This result suggests that combination of FL and CEY-XANES is useful for the speciation of Fe and Mn in geochemical material at mineral surfaces (mostly <100 nm) and for the comparison of surface-sensitive information with bulk. In particular, identification of Fe and Mn oxides at low abundances can be done only by such surface

sensitive methods. Successful detection of such phases will enable us to understand the migration of As during water-rock interactions.

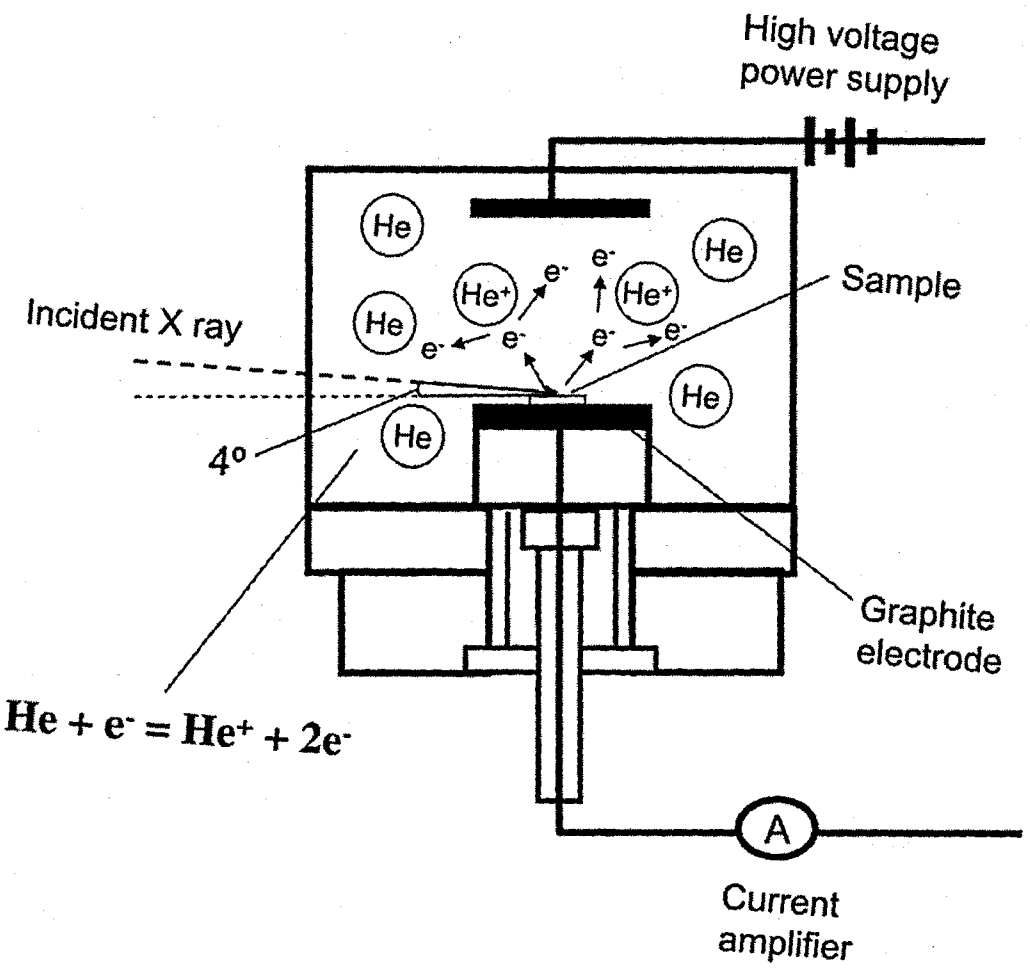

Fig. 3-1. Configuration of electrode unit of CEY-XAFS.

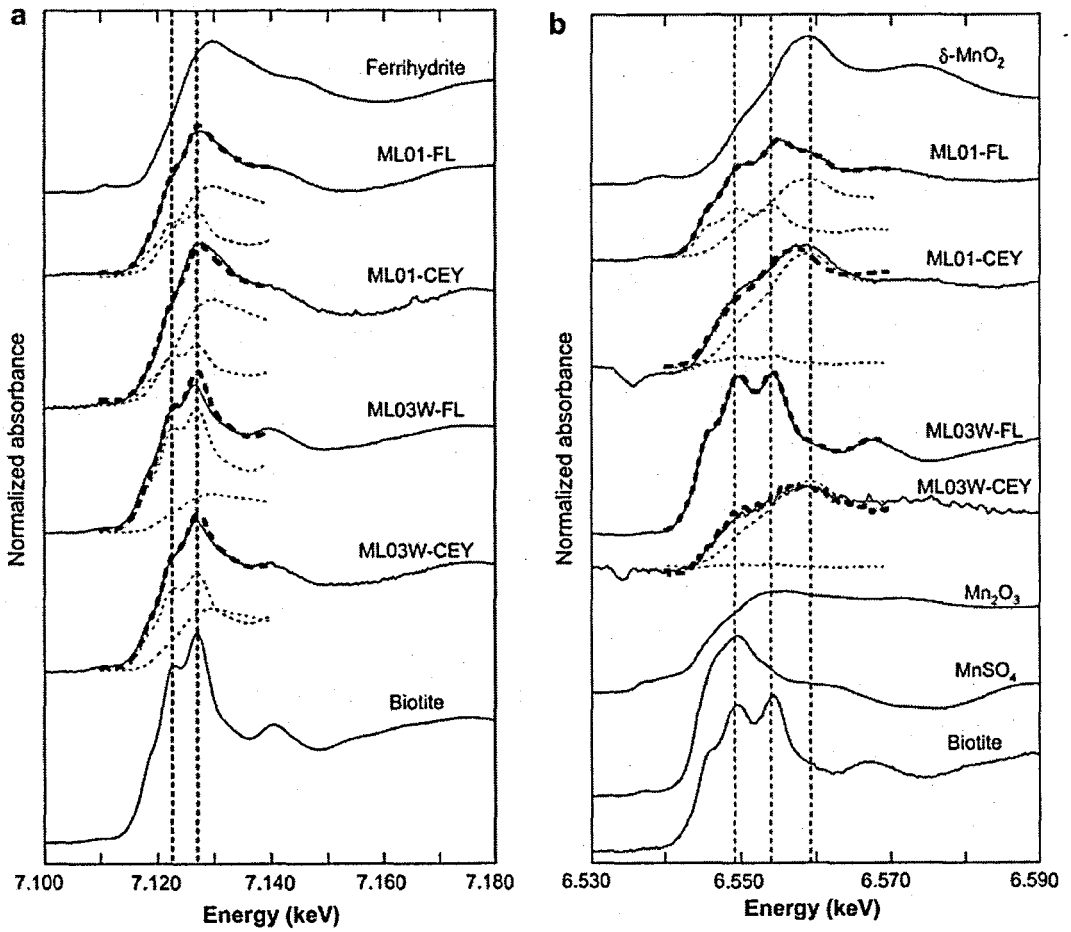

Fig. 3-2. (a) Fe-K edge and (b) Mn-K edge XANES spectra of granite samples measured by FL and CEY modes.

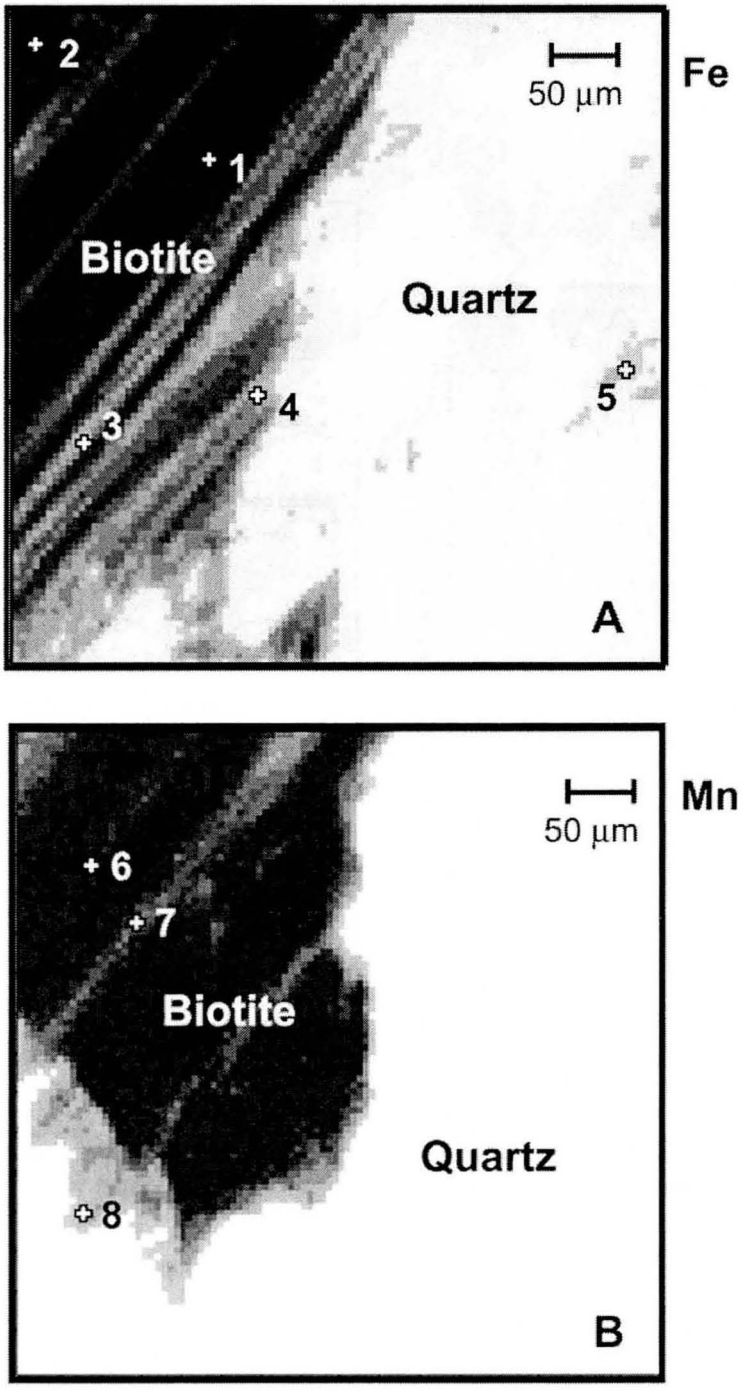

Fig. 3-3. Result of micro-XRF elemental mapping for Fe and Mn in ML03W. Thirteen points of interest where micro-XANES spectra were collected are specified.

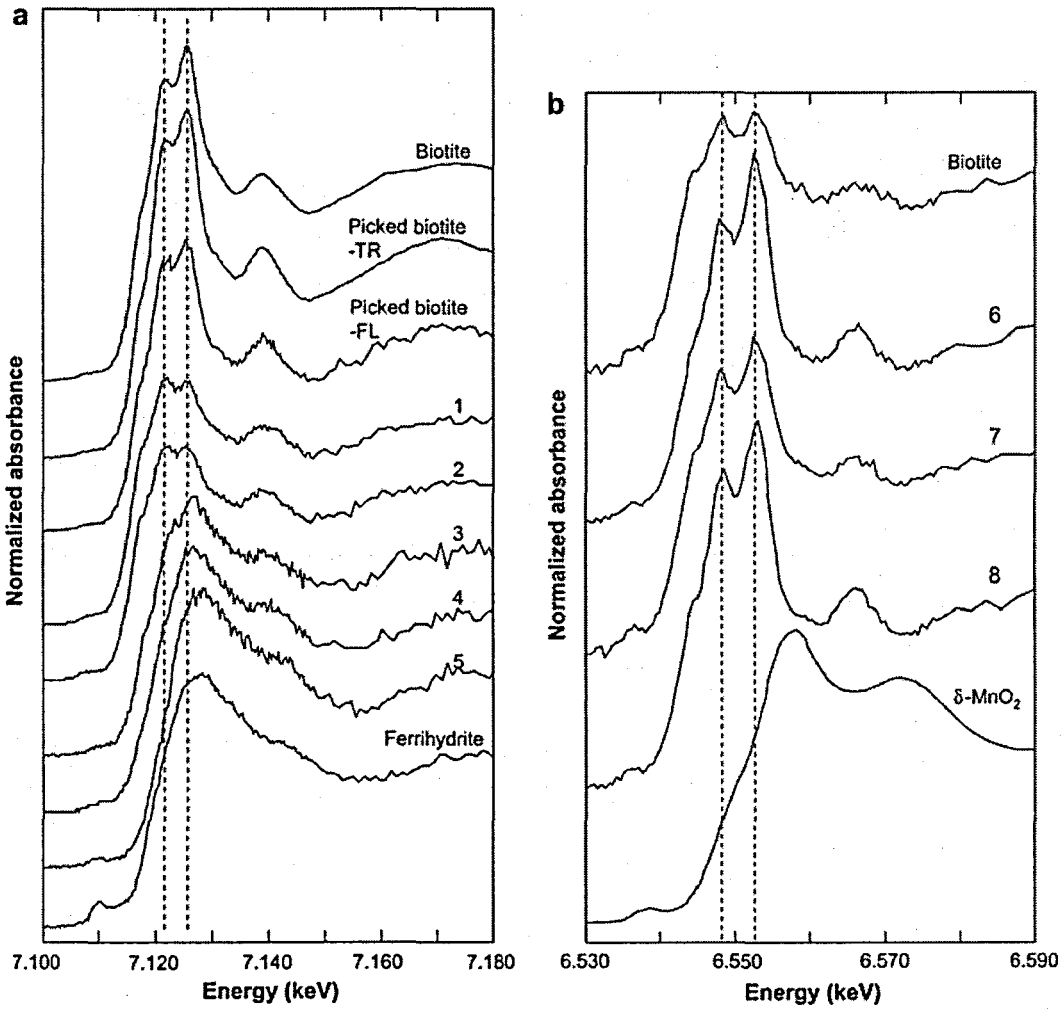

Fig. 3-4. Micro-XANES spectra of (a) Fe-K edge and (b) Mn-K edge measured at points of interest specified in Fig.3- 3. TR and FL mean the spectra recorded in transmission and fluorescence modes, respectively.

Table 3-1. Major element compositions (wt. %) of the granites and the chemical index of alteration (CIA) calculated from major element composition.

Sample	SiO_2	TiO_2	Al_2O_3	Fe_2O_3	MnO	MgO	CaO	Na_2O	K_2O	P_2O_5	CIA
ML01	77.07	0.04	13.80	0.91	0.042	0.06	0.30	1.97	4.80	0.01	61.3
ML03W	74.20	0.08	13.72	1.35	0.037	0.10	0.65	3.43	5.23	0.01	53.6

Table 3-2. Contribution of end members determined by least square fit

Fe

Sample	Measurement mode	$f_{biotite}$	$f_{ferrihydrite}$	R
ML01	FL	34%	66%	0.014
	CEY	25%	75%	0.031
ML03W	FL	69%	31%	0.037
	CEY	53%	47%	0.021

Mn

Sample	Measurement mode	$f_{biotite}$	f_{MnO2}	R
ML01	FL	42%	58%	0.024
	CEY	14%	86%	0.067
ML03W	FL	100%	0%	0.053
	CEY	9%	91%	0.074

Table 3-3. Fraction of extracted Fe (or Mn) in total Fe (or Mn) by selective extraction.

Sample	Extracted Fe	Extracted Mn
	Oxalate	*Hydroxylamine*
ML01	23%	48%
ML03W	21%	5%

Chapter 4
Adsorption properties of As-contaminated sediment: Implication for the factors controlling large variation of As concentration in groundwater

1. Chapter introduction

The cause of highly heterogeneous spatial distribution of As-contaminated groundwater in aquifer has been extensively debating. This intricate feature makes prediction of safe-well water difficult, thus it should be clarified. Two kinds of reaction should be considered in order to understand the controlling factor of great spatial variation of As concentration under subsurface: (i) dissolution–precipitation of the As host mineral; (ii) adsorption–desorption of As during groundwater flow.

Among the first processes, the reduction of iron (Fe) oxyhydroxides via microbial reductive dissolution most plausibly produces high-As groundwater (Bhattacharya *et al.*, 1997; Nickson *et al.*, 1998, 2000; Ravenscroft *et al.*, 2001; McArthur *et al.*, 2001; Dowling *et al.*, 2002; Harvey *et al.*, 2002, and Anawar *et al.*, 2003). This hypothesis is supported by an observed elevated concentration of Fe in As-contaminated groundwater, and enrichment of As in Fe oxyhydroxide fractions in sediments (Nickson *et al.*, 2000; BGS and DPHE 2001; Swartz *et al.*, 2004). The hypothesis is based on the assumption that the contaminated aquifer was initially in an oxidizing condition and this was followed by a change to a reducing state. The source of the reducing agent necessary for changing the redox condition remains a matter of debate. For example, Harvey *et al.* (2002) propose that natural organic matter supplied from surface due to recent excessive drawdown of groundwater is the cause of the redox change. McArthur *et al.* (2004) suggest that origin of the reducing agent is buried organic matter represented by interstratified peat.

Once As is released from the host minerals, an adsorption–desorption reaction is the dominant process in controlling the solid-water distribution of As in groundwater (Smedley and Kinniburgh, 2002). Because of the rapid kinetics, the dissolved As concentration in well water is likely to be controlled by the adsorption equilibrium

between sediment and water at the depth of the well screen. The adsorption–desorption reaction can be quantitatively discussed using distribution coefficient (K_d) between solid and water. The K_d of As for various solid phases has been experimentally determined (Smedley and Kinniburgh, 2002, and references therein). The most important adsorbents are amorphous Fe oxyhydroxides with K_d of 10^4–10^5 L/kg for both arsenite and arsenate at circumneutral pH (Dixit and Hering, 2003). The K_d values for various solid phases generally show higher affinities for arsenate than arsenite around neutral pH. Although there are some opposing reports concerning hydrous ferric oxides (Manning *et al.*, 1998; Dixit and Hering, 2003), a higher mobility of arsenite than arsenate in the natural environment is the likely common view. This is possibly due to a weak bonding of the surface complex of arsenite onto Fe oxyhydroxides caused by a dominant outer-sphere (or H-bonded) complex (Sun and Doner, 1996; Sverjensky and Fukushi, 2006). When compared with adsorption experiments for various minerals, the apparent value of K_d in the sediment of As-contaminated aquifers is relatively poorly reported, except for those studies on apparent K_d and retardation factors based on the comparison of labile (or adsorbed) As in sediment and dissolved As in groundwater (BGS and DPHE, 2001; Swartz *et al.*, 2004; van Geen *et al.*, 2008).

To discuss the adsorption–desorption reaction of As, it is necessary to consider the speciation of As in the contaminated aquifer. Because of the differing affinities of arsenite and arsenate for solid phases, arsenate reduction to arsenite can be a trigger for the mobilization of adsorbed As (Zobrist *et al.*, 2000; Takahashi *et al.*, 2004). This could be a more essential reaction for yielding an elevated concentration of As in groundwater rather than the reductive dissolution/transformation of Fe oxyhydroxides (Kocar *et al.*, 2006; Mitsunobu *et al.*, 2006, 2008). There is a consensus that As as arsenite is the dominant form dissolved in a contaminated aquifer (Bhattacharrya *et al.*, 1997; Swartz *et al.*, 2004; Horneman *et al.*, 2004; Stollenwerk *et al.*, 2007). However, an alternative issue is the speciation of As as a solid phase. Because the majority of As in the system occurs in the solid phase, its role here should also be clarified.

The X-ray absorption fine structure (XAFS) is a useful nondestructive method for the speciation of trace elements in the solid phase (Brown Jr. and Sturchio, 2002). However, Bangladesh sediment has not been extensively studied in this way, mainly due

to the low As concentrations (Gault *et al.*, 2003; Rowland *et al.*, 2005). Some researchers point out the importance of As-bearing sulfide as a source or sink of As in an aquifer based on XAFS results (Polizzotto *et al.*, 2005; Lowers *et al.*, 2007). For example, Polizzotto *et al.* (2005) show that As-rich sulfide of likely detrital origin is present in an aquifer using a μ-XAFS technique. However, the contribution of As bearing sulfide to the total As in the bulk sediment has not been fully revealed.

In this study, the speciation of As and Fe in cored sediment was first clarified using fluorescence (FL) and conversion electron yield (CEY) X-ray absorption near the edge structure (XANES), coupled with hot HCl extraction to consider the labile fraction of As and Fe. Secondly, the apparent distribution coefficient K_d of As between sediment and water was determined as a function of the depth using a batch experiment. The K_d for both arsenate and arsenite was determined to evaluate the effect of arsenate reduction in As mobilization. Dependence of the K_d on the As concentration was assessed by adsorption isotherms for some samples. Thirdly, the concentration of As in interstitial water was simulated based on the concentration of As adsorbed on the sediment and the apparent K_d for sediment. The depth profile of the oxidation state determined by XANES was also taken into account. The simulation results were compared with the actual As concentration profile in groundwater to investigate whether the concentration of aqueous As can be explained by the adsorption equilibrium model. Finally, factors controlling the As concentration variation in groundwater are discussed based on the adsorption equilibrium model.

2. *Site description*

Sediment cores 3.5 cm in diameter were taken by penetration drilling in the As-polluted groundwater aquifer in the Sonargaon Upazilla subdistrict of central Bangladesh. The study site of approximately 3 km^2 was located on the southeastern edge of the Madhupur Tract Pleistocene terrace deposit. There are three hydrological units distinguishable from surface to 100 m depth: an upper, arenaceous aquifer; a middle, argillite aquitard; and a lower, arenaceous aquifer (Fig. 4–1). The middle, impervious aquitard generally lies at a depth of 25–40 m beneath the surface. The sedimentation ages of the three units are estimated to be Plio-Pleistocene for the lower

aquifer, Middle-Upper Pleistocene for the middle aquitard, and Holocene for the upper aquifer. Hereafter, the upper and lower aquifers are respectively called the Holocene and Pleistocene sand aquifers.

The hydraulic conductivities are respectively 0.74×10^{-2} and 2.6×10^{-2} cm/sec in the upper 6–12 m and lower 18–27 m sections of the Holocene aquifer, and 1.6×10^{-2} cm/sec in the Pleistocene aquifer at 45–55 m depth (Mitamura *et al.*, 2008). Because the lower Holocene aquifer generally consists of medium to coarse grained, uncemented sand (e.g., SD22 and SD26 in Fig. 4–1) the hydraulic conductivity is higher than in the overlying part. For convenience, hereafter the sand layer between 18 m depth and the groundwater level is called the upper half (fine sand layer) of the Holocene aquifer, whereas the layer at 18–28 m is the lower half (coarse sand layer) (Fig. 4–1). The majority of the tube wells draw groundwater from the lower half.

3. *Materials and methods*

3.1. Sampling

The sediment cores were recovered in December 2004 using a 60 cm length split-barrel sampler used down to 100 m depth. As the sediment was tightly packed in the barrel sampler during both the drilling and recovery phases, minimal contact with air occurred and therefore the original oxidation state of Fe and As in the samples should have been preserved. The sediment recovered was immediately packed in an oxygen impermeable film bag (Escal film, Mitsubishi Gas Chemical. Japan) together with oxygen absorbent to avoid oxidation. The samples were taken to Japan within two weeks of sampling, and were stored frozen at -18 °C. The lithology of the sediment deposit with regard to grain size, texture, color, and fossil content are described elsewhere in detail (Mitamura *et al.*, 2008).

The names of the sediment samples are defined as a combination of the abbreviated lithology and depth. For example, SL2 means the silt sample from ca. 2 m depth. Groundwater was collected monthly from three observation wells, W1, W2, and W3, drilled within 7 m of the core-drilling site during the period from January to

December 2005. Procedures for sample collection were based upon Itai *et al.* (2008b). The depths of the well screens were in the range 6–12 m, 18–27 m, and 45–54 m for W1, W2, and W3, respectively.

3.2. Analytical methods

Sixteen sediments from the Holocene aquifer and two samples from the Pleistocene aquifer were selected based on the physical and chemical properties of samples listed in Tables 4–1 and 4–2. Prior to analysis, other than for XAFS, the samples were freeze-dried. The major element composition was determined by XRF (ZSX, Rigaku, Japan). Concentrations of C, H, N, and S were measured using a CHNS analyzer (CHNS/O 2400II, PerkinElmer Japan). Grain size distribution was determined by the laser scattering method (SALD3000S, Shimadzu, Japan) as described in Seddique *et al.* (2008). Total As concentration was determined by hydride generation atomic absorption spectrophotometry (HG-AAS, SAS7000, Seiko Instruments, Japan) after the decomposition of sample by the alkaline fusion method. No loss of As by volatilization during alkaline fusion was preliminarily confirmed by measurement of certified standard sedimentary rock samples provided by the Geological Survey of Japan (Imai *et al.*, 1996). The surface areas of sediment samples were determined by the multipoint BET method by N_2 adsorption using a BELSORP-mini II surface area analyzer (Bell Japan).

The concentrations of As, Fe, Mn, and phosphate dissolved in groundwater from W1 and W2 (8 samples for each) were measured for filtered (0.45 μm) and acidified (0.06N HCl) samples collected from January to October, 2005. Inductively coupled plasma mass spectrometer (ICP-MS, Agilent 7500cs, Agilent Technologies, Japan) was used for the determination of As, Fe, and Mn concentrations. Interferences of $^{40}Ar^{35}Cl$ and $^{40}Ar^{16}O^{1}H$ with ^{75}As and ^{57}Fe peaks, respectively, were reduced using a hexapole collision cell under a He atmosphere (3.0 and 4.5 mL/min, respectively). Phosphate was determined by spectrophotometry (BMP-20, Taitech, Japan) using the molybdenum blue method (Crouch and Malmstadt, 1967).

3.3. XAFS

The measurement of XAFS spectra at As and Fe K-edges was conducted at the BL12C, Photon Factory (Tsukuba, Japan). For As, XANES spectra of $KAsO_2$ and KH_2AsO_4 were measured as the reference materials purchased from Wako Pure Chemical Industries, Japan Arsenite and arsenate solutions were also prepared as the reference material by dissolving $KAsO_2$ and KH_2AsO_4 in deionized water to be 2000 mg/L of As. For Fe, XANES spectra of ferrihydrite, goethite, hematite, magnetite, pyrite, fayalite, chlorite, illite, and biotite were measured as the reference materials. Ferrihydrite and goethite were synthesized following the method developed by Schwertmann and Cornell (2000). Sulfate green rust was synthesized following the method of Mitsunobu *et al.* (2008). Magnetite, biotite, fayalite, and pyrite were purchased from the Nichika. Inc., Japan. Chlorite (CCa-1) and illite (IMt-1) were purchased from the Clay Minerals Society, USA. All the reagents used above were of analytical grade.

The XANES spectra of reference materials were measured by transmission mode, whereas the sediment samples were measured by fluorescence mode (hereafter "FL-XANES"). During the FL-XAFS measurement, sediment samples were kept frozen and sealed in oxygen impermeable films. Each sample was positioned at 45°C to the incident beam in fluorescence mode. The incident X-ray was tuned by a Si (111) monochrometer. The energy calibration was performed for As and Fe K-edges by assigning a peak of As_2O_3 in XANES as 11.865 keV and a second peak in the pre-edge region of hematite as 7.1096 keV. Incident and transmitted intensities were determined using an ionization chamber in transmission mode, whereas fluorescent X rays were measured by a Lytle detector equipped with Soller slits and Ge or Mn filters for As or Fe analyses, respectively.

XANES in conversion electron yield mode (hereafter "CEY-XANES") was measured using a CEY detector unit (Teikoku Electric, Japan). The principles and merits of this method are described in detail elsewhere (Schroeder, 1996; Itai *et al.*, 2008a). Prior to measurement, the frozen samples were freeze-dried under vacuum and kept in oxygen impermeable film under an Ar atmosphere in a globe box (1ADB-3,

Miwa Seisakusho, Japan). The powdered sample was placed on electrically conductive carbon tape (DTM9101, JEOL, Japan) at the center of a circular graphite carbon electrode connected to an amplifier. Pure He gas was allowed to flow through the cell at 300 mL/min. High voltage power was fixed at 400 V during all the measurements.

Background-removed and normalized spectra were obtained for all the XANES spectra. The oxidation state of As in sediments was estimated by simulating the spectra of the samples by the linear combination of those of reference materials. Because better fit was achieved by the spectra of As(III) and As(V) solutions as the end-members, they were used in the simulation for all the samples. Fitting was conducted in the energy range 11.850–11.880 keV.

The oxidation state of Fe was estimated by the shift of the centroid of the pre-edge position (Wilke *et al.*, 2001). The pre-edge peak was extracted by subtracting a cubic spline curve from the original spectra. The former was obtained by assuming the function using the data derived from several eV before and after the pre-edge feature in the range 7.100–7.117 keV. The energy shift of extracted pre-edge peak was assessed using the relative shift of centroid (RSC) defined as

$$RSC = \frac{EOC_{hem} - EOC_{sample}}{EOC_{hem} - EOC_{bt}} \quad (1)$$

where EOC_{hem} and EOC_{bt} are centroid positions (eV) of the spectra of hematite and biotite, respectively, whereas EOC_{sample} is that for samples. In this definition, the increase of RSC indicates an increase of ferrous species.

3.4. Chemical extraction

Acid extraction of Fe in the sediments was conducted by the method proposed by Raiswell *et al.* (1994). A weighed sample of 150 mg was decomposed by 5 mL of boiled 12 N HCl for 1 min in a Teflon beaker. Reaction was quenched by the addition of distilled water. This method used pulverized hydroxides, oxides, carbonates, and poorly crystalline sheet silicates. The concentration of extracted Fe (hereafter, labile Fe) was determined by graphite furnace atomic absorption spectroscopy (GF-AAS; AA-6650,

Shimadzu, Japan). Concentration of extracted As (hereafter, labile As or As_{HCl}) was measured by ICP-MS.

3.5. Adsorption experiment

Apparent distribution coefficients K_d of arsenite and arsenate were determined by a batch experiment under reducing conditions. To compare the partitioning ratio under identical conditions, a deoxidized buffer solution (10 mM MOPS: 3-Morpholinopropanesulfonic acid) was bubbled by 99.99% N_2 for 48 hours. The pH was adjusted to 7.3, a typical pH of ground water around the core drilling site, by addition of $NaOH_{(aq)}$. A standard stock solution of arsenite or arsenate (As concentration: 1000 mg/L) was spiked to the buffer solution. The final concentration of As in solution was adjusted to ca. 400 μg/L. Each sediment sample was put into a plastic bottle with 5 g of arsenite or arsenate standard solution, which was subsequently shaken at 20°C for 12 hours by a 120 rpm reciprocating shaker under darkness and a N_2 atmosphere. Adsorption equilibrium was achieved during this period according to preliminary experiments using SD13, SD16, and SD26. After the reaction was complete, each solution was filtered through a 0.45 μm membrane. The amount of As(III) or As(V) adsorbed was determined by the difference between the initial and final aqueous concentrations. According to the HPLC-ICP-MS analyses, the oxidation state of As in solution did not change during the experiment. The apparent distribution coefficient K_d is defined as

$$K_d = \frac{C_S}{C_A} \tag{2}$$

where C_S (mg/kg) and C_A (mg/L) respectively denote the concentrations of adsorbed and aqueous As species. Because a significant amount of As was originally adsorbed in natural sediment other than the As added by the experiment, the contribution of the initially adsorbed As should be considered. The total mass of As (m^{As}_{total}/g) active for the adsorption experiments was assumed to be the sum of initially adsorbed As (m^{As}_{ads}/g) and added As (m^{As}_{add}/g).

$$m_{total}^{As} = m_{ads}^{As} + m_{add}^{As} \quad (3)$$

The amount of initially adsorbed As onto the sediment was determined by the phosphate extraction method (Keon *et al.*, 2001). Because the mass of aqueous As after reaction can be obtained by the experiment, the C_s can be determined using difference between masses of total and aqueous As.

$$C_s = \frac{m_{total}^{As} - m_{aq}^{As}}{V_L} \quad (4)$$

where V_L is the volume of standard solution used for each experiment.

Adsorption isotherms for As(III) were determined in separate experiments for total concentrations of As in the range 10–2000 μg/L As to assess the dependence of K_d on As concentration. After equilibrium, the concentration and oxidation state of As in the aqueous phase were determined for both standard and residual solutions.

4. *Results*

4.1. Chemical and physical characteristics of sediment and groundwater samples

Among 18 samples listed in Tables 4–1 and 4–2, 15 samples SL2–SD26 were collected from the Holocene aquifer, SL29 came from the boundary between the Holocene aquifer and the aquitard, and SL39 and SD48 came from the Pleistocene aquifer. In the Holocene aquifer the SiO_2 content varied in the range 65.1–80.0 wt%, and the content of <67 wt% was clearly depleted in three silt samples SL2, SL7, and SL19. These samples showed a relatively high Al_2O_3 content of >15 wt% suggesting abundant clay minerals. Relatively high concentrations of Mg and K in these samples indicated much biotite or chlorite in these silt layers. Concentration of Fe_2O_3 was generally high at 6.24–6.48 wt% in the fine grained samples SL2–SL19 except for SD9 and SD11. A very high concentration of Fe (Fe_2O_3: 22.1 wt%) was observed in SL29. The red color of SL29 indicated Fe oxyhydroxides in the lowest part of the upper aquifer (Fig. 4–1).

Total carbon (TC), nitrogen (TN), and sulfur (TS) contents were low in the entire sections of the Holocene and Pleistocene aquifers (Table 4–2). The sum of these elements did not exceed 1 wt%. The TC was higher in the lenticular silt layers (SL7 and SL19) compared with sand layers, whereas relatively high TC was found from SD13 and SD16 within the sand layers. Organic rich layers such as peat were not found in the core, nor did they occur in the other seven cores collected in the study area (Mitamura *et al.*, 2008). TN was mostly low, and rarely detected as <0.01 wt% below 7.2 m. TS was also low, in the range 0.01–0.06 wt%.

The concentration of As in sediment was in the range 1.0–53 mg/kg in the upper aquifer. Most of the samples gave an As abundance below 10 mg/kg. These concentrations are similar or slightly higher than the average value of As in the upper continental crust of 1.5 mg/kg (Taylor and McLennan, 1994). The concentration of As was generally high in the silt layers such as SL2, SL7, and SL19. However, some coarser grained samples like SD22, SD23, and SD26 also showed relatively high concentrations. An exceptionally high concentration of As of 53 mg/kg came from SL29 found in the lowest part of the upper aquifer. The BET surface area of sediments collected from the Holocene aquifer was 0.57–2.9 m^2/g in sand samples, whereas the value was 4.0–5.6 m^2/g in silt samples.

The average concentrations of dissolved As, phosphate, Fe, and Mn in groundwater from W1 (n = 8) were 23 ± 11 μg/L, 0.40 ± 0.12 mg/L, 26.7 ± 8.1 mg/L, and 0.96 ± 0.20 mg/L, respectively, whereas these concentrations in W2 (n = 8) were 119 ± 34 μg/L, 0.89 ± 0.24 mg/L, 4.1 ± 1.4 mg/L, and 0.08 ± 0.07 mg/L, respectively. Arsenic and phosphate concentration were higher in the lower half than in the upper half, whereas Fe and Mn were higher in the upper half. The molar ratio of P/As in W1 and W2 were 16.5 ± 8.1 and 6.6 ± 3.1, respectively.

4.2. As K-edge XANES

The XANES spectra of the As(III) and As(V) solutions show a clear energy shift of the main peak between As(III) (11.865 keV) and As(V) (11.868 keV). Takahashi *et al.* (2003) confirm that the As(III)/As(V) ratio in natural solid samples can be determined

by a simulation using normalized spectra of arsenite and arsenate when these are the dominant As species. In the simulation of As K-edge XANES spectra obtained in this study, the root mean square error (R-factor) was less than 0.080, suggesting that the dominant form of As in the sediment was either arsenate or arsenite. This also suggests that the contribution of As bearing sulfide is almost negligible within total As (Fig. 4–2). The XANES spectra of SL2 and SD3 are quite similar to that of As(V) solution, whereas the proportion of arsenite gradually increases in SD5 and SD8. The XANES spectra of SD13, SD16, SD21, and SD26 are similar to that of As(III) solution, whereas the contribution of arsenate is significant in SD22 and SD23. The fraction of As(III) is greater than 0.65 below 5 m depth (Fig. 4–3).

4.3. Fe K-edge XANES

The pre-edge structure of Fe K-edge XANES after the subtraction of the baseline is shown in Fig. 4–4. The dotted vertical line corresponds to the POC of hematite and biotite. With an increasing proportion of Fe(III) compounds, the POC generally shifts to higher energy and the peak area becomes larger (Wilke *et al.*, 2001). The proportion of ferric species was high at 2 m, whereas ferrous species became increasingly important below 2 m. A higher proportion of ferric species was also observed below 14 m in SD15–SD26. A change in oxidation state with depth was shown in Fig. 4–3 using the relative shift of centroid (RSC). The RSC above 4 m is ca. 0.5 whereas RSC becomes >0.6 below that depth. SD13 and SD16 gave particularly high RSC of >0.9 suggesting that the contribution of ferric species is lowest in these depths.

Figure 4–5 shows the normalized and first derivative XANES spectra of Fe in samples and some reference minerals. The FL-XANES spectra of SD9–SD26 are similar, whereas the spectrum of SL2 is different. The FL-XANES spectra of sediments below 9 m are characterized by shoulders appearing at 7.122 keV. The shoulder is more prominent as the local minimum point of the first derivative spectrum, which appears at 7.122 keV. This peak is small in SL2 suggesting that a significant change of Fe species occurs between 2 and 9 m. Although the dominant Fe phase in the samples cannot be uniquely determined by a comparison of FL-XANES with reference materials, the sample from 2 m is similar to ferrihydrite. This is consistent with the pre-edge

information shown above. At 9–26 m, the first derivative FL-XANES is characterized by the three peaks at 7.116, 7.119, and 7.124 keV. They correspond to the three peaks found in the first derivative spectrum of biotite. This result indicates that most of Fe is present in detrital silicates as proposed by Polizzotto *et al.* (2006). Iron sulfide should be minor in the sediments, because the XANES spectrum of pyrite is totally different from that of Fe oxide, as noted in O'Day *et al.* (2004a).

The shape of CEY-XANES spectra, which are surface sensitive, is different from FL-XANES at all the depths. In particular, the shoulders found for biotite become smaller in CEY-XANES spectra from SD9–SD26. Such a difference is more distinct in the first derivative XANES spectra. Although both first derivative XANES spectra collected under FL and CEY modes gave the same peaks (7.116, 7.120, 7.124 keV), the peaks at 7.116 keV were attenuated in CEY-XANES. This change indicates an increase in the proportion of ferric compounds when measured in CEY mode. As noted above, the dominant phase of Fe at 9–26 m depth is as detrital silicate minerals, e.g., biotite or hornblende. The attenuation of the peak at 7.116 keV may reflect the alteration of such silicates at the particle surfaces and/or the formation of secondary phases, possibly Fe oxyhydroxides.

4.4. Chemical extraction

The concentration of labile Fe was generally higher in the silt samples, >2.0 mg/kg in SL2, SL7, SL19, than in the sand samples of mostly <1.2 mg/kg except for SD13. The proportion of total Fe varied in the range 15–46% in the Holocene aquifer (Fig. 4–6). The concentration of inert Fe unextracted by hot HCl solution was 2.7–3.7 mg/kg except for SL7 at 4.4 mg/kg. As noted, unextractable Fe may be mainly incorporated in crystalline silicates or sulfides. Because the concentration of S in the Holocene aquifer was very low <0.06% as noted in 3.1, the main phase of Fe should be as detrital silicate. According to optical observation and XRD analysis (Seddique *et al.*, 2008), the majority of inert Fe is likely to be contained in biotite, and chlorite, with minor contribution of smectite.

Labile As concentration varied in the range 1.7–7.3 mg/kg in the Holocene aquifer, whereas it was 1.4–1.9 mg/kg in the Pleistocene aquifer (Table 4–3). The highest

content of labile As was observed in SL2, which exhibits oxic characteristics. Similarly to Fe, labile As was generally more abundant in the silt layers than the sand layers. However, in the lower half of the upper aquifer, the abundance of labile As is high in both the silt and sand samples SL19–SD26. The proportion of labile As as total As varied in the range 30–89%. This information is important to the interpretation of the results of the As K-edge XANES, which reflects bulk information. In the hot $HCl_{(aq)}$ extraction, inert As may have been incorporated in crystalline silicates or sulfides. However, the contribution of As sulfide should be very small based on the XANES analysis for the bulk sediment. Seddique *et al.* (2008) report that the majority of inert As is in biotite, which has an As content up to 49.6 mg/kg. The oxidation state of As in separated biotite from SD13 was mainly As(III) (ca. 65%) based on the As K-edge XANES. These results indicated that a major host phase of inert As is most likely biotite.

4.5. Adsorption experiment

The apparent distribution coefficient of As(V) and As(III) is listed in Table 4–4 with the uncertainty in the range of each K_d value. In equation 3, only adsorbed As having the same oxidation state as added As should be considered as m^{As}_{ads}. However, the oxidation state of initially adsorbed As is difficult to estimate. Hence, the uncertainty of apparent K_d value defined as equation 3 can be large when As_{ads} is high. When all the initially adsorbed As formed a different species to added As, the apparent K_d should be minimum (K_{d_min}). Conversely, when all the As initially adsorbed was the same species as added As the apparent K_d should be maximum (K_{d_max}).

The apparent distribution coefficient K_d for As(V) was always higher than that for As(III) for all the samples (Fig. 4–7). This result indicates that the reduction of arsenate can be a cause of As mobilization at all depths. In the Holocene aquifer, the K_d of As(III) [$K_{d\text{-}As(III)}$] was 7.9 ± 1.7 – 56 ± 11 L/kg, whereas that of As(V) [$K_{d\text{-}As(V)}$] was 23 ± 2.4 – 672 ± 111 L/kg (Table 4–4). The $K_{d\text{-}As(III)}$ tended to be high in silt samples rather than in sand samples such as SL2, SL7, and SL19. Although $K_{d\text{-}As(V)}$ was also high in silt samples, some sand such as SD3 and SD23, gave comparable or even higher $K_{d\text{-}As(V)}$ than silt samples. Both $K_{d\text{-}As(III)}$ and $K_{d\text{-}As(V)}$ tended to be high near the surface, probably

due to the oxic nature of the sediments. The largest difference between $K_{d\text{-}As(III)}$ and $K_{d\text{-}As(V)}$ was observed for SL2. Below SL2 at 2.2 m, both $K_{d\text{-}As(III)}$ and $K_{d\text{-}As(V)}$ decreased with depth increase. This is consistent with the reduction of Fe oxyhydroxides below 5 m as noted in section 3.2. In the Pleistocene aquifer, the $K_{d\text{-}As(III)}$ were 9.4 ± 0.8 L/kg and 88 ± 4.3 L/kg in SD48 and SL39, respectively. On the other hand, $K_{d\text{-}As(V)}$ were 17 ± 1.7 L/kg and 215 ± 10 L/kg respectively.

The concentration of phosphate-extractable As (hereafter As_{ads}) was 0.08–2.1 mg/kg in the Holocene aquifer, whereas it was less than 0.17 mg/kg in the Pleistocene aquifer (Table 4–3). In the Holocene aquifer, the As_{ads} tended to be higher in silt rather than sand layers. Among the sand samples, the As_{ads} was higher in the lower rather than in the upper half of the Holocene aquifer (Fig. 4–7).

All the adsorption isotherms of As(III) for SD13, SD16, and SD26 can be fitted by a Freundlich isotherm (Fig. 4–8) indicating that when the obtained K_d values are used for discussion, the nonlinearity of K_d over the wide range of As concentration should be considered.

5. *Discussion*

5.1. Speciation of As and Fe in sediments

To clarify the reactions promoting As mobilization under reducing conditions, speciation of Fe and As in the sediments is essential. In the study area, As(V) was reduced to As (III) near the surface, whereas As dissolution occurred significantly in a deeper layer at 15–30 m (Fig. 4–3). If the reduction of As(V) is the primary cause for the mobilization of As, the concentration of As in groundwater should be high near the surface accompanied by the As reduction. The disagreement in the depths of redox boundaries and the peak of dissolved As concentration indicates that other factors should be considered to explain the "bell-shaped" depth profile of dissolved As (Fig. 4–3c). Breit *et al.* (2001) report that arsenate is dominant in shallow sediment above the water table, whereas arsenite becomes dominant in water-saturated sediment. Polizzotto *et al.* (2006) report a dramatic change in the oxidation state of As in soil from the

surface to a depth of 36 cm. Both reports support the idea that reduction of As(V) near the surface is common in other parts of Bangladesh. Because the peak of dissolved As is commonly at a depth significantly beneath the surface such as at 15–20 m depth in Araihazar (van Geen *et al.*, 2003), and 30–40 m depth in Munshiganji (Harvey *et al.*, 2002), as well as at 30 m depth in a district east of Dhaka (Stollenwerk *et al.*, 2007), the cause of the disagreement between the depths of redox boundary and peak of dissolved As-concentration must be investigated to clarify the mobilization process of As in a contaminated aquifer.

In a manner similar to As, the oxidation state of Fe indicates a reduction of Fe oxyhydroxides near the surface. A decrease of labile Fe and an increase of RSC in the Fe K-edge XANES from SL2 to SD5 support the observed reduction of Fe oxyhydroxides. These results indicate that the reduction of Fe oxyhydroxides occurred around the water table. This suggests that dissolved As concentration is not always high at the depth where Fe oxyhydroxides are unstable. Reduced Fe would be flushed out as dissolved Fe^{2+} or fixed as secondly minerals such as siderite, vivianite, mackinawite, magnetite, and green rust (Hansel *et al.*, 2003; Akai *et al.*, 2004; Ahmed *et al.*, 2004; McArthur *et al.*, 2004). A significant deficit of labile Fe at 2–5 m and a high concentration of dissolved Fe in W1 at 6–12 m indicate that reduced Fe near the surface is mostly flushed away in the sand layer just below the water table.

If the secondary Fe(II) compounds are present below the water table, they can be detected in CEY-XANES due to the clearly differentiable feature of Fe K-edge XANES for carbonates, phosphates, sulfides from silicates and oxides (O'Day *et al.*, 2004a; Taylor *et al.*, 2008). O'Day *et al.* (2004a) suggest a practical detection limit for a mineral component by Fe K-edge XANES in a binary or ternary mixture to be about 5%. However, even employing CEY-XANES, a contribution by Fe carbonates, phosphates, and sulfides was not confirmed, suggesting that the presence of these secondary phases was unlikely in the core samples.

Compared to the upper half of the Holocene aquifer, the proportion of ferric species is high in the lower half. A higher concentration of labile As in the lower rather than upper half is consistent with an increase of ferric compounds (Fig. 4–6). Although a large fixation capacity for As is predicted within this depth, dissolved As in

groundwater is highest at a depth of 20–30 m. Hence, apparent K_d should be experimentally determined for the sediments in both the upper and lower halves of the Holocene aquifer to clarify whether the depth profile is consistent with the profile predicted by the adsorption equilibrium model. If we can explain the depth profile based on certain assumptions, the controlling factors of As transport in an aquifer can be specified from the consistency between the predicted and actual values in the As depth profile.

5.2. Simulation of depth profile of aqueous As based on the As adsorption equilibrium

One approach to confirm adsorption equilibrium is a comparison of measured As concentration in groundwater with the estimated concentration in an adsorption equilibrium model. For this purpose, I estimated dissolved As (C_w) in interstitial water at various depths assuming adsorption equilibrium by the following equation:

$$C_w(mg/L) = K_d^{-1}(kg/L) \times As_{ads}(mg/kg) \qquad (5).$$

Note that $K_{d\text{-}As(V)}$ was used for the samples above 4 m, whereas $K_{d\text{-}As(III)}$ was used below 4 m based on the results of the As K-edge XANES. According to Fig. 4–9, the C_w from 6–12 m depth matches well the range of As concentration in groundwater collected from W1. Additionally, C_w values predicted for 13 and 15 m are also within the range. Because both SD13 and SD15 can also be classified into upper half in terms of lithology (Table 4–1), this result is consistent with the prediction. An increase of C_w below 15 m is also consistent with a "bell-shaped" profile of As in groundwater (Fig. 4–3c). Although C_w predicted by the model can explain qualitatively the high concentration of As in groundwater in the lower half, the C_w at 18–28 m (30–90 μg/L) is somewhat lower than that measured As in groundwater from W2 (85–153 μg/L). Considering the value of adsorbed As, the required range of $K_{d\text{-}As(III)}$ values for SD22 and SD26 are ca. 5–12 L/kg to satisfy the range of aqueous As concentration from W2. Such a value is actually observed in SD16, which can be classified into the lower half in terms of lithology (Table 4–1). Thus, the difference between the predicted and measured values in the lower half can be ascribed to the spatial heterogeneity in sediment property. As

shown in Fig. 4–3c, aqueous As concentration in well waters from the entire 3 km^2 study area can vary from <1–>1000 μg/L in the Holocene aquifer (Itai *et al.*, 2008b). Considering this large variation, the simulation result for the C_w value can explain the measured aqueous As concentration, suggesting that the adsorption equilibrium primarily governs the aqueous As concentration in groundwater.

5.3. Factors controlling K_d

As discussed in the previous section, variation of apparent K_d can directly affect the variation of aqueous As concentration in groundwater. Hence, factors controlling K_d should be clarified to understand the cause of the large variation in aqueous As concentration.

According to the depth profile of K_d, both $K_{d\_As(III)}$ and $K_{d\_As(V)}$ tend to be larger near the surface, i.e., in an oxic environment. However, the apparent variation of K_d is more marked for $K_{d\_As(V)}$ and $K_{d\_As(III)}$. Possible factors controlling K_d are (i) mineral composition, particularly the abundance of Fe oxyhydroxides, and (ii) surface area of sediments. To clarify the controlling factors of K_d, I compared the relationships of K_d with (i) RSC of Fe K-edge XANES, and (ii) BET surface area (Fig. 4–10). Both $K_{d\_As(III)}$ and $K_{d\_As(V)}$ for sand samples are negatively correlated to the RSC of Fe K-edge XANES. That is, both K_d values increase with increasing amount of Fe oxyhydroxides. In particular, $K_{d\_As(V)}$ shows clearer correlation (r^2 = 0.8572 for sand, n = 7) than $K_{d\_As(III)}$ (r^2 = 0.6563 for sand, n = 7). The relationship between $K_{d\_As(III)}$ and the BET surface area shows a linear relationship irrespective of the difference in the type of lithology (Fig. 4–10c). The data are distributed along an empirical line: $K_{d\_As(III)}/(L/kg) = 8.4\ S_B/(m^2/g) + 4.8$ [r^2 = 0.9059, n = 10), where S_B is the BET surface area. In contrast, $K_{d\_As(V)}$ does not show a distinctive relation with the surface area. Consequently, a primary factor controlling $K_{d\_As(III)}$ is the surface area of sediment, whereas the amount of Fe oxyhydroxides strongly relates to $K_{d\_As(V)}$.

Our results indicate that if As(V) is present in an aquifer, the host phase in the sediment is likely to be Fe oxyhydroxide. This is consistent with EXAFS results presented by Gault *et al.* (2003) showing that As(V) is adsorbed as bidentate arsenate tetrahedra on metal (Fe and/or Al) oxyhydroxide surfaces. Conversely, the host phase of

As(III) is not very clear in the sample.

The most important solid phase as an adsorbent of As(III) is Fe oxyhydroxide according to the laboratory experiments (Smedley and Kinniburgh, 2002 and references therein). Because the concentration of As in a contaminated aquifer is not high, only small amounts of Fe oxyhydroxides can suppress aqueous As to the natural baseline level of <10 μg/L. Polizzotto *et al.* (2006) experimentally confirmed that the addition of 0.04 wt% of Fe (as Fe oxyhydroxide) to sediment, which was collected from an As-contaminated aquifer in Bangladesh, could reduce 88% of dissolved As in coexisting water at ca. 100 μg/L before the addition. This amount of Fe oxyhydroxide is at least 10 times lower than that of labile Fe in the sediments determined in this study. Such a small amount of Fe oxyhydroxide is possibly available below 16 m based on the decrease of RSC in this depth and increase of the contribution of Fe(III) in CEY-XANES rather than in FL-XANES. Nevertheless, $K_{d\_As(III)}$ does not show any distinct difference between the upper half (reducing environment) and lower half (less reducing environment). Consequently, (i) a clear positive correlation between As(III) and the BET surface area, and (ii) less sensitive change in $K_{d\_As(III)}$ to the redox state of Fe compounds both indicate that $K_{d\_As(III)}$ is not solely controlled by the amount of Fe oxyhydroxides, but also that the surface area is important.

5.4. Primary factor controlling depth profile of aqueous As concentration

As suggested in 5.1, aqueous As in groundwater is not always high where arsenite is stable and Fe oxyhydroxides are unstable. Other factors should be considered in explaining the depth profile of aqueous As concentration. Because the affinity of As(III) to sediment (i.e., $K_{d\_As(III)}$) does not show a systematic difference between the upper and lower halves of the Holocene aquifer, a primary factor controlling the contrast of aqueous As concentration can be the amount of As adsorbed in the sediment. When K_d values are similar over the depth, the difference found in the amount of adsorbed As reflects that of As supplied to each sediment in the past. Conversely, the amount of As accumulated so far by the groundwater flow can be discussed from the difference of adsorbed As.

For example, SD13 and SD22 have an apparently similar $K_{d\_As(III)}$, but the amount

of As adsorbed to SD13 is almost half that of SD22. There are two possible explanations for such a difference. One process is the selective flow of high-As groundwater into the 18–30 m interval. Conversely, As initially adsorbed in the 5–18 m stratum that has been flushed out due to the flow of low-As groundwater presents another possible process. Although both are in-principle possibilities, the former process is likely to have been dominant in the study area, because the permeability coefficient of the lower half is 3.5 times higher than the upper half. Either increase or decrease of adsorbed As should be more noticeable in the lower half rather than the upper. However, the amount of adsorbed As is significantly greater in the lower half, suggesting that groundwater flows in the upper and lower sections are hydrologically separated, and a large amount of As should be released from the host mineral in a hydrological up gradient of groundwater flow in the upper half.

An opposite example is sample SD48 collected from the Pleistocene aquifer. It is well known that this aquifer is generally not contaminated by As (e.g., BGS and DPHE. 2001; Zhang *et al.*, 2005) as was also found in the study area (Mitamura *et al.*, 2008). Despite the oxic nature of SD48, the apparent $K_{d\_As(III)}$ is not high relative to the samples from the Holocene aquifer (Table 4–4), suggesting that if the amount of labile As in the Pleistocene aquifer is comparable to that in the Holocene aquifer, aqueous As concentration could be high. It is obvious that a low aqueous As concentration in the Pleistocene aquifer is caused by a low concentration of adsorbed As (Table 4–4). Flushing is the most plausible explanation for this depletion of adsorbed As.

The two examples above suggest that groundwater flow in the past has caused a large variation in aqueous As concentration, not only by the decrease of As following flushing, but also through accumulation of As following high-As groundwater flow.

5.5. Physico-chemical factors controlling variation of aqueous As concentration

According to the adsorption equilibrium model, aqueous As concentration is basically controlled by the three factors of: the oxidation state of As; the affinity of As to sediment (K_d); and the amount of As adsorbed in sediment. In the study area the concentration of As was in the range <1 μg/L–>1000 μg/L in the Holocene aquifer (Itai *et al.*, 2008b). We can give some constraints for the causes of the large variation in As

concentration in groundwater using the three parameters shown above.

Figure 4–11 shows the chemical conditions required to form aqueous As concentration under adsorption equilibrium. According to Fig. 4–11, and the factors controlling the K_d value discussed in 5.3, the physico-chemical conditions needed to form various aqueous As concentrations can be summarized as follows.

(I) <1 μg/L region. Both As(V) and Fe oxyhydroxides are stable, when adsorbed As is very low (<0.5 mg/kg as in SD48).

(II) 1–10 μg/L region: As(V) is stable. If As(III) is dominant, the amount of adsorbed As(III) should be low (<1 mg/kg).

(III) 10–100 μg/L region. As(III) is stable. The amount of adsorbed As(III) is more than 0.5 mg/kg.

(IV) 100–1000 μg/L region. As(III) is stable. The apparent K_d should be low due to the dominance of coarse-grained sediments and/or the competition effect.

(V) >1000 μg/L region. As(III) is stable. Coarse-grained sediment is dominant and considerable competition effect is needed.

The ranges of K_d values and amount of adsorbed As were obtained from only one drill core, it is therefore conceivable that the K_d value variation could be larger across the entire study area. As an illustration the reported apparent K_d values based on the simultaneous measurement of As in both sediment and coexisting water are ca. 4 L/kg and 2–6 L/kg in van Geen *et al.* (2008) and BGS and DPHE (2001) respectively, and these are lower than $K_{d\_As(III)}$ determined in this study (Fig. 4–11). As discussed in 5.3 the primary factors controlling $K_{d\_As(III)}$ are surface area and the amount of Fe oxyhydroxide. If the coarse-grained sediment is dominant and the amount of Fe oxyhydroxide is very small $K_{d\_As(III)}$ can take a smaller value as reported in other studies. The sample collected from the most reducing environment, SD16, actually shows the lowest $K_{d\_As(III)}$ value of 6.2–10 L/kg. If the apparent K_d is as low as 2 L/kg reflecting the variation of these controlling factors, it is possible to explain the formation of an aqueous As concentration of more than 1000 μg/L.

The adsorption equilibrium model permits implications for the temporal variation of aqueous As in well waters. Because the majority of As is adsorbed onto the solid

phase, the concentration of aqueous As is buffered when water having a different composition meets the water–rock system at the tube well screen placement. This buffering effect prevents a drastic change in concentration of aqueous As over time. In the study area, the change in concentration of aqueous As was mostly within 20% for ca. 230 tube wells during one and a half years despite a large spatial variation of As concentration amongst the different wells (Itai *et al.*, 2008b). Cheng *et al.* (2005) also reported a limited temporal variation within 15% at Araihazar, based on the continuous monitoring of As in ten shallow wells <20 m over three years, although two of the shallowest wells about 8 m deep showed a significant seasonal variation of 21–63%. The adsorption equilibrium model has the potential to explain not only the spatial variation of aqueous As concentration, but also the limited temporal variation of As concentration in groundwater in Bangladesh.

6. *Conclusions*

In Chapter 4, I focused on the speciation of As and Fe in the solid phase, and the adsorption properties of As(V) and As(III) in sediment to confirm the adsorption equilibrium in an As-contaminated aquifer. Although the variation of As concentration in groundwater is very large (<1 to >1200 μg/L), a most important factor in the generation of high-As groundwater of >100 μg/L is the oxidation state of As. According to the adsorption equilibrium model, the aqueous As concentration can easily exceed the WHO provisional guide value for drinking water of 10 μg/L when the As(III) is stable irrespective of the mineralogy of the sediment. Although many studies have considered As-contaminated aquifers in Asia, there have been few experimental approaches dealing with the adsorption–desorption reaction taking into account the As oxidation state. It is difficult to design a mitigation strategy for a great spatial variation in the As contamination of groundwater. The adsorption equilibrium model has the potential to account for the inhomogeneity of spatial variation and limited temporal variation in the As concentration of tube well waters. A quantitative evaluation based on the adsorption–desorption reaction at a local scale is needed to identify the factors controlling the present As distribution, together with hydrogeochemical modeling that

considers a complex regional groundwater flow.

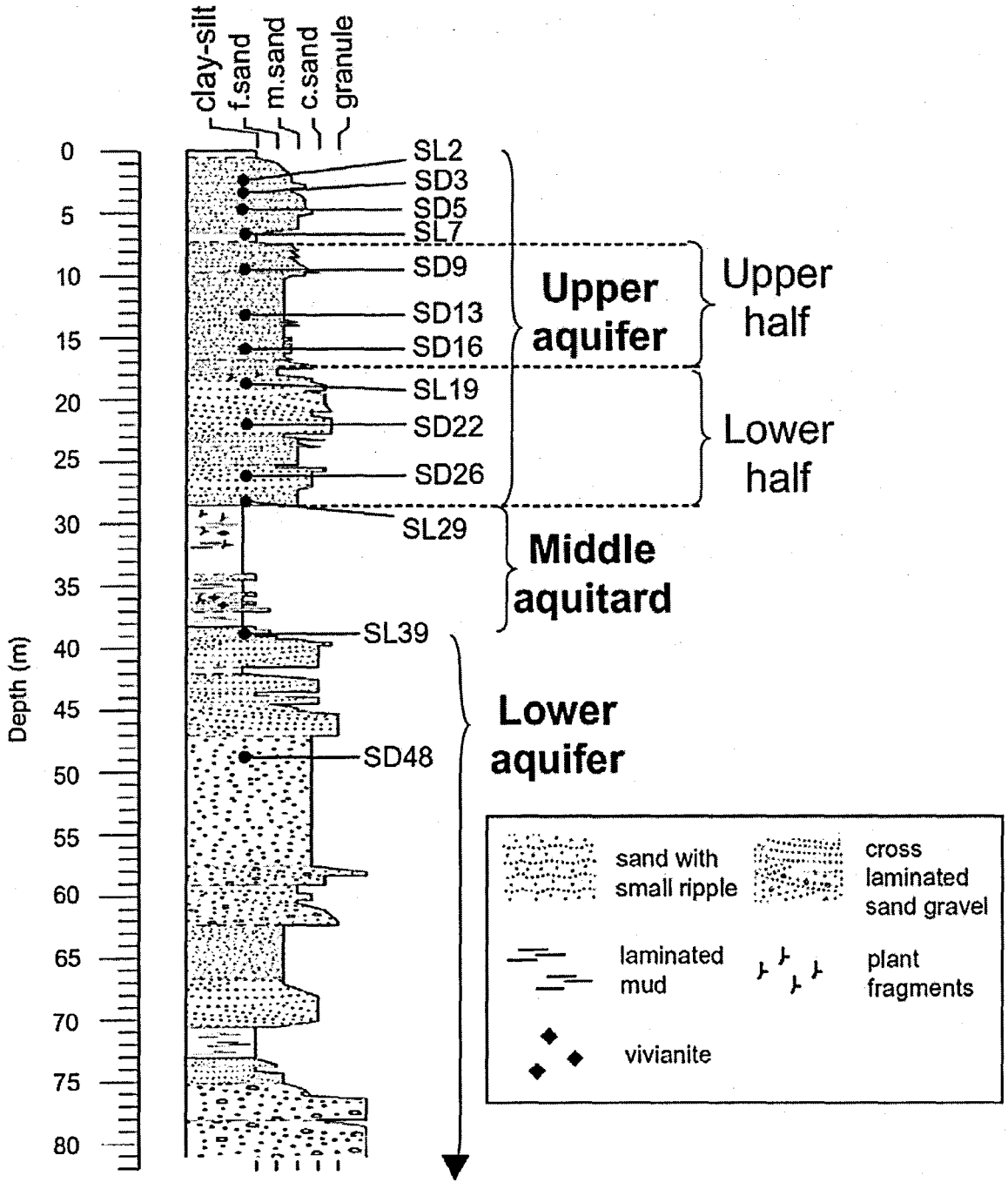

Fig. 4-1. Lithologic profile of cored sediment from surface to 80 m depth collected from the study area. The thickness of column indicates the grain size of the sediments.

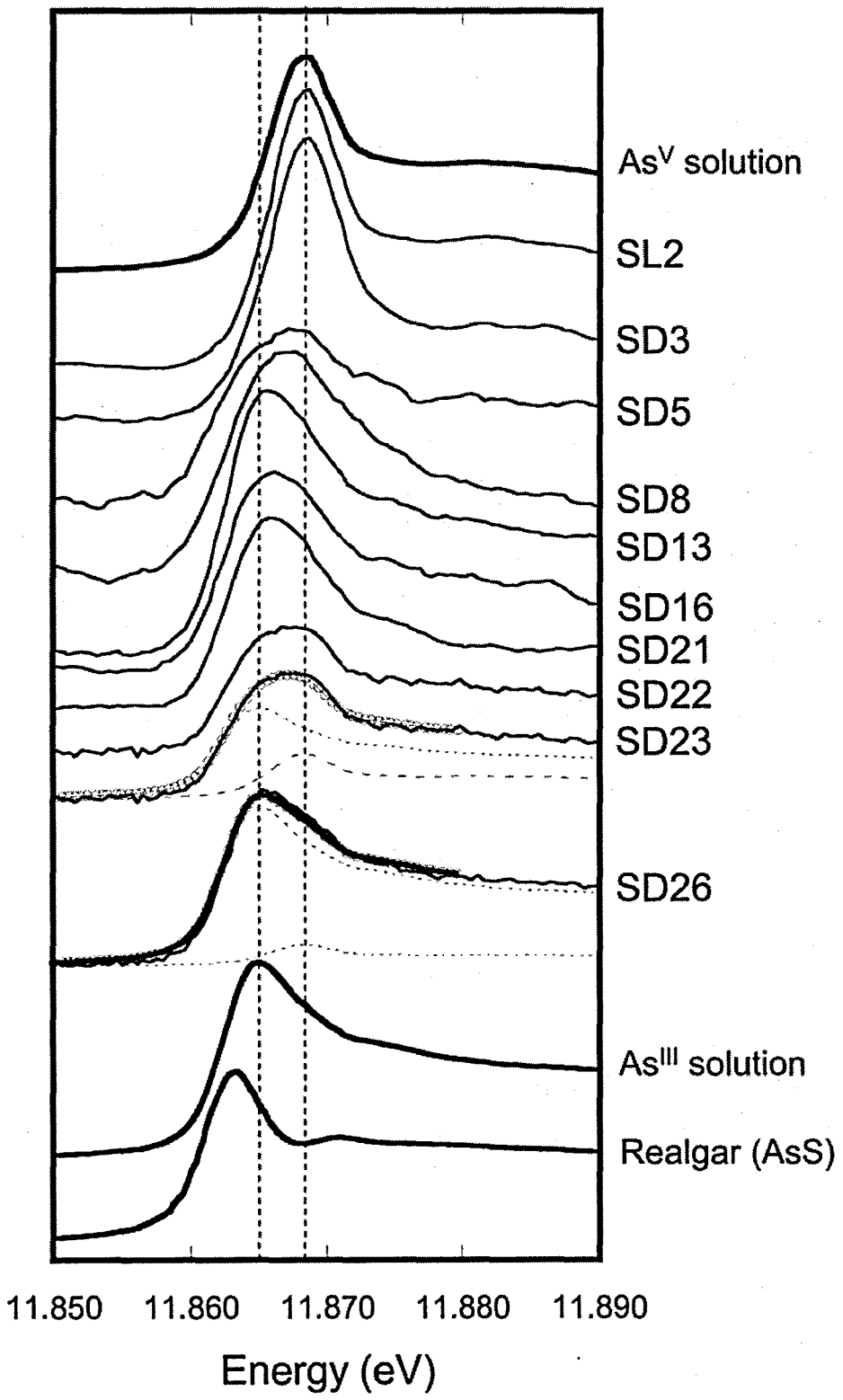

Fig. 4-2. Normalized As K-edge XANES spectra for sediments. The depth of each sample is shown in Tables 4-1 and 4-2.

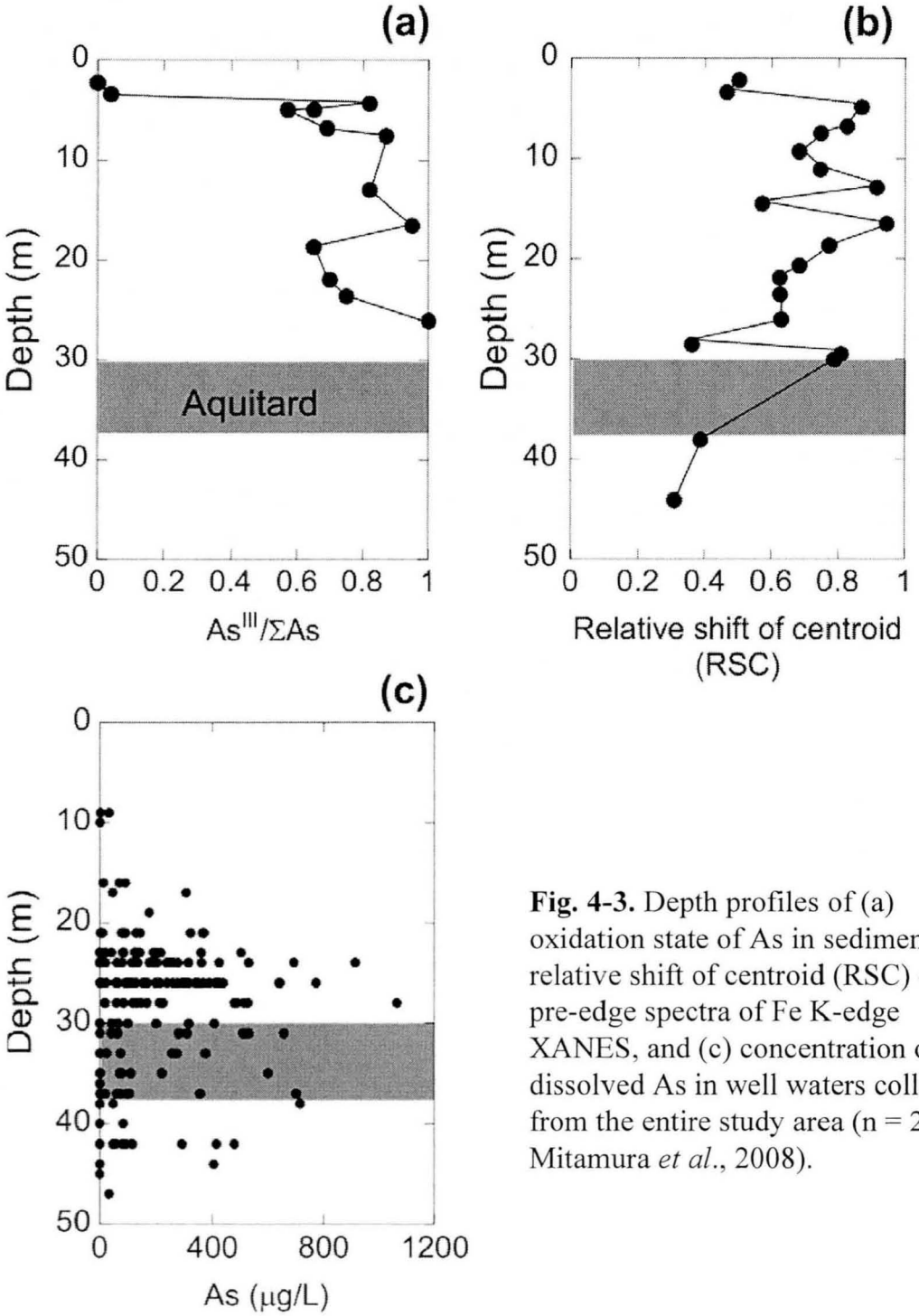

Fig. 4-3. Depth profiles of (a) oxidation state of As in sediment, (b) relative shift of centroid (RSC) of pre-edge spectra of Fe K-edge XANES, and (c) concentration of dissolved As in well waters collected from the entire study area (n = 228, Mitamura *et al.*, 2008).

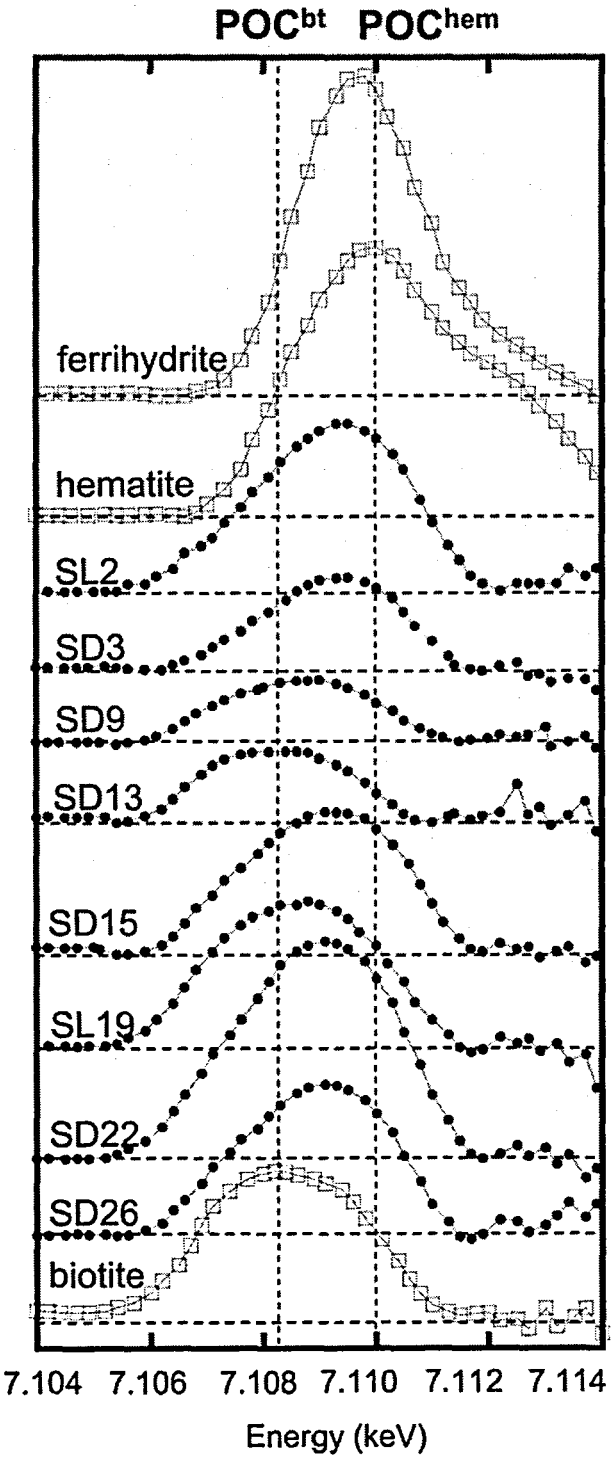

Fig. 4-4. The pre-edge of Fe K-edge XANES spectra after background subtraction. The depth of each sample is shown in Tables 1 and 2.

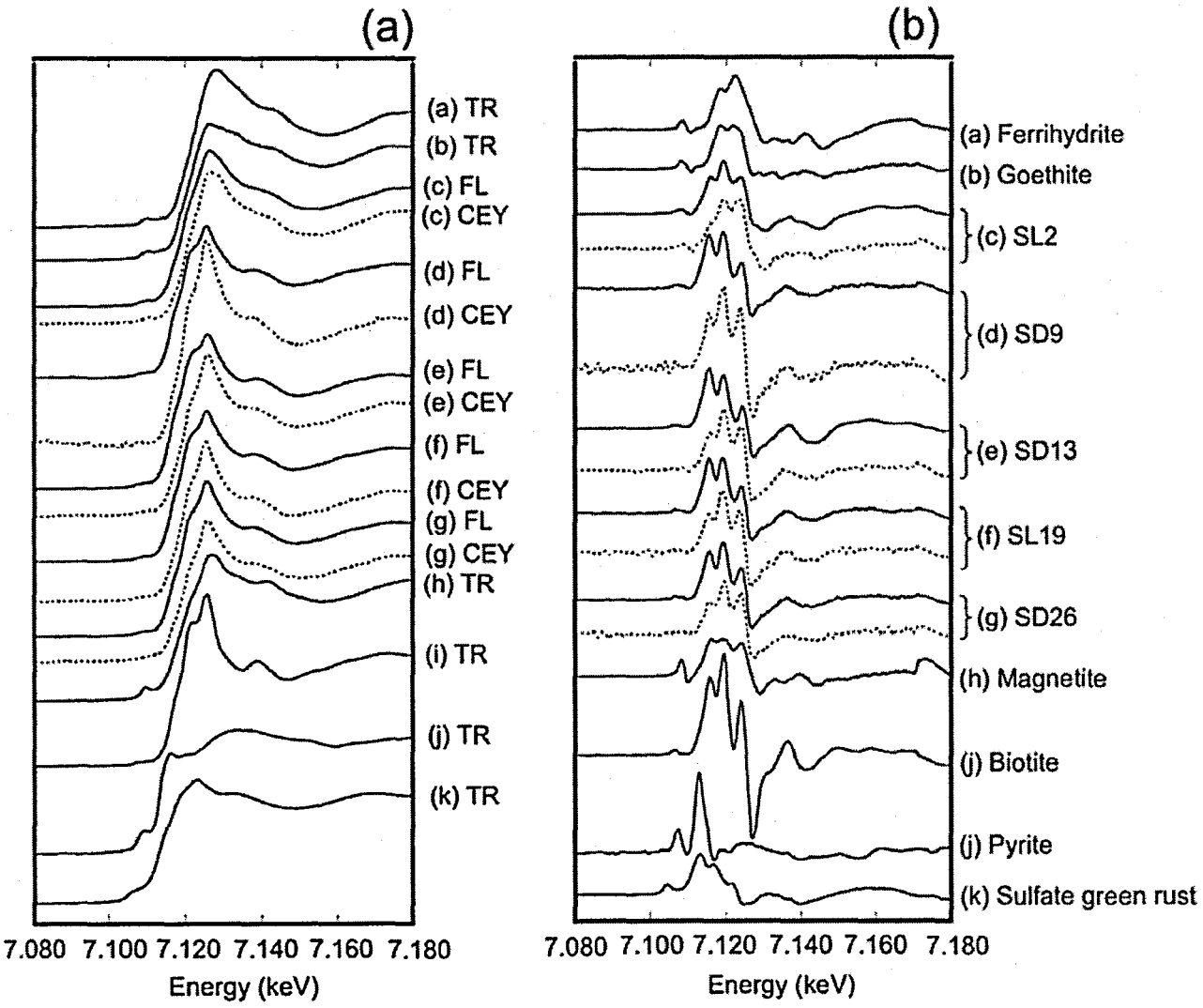

Fig. 4-5. (a) Normalized, and (b) first derivative Fe K-edge XANES spectra. Solid and dotted line spectra represent FL and CEY-XANES, respectively.

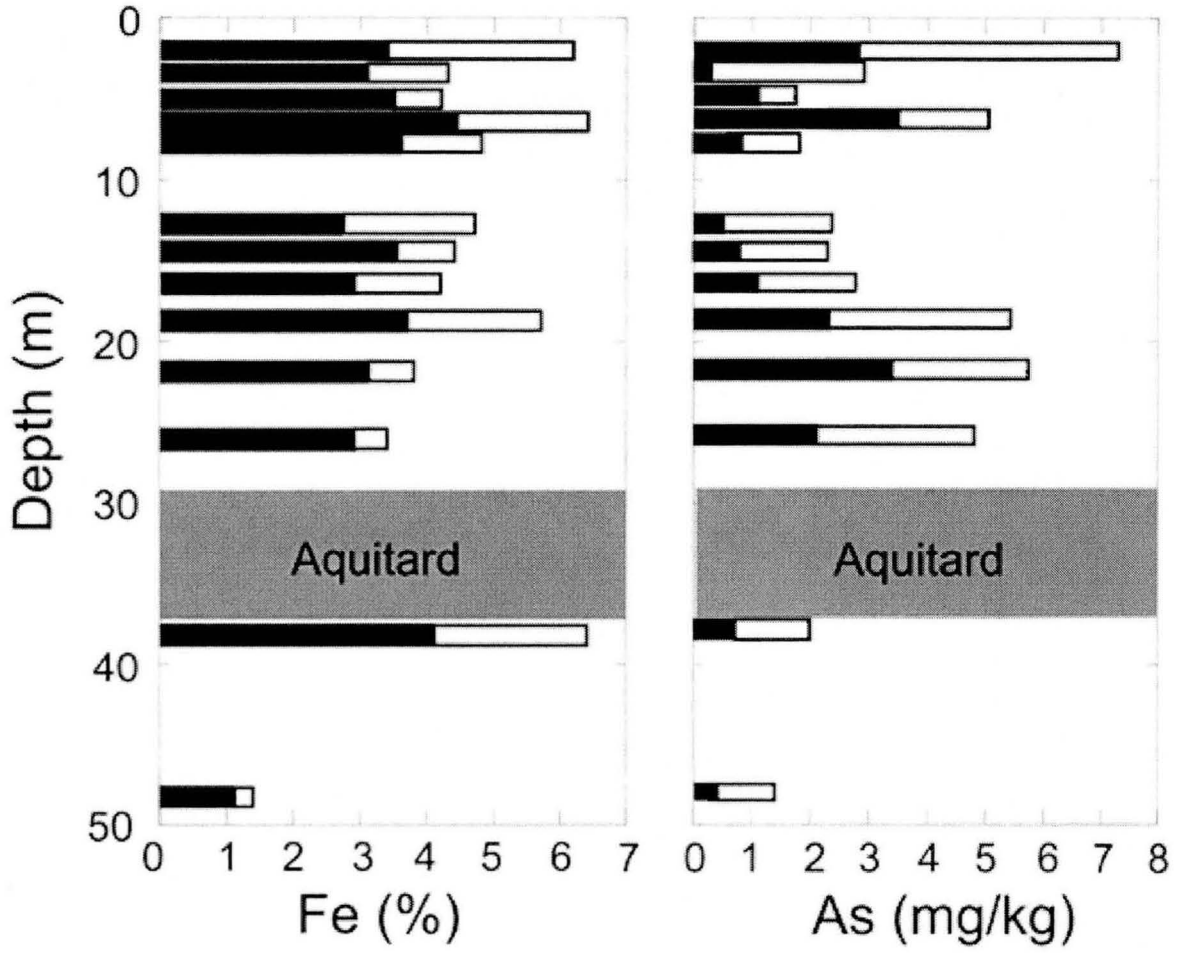

Fig. 4-6. Results of acid extraction of Fe and As as a function of depth. White and black bars respectively represent HCl extractable and unextractable phases.

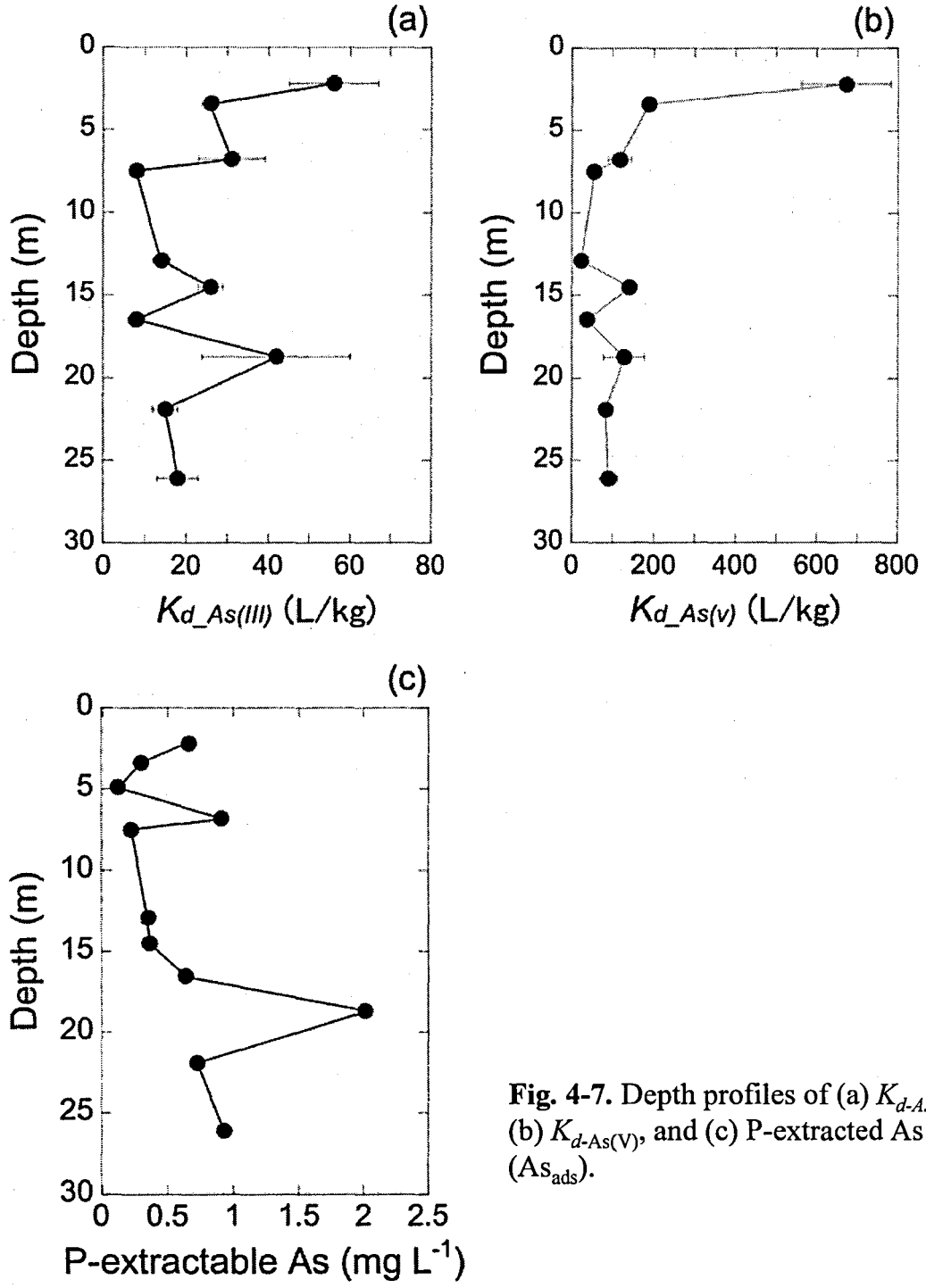

Fig. 4-7. Depth profiles of (a) $K_{d\text{-}As(III)}$, (b) $K_{d\text{-}As(V)}$, and (c) P-extracted As (As_{ads}).

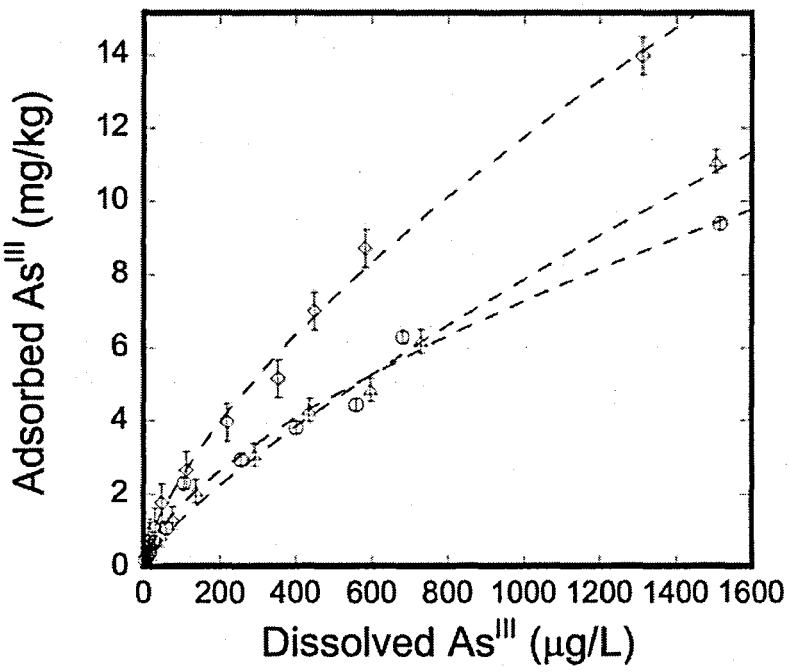

Fig. 4-8. Adsorption isotherm of As(III) at pH 7.3 for three sediments. ○, △, and ◇ are SD13, SD16, and SD26, respectively. The dashed line shows a fitted curve using the Freundlich equation.

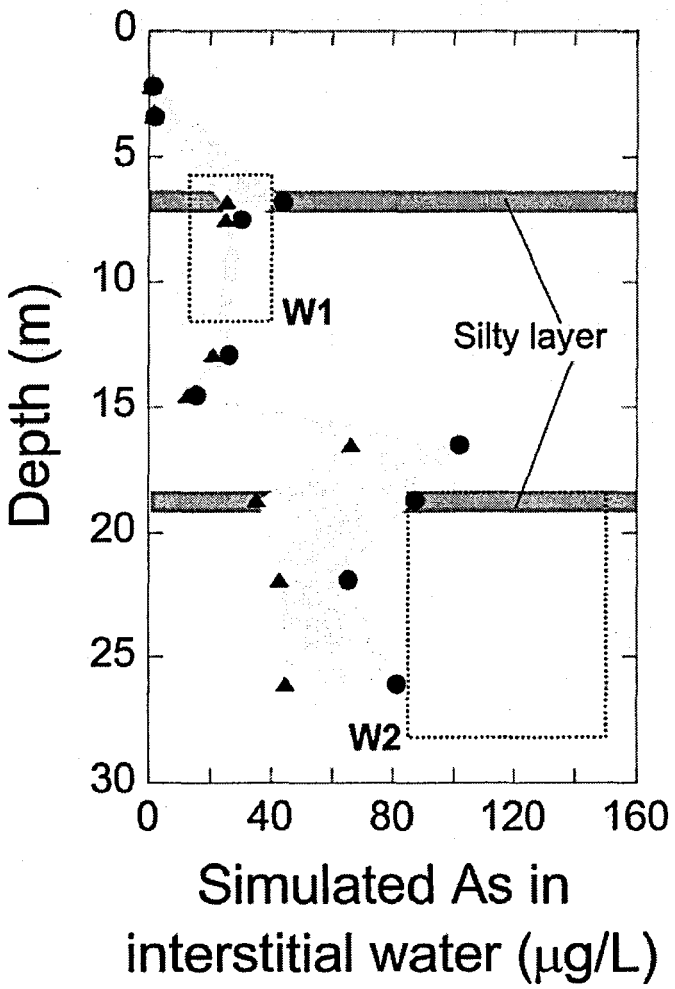

Fig. 4-9. Simulation of aqueous As concentration in groundwater equilibrated with sediment in each depth. ▲ and ● show the simulated value using the minimum and maximum values of K_d shown in Table 4. Square regions by dotted line indicate range of measured As concentration in groundwater from W1 and W2 from January to October 2005 (n = 8).

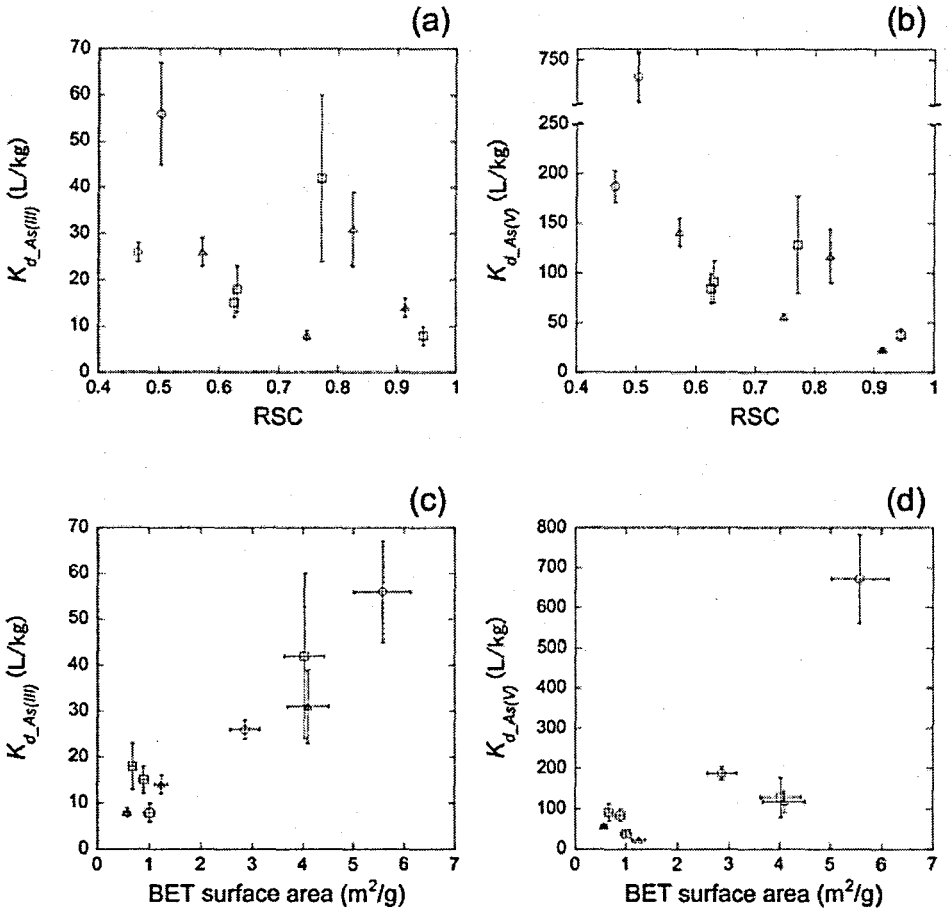

Fig. 4-10. Relationships between (a) $K_{d\text{-}As(III)}$ and RSC (Relative shift of centroid) of Fe K-edge XANES, (b) $K_{d\text{-}As(V)}$ and RSC, (c) $K_{d\text{-}As(III)}$ and BET surface area, and (d) $K_{d\text{-}As(V)}$ and BET surface area. ○, △, and □ represent samples.

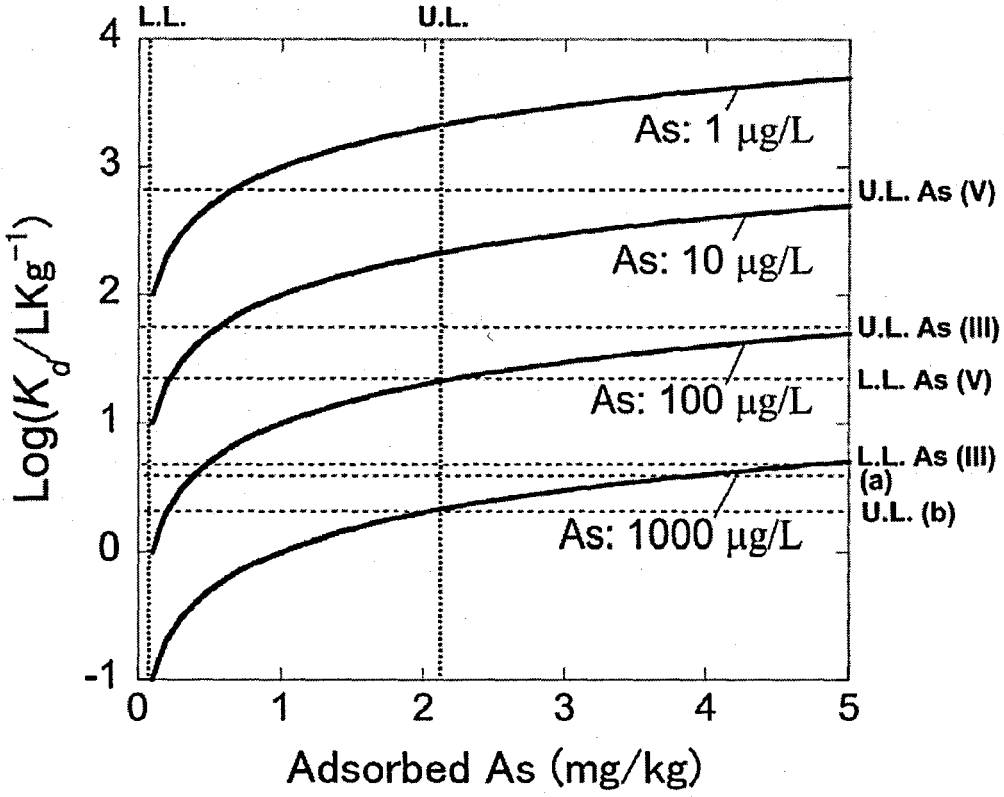

Fig. 4-11. Chemical condition to form a given concentration of aqueous As in groundwater based on the adsorption equilibrium model. Dotted horizontal lines show K_d values. U.L. and L.L. respectively represent the upper and lower limits. (a) and (b) respectively represent the value of apparent K_d as reported by van Geen *et al.* (2008) and BGS and DPHE (2001). The dotted vertical lines are the upper and lower limits of adsorbed As obtained from this study.

Table 1. Lithological characteristics of sediment samples

Sample	middle depth (m)	Lithology	clay (%)	Silt (%)	fine sand (%)	medium sand (%)	course sand (%)	BET surface area (m^2/g)	a* (redness)
SL2	2.20	Silt	10.1	75.5	14.4	0.0	0.0	5.6	-0.7
SD3	3.40	silty fine sand - fine sand	0.7	32.2	58.6	6.6	0.2	2.7	0.9
S8	4.90	silty fine sand - fine sand	1.4	34.1	60.1	4.2	0.2	0.80	-1.4
SL7	6.80	Silt	8.9	75.6	15.5	0.0	0.0	4.1	-1.5
SD8	7.50	silty fine sand - fine sand	0.9	36.9	55.0	7.4	0.2	0.57	-1.4
SD9	9.30	vary fine - fine sand	0.0	13.4	79.4	6.9	0.3	N/A	-1.4
SD11	11.10	very fine - fine sand	0.0	13.2	79.7	5.6	1.5	N/A	-1.3
SD13	12.90	very fine - fine sand	0.3	28.6	67.0	4.1	0.1	1.2	-1.9
SD15	14.50	very fine - fine sand	0.1	14.6	71.6	7.8	5.2	N/A	-1.5
SD16	16.45	silty fine sand - fine sand	0.1	38.8	56.0	4.4	0.8	1.0	-1.8
SL19	18.70	Silt	3.7	64.1	32.1	0.1	0.0	4.0	-1.3
SD21	20.70	medium - course sand	0.2	3.90	19.3	65.6	9.8	N/A	-1.4
SD22	21.90	fine - medium sand	0.0	21.8	58.6	18.6	1.1	0.89	-1.8
SD23	23.15	fine - midium sand	0.5	25.8	54.2	18.0	1.5	N/A	-1.8
SD26	26.10	fine - medium sand	0.0	15.2	60.1	22.5	2.2	0.67	-1.7
SL29	28.55	fine - medium sand	0.9	16.7	50.5	26.4	5.3	N/A	3.4
SL39	38.95	Clay	23.6	72.2	4.2	0.0	0.0	N/A	-2.6
SD48	48.25	medium – course sand	0.0	0.0	59.2	39.1	1.7	N/A	7.3

Table 2. Chemical composition of sediment samples

Sample	middle depth (m)	SiO_2 (%)	TiO_2 (%)	Al_2O_3 (%)	Fe_2O_3 (%)	MnO (%)	MgO (%)	CaO (%)	Na_2O (%)	K_2O (%)	As (mg/kg)	TC (%)	TN (%)	TS (%)
SL2	2.20	65.13	0.85	15.28	6.24	0.10	2.46	2.18	1.69	2.81	7.3	0.18	0.025	0.04
SD3	3.40	74.30	0.66	11.66	4.36	0.07	1.65	2.30	2.32	2.33	2.9	0.095	0.065	0.06
S8	4.90	74.78	0.71	11.10	4.23	0.07	1.62	2.46	1.91	2.15	1.7	0.06	0.07	0.05
SL7	6.80	66.28	0.87	15.77	6.43	0.11	2.72	1.99	1.66	3.03	5.0	0.55	0.025	0.03
SD8	7.50	73.46	0.82	11.13	4.82	0.09	1.78	2.75	1.83	2.10	1.8	0.085	<0.01	0.01
SD9	9.30	78.89	0.32	10.68	2.36	0.03	0.96	1.56	2.15	2.43	1.0	0.08	<0.01	0.05
SD11	11.10	79.97	0.37	9.44	2.44	0.04	1.05	1.98	1.97	1.88	1.6	N/A	N/A	N/A
SD13	12.90	73.31	0.56	12.29	4.68	0.07	1.73	1.73	2.01	2.77	2.4	0.24	0.01	0.05
SD15	14.50	73.86	0.85	10.72	4.74	0.10	1.63	3.17	1.95	1.90	2.3	0.15	<0.01	0.05
SD16	16.45	74.56	0.74	10.56	4.36	0.09	1.58	3.04	1.87	1.95	2.8	0.51	<0.01	0.03
SL19	18.70	66.40	0.89	15.81	6.48	0.10	2.65	2.03	1.78	3.00	5.4	0.75	0.01	0.06
SD21	20.70	76.44	0.47	10.98	3.83	0.06	1.20	1.62	1.89	2.64	2.0	N/A	N/A	N/A
SD22	21.90	79.35	0.44	9.43	3.15	0.06	0.88	1.76	1.70	2.23	5.7	0.065	<0.01	0.03
SD23	23.15	75.69	0.39	11.80	3.89	0.06	1.26	1.24	1.94	3.04	8.2	N/A	N/A	N/A
SD26	26.10	76.86	0.51	10.32	3.49	0.07	1.31	2.51	2.15	2.08	4.8	0.065	<0.01	0.01
SL29	28.55	57.96	0.76	14.19	22.06	0.15	1.07	0.64	0.63	2.41	53	N/A	N/A	N/A
SL39	38.95	70.31	1.03	15.85	6.42	0.11	1.22	0.45	0.72	2.43	1.9	0.45	0.035	0.065
SD48	48.25	89.07	0.28	5.09	1.37	0.03	0.33	0.75	0.76	1.45	3.3	0.055	<0.01	0.005

Table 3. Result of chemical extraction

Sample	Fe_{HCl} (%)	Inert Fe (%)	$Fe_{HCl}/\Sigma Fe$ (%)	As_{HCl} (mg/kg)	Inert As (mg/kg)	$As_{HCl}/\Sigma As$ (%)	As_{ads} (mg/kg)	As_{ads}/As_{HCl}
SL2	2.9	3.4	46	7.3	2.8	62	0.71	10
SD3	1.1	3.1	27	2.9	0.3	89	0.32	11
SD5	0.74	3.5	18	1.7	1.1	35	0.08	4
SL7	2.0	4.4	32	5.0	3.5	30	1.0	20
SD8	1.2	3.6	26	1.8	0.8	57	0.22	12
SD13	1.9	2.7	41	2.4	0.5	78	0.33	14
SD15	0.91	3.5	21	2.3	0.8	67	0.36	15
SD16	1.2	2.9	30	2.8	1.1	60	0.63	22
SL19	1.9	3.7	34	5.4	2.3	58	2.1	39
SD22	0.71	3.1	19	5.7	3.4	40	0.75	13
SD26	0.51	2.9	15	4.8	2.1	56	1.0	21
SL39	2.4	4.1	37	1.9	1.0	44	0.17	9
SD48	0.27	1.1	20	1.4	0.4	70	U.D.	N/A

Table 4. Result of the adsorption experiment

Sample	Previously adsorbed As (mg/kg)	Aqueous As(III) (ug/L)	Newly adsorbed As(III) (mg/kg)	$K_{d\_As(III)}$[a] min (L/kg)	$K_{d\_As(III)}$[b] max (L/kg)	Aqueous As(V) (mg/kg)	Newly adsorbed As(v) (mg/kg)	$K_{d\_As(V)}$[c] min (L/kg)	$K_{d\_As(V)}$[d] max (L/kg)
SL2	0.71	33.4	1.53	46	67	3.19	1.79	561	783
SD3	0.32	69.9	1.64	23	28	10.1	1.73	171	203
SL7	1.0	60.2	1.39	23	40	18.4	1.64	89	144
SD8	0.22	147	1.07	7.3	8.8	31.8	1.66	52	59
SD13	0.33	102	1.30	13	16	69.7	1.44	21	25
SD15	0.36	69.7	1.63	23	29	13.4	1.71	128	155
SD16	0.63	189	1.17	6.2	10	50.2	1.58	31	44
SL19	2.1	59.0	1.43	24	60	21.5	1.71	79	178
SD22	0.75	123	1.41	11	18	24.4	1.68	69	100
SD26	1.0	99.3	1.26	13	23	24.2	1.68	69	112
SL39	0.17	19.4	1.64	84	93	8.20	1.68	205	225
SD48	U.D.	128	1.19	8.6	10	80.0	1.39	15	19

Notes

[a] Assuming that all initially adsorbed As was not As(III).

[b] Assuming that all initially adsorbed As was As(III).

[c] Assuming that all initially adsorbed As was not As(V).

[d] Assuming that all initially adsorbed As was As(V).

Chapter 5 Discussion

In the Chapter 5, I will discuss some common controversial issues in this research field. As mentioned in Chapter 1, there are many common scientific issues, e.g., trigger of As release from sediment, cause of patchy spatial variation and bell shaped depth profile of aqueous As concentration, temporal change in As concentration, source of organic matter, and ultimate source of As. Although the data shown in this study are still not enough to clarify all the issues, my data could give many important constraints. I also mention implications for the mitigation policy, and future prospects of the research about natural occurrence of As-contamination.

1 Cause of bell-shaped profile

Throughout this thesis, particularly in Chapter 4, formation process of bell-shaped profile which commonly observed from various contaminated regions has been discussed. One important assumption based on this study is that aqueous As concentration is consistent with the adsorption equilibrium. Under this assumption, we should consider two types of the effects which are tentatively named as "mass effect" and "partition effect" (Fig. 5–1). The basis of mass effect is that aqueous As concentration is proportional to the amount of As (= sum of As in solid and solution) in the system. If apparent K_d is constant at all the depths, the mass effect is the dominant cause to form difference in As concentration with depth. On the other hand, the partition effect is derived from variation of apparent K_d in each depth. Although the variation of apparent K_d is controlled by various factors (Chapter 4), most important factors are the concentration of Fe oxyhydroxide and the oxidation state of As at least in my research area, Bangladesh. If the amount of As in the system is constant at all the depths, the partition effect should be the dominant factor.

In our study area, the sediment core can be classified into three parts according to the above reasoning (Fig. 5–2). The shallowest layer, named as layer A, is oxic environment where both Fe oxyhydroxide and arsenate are stable. Low aqueous concentration of As is predicted in this layer despite its higher concentration of adsorbed As than the layer below (Fig. 4–7). This is the typical situation where the partition

effect dominantly alters the aqueous As concentration. Below the layer A, both Fe oxyhydroxide and arsenate become unstable. Apparent K_d of arsenite are almost similar at all the depths below layer A. Nevertheless, aqueous concentration of As is higher in the lower part (layer C) than the upper part (layer B). Hence, this difference can be attributed to the mass effect. Using this approach, I can conclude that the difference in amount of As should be attributed to the different mass flux of As for each layer.

Is the process shown above able to extend to the entire part of Bengal Basin? As I noted, bell shaped profile are common in Bangladesh (Chapter 1). In order to generalize my idea, the variation of apparent K_d needs to be known at various study areas. Unfortunately, this information is unavailable in most of intensive study areas. However, several reports confirmed that redox boundary of Fe and As appears around the water table (Breit *et al.*, 2001; Horneman *et al.*, 2004; Polizzotto *et al.*, 2006), indicating that contaminated depth is significantly lower than the redox boundary in several contaminated regions as well as our study area. Under reducing condition where both Fe oxyhydroxide and arsenate are unstable, the variation of apparent K_d is likely small (Chapter 4). Therefore, I suppose that the formation of bell-shaped profile from various parts of Bangladesh is mainly attributed to the mass effect.

2 *Cause of patchy distribution of aqueous As in aquifer*

Controlling factors of lateral distribution of As in groundwater seems more complex than that for vertical direction. Similar to the discussions above, both mass effect and partitioning effect should control the present distribution. Figure 4–11 is helpful to constrain the process of formation of large spatial variation of As concentration. The condition where concentration of aqueous As is very high (>1000 μg/L) or very low (<1 μg/L) can be constrained. For the regions showing low aqueous As, such as spot A (Fig. 5–3), the predominance of arsenate is a necessary factor. Additionally, relatively low adsorbed As (<0.3 mg/kg) is also needed. Such a low concentration of arsenate in solid phase is only formed by the flushing of As by the continuous flowing of low As groundwater. On the other hand, for the regions showing high aqueous As, such as spot B, the prevalence of arsenite and very high adsorbed As (>5 mg/kg) are needed.

According to the above assumption, spot A and spot B should hydrologically separated. The oxygen isotope data supports this scenario. Very low As groundwater coincides with the low $\delta^{18}O$ (mostly -5 to -3‰), whereas very high As groundwater show the high $\delta^{18}O$ (mostly -3 to -2 ‰, Fig. 2–4). Such contrast indicates limited mixing of two water bodies. Additionally, as I mentioned in Chapter 2, total dissolved components of the groundwater flowing spot A (HHD-N) is significantly smaller than the spot B (DRK) implying the smaller residence time of the groundwater beneath the spot A. If this interpretation is correct, depletion of labile As due to flushing should be more marked beneath the spot A than spot B. Therefore, the regions showing very low concentration of As plausibly corresponds to the highly permeable region.

Being different from the case of spot A, two processes should be considered for the reason of very high concentration of aqueous As beneath the spot B. One process is selective flowing of As-rich water. Another process is the release of As in the depth where As-rich groundwater exists with dissolution of host mineral, possibly Fe oxyhydroxide. If the As is dominantly released from surface as some researchers suggested (Harvey *et al.*, 2006; Polizzotto *et al.*, 2008), former process is reasonable. However, it is necessary to accumulate >5 mg/kg of As as adsorbed phase, to form >1000 μg/L of As in groundwater (Fig. 4–11). It is quite difficult to supply such a large amount of As solely from the surface sediment. Therefore, reductive dissolution of Fe oxyhydroxide is, at least some parts, occurring in the aquifer far from surface.

Summarizing the above, the spots showing very low concentration of As is likely correspond to the highly permeable regions, whereas the spots showing very high concentration, so called "hot spot", should be corresponded to the regions where reductive dissolution of Fe oxyhydroxide is intensively occurring. The reason of highly heterogeneous occurrence of the hot spots is unclear. According to the Fig. 4–11, even if the reductive dissolution is occurring in aquifer, further effects to decrease the apparent K_d, e.g., presence of large amount of competitive ions, are necessary to form more than 1000 μg/L of As.

3. *Cause of reductive dissolution of Fe oxyhydroxides –Source of organic matters-*

The Fe oxyhydroxides reduction hypothesis has been widely believed as the trigger of As release. High concentration of dissolved Fe strongly indicated that aquifer is sufficiently reducing to mobilize Fe^{2+} (Chapter 2). However, there are still some questions (Chapter 1). Firstly, in previous studies, amount and speciation of labile Fe in Holocene aquifer is still not very clear despite the necessity of this basic information. This is attributed to the low concentration of secondly Fe mineral and the unavoidable analytical limitation of extraction methods. Secondly, the timing of reductive dissolution since recharge is unclear. Although some experiments demonstrated that dissolution of Fe oxyhydroxide can occur at the contaminated depth (Harvey *et al.*, 2002; Islam *et al.*, 2004; and studies shown in Table 1–7), clear redox boundary is found around water table as I proposed in Chapter 4. If majority of dissolved Fe in aquifer is transported from the redox boundary, it gives strong constraint for the interpretation of spatial distribution of As. Thirdly, the rate of reductive dissolution after sedimentation is unclear. The amount of labile Fe in aquifer must have decreased since sedimentation. The history of the decrease is important to interpret the history of As contamination.

Our data provides an important example for the first question. The result of CEY-XAFS indicated that Fe oxyhydroxide is clearly unstable just below the water table. Majority of reduced Fe is as aqueous Fe^{2+}, and reduced secondly Fe(II) minerals, such as siderite, magnetite, and green rust, should be minor. However, the result of CEY-XAFS suggested that Fe oxyhydroxide is partially remaining in the aquifer. Because the amount of HCl extractable As is enough to form As concentration observed in this study, both reductive dissolution of Fe oxyhydroxides and reductive desorption of arsenite can be a cause of As release in aquifer.

For second and third questions, source of reducing agent, possibly labile organic matter, is necessary to be clarified. As mentioned in Chapter 1, there are several hypotheses about the source of organic matter: (i) surface origin hypothesis (Harvey *et al.* 2002), (ii) co-deposition hypothesis (Smedley and Kinniburgh, 2002; Meharg *et al.* 2006), (iii) peat origin hypothesis (McArthur *et al.* 2001, 2004; Ravenscroft *et al.* 2001),

and (iv) petroleum origin hypothesis (Rowland *et al.* 2006; van Dongen *et al.* 2008). In my opinion, 4 hypotheses shown above can be classified into two groups: internal source and external source hypotheses. The surface origin hypothesis is classified into external source hypothesis, whereas co-deposition hypothesis and peat origin hypothesis are into internal source hypothesis because these organic matters have likely been present since sedimentation of Holocene aquifer. Petroleum origin hypothesis is not simply classifiable but tentatively classified into external source hypothesis.

According to the assumption of internal source hypothesis, organic matter decomposition should have continued since the deposition of the sediments. The rate of organic matter degradation should be higher in the past than the present day because lability of organic matter in sediment decreases with increasing age of sediment (Appelo and Postoma, 2005). Hence, the rate of reductive dissolution of Fe oxyhydroxide should be higher in the past than that at present. According to this process, formation of reducing condition and subsequent As release seem very common processes during early sedimentation, and thus this is plausible contamination processes. One point that should be considered is the rate of flushing of Fe and As from aquifer. As I pointed out, rate of reduction of Fe oxyhydroxide and consequent As release were plausibly higher in the past than at present. If these processes have continued since the initiation of sediment deposition, it is somewhat strange that why Fe oxyhydroxide is still survived, and As contamination is still significant. Rate of flushing of As from aquifer is the function of K_d and residence time of groundwater. Determination of apparent K_d is eventually important in terms of the estimation of the rate of flushing.

The notable difference of internal and external source hypotheses is the constraint for the mass balance of Fe and As in aquifer. Different from internal source hypothesis, As can be transported from the outside of aquifer according to the external source hypothesis. Polizzotto et al. (2008) actually proposed that influx of As to surface wetland is identical to the outflux from aquifer to adjacent river, although this study is conducted in Cambodia. In my study area, some evidences are consistent with the surface origin hypothesis: (i) redox boundaries of Fe and As clearly exist near the surface, and (ii) the concentration of buried organic matter in the lower part of Holocene aquifer is low (<0.3% as TC). The observation against this hypothesis is the vertical

profile of aqueous As concentration. The bell-shaped profile which has been confirmed in various parts of contaminated regions in Bangladesh is not consistent with the surface origin hypothesis. Even if labile organic matter is originated from the surface, decomposition of Fe oxyhydroxide and concomitant mobilization of As is likely marked in aquifer.

With the situation described above, the rate of reductive dissolution and mass balance of Fe and As in aquifer should be further investigated. Intensively detail field survey and characterization of organic matter are needed to clarify this issue.

4 *Buffering effect of aqueous As concentration of tube-well water*

Prediction of temporal change in aqueous As of well water is very important. There have been two opposite arguments about the temporal variation of aqueous As of well water (Chapter 1, section 5.2). In my study area, change in aqueous As concentration with time was limited, although monitoring period is only one half years (Chapter 2). I think this limited temporal variation is reasonable result according to the adsorption equilibrium model.

According to the adsorption experiments performed in Chapter 4, more than 80% of As in the aquifer system is partitioned into the solid phase as exchangeable phase. Because As in groundwater has likely reached adsorption equilibrium, chemical buffering effect contributes to keep the level of aqueous As constant even if water having higher or lower concentration of As flows in. Temporal change in aqueous As concentration should consequently be limited.

Although strong buffering effect likely prevents drastic change in aqueous As concentration with time, there are several reports showing significant temporal variation of aqueous As by continuous monitoring (Chapter 1, Section 5.2). The cause of this fact should be explained according to the principle of adsorption equilibrium. Some artifacts during sampling and chemical analysis are one possibility as suggested by McArthur *et al.* (2004). Other possibility is saturation of surface site of adsorbents. In my experiment, adsorption isotherm of arsenite and arsenate to sediment show the Freundrich type isotherm (Chapter 4, Fig. 4–8). The isotherm becomes convex with increasing the amount of adsorbed As indicating that the buffering becomes less effective with

increasing adsorbed As. If the adsorption isotherm becomes Langmuir type (Harvey *et al.*, 2002), attenuation of buffering capacity is more prominent when adsorbed As beyond the adsorption maxima. It is suggested that groundwater showing relatively large temporal change possibly reflect the high saturation state of adsorption site due to continuous flowing of As rich groundwater. Hence, the important parameters to predict the change in aqueous concentration in future is adsorption capacity of sediment and amount of adsorbed As. It may be important to evaluate the saturation state of the surface of sediment relative to the amount of adsorbed As before further developing the use of tube-well.

5 *Vulnerability of low-As aquifers – policy implications*

Here, an implication for the mitigation policy of this serious contamination is highlighted. Presently, majority of tube-well water in south west Bangladesh is contaminated by As. Following policies are effective for mitigation of health hazard.

(i) Use other water resources, such as rain water.

(ii) Use groundwater after removing the As.

(iii) Use groundwater from As free aquifer.

Actually, policies (i) and (ii) have been applied with the great help of various NGOs, e.g., construction of rain water reservoir, inexpensive filtration unit, and attaching the specific adsorbent to tube-well. The policy (iii) is also useful. Well-switching policy has been employed as low cost remediation method (van Geen *et al.*. 2003, 2004). It is well known that deep groundwater is generally less contaminated. In our study area, groundwater from Pleistocene aquifer (>60 m), consisting of brown colored sand, is not contaminated. Hence, installing the deep well water is one useful policy to obtain the safe water. However, there is one wariness that increasing use of deep groundwater can promote downward movement of As-contaminated shallow water. Assessing the vulnerability of Pleistocene aquifer against the penetration of As-rich groundwater is thus very important.

Previously, two factors are considered as the cause of low aqueous As in Pleistocene aquifer. Firstly, adsorption capacity of sediment is likely high in Pleistocene aquifer because of the oxic nature. Secondly, concentration of labile As is possibly low

due to the long time flushing of groundwater. According to the result of my study, however, apparent distribution coefficient (K_d) is not higher in Pleistocene aquifer than in Holocene aquifer. Hence, if large volume of As-rich groundwater flows in from Holocene aquifer, expansion of As contamination to Pleistocene aquifer is possible. Although only one sample was measured, adsorbed As is still very low in Pleistocene aquifer suggesting that the adsorption site in this aquifer has been unsaturated so far. Stable form of As is plausibly less-mobile arsenate due to oxic feature of Pleistocene aquifer. Very low apparent $K_{d\_As(V)}$ (Chapter 4, Table 4–4) for Pleistocene aquifer, however, implies high vulnerability of Pleistocene aquifer to the inflow of As-contaminated groundwater (Fig. 4–11). Because data of adsorption capacity of Pleistocene aquifer is still poor, experimental evaluation should be more focused to assess the vulnerability of low As aquifer to the inflow of As rich water.

6 *A consideration for the primary source*

As mentioned in Chapter 1, it has been most widely believed that As in Bengal Basin is originated from Himalaya. Although As-rich sulfide is a plausible candidate as the specific mineral source, other minerals are also proposed. Seddique et al. (2008) reported As concentration in biotite separated from same sediment core used in my study, and suggested that majority of As in residual phase in sequential extraction is derived from biotite. Biotite is ubiquitous mineral, and is relatively easy to weather in the surface environment (Wilson et al., 2004).

I would point out the importance to assess the rate of releasing of As from inert phases to labile phase after sedimentation. Many reports suggested the high contribution of As in inert phases, which can not be decomposed by weak acids, in bulk As (Chapter 1, Table 1–3). However, the identity of the As in the inert phases has been unclear. According to the target phase of sequential extraction procedure, possible inert phases are sulfides and silicates. As mentioned above, Seddique *et al.* (2008) argued that host phase of As in residual is biotite. The XAFS result of this study partly supports this finding, because no contribution of sulfides was confirmed in Chapter 4. However, there are some contradict reports. Polizzotto *et al.* (2006) suggested that ca. 60% of As would be associated with sulfide in aquifer based on the μ-XANES analysis. Lowers *et al.*

(2007) was also claimed that authigenic sulfide act as the sink of As in aquifer based on the bulk and μ-XANES analyses.

If sulfides are the host of inert As, these As can be extremely insoluble under reducing condition. Actually, As-rich groundwater show very low concentration of sulfate ions indicating that As in sulfides should not be released in aquifer (Chapter 1). If As bearing sulfide present in the aquifer, it is plausibly authigenic, and may be act as sink of As. Although our data are from only one drilling site, contribution of As-bearing sulfide must be low in our study area based on the bulk XANES result.

Being different from sulfide, incongruent dissolution of silicate mineral is irreversible reaction. Therefore, if certain silicate is the host of inert As, it should contribute as the source of As. In my study area, silicate is the most plausible host mineral of inert As. Actually, Seddique et al. (2008) reported ca. 10 times higher concentration of As in biotite relative to bulk. Because weathering rate of biotite is high under oxic condition, this reaction might be important when the sediment was freshly deposited with exposure to air. The As released from biotite would be adsorbed onto Fe oxyhydroxide followed by the remobilization by further sedimentation. Additionally, it is well known that content of mica is high in the detritus derived from Himalaya. Therefore, weathering of biotite is valuable hypothesis to be tested as the primary mechanism of extraordinarily global As-contamination in Bengal Basin.

7 *Why is natural occurrence of As contamination remarkable in Asia?*

I have two ideas for this question. One reason is the large supply of source materials from Himalaya, whereas the other is the tropical climate. Many As-polluted regions, such as Bengal Delta (Bangladesh and West Bengal), Mekong Delta (North Vietnam), Red River Delta (South Vietnam and Cambodia), and Terai Basin (Nepal), are located on the down stream of large rivers derived from Himalaya. Huge amount of detritus from Himalaya would transport As to the young sediments in these regions. However, it should be noted that natural occurrences of As-contaminations are not limited in the downstream of Himalaya. For example, As rich groundwaters (>1000 μg/L) are reported from Inner Mongolia and Taiwan. The As rich groundwaters in these regions are observed in Holocene aquifer, but the sediment is not derived from

Himalaya. Cause of As release in these regions may be similar to the deltaic regions, because of common feature of groundwater quality. This fact indicates that the large supply of detritus from Himalaya is not always necessary to form high As groundwater.

Tropical climate of south-east Asia is another potential cause of As-contamination. Drastic change in the amount of precipitation between rainy and dry seasons can be a cause of large variation of redox condition near the surface. Such condition likely promotes the cycle of As accumulation/release from soil. Actually, I found the clear redox boundary of As and Fe near the water table (Chapter 4). Oscillation of water table between rainy and dry season should promote annual redox change followed by the mobilization of Fe and As. In addition, high rate of chemical weathering in tropical climate would cause the transport of As from primary minerals to secondary minerals. If those factors are really promoting the As-contamination, other tropical regions in the world, e.g., south America and Oceania, may have potential to be being exposed by serious contamination. Same to the factor of Himalaya, tropical climate is also not the necessary condition, because there are some exceptionally contaminated regions other than tropical region, such as Nepal and Inner Mongolia.

With this situation, comparative study among various contaminated regions should be important to evaluate the relative contribution of the factors shown above for the mechanism of natural occurrence of As-contaminated groundwater.

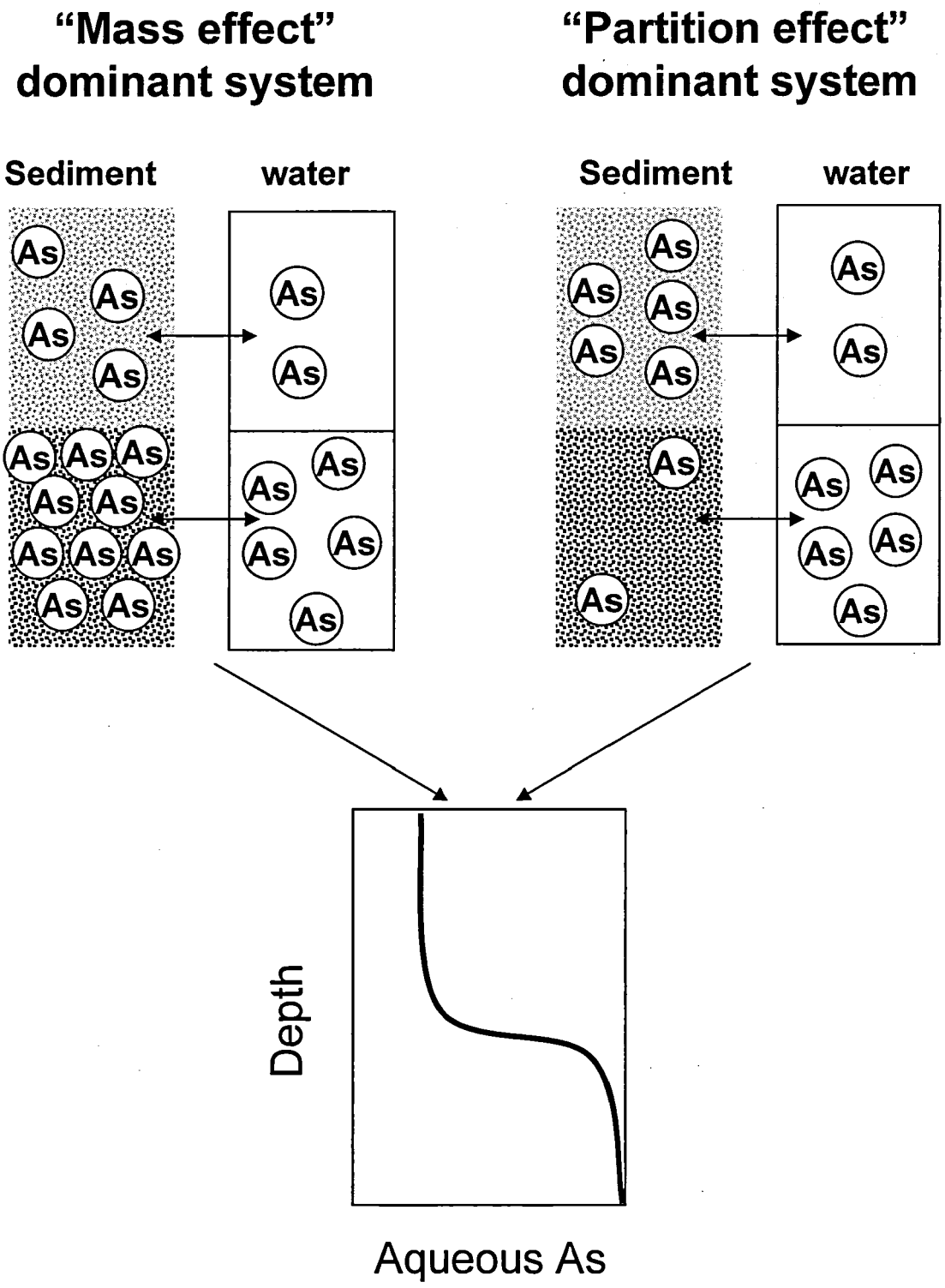

Fig. 5-1. A schematic of the concepts of mass and partition effects.

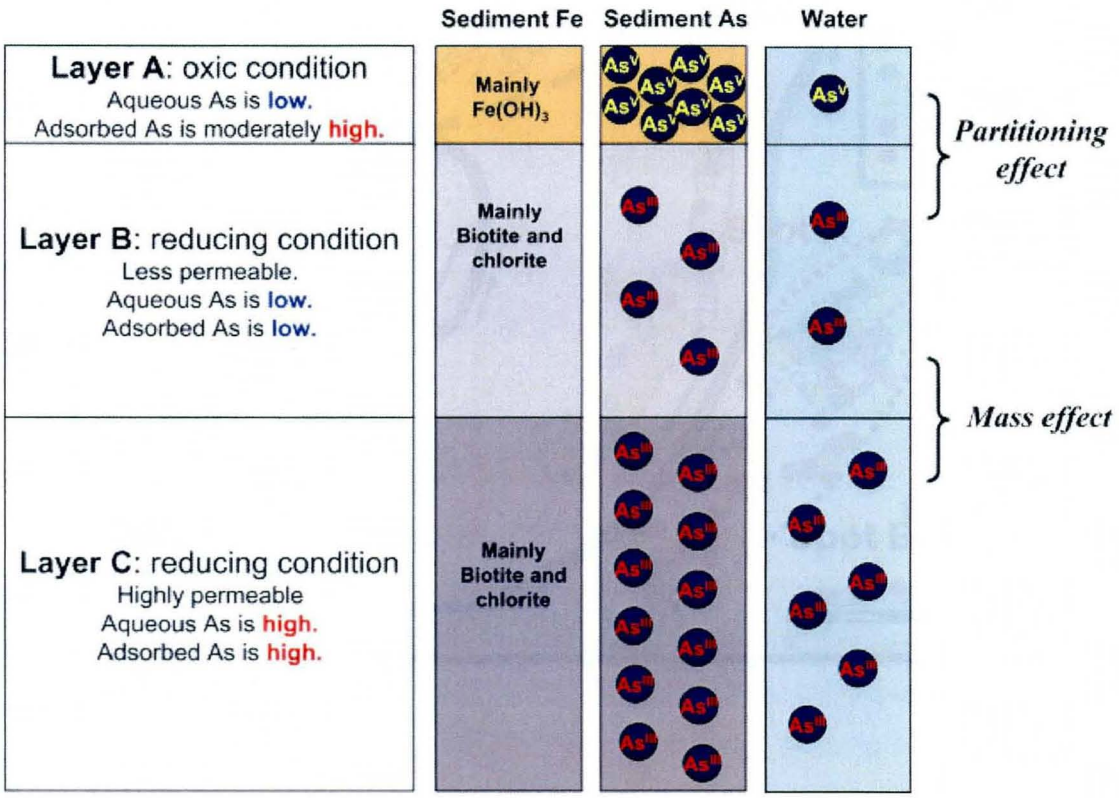

Fig. 5-2. A schematic of the classification of three layers in the drilling core.

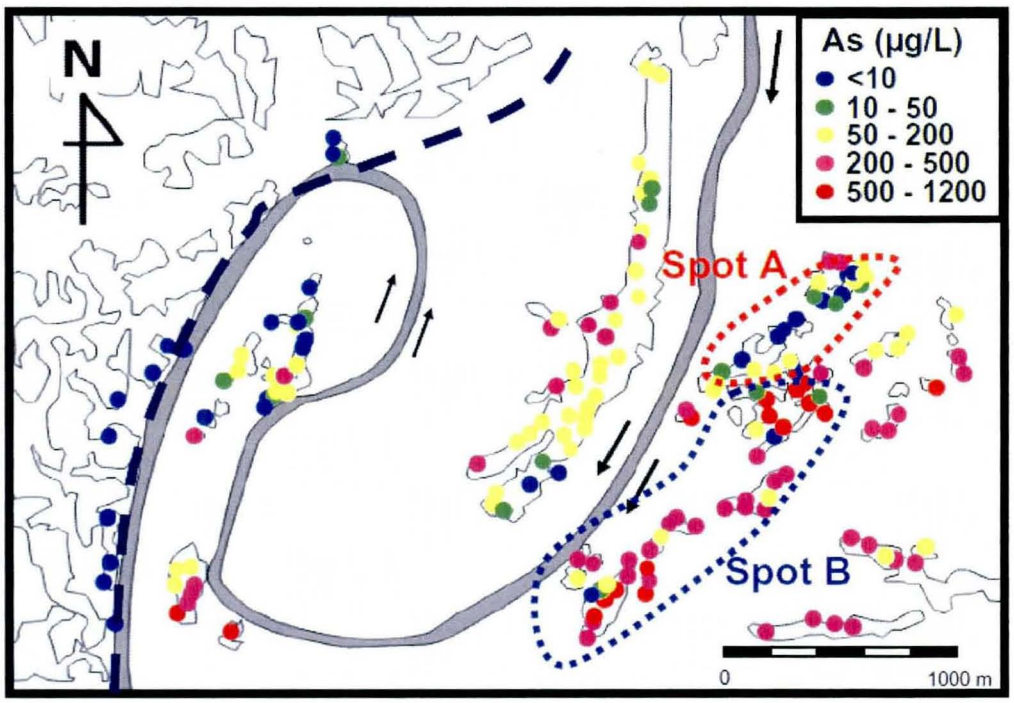

Fig. 5-3. A map of the distribution of As concentration in groundwater. In spot A, low-As water is predominant, whereas high-As water is predominant in spot B.

Chapter 6 Conclusions

Throughout my PhD work, I have attempted two approaches to clarify the factor controlling variation of aqueous concentration in groundwater (Fig. A-1). Hydrogeological study described in Chapter 1 revealed following things.

(i) Arsenic-rich groundwater is only present in Holocene aquifer, whereas Pleistocene aquifer is not contaminated

(ii) Concentration of As in groundwater is low near the surface (<15 m), and gradually increased from middle to deep part of Holocene aquifer (15 ~ 30 m). (so-called bell shaped profile)

(iii) Arsenic-rich groundwaters show high concentration of NH_4^+, whereas NO_3^- and SO_4^{2-} are rarely detected, suggesting that these groundwaters are under strongly reducing condition.

(iv) Arsenite is the dominant species of dissolved As.

(v) The residence time of groundwater in Holocene aquifer is mostly <50 years, whereas that in Pleistocene aquifer is >50 years.

(vi) Recharge/discharge cycle of groundwater in Holocene aquifer is occurring in localized spatial scale, proved by large spatial variation of $\delta^{18}O$.

(vii) Decomposition of As-rich biotite can be important to increase amount of labile As in aquifer.

With above findings, I then focused on the controlling factors of variation of aqueous As concentration in Holocene aquifer. Particularly, speciation of As and Fe in solid phase is the key point of this approach. The following conclusions were extracted from the approaches introduced in Chapter 3 and 4.

(i) Oxidation states of As in sediment change around the water table, and hence arsenite is dominant in the depth where As-rich groundwater prevails.

(ii) Oxidation states of Fe in sediment also change around the water table. Reduced Fe would be flushed as Fe^{2+}, and formation of secondly Fe(II) mineral is likely negligible according to the result of CEY-XAFS.

(iii) Fraction of HCl extractable As is generally lower than unextractable fraction. The unextractable As is likely associated with inert silicates, such as biotite.

(iv) Apparent distribution coefficient of arsenate is always larger than arsenite, suggesting that arsenate reduction always enhances the mobility of As.

(v) Amount of adsorbed As determined by phosphate extraction is larger in lower part than upper part of Holocene aquifer, and that is very low in Pleistocene aquifer.

(vi) Apparent K_d of As(V) is proportional to the amount of Fe oxyhydroxide, whereas that of As(III) is less sensitive to Fe oxyhydroxide.

(vii) The simulated concentration of aqueous As under adsorption equilibrium is consistent with the measured As concentration in the monitoring wells.

The findings in this study from Chapter 2 to 4 provide some constraints for various controversial issues, such as redox chemistry of Fe in aquifer, cause of bell-shaped profile, and controlling factor of temporal variation of As concentration (Chapter 5).

The most important finding throughout my studies is that aqueous As concentration in groundwater is regulated by the adsorption-desorption equilibrium. I claim that two factors: "mass effect" and "partition effect", must be considered to discuss the spatial variation of As concentration (Fig. 5−1). Particularly, the contribution of "partition effect" has been rather overlooked. The difficulty to assess the contribution of this effect is in the variable speciation of As and Fe in natural sample. I succeeded to overcome this difficulty by the adsorption experiment coupled with the speciation of As and Fe using XAFS technique. According to the result of this study, large variation of aqueous As concentration in groundwater can not be explained by the single factor. Both "mass effect" and "partition effect" need to be combined to explain very high (>100 μg/L) and very low (<100 μg/L) concentration of As (Fig. 4−11). Additionally, I revealed that oxidation state of As is the most important factor to generate high-As groundwater of >100 μg/L (Fig. 4−11). I believe these finding should contribute to predict the spatial and temporal variation of As-contaminated groundwater in Bengal Basin and other As affected countries.

References

Acharyya, S. K., Chakraborty, P., Lahiri, S., Raymahashay, B. C., Guha, S., Bhowmik, A., 1999. Arsenic poisoning in the Ganges delta. *Nature* 401, 545–545.

Acharyya, S. K., Lahiri, S., Raymahashay, B. C., Bhowmik, A., 2000. Arsenic toxicity of groundwater in parts of the Bengal Basin in India and Bangladesh: the role of Quaternary stratigraphy and Holocene sea-level fluctuation. *Environ. Geol.* 39, 1127–1137.

Aggarwal, P. K., Basu, A. R., Poreda, R.J., 2000. Isotope hydrology of groundwater in Bangladesh: implications for characterization and mitigation of arsenic in groundwater, IAEA-TC Project Report: BGD/8/016, IAEA, Vienna.

Agusa, T., Kunito, T., Fujihara, J., Kubota, R., Minh, T. B., Trang, P. T. K., Iwata, H., Subramanian, A., Viet, P. H., Tanabe, S., 2006. Contamination by arsenic and other trace elements in tube-well-water and its risk assessment to humans in Hanoi, Vietnam. *Environ. Poll.* 139, 95–106.

Ahamed, S., Sengupta, M. K., Mukherjee, A., Hossain, A. M., Das, B., Nayak, B., Pal, A., Mukherjee, S. C., Pati, S., Dutta, R. N., Chatterjee, G., Mukherjee, A., Srivastava, R., Chakraborti, D., 2006. Arsenic groundwater contamination and its health effects in the state of Uttar Pradesh (UP) in upper and middle Ganga plain, India: A severe danger. *Sci. Total Environ.* 370, 310–322.

Ahmed, K. M., Bhattacharya, P., Hasan, M. A., Akhter, S. H., Alam, S. M. M., Bhuyian, M. A. H., Imam, M. B., Khan, A. A., Sracek, O., 2004a. Arsenic enrichment in groundwater of the alluvial aquifers in Bangladesh: an overview. *Appl. Geochem.* 19, 181–200.

Akai, J., Izumi, K., Fukuhara, H., Masuda, H., Nakano, S., Yoshimura, T., Ohfuji, H., Anawar, H. M., Akai, K., 2004. Mineralogical and geomicrobiological investigations on groundwater arsenic enrichment in Bangladesh. *Appl. Geochem.* 19, 215–230.

Allison, J. D., Brown, D. S., Novo-Gradac, J., 1991. MINTEQ2/PRODEFA2, A geochemical assessment database and test cases for environmental systems: Vers. 3.0 user's manual. Report EPA/600/3–91/–21. Athens, GA: U.S. EPA.

Anawar, H. M., Akai, J., Komaki, K., Terao, H., Yoshioka, T., Ishizuka, T., Safiullah, S., Kato, K., 2003. Geochemical occurrence of arsenic in groundwater of Bangladesh: sources and mobilization processes. *J. Geochem. Explor.* 77, 109–131.

Anawar, H. M., Akai, J., Sakugawa, H., 2004. Mobilization of arsenic from subsurface

sediments by effect of bicarbonate ions in groundwater. *Chemosphere* 54, 753–762

Appelo, C. A. J., Van der Weiden, M. J. J., Tournassat, C., Charlet, L., 2002. Surface complexation of ferrous iron and carbonate on ferrihydrite and the mobilization of arsenic. *Environ. Sci. Technol.* 36, 3096–3103.

Appelo, C.A.J., Postma, D., 2005. Geochemistry, groundwater and pollution, 2nd edition, Balkema, Rotterdam, p. 536.

Arai, Y., Elzinga, E. J., Sparks, D. L., 2001. X-ray absorption spectroscopic investigation of arsenite and arsenate adsorption at the aluminum oxide-water interface. *J. Colloid Interface Sci.* 235, 80–88.

Aziz, Z., van Geen, A., Stute, M., Versteeg, R., Horneman, A., Zheng, Y., Goodbred, S., Steckler, M., Weinman, B., Gavrieli, I., Hoque, M. A., Shamsudduha, M., Ahmed, K. M., 2008. Impact of local recharge on arsenic concentrations in shallow aquifers inferred from the electromagnetic conductivity of soils in Araihazar, Bangladesh. *Water Resour. Reser.* 44.

Beak DG, Wilkin RT, Ford RG, Kelly SD., 2008. Examination of arsenic speciation in sulfidic solutions using X-ray absorption spectroscopy. *Environ. Sci. Technol.*42, 1643–1650.

Bethke, C. M., 2006. A user's guide to Rxn, Act2, Tact, SpecE8, and Aqplot. Hydrogeology Program. Urbana, IL: University of Illinois.

Berg, M., Tran, H. C., Nguyen, T. C., Pham, H. V., Schertenleib, R., Giger, W., 2001. Arsenic contamination of groundwater and drinking waiter in Vietnam: A human health threat. *Environ. Sci. Technol.* 35, 2621–2626.

Berg, M., Luzi, S., Trang, P. T. K., Viet, P. H., Giger, W., Stüben, D., 2006. Arsenic removal from groundwater by household sand filters: Comparative field study, model calculations, and health benefits. *Environ. Sci. Technol.* 40, 5567–5573.

Berg, M., Trang, P. T. K., Stengel, C., Buschmann, J., Viet, P. H., Van Dan, N., Giger, W., Stüben, D., 2008. Hydrological and sedimentary controls leading to arsenic contamination of groundwater in the Hanoi area, Vietnam: The impact of iron-arsenic ratios, peat, river bank deposits, and excessive groundwater abstraction. *Chem. Geol.* 249, 91–112.

BGS and DPHE, 2001. Arsenic contamination of groundwater in Bangladesh, In: Kinniburgh, D. G. and Smedley, P. L., Editors, BGS Technical Report WC/00/19, British Geological Survey, Keyworth, UK.

Bhattacharya, P., Chatterjee, D., Jacks, G., 1997. Occurrence of Arsenic-contaminated groundwater in alluvial aquifers from Delta Plains, Eastern India: Options for safe drinking water supply. *Int. J. Water Resour. Develop.*13, 79–92.

Bhattacharya, P., Jacks, G., Ahmed, K. M., Khan, A. A., Routh, J., 2002. Arsenic in groundwater of the Bengal Delta Plain aquifers in Bangladesh. *Bull. Environ. Contam. Toxicol.* 69, 538–545.

Bostick, B. C., Fendorf, S., 2003. Arsenite sorption on troilite (FeS) and pyrite (FeS_2). *Geochim. Cosmochim. Acta* 67, 909–921.

Bostick, B. C., Fendorf, S., Manning, B. A., 2003. Arsenite adsorption on galena (PbS) and sphalerite (ZnS). *Geochim. Cosmochim. Acta* 67, 895–907.

Brown, G. E., Sturchio, N. C., 2002. An overview of synchrotron radiation applications to low temperature geochemistry and environmental science, Applications of Synchrotron Radiation in Low-Temperature Geochemistry and Environmental Sciences. Mineralogical Soc America, Washington.

Breit, G. N., Whiteney, J., Foster, A., Welch, A. H., Yount, J., Sanxolone, R., Islam, M. M., Sutton, S., Newville, M., 2001. Preliminary evaluation of arsenic cycling in the sediments of Bangladesh. Abstract in USGS Workshop on Arsenic in the Environment, Denver.

Burnol, A., Garrido, F., Baranger, P., Joulian, C., Dictor, M. C., Bodenan, F., Morin, G., Charlet, L., 2007. Decoupling of arsenic and iron release from ferrihydrite suspension under reducing conditions: a biogeochemical model. *Geochem. Trans.* 8, 12.

Buschmann, J., Berg, M., Stengel, C., Sampson, M. L., 2007. Arsenic and manganese contamination of drinking water resources in Cambodia: Coincidence of risk areas with low relief topography. *Environ. Sci. Technol.* 41, 2146–2152.

Buschmann, J., Kappeler, A., Lindauer, U., Kistler, D., Berg, M., Sigg, L., 2006. Arsenite and arsenate binding to dissolved humic acids: Influence of pH, type of humic acid, and aluminum. *Environ. Sci. Technol.* 40, 6015–6020.

Campbell, K. M., Malasarn, D., Saltikov, C. W., Newman, D. K., Hering, J. G., 2006. Simultaneous microbial reduction of iron(III) and arsenic(V) in suspensions of hydrous ferric oxide. *Environ. Sci. Technol.* 40, 5950–5955.

Canfield, D. E., Thamdrup, B., Hansen, J. W., 1993. The anaerobic degradation of organic matter in Danish coastal sediments: iron reduction, manganese reduction, and sulfate reduction. *Geochim. Cosmochim. Acta* 57, 3867–3885.

Chakraborti, D., Rahman, M.M., Paul, K., Chowdhury, U.K., Sengupta, M.K., Lodh, D., Chanda, C.R., Saha, K.C., Mukherjee, S.C., 2002. Arsenic calamity in the Indian subcontinent what lessons have been learned? *Talanta* 58, 3–22.

Chakraborti, D., Mukherjee, S. C., Pati, S., Sengupta, M. K., Rahman, M. M., Chowdhury, U. K., Lodh, D., Chanda, C. R., Chakraborty, A. K., Basul, G. K., 2003. Arsenic groundwater contamination in Middle Ganga Plain, Bihar, India: A future danger? *Environ. Health Perspec.* 111, 1194–1201.

Chakraborty, A. K., Saha, K. C., 1987. Arsenic dermatosis from tubewell-water in West Bengal. *Indian J. Med. Resear.* 85, 326–334.

Chakraborty, S., Wolthers, M., Chatterjee, D., Charlet, L., 2007. Adsorption of arsenite and arsenate onto muscovite and biotite mica. *J. Colloid Interface Sci.* 309, 392–401.

Chao, T. T., Zhou, L., 1983. Extraction techniques for selective dissolution of amorphous iron oxides from soils and sediments. *Soil Sci. Soc. Am. J.* 47, 225–232.

Charlet, L., Chakraborty, S., Appelo, C. A. J., Roman-Ross, G., Nath, B., Ansari, A. A., Lanson, M., Chatterjee, D., and Mallik, S. B., 2007. Chemodynamics of an arsenic "hotspot" in a West Bengal aquifer: A field and reactive transport modeling study. *Appl. Geochem.* 22, 1273–1292.

Charlet, L., Polya, D. A., 2006. Arsenic in shallow, reducing groundwaters in southern Asia: An environmental health disaster. *Elements* 2, 91–96.

Chatterjee, A., Das, D., Mandal, B. K., Chowdhury, T. R., Samanta, G., Chakraborti, D., 1995. Arsenic in groundwater in six districts of West Bengal, India: the biggest arsenic calamity in the world. Part 1. Arsenic species in drinking water and urine of the affected people. *Analyst* 120, 643–650.

Chatterjee, D., Roy, R. K., Basu, B. B., 2005. Riddle of arsenic in groundwater of Bengal Delta Plain - role of non-inland source and redox traps. *Environ. Geol.* 49, 188–206.

Chen, S. L., Dzeng, S. R., Yang, M. H., Chiu, K. H., Shieh, G. M., Wai, C. M., 1994. Arsenic species in groundwaters of the blackfoot disease areas, Taiwan. *Environ. Sci. Technol.* 28, 877–881.

Cheng, L. W., Fenter, P., Sturchio, N. C., Zhong, Z., Bedzyk, M. J., 1999. X-ray standing wave study of arsenite incorporation at the calcite surface. *Geochim. Cosmochim. Acta* 63, 3153–3157.

Cheng, Z., Van Geen, A., Seddique, A. A., Ahmed, K. M., 2005. Limited temporal

variability of arsenic concentrations in 20 wells monitored for 3 years in Araihazar, Bangladesh. *Environ. Sci. Technol.* 39, 4759–4766.

Cheng, Z. Q., van Geen, A., Seddique, A. A., Ahmed, K. M., 2006. Response to comments on "Limited temporal variability of arsenic concentration in 20 wells monitored for 3 years in Araihazar, Bangladesh". *Environ. Sci. Technol.* 40, 1718–1720.

Chiu, V. Q., Hering, J. G., 2000. Arsenic adsorption and oxidation at manganite surfaces. 1. Method for simultaneous determination of adsorbed and dissolved arsenic species. *Environ. Sci. Technol.* 34, 2029–2034.

Chowdhury, T. R., Basu, G. K., Mandal, B. K., Biswas, B. K., Samanta, G., Chowdhury, U. K., Chanda, C. R., Lodh, D., Lal Roy, S., Saha, K. C., Roy, S., Kabir, S., Quamruzzaman, Q., Chakraborti, D., 1999. Arsenic poisoning in the Ganges delta. *Nature* 401, 545–546.

Concepcíon, J. L., Christopher, S. R., 2004. Precipitation kinetics and carbon isotope partitioning of inorganic siderite at 25°C and 1 atm. *Geochim. Cosmochim. Acta* 68, 557–571.

Craig, H., 1961. Isotopic variations in meteoric waters, *Science* 133, 1702–1703.

Criss, R. E., 1999. Principles of stable isotope distribution. Oxford University Press.

Crouch, S. R., Malmstadt, H. V., 1967. A mechanistic investigation of molybdenum blue method for determination of phosphate. *Anal. Chem.* 39, 1084–1089.

Curray, J.R., Moore, D. G., 1974. Sedimentary and tectonic processes in the Bengal deep-sea fan and geosyncline. In: C.A. Burk and C.L. Drake, Editors, The Geology of Continental Margins, Springer, New York, NY, pp. 617–628.

Das, D., Samanta, G., Mandal, B. K., Chowdhury, T. R., Chanda, C. R., Chowdhury, P. P., Basu, G. K., Chakraborti, D., 1996. Arsenic in groundwater in six districts of West Bengal, India. *Environ. Geochem. Health* 18, 5–15.

Datta, D. K., Subramanian, V., 1998. Distribution and fractionation of heavy metals in the surface sediments of the Ganges-Brahamputra-Meghna river system in the Bengal Basin. *Environ. Geol.* 36, 93–101.

Daus, B., Mattusch, B., Wennrich, R., Weiss, H., 2002. Investigation on stability and preservation of arsenic species in iron rich water samples. *Talanta* 58, 57–65.

De Vitre, R., Belzile, N., Tessier, A., 1991. Speciation and adsorption of arsenic on diagenetic iron oxyhydroxides. *Limnol. Oceanog.* 36, 1480–1485.

Dhar, R. K., Zheng, Y., Stute, M., van Geen, A., Cheng, Z., Shanewaz, M., Shamsudduha, M., Hoque, M. A., Rahman, M. W., Ahmed, K. M., 2008. Temporal variability of groundwater chemistry in shallow and deep aquifers of Araihazar, Bangladesh. *J. Contam. Hydrol.* 99, 97–111.

Dixit, S., Hering, J. G., 2003. Comparison of arsenic(V) and arsenic(III) sorption onto iron oxide minerals: Implications for arsenic mobility. *Environ. Sci. Technol.* 37, 4182–4189.

Dixit, S., Hering, J. G., 2006. Sorption of Fe(II) and As(III) on goethite in single- and dual-sorbate systems. *Chem. Geol.* 228, 6–15.

Dowling, C. B., Poreda, R. J., Basu, A. R., Peters, S. L., 2002. Geochemical study of arsenic release mechanisms in the Bengal Basin groundwater. *Water Res. Resear.* 38, 1–17.

DPHE/MMD/BGS, 1999. DPHE/Mott MacDonald Ltd/British Geological Survey, Groundwater Studies for Arsenic Contamination in Bangladesh, Main Report.

Drever, J. I., 2002. The geochemistry of natural waters, Prentice Hall, Inc.

Dyar, M. D., Lowe, E. W., Guidotti, C. V., Delaney J. S., 2002. Fe^{3+} and Fe^{2+} partitioning among silicates in metapelites: A synchrotron micro-XANES study, *Am. Mineral.* 87, 514–522.

Epstein, S., Mayeda, M., 1953. Variation of O^{18} content of waters from natural sources. *Geochim. Cosmochim. Acta* 4, 213–224.

Erbil, A., Cargill G. S., Frahm, R., Boehme, R. F., 1988. Total-electron-yield current measurements for near-surface extended x-ray-absorption fine structure. *Phys. Rev. B.* 37, 2450–2464.

Farooqi, A., Masuda, H., Firdous, N., Naseem, M., Firdous, N., 2007a. Toxic fluoride and arsenic contaminated groundwater in the Lahore and Kasur districts, Punjab, Pakistan and possible contaminant sources. *Environ. Poll.* 145, 839–849.

Farooqi, A., Masuda, H., Kusakabe, M., Naseem, M., Firdous, N., 2007b. Distribution of highly arsenic and fluoride contaminated groundwater from east Punjab, Pakistan, and the controlling role of anthropogenic pollutants in the natural hydrological cycle. *Geochem. J.* 41, 213–234.

Farquhar, M. L., Charnock, J. M., Livens, F. R., Vaughan, D. J., 2002. Mechanisms of arsenic uptake from aqueous solution by interaction with goethite, lepidocrocite, mackinawite, and pyrite: An X-ray absorption spectroscopy study. *Environ. Sci.*

Technol. 36, 1757–1762.

Fernandez-Martinez, A., Roman-Ross, G., Cuello, G. J., Turrillas, X., Charlet, L., Johnson, M. R., Bardelli, F., 2006. Arsenic uptake by gypsum and calcite: Modeling and probing by neutron and X-ray scattering. *Physica B-Condensed Matt.* 385–86, 935–937.

Ford, R. G., Fendorf, S., Wilkin, R. T., 2006. Introduction: Controls on arsenic transport in near-surface aquatic systems. *Chem. Geol.* 228, 1–5.

Foster, A.L., 2003. Spectroscopic investigations of arsenic species in solid phases. In: A.H. Welch and K.G. Stollenwerk, Editors, Arsenic in Ground Water, Geochemistry and Occurrence, Kluwer Academic Publishers, Boston, pp. 27–65.

Fukushi, K., Sverjensky, D. A., 2007. A predictive model (ETLM) for arsenate adsorption and surface speciation on oxides consistent with spectroscopic and theoretical molecular evidence. *Geochim. Cosmochim. Acta* 71, 3717–3745.

Galy, A., France-Lanord, C., 1999. Weathering processes in the Ganges-Brahmaputra basin and the riverine alkalinity budget. *Chem. Geol.* 159, 31–60.

Gao, S., Luo, T.C., Zhang, B.R., Zhang, H.F., Han, Y.W., Zhao, Z.D., Hu, Y.K., 1998. Chemical composition of the continental crust as revealed by studies in East China. *Geochim. Cosmochim. Acta* 62, 1959–1975.

Garai, R., Chakraborty, A. K., Dey, S. B., Saha, K.C., 1984. Chronic arsenic poisoning from tube-well water. *J. Indian Med. Assoc.* 82, 34–35.

Gault, A. G., Polya, D. A., Charnock, J. M., Islam, F. S., Lloyd, J. R., Chatterjee, D., 2003. Preliminary EXAFS studies of solid phase speciation of As in a West Bengali sediment. *Mineral. Magazine* 67, 1183–1191.

Gault, A. G., Islam, F. S., Polya, D. A., Charnock, J. M., Boothman, C., Chatterjee, D., Lloyd, J. R., 2005a. Microcosm depth profiles of arsenic release in a shallow aquifer, West Bengal. *Mineral. Magazine* 69, 855–863.

Gault, A. G., Jana, J., Chakraborty, S., Mukherjee, P., Sarkar, M., Nath, B., Polya, D. A., Chatterjee, D., 2005b. Preservation strategies for inorganic arsenic species in high iron, low-Eh groundwater from West Bengal, India. *Anal. Bioanal. Chem.* 381, 347–353.

Goldberg, S., 2002. Competitive adsorption of arsenate and arsenite on oxides and clay minerals. *Soil Sci. Soc. Am. J.* 66, 413–421.

Gong, Z., Lu, X., Ma, M., Watt, C., Le, X. C., 2002. Arsenic speciation analysis.

Talanta 58, 77–96.

Gong, Z. L., Lu, X. F., Watt, C., Wen, B., He, B., Mumford, J., Ning, Z. X., Xia, Y. J., Le, X. C., 2006. Speciation analysis of arsenic in groundwater from Inner Mongolia with an emphasis on acid-leachable particulate arsenic. *Anal. Chim. Acta* 555, 181–187.

Goodbred, S. L., Kuehl, S. A., 1999. Holocene and modern sediment budgets for the Ganges-Brahmaputra river system; evidence for highstand dispersal to flood-plain, shelf, and deep-sea depocenters. *Geology* 27, 559–562.

Goodbred, S. L., Kuehl, S. A., 2000. The significance of large sediment supply, active tectonism, and eustasy on margin sequence development: Late Quaternary stratigraphy and evolution of the Ganges-Brahmaputra delta. *Sediment. Geol.* 133, 227–248.

Goodbred, S. L., Kuehl, S. A., Steckler, M. S., Sarker, M. H., 2003. Controls on facies distribution and stratigraphic preservation in the Ganges-Brahmaputra delta sequence. *Sediment. Geol.* 155, 301–316.

Guillot, S., Charlet, L., 2007. Bengal arsenic, an archive of Himalaya orogeny and paleohydrology. *J. Environ. Sci. Health Part A* 42, 1785–1794.

Guo, H. M., Yang, S. Z., Tang, X. H., Li, Y., Shen, Z. L., 2008. Groundwater geochemistry and its implications for arsenic mobilization in shallow aquifers of the Hetao Basin, Inner Mongolia. *Sci. Total Environ.* 393, 131–144.

Gurung, J. K., Ishiga, H., Khadka, M. S., 2005. Geological and geochemical examination of arsenic contamination in groundwater in the Holocene Terai basin, Nepal. *Environ. Geol.* 49, 98–113.

Gurung, J. K., Ishiga, H., Khadka, M. S., Shrestha, N. R., 2007. The geochemical study of fluvio-lacustrine aquifers in the Kathmandu Basin (Nepal) and the implications for the mobilization of arsenic. *Environ. Geol.* 52, 503–517.

Hansel, C. M., Benner, S. G., Neiss, J., Dohnalkova, A., Kukkadapu, R. K., Fendorf, S., 2003. Secondary mineralization pathways induced by dissimilatory iron reduction of ferrihydrite under advective flow. *Geochim. Cosmochim. Acta* 67, 2977–2992.

Harbel, M., Fendorf, S., 2006. Biogeochemical processes controlling the speciation and transport of arsenic within iron coated sands, *Chem. Geol.* 228, 16–32.

Harvey, C. F., Swartz, C. H., Badruzzaman, A. B. M., Keon-Blute, N., Yu, W., Ali, M. A., Jay, J., Beckie, R., Niedan, V., Brabander, D., Oates, P. M., Ashfaque, K. N.,

Islam, S., Hemond, H. F., Ahmed, M. F., 2002. Arsenic mobility and groundwater extraction in Bangladesh. *Science* 298, 1602–1606.

Harvey, C. F., Ashfaque, K. N., Yu, W., Badruzzaman, A. B. M., Ali, M. A., Oates, P. M., Michael, H. A., Neumann, R. B., Beckie, R., Islam, S., Ahmed, M. F., 2006. Groundwater dynamics and arsenic contamination in Bangladesh. *Chem. Geol.* 228, 112–136.

Helz, G.. R., Tossell, J. A., Charnock, J. M., Pattrick, R. A. D., Vaughan, D. J., Garner, C. D., 1995. Oligomerization in As(III) sulfide solutions. Theoretical constraints and spectroscopic evidence. *Geochim. Cosmochim. Acta* 59, 4591–4604.

Heltz, G. R., Tossell, J. A., 2008. Thermodynamic model for arsenic speciation in sulfidic waters: A novel use of ab initio computations. *Geochim. Cosmochim. Acta* 72, 4457–4468.

Hochella, M. F., Kasama, T., Putnis, A., Putnis, C. V., Moore, J. N. 2005. Environmentally important, poorly crystalline Fe/Mn hydrous oxides: Ferrihydrite and a possibly new vernadite-like mineral from the Clark Fork River Superfund Complex. *Amer. Mineral.* 90, 718–724.

Holak, W., 1980. Determination of arsenic by cathodic stripping voltammetry with a hanging mercury electrode. *Anal. Chem.* 52, 2189–2192.

Holeman, J. N., 1968. The Sediment Yield of Major Rivers of the World. *Water Resour. Resear.* 4, 737–747.

Hoque, M. A., Khan, A. A., Shamsudduha, M., Hossain, M. S., Islam, T., Chowdhury, S. H., 2008. Near surface lithology and spatial variation of arsenic in the shallow groundwater: southeastern Bangladesh. *Environ. Geol.* doi: 10.1007/s00254–008–1267–3

Horneman, A., Van Geen, A., Kent, D. V., Mathe, P. E., Zheng, Y., Dhar, R. K., O'Connell, S., Hoque, M. A., Aziz, Z., Shamsudduha, M., Seddique, A. A., Ahmed, K. M., 2004. Decoupling of As and Fe release to Bangladesh groundwater under reducing conditions. Part 1: Evidence from sediment profiles. *Geochim. Cosmochim. Acta* 68, 3459–3473.

Hu, Z., Ga, S., 2008. Upper crustal abundances of trace elements: A revision and update. *Chem. Geol.* 253. 205–221.

Hudson-Edwards, K. A., Houghton, S. L., Osborn, A., 2004. Extraction and analysis of arsenic in soils and sediments. *Trends Anal. Chem.* 23. 745–752

Hug, S. J., Leupin, O. X., Berg, M., 2008. Bangladesh and Vietnam: Different Groundwater Compositions Require Different Approaches to Arsenic Mitigation. 2008.*Environ. Sci. Technol.* 42, 6318–6323.

Hung, D. Q., Nekrassova, O., Compton, R. G., 2004. Analytical methods for inorganic arsenic in water: a review. *Talanta* 64, 269–277.

Imai, N., Terashima, S., Itoh, S., Ando, A., 1996. Compilation of analytical data on nine GSJ geochemical reference samples, "Sedimentary rock series". *Geostand. Newslett.* 20, 165–216.

Islam, F. S., Gault, A. G., Boothman, C., Polya, D. A., Charnock, J. M., Chatterjee, D., Lloyd, J. R., 2004. Role of metal-reducing bacteria in arsenic release from Bengal delta sediments. *Nature* 430, 68–71.

Itagaki, K., Nishimura, T., 1986. Thermodynamic properties of compounds and aqueous species of VA elements. *Metallurg. Rev.* 3, 29–48.

Itai, T., Kusakabe, M., 2004. Some practical aspects of an on-line chromium reduction method for D/H analysis of natural waters using a conventional IRMS. *Geochem. J.* 38, 435–440.

Itai, T., Masuda, H., Takahashi, Y., Mitamura, M., Kusakabe, M., 2006. Determination of As^{III}/As^{V} ratio in alluvial sediments of the Bengal Basin using X-ray absorption near-edge structure. *Chem. Lett.* 35, 866–867.

Itai, T., Takahashi, Y., Uruga, T., Tanida, H., Iida, A., 2008a. Selective detection of Fe and Mn species at mineral surfaces in weathered granite by conversion electron yield X-ray absorption fine structure, *Appl. Geochem.* 23, 2667–2675.

Itai, T., Masuda, H., Seddique, A. A., Mitamura, M., Maruoka, T., Li, X., Kusakabe, M., Dipak, B. K., Farooqi, A., Yamanaka, T., Nakaya, S., Matsuda, J., Ahmed, K. M., 2008b. Hydrological and geochemical constraints on the mechanism of formation of arsenic contaminated groundwater in Sonargaon, Bangladesh. *Appl. Geochem.* 23, 3155–3176.

Itai, T., Takahashi, Y., Seddique, A. A., Mitamura, M., Maruoka, T., Masuda, H., Variations in the redox state of As and Fe measured by X-ray absorption spectroscopy in aquifers of Bangladesh and their effect on As adsorption. *Appl. Geochem.* in revision.

Jain, A., Raven, K. P., Loeppert, R. H., 1999. Arsenite and arsenate adsorption on ferrihydrite: Surface charge reduction and net OH^- release stoichiometry. *Environ. Sci. Technol.* 33, 1179–1184.

Jain, A., Loeppert, R. H., 2000. Effect of competing anions on the adsorption of arsenate and arsenite by ferrihydrite. *J. Environ. Qual.* 29, 1422–1430.

Jones, C. A., Langner, H. W., Anderson, K., McDermott, T. R., Inskeep, W. P., 2000. Rates of microbially mediated arsenate reduction and solubilization. *Soil Sci. Soc. Am. J.* 64, 600–608.

Jönsson, J., Sherman, D. M., 2008. Sorption of As(III) and As(V) to siderite, green rust (fougerite) and magnetite: Implications for arsenic release in anoxic groundwaters. *Chem. Geol.* 255, 173–181.

Joy, D. C., Luo, S., 1989. An empirical stopping power relationship for low-energy electrons. *Scanning* 11, 176.

Jung, H. B., Zheng, Y., 2006. Enhanced recovery of arsenite sorbed onto synthetic oxides by L-ascorbic acid addition to phosphate solution: calibrating a sequential leaching method for the speciation analysis of arsenic in natural samples. *Water Resear.* 40, 2168–2180.

Karim, M., 2000. Arsenic in groundwater and health problems in Bangladesh. *Water Resear.* 34, 304–310.

Kawai, J., Yamamoto, T., Tohno, S., Kitajima, Y., 1999. Comparison between X-ray photoelectron and X-ray absorption spectra of an environmental aerosol sample measured by synchrotron radiation. *Spectrochim. Acta Part B* 54, 241–245.

Keon, N. E., Swartz, C. H., Brabander, D. J., Harvey, C., Hemond H. F., 2001. Validation of an arsenic sequential extraction method for evaluating mobility in sediments. *Environ. Sci. Technol.* 35, 2778–2784.

Kim, M. J., Nriagu, J., Haack, S., 2000. Carbonate ions and arsenic dissolution by groundwater. *Environ. Sci. Technol.* 34, 3094–3100.

Klump, S., Kipfer, R., Cirpka, O. A., Harvey, C. F., Brennwald, M. S., Ashfaque, K. N., Badruzzaman, A. B. M., Hug, S. J., Imboden, D. M., 2006. Groundwater dynamics and arsenic mobilization in Bangladesh assessed using noble gases and tritium. *Environ. Sci. Technol.* 40, 243–250.

Kocar, B. D., Herbel, M. J., Tufano, K. J., Fendorf, S., 2006. Contrasting effects of dissimilatory iron(III) and arsenic(V) reduction on arsenic retention and transport. *Environ. Sci. Technol.* 40, 6715–6721.

Koscihnsky, A., Halbach, P., Sequential leaching of marine ferromanganese precipitates: Genetic implications. 1995. *Geochim. Cosmochim. Acta* 59, 5113–5132.

Kostroun, V. O., Atomic radiation transition probabilities to the 1s state and theoretical K-shell fluorescence yields, 1971, *Phys. Rev. A* 3, 533–545.

Lafferty, B. J., Loeppert, R. H., 2005. Methyl arsenic adsorption and desorption behavior on iron oxides. *Environ. Sci. Technol.* 39, 2120–2127.

La Force, M. J., Fendorf, S., Solid-phase iron characterization during common selective sequential extractions. 2000. *Soil Sci. Soc. Am. J.* 64, 1608–1615.

Langner, H. W., Inskeep, W. P., 2000. Microbial reduction of arsenate in the presence of ferrihydrite. *Environ. Sci. Technol.* 34, 3131–3136.

Lear, G., Song, B., Gault, A. G., Polya, D. A., Lloyd, J. R., 2007. Molecular analysis of arsenate-reducing bacteria within Cambodian sediments following amendment with acetate. *Appl. Environ. Microbiol.* 73, 1041–1048.

Lee J. S., Nriagu, J. O., 2003. Arsenic carbonate complexes in aqueous systems. In Biogeochemistry of environmentally important trace metals, American Chemical Society, pp. 33–41.

Lin, H. T., Wang, M. C., Li, G. C., 2004. Complexation of arsenate with humic substance in water extract of compost. *Chemosphere* 56, 1105–1112.

Liu, C. W., Lin, K. H., Kuo, Y. M., 2003. Application of factor analysis in the assessment of groundwater quality in a blackfoot disease area in Taiwan. *Sci. Total Environ.* 313, 77–89.

Loomer, D. B., Al, T. A., Weaver, L., Cogswell, S., 2007. Manganese valence imaging in Mn minerals at the nanoscale using STEM-EELS. *Am. Mineral.* 92, 72–79.

Lowers, H. A., Breit, G. N., Foster, A. L., Whitney, J., Yount, J., Uddin, N., Muneem, A., 2007. Arsenic incorporation into authigenic pyrite, Bengal Basin sediment, Bangladesh. *Geochim. Cosmochim. Acta* 71, 2699–2717.

Luxton, T. R., Tadanier, C. J., Eick, M. J., 2006. Mobilization of arsenite by competitive interaction with silicic acid. *Soil Sci. Soc. Am. J.* 70, 204–214.

Mallick, S., Rajagopal, N. R., 1996. Groundwater development in the arsenic-affected alluvial belt of West Bengal - Some questions. *Current Sci.* 70, 956–958.

Manceau, A., Tamura, N., Celestre, R. S., MacDowell, A. A., Geoffroy, N., Sposito, G., Padmore, H. A., 2003. Molecular-scale speciation of Zn and Ni in soil ferromanganese nodules from loess soils of the Mississippi Basin. *Environ. Sci. Technol.* 37, 75–80.

Mandal, B. K., Chowdhury, T. R., Samanta, G., Basu, G. K., Chowdhury, P. P., Chanda,

C. R., Lodh, D., Karan, N. K., Dhar, R. K., Tamili, D. K., Das, D., Saha, K. C., Chakraborti, D., 1996. Arsenic in groundwater in seven districts of West Bengal, India - The biggest arsenic calamity in the world. *Current Sci.* 70, 976–986.

Manning, B. A., Goldberg, S., 1997. Adsorption and Stability of Arsenic(III) at the clay mineral-water interface. *Environ. Sci. Technol.* 31, 2005–2011.

Manning, B. A., Fendorf, S. E., Goldberg, S., 1998. Surface structures and stability of arsenic(III) on goethite: Spectroscopic evidence for inner-sphere complexes. *Environ. Sci. Technol.* 32, 2383–2388.

Manning, B. A., Fendorf, S. E., Bostick, B., Suarez, D. L., 2002. Arsenic(III) oxidation and arsenic(V) adsorption reactions on synthetic birnessite. *Environ. Sci. Technol.* 36, 976–981.

Marini, L., Accornero, M., 2007. Prediction of the thermodynamic properties of metal-arsenate and metal-arsenite aqueous complexes to high temperatures and pressures and some geological consequences. *Environ. Geol.* 52, 1343–1363.

Martin, J.M., Meybeck, M., 1979. Elemental mass-balance of material carried by major world rivers. *Mar. Chem.* 7, 173–206.

Mazumder, G.. D. N., Haque, R., Ghosh, N., De, B. K., Santra, A., Chakraborti, D., Smith, A. H., 1998. Arsenic levels in drinking water and the prevalence of skin lesions in West Bengal, India, *Int. J. Epidemiol.* 27, 871– 877.

McArthur, J. M., Ravenscroft, P., Safiulla, S., Thirlwall, M. F., 2001. Arsenic in groundwater: Testing pollution mechanisms for sedimentary aquifers in Bangladesh. *Water Resour. Reser.* 37, 109–117.

McArthur, J. M., Banerjee, D. M., Hudson-Edwards, K. A., Mishra, R., Purohit, R., Ravenscroft, P., Cronin, A., Howarth, R. J., Chatterjee, A., Talukder, T., Lowry, D., Houghton, S., Chadha, D. K., 2004. Natural organic matter in sedimentary basins and its relation to arsenic in anoxic ground water: the example of West Bengal and its worldwide implications. *Appl. Geochem.* 19, 1255–1293.

McCleskey, R. B., Nordstorm, D. K., Maest, A. S., 2004. Preservation of water samples for arsenic(III/V) determinations: an evaluation of the literature and new analytical results. *Appl. Geochem.* 19, 995–1009.

McGuire, E. J., 1970. K-Shell Auger transition rates and fluorescence yields for elements Ar-Xe, *Pys. Rev. A* 2, 273–278.

Meharg, A. A., Scrimgeour, C., Hossain, S. A., Fuller, K., Cruickshank, K., Williams, P.

N., Kinniburgh, D. G., 2006. Codeposition of organic carbon and arsenic in Bengal Delta aquifers. *Environ. Sci. Technol.* 40, 4928–4935.

Meng, X. G., Korfiatis, G. P., Bang, S. B., Bang, K. W., 2002. Combined effects of anions on arsenic removal by iron hydroxides. *Toxicol. Lett.* 133, 103–111.

Michael, H. A., Voss, C. I., 2008. Evaluation of the sustainability of deep groundwater as an arsenic-safe resource in the Bengal Basin. *Proc. Natl. Acad. Sci. U.S.A.* 105, 8531–8536.

Mitamura, M., Masuda, H., Itai, T., Minowa, T., Maruola, T., Ahmed K. M., Seddique, A. A. Dipak, B. K., Nakaya, S., Li, X. D., Uesugi, K., Kusakabe, 2008. M., Aquifer structure of arsenic contaminated groundwater in Sonargaon, Narayanganj, Bangladesh. *J. Geol.* 116. 288–302.

Mitsunobu, S., Harada, T., Takahashi, Y., 2006. Comparison of antimony behavior with that of arsenic under various soil redox conditions *Environ. Sci. Technol.* 40, 7270–7276.

Mitsunobu, S., Takahashi, Y., Sakai, Y., 2008. Abiotic reduction of antimony(V) by green rust ($Fe_4(II)Fe_2(III)(OH)_{12}SO_4 \cdot 3H_2O$). *Chemosphere* 70, 942–94.

Mueller, D. K., Helsel, D. R., 1996. Nutrients in the Nation's waters. Too much of a good thing? U.S. Geological Survey Circular 1136, 24.

Mukherjee-Goswami, A., Nath, B., Jana, J., Sahu, S. J., Sarkar, M. J., Jacks, G., Bhattacharya, P., Mukherjee, A., Polya, D. A., Jean, J. S., Chatterjee, D., 2008. Hydrogeochemical behavior of arsenic-enriched groundwater in the deltaic environment: Comparison between two study sites in West Bengal, India. *J. Contam. Hydrol.* 99, 22–30.

Murray, J.W., 1974. The surface chemistry of hydrous manganese dioxide. *J. Colloid Interface Sci.* 18, 357–371.

Myneni, S. C. B., Traina, S. J., Waychunas, G. A., Logan, T. J., 1998. Experimental and theoretical vibrational spectroscopic evaluation of arsenate coordination in aqueous solutions, solids, and at mineral-water interfaces. *Geochim. Cosmochim. Acta* 62, 3285–3300.

Nath, B., Berner, Z., Chatterjee, D., Mallik, S. B., Stuben, D., 2008a. Mobility of arsenic in West Bengal aquifers conducting low and high groundwater arsenic. Part II: Comparative geochemical profile and leaching study. *Appl. Geochem.* 23, 996–1011.

Nath, B., Jean, J. S., Lee, M. K., Yang, H. J., Liu, C. C., 2008b. Geochemistry of high arsenic groundwater in Chia-Nan plain, Southwestern Taiwan: Possible sources and reactive transport of arsenic. *J. Contam. Hydrol.* 99, 85–96.

Nath, B., Stuben, D., Mallik, S. B., Chatterjee, D., Charlet, L., 2008c. Mobility of arsenic in West Bengal aquifers conducting low and high groundwater arsenic. Part I: Comparative hydrochemical and hydrogeological characteristics. *Appl. Geochem.* 23, 977–995.

Naumov, G.. B., Ryzhenks, B. N., Khodakovsky, I. L. 1974. Handbook of Thermodynamic Data. U. S. Geol. Surv. PB. 226–722: Rept. No. USGS–WRD–74–001.

Nesbitt, H.W., Young, G.M., 1982. Early proterozoic climates and plate motions inferred from major element chemistry of lutites, *Nature* 299, 715–717.

Neuberger, C. S. Helz, G. R., 2005. Arsenic(III) carbonate complexing. *Appl. Geochem.* 20, 1218–1225.

Nickson, R., McArthur, J., Burgess, W., Ahmed, K. M., Ravenscroft, P., Rahman, M., 1998. Arsenic poisoning of Bangladesh groundwater. *Nature* 395, 338–338.

Nickson, R. T., McArthur, J. M., Ravenscroft, P., Burgess, W. G., Ahmed, K. M., 2000. Mechanism of arsenic release to groundwater, Bangladesh and West Bengal. *Appl. Geochem.* 15, 403–413.

Nickson, R. T., McArthur, J. M., Shrestha, B., Kyaw-Myint, T. O., Lowry, D., 2005. Arsenic and other drinking water quality issues, Muzaffargarh District, Pakistan. *Appl. Geochem.* 20, 55–68.

Nishimura, T., Ito, C. T., Tozawa, K., 1988. Stabilities and solubilities of metal arsenites and arsenates in water and effect of sulfate and carbonate ions on their solubilities. In Arsenic Metallurgy Fundamentals and Applications. Metallurgical Society, Warrendale, PA, pp. 77–98.

O'Day, P. A., Rivera, N., Root, R., Carroll, S. A., 2004a. X-ray absorption spectroscopic study of Fe reference compounds for the analysis of natural sediments. *Am. Mineral.* 89, 572–585.

O'Day, P. A., Vlassopoulos, D., Root, R., Rivera, N., 2004b. The influence of sulfur and iron on dissolved arsenic concentrations in the shallow subsurface under changing redox conditions. *Proc. Natl. Acad. Sci. U.S.A.* 101, 13703–13708.

O'Day, P., 2006. Chemistry and mineralogy of arsenic. *Elements* 2, 77–83.

Ona-Nguema, G., Morin, G., Juillot, F., Calas, G., Brown, G. E., 2005. EXAFS analysis of arsenite adsorption onto two-line ferrihydrite, hematite, goethite, and lepidocrocite. *Environ. Sci. Technol.* 39, 9147–9155.

Oremland, R. S., Stola, J. G., 2003. The ecology of arsenic. Science 300. 939–944.

Oremland, R. S., Stolz, J. F., 2005. Arsenic, microbes and contaminated aquifers. *Trends in Microbiol.* 13, 45–49.

Pal, T., Mukherjee, P. K., 2009. Study of subsurface geology in locating arsenic-free groundwater in Bengal delta, West Bengal, India. *Environ. Geol.* 56,1211–1225.

Pedersen, H. D., Postma, D., Jakobsen, R., 2006. Release of arsenic associated with the reduction and transformation of iron oxides. *Geochim. Cosmochim. Acta* 70, 4116–4129.

Pierce, M. L., Moore, C. B., 1982. Adsorption of arsenite and arsenate on amorphous iron hydroxide. *Water Res.* 16, 1247–1253.

Polizzotto, M. L., Harvey, C. F., Sutton, S. R., Fendorf, S., 2005. Processes conducive to the release and transport of arsenic into aquifers of Bangladesh. *Proc. Natl. Acad. Sci. U.S.A.* 102, 18819–18823.

Polizzotto, M. L., Harvey, C. F., Li, G. C., Badruzzman, B., Ali, A., Newville, M., Sutton, S., Fendorf, S., 2006. Solid-phases and desorption processes of arsenic within Bangladesh sediments. *Chem Geol.* 228, 97–111.

Polizzotto, M. L., Kocar, B. D., Benner, S. G., Sampson, M., Fendorf, S., 2008. Near-surface wetland sediments as a source of arsenic release to ground water in Asia. *Nature* 454, 505–U5.

Post, J. E., 1999. Manganese oxide minerals: Crystal structures and economic and environmental significance. *Proc. Natl. Acad. Sci. U.S.A.* 96, 3447–3454.

Postma, D., Larsen, F., Hue, N. T. M., Duc, M. T., Viet, P. H., Nhan, P. Q., Jessen, S., 2007. Arsenic in groundwater of the Red River floodplain, Vietnam: Controlling geochemical processes and reactive transport modeling. *Geochim. Cosmochim. Acta* 71, 5054–5071.

Radloff, K. A., Cheng, Z. Q., Rahman, M. W., Ahmed, K. M., Mailloux, B. J., Juhl, A. R., Schlosser, P., van Geen, A., 2007. Mobilization of arsenic during one-year incubations of grey aquifer sands from Araihazar, Bangladesh. *Environ. Sci. Technol.* 41, 3639–3645.

Radu, T., Subacz, J. L., Phillippi, J. M., Barnett, M. O., 2005. Effects of dissolved

carbonate on arsenic adsorption and mobility. *Environ. Sci. Technol.* 39, 7875–7882.

Raiswell, R., Canfield D. E., Berner R. A., 1994. A comparison of iron extraction methods for the determination of degree of pyritisation and the recognition of iron-limited pyrite formation. *Chem. Geol.* 111, 101–110.

Raven, K. P., Jain, A., Loeppert, R. H., 1998. Arsenite and arsenate adsorption on ferrihydrite: Kinetics, equilibrium, and adsorption envelopes. *Environ. Sci. Technol.* 32, 344–349.

Ravenscroft, P., McArthur, J. M., Hoque, B. A., 2001. Geochemical and palaeohydrological controls on pollution of groundwater by arsenic. Arsenic Exposure and Health Effects IV, Elsevier Science Ltd. Oxford. 53–78.

Ravenscroft, P., Burgess, W. G., Ahmed, K. M., Burren, M., Perrin, J., 2005. Arsenic in groundwater of the Bengal Basin, Bangladesh: Distribution, field relations, and hydrogeological setting. *Hydrogeol. J.* 13, 727–751.

Ravenscroft, P., Howarth, R. J., McArthur, J. M., 2006. Comment on "Limited temporal variability of arsenic concentrations in 20 wells monitored for 3 years in Araihazar, Bangladesh". *Environ. Sci. Technol.* 40, 1716–1717.

Ritter, K., Aiken, G. R., Ranville, J. F., Bauer, M., Macalady, D. L., 2006. Evidence for the aquatic binding of arsenate by natural organic matter-suspended Fe(III). *Environ. Sci. Technol.* 40, 5380–5387.

Robins R. G., 1990. The stability and solubility of ferric arsenate: an update. In EPD Congress 90' Minerals, Metals and Materials Society, Warrendale, PA. pp. 93–104.

Roman-Ross, G., Cuello, G. J., Turrillas, X., Fernandez-Martinez, A., Charlet, L., 2006. Arsenite sorption and co-precipitation with calcite. *Chem. Geol.* 233, 328–336.

Rowland, H. A. L., Gault, A. G., Charnock, J. M., Polya, D. A. 2005. Preservation and XANES determination of the oxidation state of solid-phase arsenic in shallow sedimentary aquifers in Bengal and Cambodia. *Mineral. Magazine* 69, 825–839.

Rowland, H. A. L., Polya, D. A., Lloyd, J. R., Pancost, R. D., 2006. Characterization of organic matter in a shallow, reducing, arsenic-rich aquifer, West Bengal. *Organ. Geochem.* 37, 1101–1114.

Rowland, H. A. L., Pederick, R. L., Polya, D. A., Pancost, R. D., Van Dongen, B. E., Gault, A. G., Vaughan, D. J., Bryant, C., Anderson, B., Lloyd, J. R., 2007. The control of organic matter on microbially mediated iron reduction and arsenic release in shallow alluvial aquifers, Cambodia. *Geobiol.* 5, 281–292.

Rowland, H. A. J., Gault, A. G., Lythgoe, P., Polya, D. A., 2008. Geochemistry of aquifer sediments and arsenic-rich groundwaters from Kandal Province, Cambodia. *Appl. Geochem.* 23, 3029–3046.

Rudnick, R., Gao, S., 2003. Composition of the continental crust. In: Rudnick, R.L. (Ed.), The Crust. In: Holland, H.D., Turekian, K.K. (Eds.), Treatise on Geochemistry, vol. 3. Elsevier-Pergamon, Oxford, pp. 1–64.

Ryu, J.F., Gao, S., Dahlgren, R. A., Zierenberg, R. A., 2002. Arsenic distribution, speciation and solubility in shallow groundwater of Owens Dry lake, California. *Geochim. Cosmochim. Acta* 66, 2981–2994.

Sadiq M., Lindsay, W, L., 1981. Arsenic supplement to technical bulletin 134: Selection of standard free energies of formation for use in soil chemistry. Colorado State University Experiment Station, Fort Collins, Colorado.

Samanta, G., Clifford, D. A., 2005. Preservation of inorganic arsenic species in groundwater. *Environ. Sci. Technol.* 39, 8877–8882.

Savage, K. S., Bird, D. K., O'Day, P. A., 2005. Arsenic speciation in synthetic jarosite. *Chem. Geol.* 215, 473–498.

Savarimuthu, X., Hira-Smith, M. M., Yuan, Y., von Ehrenstein, O. S., Das, S., Ghosh, N., Mazumder, D. N. G., Smith, A. H., 2006. Seasonal variation of arsenic concentrations in tubewells in West Bengal, India. *J. Health Popul. Nutr.* 24, 277–281.

Schroeder, S. L. M., 1996. Towards a 'universal curve' for total electron-yield XAS. *Solid State Commun.* 98, 405–409.

Schwertmann, U., Cornell, R. M., 2000. Iron oxides in the laboratory: preparation and characterization. Wiley-VCH. 103–110.

Seddique, A. A., Masuda, H., Mitamura, M., Shinoda, K., Yamanaka, T., Itai, T., Maruoka, T., Uesugi, K., Ahmed, K. M., Biswas, D. K., 2008. Arsenic release from biotite into a Holocene groundwater aquifer in Bangladesh. *Appl. Geochem.*. 23, 2236–2248.

Sengupta, S., Mukherjee, P. K., Pal, T., Shome, S., 2004. Nature and origin of arsenic carriers in shallow aquifer sediments of Bengal Delta, India. *Environ. Geol.* 45, 1071 –1081.

Sengupta, M. K., Mukherjee, A., Ahamed, S., Hossain, M. A., Das, B., Nayak, B., Chakraborti, D., Goswami, A. B., 2006. Comment on "Limited temporal variability

of arsenic concentrations in 20 wells monitored for 3 years in Araihazar, Bangladesh". *Environ. Sci. Technol.* 40, 1714–1715.

Sengupta, S., McArthur, J. M., Sarkar, A., Leng, M. J., Ravenscroft, P., Howarth, R. J., Banerjee, D. M., 2008. Do ponds cause arsenic-pollution of groundwater in the Bengal Basin? An answer from West Bengal. *Environ. Sci. Technol.* 42, 5156–5164.

Shamsudduha, M., Uddin, A., 2007. Quaternary shoreline shifting and hydrogeologic influence on the distribution of groundwater arsenic in aquifers of the Bengal Basin. *J.Asian Earth Sci.* 31, 177–194.

Shamsudduha, M., Uddin, A., Saunders, J. A., Lee, M. K., 2008. Quaternary stratigraphy, sediment characteristics and geochemistry of arsenic-contaminated alluvial aquifers in the Ganges-Brahmaputra floodplain in central Bangladesh. *J. Contam. Hydrol.* 99, 112–136.

Sherman, D. M., Randall, S. R., 2003. Surface complexation of arsenic(V) to iron(III) (hydr)oxides: Structural mechanism from ab initio molecular geometries and EXAFS spectroscopy. *Geochim. Cosmochim. Acta* 67, 4223–4230.

Shrestha, R. R., Shrestha, M. P., Upadhyay, N. P., Pradhan, R., Khadka, R., Maskey, A., Maharjan, M., Tuladhar, S., Dahal, B. M., Shrestha, K., 2003. Groundwater arsenic contamination, its health impact and mitigation program in Nepal. *J. Environ. Sci. Health* 38, 185–200.

Simeoni, M. A., Batts, B. D., McRae, C., 2003. Effect of groundwater fulvic acid on the adsorption of arsenate by ferrihydrite and gibbsite. *Appl. Geochem.* 18, 1507–1515.

Smedley, P. L., Kinniburgh, D. G., 2002. A review of the source, behavior and distribution of arsenic in natural waters. *Appl. Geochem.* 17, 517–568.

Smedley, P. L., Zhang, M., Zhang, G., Luo, Z., 2003. Mobilisation of arsenic and other trace elements in fluviolacustrine aquifers of the Huhhot Basin, Inner Mongolia. *Appl. Geochem.* 18, 1453–1477.

Smith, A. H., Lingas, E. O., Rahman, M., 2000. Contamination of drinking-water by arsenic in Bangladesh: a public health emergency. *Bull. World Health Organ.* 78, 1093–1103.

Smith, P. G., Koch, I., Gordon, R. A., Mandoli, D. F., Chapman, B. D., Reimer, K. J., 2005. X-ray absorption near-edge structure analysis of arsenic species for application to biological environmental samples. *Environ. Sci. Technol.* 39, 248–254.

Sø, H. U., Postma, D., Jakobsen, R., Larsen, F., 2008. Sorption and desorption of

arsenate and arsenite on calcite. *Geochim. Cosmochim. Acta* 72. 5871–5884.

Stachowicz, M., Hiemstra, T., van Riemsdijk, W. H., 2008. Multi-competitive interaction of As(III) and As(V) oxyanions with Ca^{2+}, Mg^{2+}, PO_4^{3-}, and CO_3^{2-} ions on goethite. *J. Colloid Interface Sci.* 320, 400–414.

Stanger, G., 2005a. A palaeo-hydrogeological model for arsenic contamination in southern and south-east Asia. *Environ. Geochem. Health* 27, 359–367.

Stanger, G., VanTruong, T., Ngoc, K., Luyen, T. V., Thanh, T. T., 2005b. Arsenic in groundwaters of the Lower Mekong. *Environ. Geochem. Health* 27, 341–357.

Stollenwerk, K. G., 2003. Geochemical processes controlling transport of arsenic in groundwater: a review of adsorption. In: Welch, A. H., and Stollenwerk, K. G., Editors, Arsenic in Ground Water: Geochemistry and Occurrence, Kluwer Academic Publishers, Boston, MA, pp. 67–100.

Stollenwerk, K. G., Breit, G. N., Welch, A. H., Yount, J. C., Whitney, J. W., Foster, A. L., Uddin, M. N., Majumder, R. K., Ahmed, N., 2007. Arsenic attenuation by oxidized aquifer sediments in Bangladesh. *Sci. Total Environ.* 379, 133–150.

Stolz, J. F., Oremland, R. S., 1999. Bacterial respiration of arsenic and selenium. *FEMS Microbiol. Rev.* 23, 615–627.

Stumm, W., Morgan, J. J., 1996. *Aqua. Chem.* Wiley, New York, 780–792.

Stummeyer, J., Marchig, V., Knabe, W., 2002. The composition of suspended matter from Ganges-Brahmaputra sediment dispersal system during low sediment transport season. *Chem. Geol.* 185, 125–147.

Stute, M., Zheng, Y., Schlosser, P., Horneman, A., Dhar, R. K., Datta, S., Hoque, M. A., Seddique, A. A., Shamsudduha, M., Ahmed, K. M., van Geen, A., 2007. Hydrological control of As concentrations in Bangladesh groundwater. *Water Resour. Reser.* 43.

Subramaniana, V., 1979. Chemical and suspended-sediment characteristics of rivers of India. *J. Hydrol.* 44, 37–55.

Sun, X. H., Doner, H. E., 1996. Adsorption and oxidation of arsenite on goethite. *Soil Sci.* 163, 278–287.

Sverjensky, D. A., Fukushi, K., 2006. A predictive model (ETLM) for As(III) adsorption and surface speciation on oxides consistent with spectroscopic data. *Geochim. Cosmochim. Acta* 70, 3778–3802.

Swartz, C. H., Blute, N. K., Badruzzman, B., Ali, A., Brabander, D., Jay, J., Besancon, J.,

Islam, S., Hemond, H. F., Harvey, C. F., 2004. Mobility of arsenic in a Bangladesh aquifer: Inferences from geochemical profiles, leaching data, and mineralogical characterization. *Geochim. Cosmochim. Acta* 68, 4539–4557.

Swedlund, P. J., Webster, J. G., 1999. Adsorption and polymerisation of silicic acid on ferrihydrite, and its effect on arsenic adsorption. *Water. Res.* 33, 2413–3422.

Takahashi, Y., Yoshida, H., Sato, N., Hama, K., Yusa, Y., Shimizu, H., 2002. W- and M-type tetrad effects in REE patterns for water-rock systems in the Tono uranium deposit, central Japan. *Chem. Geol.* 184, 311–335.

Takahashi, Y., Ohtaku, N., Mitsunobu, S., Yuita, K., Nomura, M., 2003. Determination of the As(III)/As(V) ratio in soil by X-ray absorption near-edge structure (XANES) and its application to the arsenic distribution between soil and water. *Anal. Sci.* 19, 891–896.

Takahashi, Y., Minamikawa, R., Hattori, K. H., Kurishima, K., Kihou, N., Yuita, K., 2004. Arsenic Behavior in paddy fields during the cycle of flooded and non-flooded periods, *Environ. Sci. Technol.* 38, 1038–1044.

Takahashi, Y., Kanai, Y., Kamioka, H., Ohta, A., Maruyama, H., Song, Z., Shimizu, H., 2006. Speciation of sulfate in size-fractionated aerosol particles using sulfur K-edge X-ray absorption near-edge structure. *Environ. Sci. Technol.* 40, 5052–5057.

Taylor, S. R., McLennan, S. M., 1995. The geochemical evolution of the continental crust. *Rev. Geophys.* 33, 241–265.

Taylor, K. G., Hudson-Edwards, K. A., Bennett, A. J., Vishnyakov, V., 2008. Early diagenetic vivianite [$Fe_3(PO_4)_2 \cdot 8H_2O$] in a contaminated freshwater sediment and insights into zinc uptake: A μ-EXAFS, μ-XANES and Raman study. *Appl. Geochem.* 23, 1623–1633.

Tebo, B. M., Johnson, H. A., McCarthy, J. K., Templeton, A. S., 2005. Geomicrobiology of manganese(II) oxidation. *Trends Microbiol.* 13, 421–428.

Tohno, S., Kawai, J., Chatani, S., Ohta, M., Kitajima, Y., Yamamoto, K., Kitamura, Y., Kasahara, M., 1998. Application of X-ray absorption fine structure (XAFS) spectrometry to identify the chemical states of atmospheric aerosols. *J. Aerosol Sci.* 29, 235–236.

Tohno, S., Kawai, J., Kitajima, Y., 2001. Identification of the chemical states of phosphorus in atmospheric aerosols by XANES spectrometry, *J. Synchrotron Rad.* 8, 958–960.

Tossel, J. A., 1997. Theoretical studies on arsenic oxide and hydroxide species in minerals and in aqueous solution. *Geochim. Cosmochim. Acta* 61, 1613–1623.

Tossell, J. A., Zimmermann, M. D., 2008. Calculation of the structures, stabilities, and vibrational spectra of arsenites, thioarsenites and thioarsenates in aqueous solution. *Geochim. Cosmochim. Acta* 72, 5232–5242.

Tournassat, C., Charlet, L., Bosbach, D., Manceau, A., 2002. Arsenic(III) oxidation by birnessite and precipitation of manganese(II) arsenate. *Environ. Sci. Technol.* 36, 493–500.

Toyoda, T., Nishi, S., Oki, T., Kuwahara, K., Ichikawa, K., Kutara, K., Hirano, I., 1999. A Guide to Draw Geological Column for Drilling Core (Bohring Chujyouzu Sakusei Yoryou Kaisetsusho). *Japan Construction Information Center*, p. 10 (in Japanese).

Tufano, K. J., Fendorf, S., 2008a. Confounding impacts of iron reduction on arsenic retention. *Environ. Sci. Technol.* 42, 4777–4783.

Tufano, K. J., Reyes, C., Saltikov, C. W., Fendorf, S., 2008b. Reductive processes controlling arsenic retention: revealing the relative importance of iron and arsenic reduction. *Environ. Sci. Technol.* 42, 8283–8289.

Umitsu, M., 1993. Late quaternary sedimentary environments and landforms in the Ganges Delta. *Sediment. Geol.* 83, 177–186

van Geen, A., Ahsan, H., Horneman, A. H., Dhar, R. K., Zheng, Y., Hussain, I., Ahmed, K. M., Gelman, A., Stute, M., Simpson, H. J., Wallace, S., Small, C., Parvez, F., Slavkovich, V., Lolacono, N. J., Becker, M., Cheng, Z., Momotaj, H., Shahnewaz, M., Seddique, A. A., Graziano, J. H., 2002. Promotion of well-switching to mitigate the current arsenic crisis in Bangladesh. *Bull. World Health Org.* 80, 732–737.

van Geen, A., Zheng, Y., Versteeg, R., Stute, M., Horneman, A., Dhar, R., Steckler, M., Gelman, A., Small, C., Ahsan, H., Graziano, J. H., Hussain, I., Ahmed, K. M., 2003. Spatial variability of arsenic in 6000 tube wells in a 25 km^2 area of Bangladesh. *Water Resour. Reser.* 39.

van Geen, A., Rose, J., Thoral, S., Garnier, J. M., Zheng, Y., Bottero, J. Y., 2004. Decoupling of As and Fe release to Bangladesh groundwater under reducing conditions. Part II: Evidence from sediment incubations. *Geochim. Cosmochim. Acta* 68, 3475–3486.

van Geen, A., Aziz, Z., Horneman, A., Weinman, B., Dhar, R. K., Zheng, Y., Goodbred, S., Versteeg, R., Seddique, A. A., Hoque, M. A., Ahmed, K. M., 2006a. Preliminary evidence of a link between surface soil properties and the arsenic

content of shallow groundwater in Bangladesh, *J. Geochem. Explor.* 88, 157–161.

van Geen, A., Zheng, Y., Cheng, Z., He, Y., Dhar, R. K., Garnier, J. M., Rose, J., Seddique, A., Hoque, M. A., Ahmed, K. M., 2006b. Impact of irrigating rice paddies with groundwater containing arsenic in Bangladesh. *Sci. Total Environ.* 367, 769–777.

van Geen, A., Zheng, Y., Goodbred, S., Horneman, A., Aziz, Z., Cheng, Z., Stute, M., Mailloux, B., Weinman, B., Hoque, M. A., Seddique, A. A., Hossain, M. S., Chowdhury, S. H., Ahmed, K. M., 2008. Flushing history as a hydrogeological control on the regional distribution of arsenic in shallow groundwater of the Bengal Basin. *Environ. Sci. Technol.* 42, 2283–2288.

van Herreweghe, S., Swennen, R., Vandecasteele, C., Cappuyns, V., 2003. Solid phase speciation of arsenic by sequential extraction in standard reference materials and industrially contaminated soil samples. *Environ. Poll.* 122, 323–342.

Wagman, D. D., Evans, W. H., Parker, V. B., Halow, I., Bailey, S. M., Schumm, R. H. 1968. Selected values of chemical thermodynamic properties. *Nat. Bur. Std. Tech. Note* pp. 270–273.

Wang, G., 1984. Arsenic poisoning from drinking water in Xinjiang. *Chin. J. Prevent. Med.* 18, 105–107.

Wang, S. W., Liu, C. W., Jang, C. S., 2007. Factors responsible for high arsenic concentrations in two groundwater catchments in Taiwan. *Appl. Geochem.* 22, 460 –476.

Webster J. G., 1990, The solubility of As_2S_3 and speciation of As in dilute and sulphide-bearing fluids at 25 and 90°C. *Geochim. Cosmochim. Acta* 54, 1009 –1017.

WHO (World Health Organization), 2004 WHO (World Health Organization), Guidelines for drinking-water quality recommendations vol. 1, WHO, Geneva, 515 pp.

Wilke, M., Farges, F., Petit, P., Brown JR, G. E., Martin, F., 2001. Oxidation state and coordination of Fe in minerals: An Fe K-XANES spectroscopic study. *Am. Mineral.* 86, 714–730.

Wilkie, J. A., Hering, J. G., 1996. Adsorption of arsenic onto hydrous ferric oxide: effects of adsorbate/adsorbent ratios and co-occurring solutes. *Colloid. Surface.* A. 107, 97–110.

Wilson, M. J., 2004. Weathering of the primary rock-forming minerals: processes,

products and rates. *Clay Min.* 39, 233–266.

Winkel, L., Berg, M., Amini, M., Hug, S. J., Johnson, C. A., 2008. Predicting groundwater arsenic contamination in Southeast Asia from surface parameters. *Nature Geosci.* 1, 536–542.

Yu, W. H., Harvey, C. M., Harvey, C. F., 2003. Arsenic in groundwater in Bangladesh: A geostatistical and epidemiological framework for evaluating health effects and potential remedies. *Water Resour. Reser.* 39.

Zhang, N. L., Blowers, P., Farrell, J., 2005. Evaluation of density functional theory methods for studying chemisorption of arsenite on ferric hydroxides. *Environ. Sci. Technol.* 39, 4816–4822.

Zheng, Y., Stute, M., van Geen, A., Gavrieli, I., Dhar, R., Simpson, H. J., Schlosser, P., Ahmed, K. M., 2004. Redox control of arsenic mobilization in Bangladesh groundwater. *Appl. Geochem.* 19, 201–214.

Zheng, Y., van Geen, A., Stute, M., Dhar, R., Mo, Z., Cheng, Z., Horneman, A., Gavrieli, I., Simpson, H. J., Versteeg, R., Steckler, M., Grazioli-Venier, A., Goodbred, S., Shahnewaz, M., Shamsudduha, M., Hoque, M. A., Ahmed, K. M., 2005. Geochemical and hydrogeological contrasts between shallow and deeper aquifers in two villages of Araihazar, Bangladesh: Implications for deeper aquifers as drinking water sources. *Geochim. Cosmochim. Acta* 69, 5203–5218.

Zobrist, J., Dowdle, P. R., Davis, J. A., Oremland, R. S., 2000. Mobilization of arsenite by dissimilatory reduction of adsorbed arsenate. *Environ. Sci. Technol.* 34, 4747–4753.

Acknowledgements

I am grateful to **Dr. Yoshio Takahashi** for his encouragements and suggestions throughout entire period of my study. I have learned various things from his behavior, not only scientific skills and knowledge, but also the positive and creative attitudes toward science and education.

I am grateful to **Prof. Harue Masuda** (Osaka-City University). This work was initiated by her introduction, and she has given me many scientific advices and encouragements.

I would like to express my thanks to the following financial supports.

The study described in Chapter 2 is supported by Grant-in-Aid for Scientific Research, No. 15403017 from the Scientific Research Fund of the Japan Society for the Promotion of Science (JSPS).

The study described in Chapter 3 was performed with the approval of the Japan Synchrotron Radiation Research Institute (JASRI, Proposal No. 2006B1099, 2007A1804, and 2006A1596) and the High Energy Accelerator Research Organization (KEK, Proposal No. 2006G347). This study was partially supported by the JSPS Research Fellowship for Young Scientist dedicated to me.

The study described in Chapter 4 was supported by a Grant-in-Aid for Scientific Research from the JSPS, No. 15403017. Valuable sponsorship was also derived via the KEK (proposal No. 2004G334), and JASRI (proposals No. 2005A0628 and 2006B1701). This study was partially supported by the JSPS Research Fellowship for Young Scientist dedicated to me.

Some traveling fees for a field survey and an international conference were supported by "Education and Training of World-class Geoexperts" selected by the Ministry of Education, Culture, Sports, Science and Technology (MEXT) for its "Support Program for Improving Graduate School Education".

In addition to the above funds, I really appreciate the research fellowship (DC2) by JSPS awarded for 2 years.

This PhD study is greatly improved by supports from following people.

I am grateful to **Prof. Hiroshi Shimizu** for his valuable scientific comments and encouragements.

I would like to express my thanks to my seniors: **Dr. Kazuya Tanaka, Dr. Satoshi Mitsunobu, Dr. Fumito Shiraishi, Dr. Anirban Das**, and **Mr. Yuhei Yamamoto**. Scientific discussions with them were valuable to improve my study.

I would like to express my thanks to the researchers: **Dr. Muneki Mitamura** (Osaka-city University), **Dr. Teruyuki Maruoka** (University of Tsukuba), **Mr. Seddique Ashraf Ali** (Osaka-city University), and **Prof. Minoru Kusakabe** (Toyama University) for their various helps to conduct this PhD studies.

I would like to express my thanks to the people in charge of the beamlines of synchrotron facilities: **Dr. Tomoya Uruga** and **Dr. Hajime Tanida** (BL01B1, Spring-8); **Dr. Yasuko Terada** and **Mr. Satoshi Endo** (BL37XU), **Dr. Atsuo Iida** (BL4A, KEK-PF); **Dr. Masaharu Nomura** and **Dr. Yasuhiro Inada** (BL12C, KEK-PF), for their helps for XAFS experiments.

I would like to express my thanks to the editors and referees of my papers: **Dr. David Polya** (editor in Applied Geochemistry), **Dr. Yoshito Ohshima** (editor in Chemistry Letters), **Dr. David Rickard** (editor in Chemical Geology), **Dr. Lex van Geen, Dr. John Uh Lee**, and some anonymous referees. Their comments greatly improved my studies.

I wish to thank the following people for their technical supports.

The field survey in Bangladesh was helped by the scientists and graduate students of Dhaka University. The core drilling was conducted by the Eastern Geotechnical, Dhaka. Total As concentration in sediment was analyzed by **Ms. Kaori Okazaki** (Osaka-city University). Total dissolved carbon was analyzed by **Dr. Toshiro Yamanaka** and **Mr. Hironori Akashi** (Okayama University). **Mr. Yoshiaki Ishitobi** prepared some instruments. **Mr. Yutaka Mouri** analyzed volatile components in sediment samples. **Mr. Hayami Ishisako** helped to prepare thin sections. The EPMA analyses were conducted by **Mr. Yasuhiro Shibata. Mr. Osamu Fushiki** and **Mr. Yoshiyuki Watanabe** helped XRF analyses. **Ms. Masako Hori** made guidance for oxygen isotope analysis.

Following people also supported my study and life in PhD course.

I am grateful to the faculties in Department of Earth and Planetary Systems Science, Hiroshima University. They have encouraged me for three years.

I would like to express my sincere thanks to **Ms. Hiroko Hirano, Ms. Chikako Kobayashi, Ms. Satoko Harada**, and **Ms. Natsumi Matsui** (the office in the Department of Earth and Planetary Systems Science, Hiroshima University) for their great many supports.

I wish to thank to **Dr. Nachiketa Das** for his English teaching.

I wish to express my sincere appreciation to **my parents** and **Ms. Yukiko Kajikawa** who always kept thoughtful encouragements for three years.

Finally, I would like to express my sincere thanks to the laboratory members. Daily discussions with following people were really exciting and greatly matured my scientific skills, **Mr. Yoshiro Yamashita, Ms. Taeko Hirata, Mr. Tomonari Fujimoto, Mr. Kenji Furukawa, Mr. Teppei Harada, Ms. Yoko Shimamoto, Mr. Yusuke Araki, Mr. Takuro Miyoshi, Mr. Koichi Morita, Ms. Mika Yamamoto, Ms. Masayuki Higashi, Ms. Mika Sakamitsu, Ms. Kyoko Sakuma, Ms. Yuka Yokoyama, Mr. Takuya Ishibashi, Mr. Ryoichi Nakada, Ms. Nozomi Raito**, and **Mr. Teruhiko Kashiwabara.**

Thank you very much.